THE FORMATION AND OBDUCTION OF OPHIOLITES SINCE THE LATE PRECAMBRIAN

by

STACEY ELAINE METZLER

Presented to the Faculty of the Graduate School of

The University of Texas at Arlington in Partial Fulfillment

of the Requirements

for the Degree of

MASTER OF SCIENCE IN GEOLOGY

THE UNIVERSITY OF TEXAS AT ARLINGTON

December 2006

DEDICATION

This work is dedicated to my two daughters Emily and Evelynne who have inspired me to keep reaching for the stars... someday you girls will reach yours too.

- Mom

ACKNOWLEDGEMENTS

It is difficult to say what is impossible, for the dream of yesterday is the hope of today and the reality of tomorrow.

- Robert Goddard

This work would not have been possible without the many ophiolite researchers from around the world. Christopher Scotese has been an invaluable source of information on tectonics and ophiolites. I would like to thank him for giving me a wealth of information and guidance during my research, mapping, and writing process. I would like to thank the firm Freese and Nichols Inc. in Fort Worth, Texas for partial financial support of my degree and for support with many GIS questions. I would like to thank my parents Eric and Deborah for an overwhelming amount of support; Deborah helped with preliminary editing. Last, I would like to thank my husband Steve and my two daughters Emily and Evelynne who have been patient and forgiving during the time I have given up with them in order to take on this endeavor of research and writing. Thank you all; this research would never have been possible without all of your support.

November 13, 2006

ABSTRACT

THE FORMATION AND OBDUCTION OF OPHIOLITES

SINCE THE LATE PRECAMBRIAN

Publication No. _____

Stacey Elaine Metzler, MS

The University of Texas at Arlington, 2006

Supervising Professor: Christopher Scotese

Ophiolite formation and emplacement has been episodic since the Late Precambrian. This research study examines ophiolites that formed during the Cenozoic, Mesozoic, Paleozoic and Late Precambrian. The ophiolites were plotted on paleogeographic reconstructions using PALEOMAP Project maps, and the ophiolite localities were analyzed by their temporal distribution in relation to the tectonic framework in which they were emplaced. The ophiolites appear to show episodic events linked to global plate reorganization. These episodes coincide with collisional

events from the supercontinents of Gondwana and Pangea. The primary mechanisms of formation and emplacement proved to be mid-ocean ridge systems and back arc basins as well as accretionary prisms and continent-continent collisions respectively. The data was refined to remove any bias and the results yield pulses of ophiolite formation and emplacement during the key intervals of late Cretaceous, middle to late Jurassic, and early Devonian and Silurian.

TABLE OF CONTENTS

LIST OF ILLUSTRATIONS

LIST OF TABLES

CHAPTER 1

OPHIOLITES

Watch the stars, and from them learn. To the Master's honor all must turn, each in its track, without a sound, forever tracing Newton's ground.

-Albert Einstein

The term ophiolite comes from the Greek "*ophis,*" meaning snake and "*lithos,*" meaning rocks. Ophiolites are generally thought of as slices of old oceanic crust and have proven to be reliable indicators of tectonic activity through geologic time. The presence of an ophiolite often indicates the existence of an ancient ocean basin and the timing of closure. Mapping ophiolite locations and describing both the age of the oceanic crust that comprises ophiolites, and the timing of the emplacement of ophiolites (obduction) are important lines of evidence that can be used to reconstruct the tectonic history of the ancient ocean basin that aids in understanding tectonic reconstructions. This study has identified and mapped most of the known ophiolites on a global scale (Figure1.1). These ophiolites were then restored to their paleo-locations at the time of emplacement and plotted on paleogeographic maps that illustrate the ancient tectonic environments.

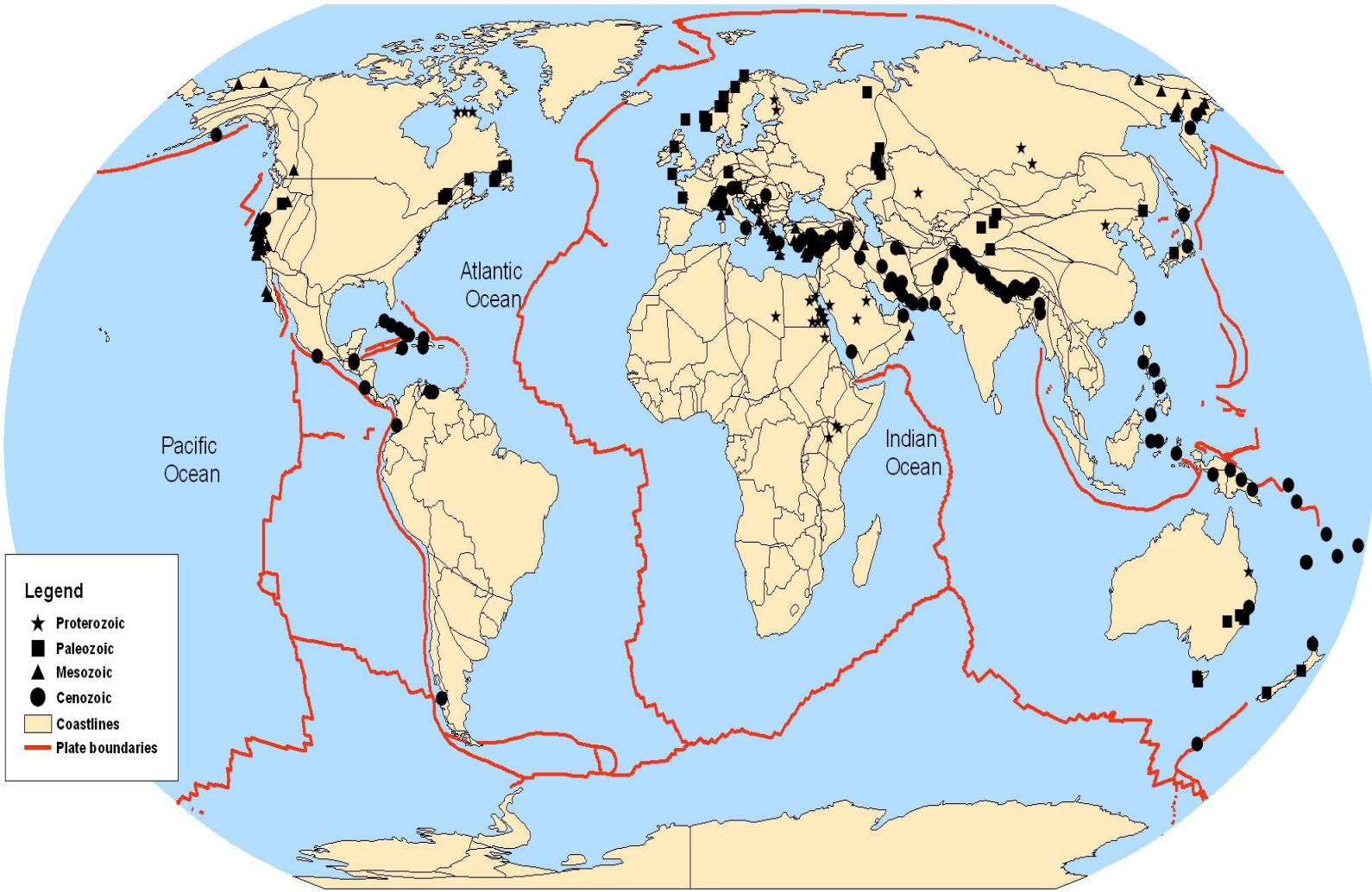

Figure 1.1 Localities of modern ophiolites with present-day plate boundaries (Scotese, 2004)

1.1 Historical Perspective on Ophiolites

1.1.1 Previous Work on Ophiolites

The three main periods of ophiolite discovery tend to follow other times of major geologic breakthroughs. The first line of thought regarding ophiolites stemmed from Alexander Brongniart's initial proposal of the term "ophiolite" in 1813, and continued until the 1960's when the plate tectonic revolution took place. The initial ideas regarding ophiolites focused on their tectonic context and recognized that they were associated with oceanic crust. The true nature of ophiolites was still debated and there were many conflicting proposals regarding the emplacement process and petrology of the rocks that comprise the ophiolitic suite. Most scientists could not and were not willing to agree on any one definition for ophiolites. The second phase in the development of the ophiolite concept took place after the acceptance of the theory of plate tectonics in the late 1960's. Scientists were looking for geological evidence to test and prove plate tectonic theories. Ophiolites provided this support. With the advent of high-speed computers and digital technology during the 1980's, new equipment such as marine seismic surveys have allowed the modern era of study in ophiolites to evolve. This has provided evidence that further validated the hypotheses describing how the ocean floor is related to ophiolite formation and how ophiolites are obducted (Nicolas & Boudier, 2003).

Before the plate tectonic revolution, the work of Alexander Brongniart, Gustav Steinmann, Norman Bowen, Harry Hess, and Robert G. Coleman, among others was

pivotal in introducing and expanding this field of study. As previously mentioned, in the early 1800's Brongniart introduced the concept of an ophiolite to describe serpentinized mélanges. He later redefined the term to include the suite of magmatic rocks composed of volcanic rocks, diabase, gabbro, and ultramafic rocks. Steinmann believed they formed as 'in situ' intrusions along the axial parts of geosynclines. These intrusions were made up of three principal components: 1) serpentinite, 2) diabase-spilite, and 3) chert. The three components of an ophiolite are now referred to as the "Steinmann Trinity." American geologists of the 1920's to the 1960's were not mobilists and generally did not accept the European concept of an ophiolite, which implied large-scale tectonic movements. Hess and Bowen studied the petrology of harzburgite and lherzolite peridotites in the 1950s, which helped to differentiate the magmas and igneous rocks that comprised ophiolites. In 1955, Hess linked the occurrence of peridotite to orogenic events (Dilek, 2003a). He also suggested that the change in seismic velocity observed at the boundary between the lower and upper mantle, or Moho, was due to a change in petrology from harzburgite to lherzolite peridotites. Because this same transition in mafic rocks was observed in ophiolite sequences, he concluded that ophiolites must represent a preserved section of the crust and mantle (Dilek, 2003a).

Robert Coleman was one of the principal scientists promoting the study of ophiolites, suggested in the late 1950's that fault contacts, rather than the intrusive contacts, indicated that ophiolites were tectonically emplaced rather than intruded from below. His book, 'Ophiolites' (1977), has been a resource for many scientists who have

chosen to further examine the many ophiolite complexes around the globe. In his book, Coleman points out the complexities and disagreements among scientists regarding the association of mafics and ultramafics within ophiolites (Dilek, 2003a; Coleman, 1977).

At the Geological Society of America Penrose Field Conference in 1972, many scientists gathered to discuss the ophiolite concept and attempted to come to a consensus concerning the definition of ophiolites. The members of the conference determined that an ophiolite is a "distinctive assemblage of mafic to ultramafic rocks" (Dilek, 2000a). The general description of this new 'layer-cake' sequence of rocks was from bottom to top: 1) an ultramafic complex consisting of harzburgite, lherzolite, and dunite, which may be serpentinized, 2) a gabbro complex including cumulus texture, 3) a mafic sheeted dike complex, 4) a mafic volcanic complex pillows, and 5) topped with a pelagic sedimentary cherty layer.

Other scientists that have made important contributions to our understanding of ophiolites include: Yildrem Dilek, Cathy Busby, Robert Hall, Thomas Moores, and Akira Ishiwatari, to name a few. Most of these modern researchers have focused on the link between ophiolites and the tectonic environments in which they formation and obduction takes place (Dilek, 2003a).

Students at the University of Texas at Arlington (UTA) Roy, Chaudhuri, and Karadeniz assembled some of the information compiled in this study in the fall of 2001. Preliminary results of this work were presented at the Annual Meeting of the Geological Society in Denver, Colorado in 2004 (Scotese et al., 2004).

1.2 Description of Ophiolites

1.2.1 What is an Ophiolite?

Many geoscientists have attempted to define what makes up an ophiolite. For simplicity, the definition presented here is the most common and widely accepted description of an ophiolite. An ophiolite is a vertical cross section of oceanic crust that has been removed or obducted during a tectonic event (Figure 1.2). The typical layers include from bottom to top: 1) mantle-ultramafic cumulates, 2) moho-seismic rocks, 3) mafic cumulates, 4) massive gabbros, 5) mafic sheeted dike complex, 6) pillow basalts, and 7) pelagic/ abyssal cherty sediments. It is noteworthy that there are some slight variations form the Penrose definition; however, the definition is still a general synthesis.

At the Penrose conference in 1972, a definition of a seven-part ophiolite complex was prepared. The definition consisted of these layers from the "bottom" up: 1) an ultramafic complex with harzburgite, lherzolite, and or dunite with a metamorphic tectonic fabric, 2) a gabbroic complex with cumulate textures consisting of peridotites and pyroxenites, 3) a mafic sheeted dike complex, 4) a mafic volcanic complex often as pillow basalts, and lastly, 5) pelagic, often cherty, sediment as a cover (Ingersoll & Busby, 1995; Dilek, 2003a). For this study, this definition of an ophiolite has been adopted and the author has added two additional units: 1) a massive gabbro layer that occurs between the gabbro cumulates and sheeted dikes, and 2) the contact between the petrologic crust and mantle (Moho). A composite ophiolite section is given in Figures

1.3 – 1.4 and shows representative images of some of the rocks typically found in ophiolites.

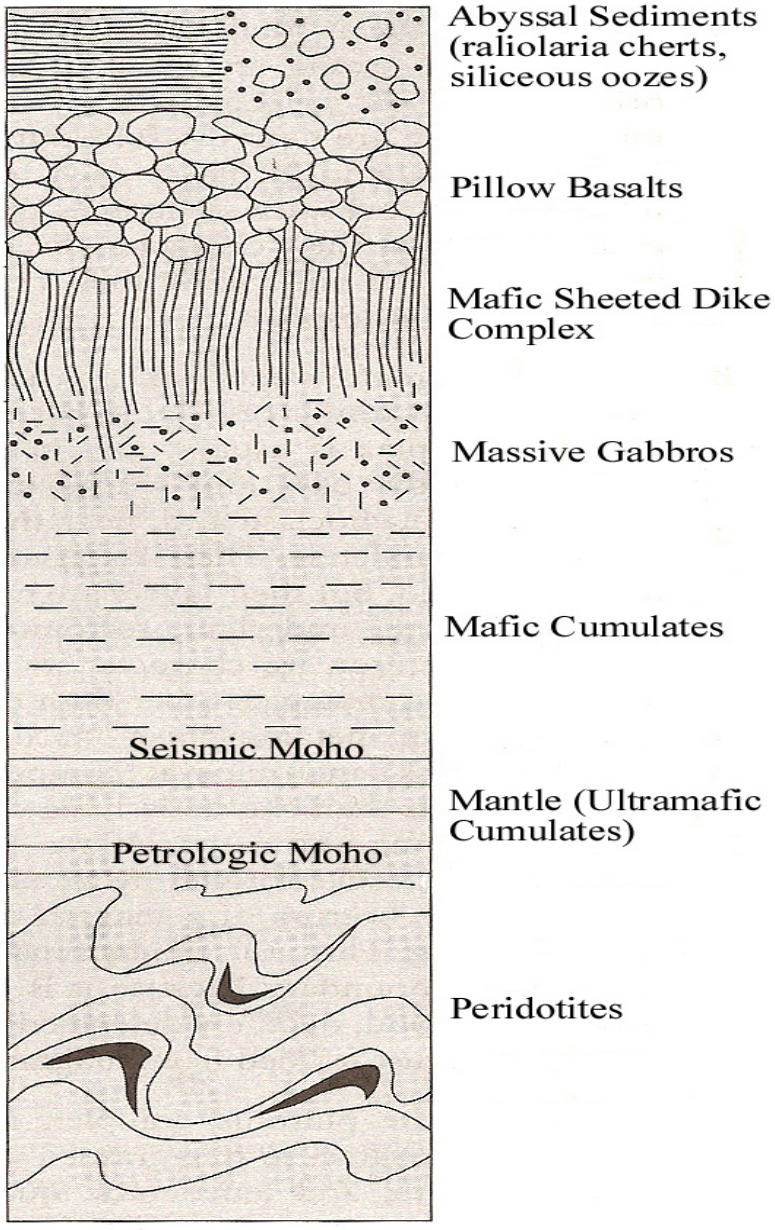

Figure 1.2 Depiction of the typical ophiolite sequence (modified from Moores and Twiss, 1995)

Figure 1.3 Pillow basalts in the Quebec ophiolites
(photo used with permission by Stein)
website: http://www.earth.northwestern.edu/people/seth/107/Ridges/ophiolite.htm

Figure 1.4 Troodos ophiolite near Cyprus with sheeted dike complexes
(photo used with permission by Tauxe)
website: http://www.digistar.mb.ca/minsci/future/deposits.htm

Gustav Steinmann is the one of the modern pioneers of the ophiolite concept. In 1927, Steinman proposed that ophiolites consisted of three principal rock types: serpentinite, gabbro, and diabase/spilite. Serpentine, a hydrated iron/magnesium-rich rock, forms when peridotite is hydrothermally altered by seawater percolating along the faults associated with seafloor spreading (Harper, 1984). Diabase is an intrusive rock comprised of mostly labradorite and pyroxene with ophitic textures. Spilite is an altered vesicular basalt and typically occurs in submariner lava flows with pillow structures. Chert is a microcrystalline sedimentary rock that typically occurs as nodules within limestones and dolomites and precipitates from organic and inorganic matter in seawater. These three typical rock types are easily identified as occurring in abyssal environments.

Steinmann initially began studying the petrologic and structural nature of what is now called the Ligurian ophiolite in the Apennines of Italy. He also described the crucial cross-cutting relationships that established the relative age and tectonic setting of ophiolites. Steinmann proposed that the serpentinite was never crosscut by the gabbro and diabase, therefore making it the oldest member of the suite. The gabbros only crosscut the serpentinite, never the diabase, and the diabase often crosscut both the serpentinite and the gabbro, making it the youngest member of the suite. Steinmann also established the crucial link between the radiolarites and the volcanic extrusions often found at the top of an ophiolite section. This relationship was important because it linked the "geosynclinal" oceanic abyssal sediments and volcanics to the ophiolite.

Although his tectonic models were incorrect, Steinmann laid the foundation for the further study of ophiolites (Juteau, 2003; Coleman, 1977).

1.2.2 How Oceanic Crust is Preserved as Ophiolites

The opinion that is widely accepted is that ophiolites form in rifting basins; however, there are a few other environments in which they can form. Ophiolites can form in environments such as back arc basins, along a continental strike-slip zone, oceanic fracture zones, pull-apart basins, and as seamounts, guyots, and hot spots. The mid-ocean ridge, or rifting, back arc basins and island arc systems are the most common of all the environments for ophiolite formation (Metzler, this work- chapter 6).

1.2.3 Ophiolite Obduction

Ophiolites can be preserved in several tectonic environments (Figure 1.5). The cartoon diagram shows how ophiolites can be "trapped" and preserved on other landmasses under the right conditions. Robert Coleman first introduced the concept of the obduction of an ophiolite in 1971 (Moores, 2003). Obduction is generally accepted as the tectonic mechanism by which the ophiolite is emplaced (see Figure 1.5). Ophiolite obduction generally occurs during the thrusting of oceanic lithosphere onto a passive continental margin during continental collision. (Coleman, 1977; Pearce, 2003).

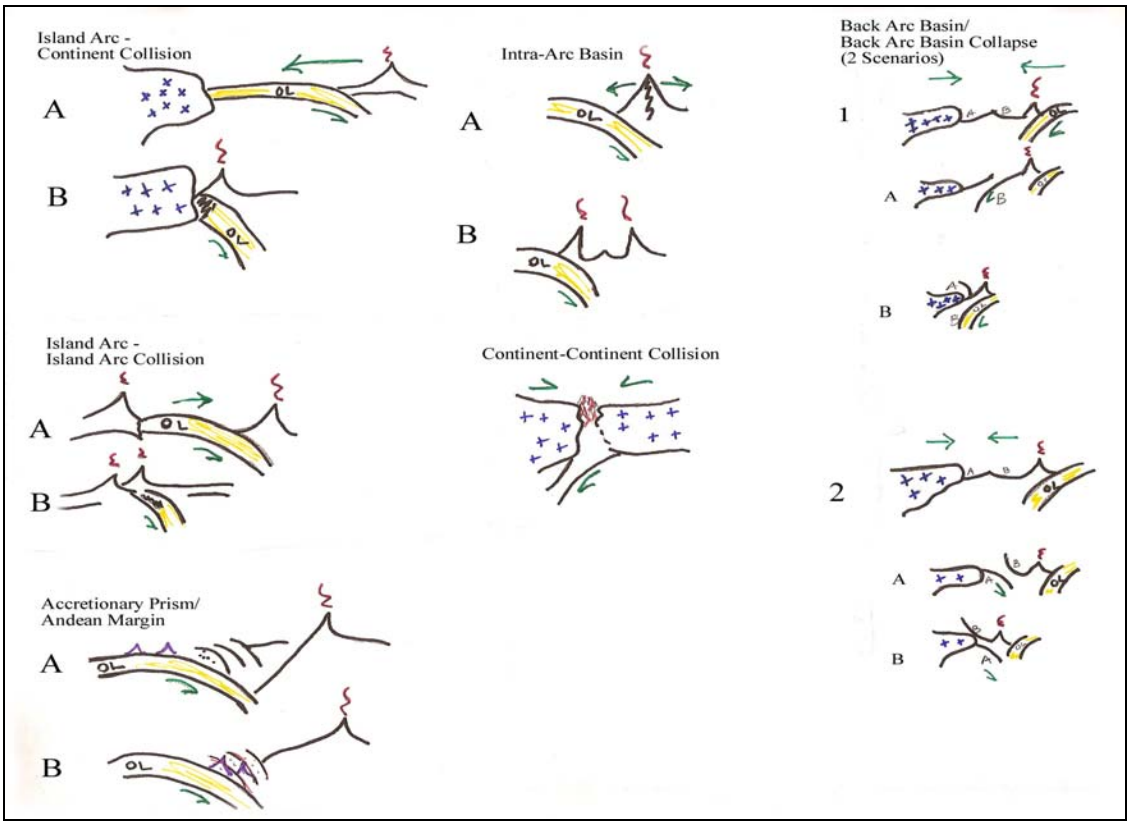

Figure 1.5 Tectonic environments for ophiolites

Another opportunity for ophiolite obduction occurs when oceanic lithosphere splits off the top of the descending slab leaving some of the slab to be placed onto the continent. The lower portion of the oceanic lithosphere is then thrust under the continental slab. (Coleman, 1977; Pearce, 2003). Another mechanism for emplacement is when a slab of oceanic crust is added to an accretionary prism in an arc system (Coleman, 1977; Pearce, 2003). As the descending slab is subducted, the portions of the oceanic lithosphere are sliced off and emplaced onto the adjacent arc. The most common environments for ophiolite emplacement are accretionary prisms, continent-continent collision, and arc-continent collisions (Metzler, this work- chapter 6).

Chapter two of this work has a further discussion of the tectonic environments for ophiolite obduction.

1.2.4 Classification of Ophiolites

The typical "layer cake stratigraphy" was generally accepted during the 1972 Penrose conference on ophiolites and still used today. A layer cake stratigraphy is useful in initial identification during field mapping, but it does not identify the tectonic setting in which the ophiolite was obducted (Dilek, 2003b). Some scientists have tried to classify ophiolites based on tectonic setting and others based on the rocks present within the complex (Nicolas, 1989). Often ophiolites are identified as more than one type depending on how the ophiolite is described: by environment, by rocks, or by tectonic regime. An example of this is to say that an ophiolite is a lherzolite-alpine type. This description suggests that the ophiolites formed in rift basins and have a normal oceanic crustal sequence yet exhibits the presence of lherzolite with deformed and possibly partial recrystallization evident in the peridotites. This nomenclature can be confusing and ambiguous (Dilek, 2003b; Nicolas, 1989).

Most scientists agree on two main types of ophiolites: the lherzolite and the harzburgite types, which are most commonly used to describe the formation environment of the ophiolite. These categories can present a problem if used as the only description for 'type' of ophiolite because the lherzolite and harzburgite type descriptors cannot differentiate between subduction or ridge crest environments. The lherzolite-types are generally ultramafic and have alpine-type, or deformed peridotites.

These generally consist of lherzolite, plagioclase peridotites, troctolites, gabbros, and Fe-gabbros. The harzburgite-type generally consists of harzburgite, dunite, chromite, pyroxenite, norite, and olivine gabbro. This type generally has the typical platinum group elements as key indicators (Pearce, 2003). Below is a further description of the 'types' of ophiolites commonly used.

In the early 1980's many ophiolite researchers made a distinction among ophiolites dividing them into two types: Tethyan/Cordilleran. Tethyan-type ophiolites are generally found in Europe, Arabia, and the Caribbean, are typically Jurassic to Cretaceous in age, and are often found on passive continental margins (Dilek, 2003b and 2000a). Moores et al. (2000) describes Tethyan ophiolites as rocks that "tectonically overlie continental crust and shallow-water continental-margin or platform sediments," which typically consist of pelagic sediments with little or no volcanics intermixed. As Spaggiari et al. (2003) describes them, these Tethyan ophiolites are typically "dominated by mantle and gabbroic sequences" and have a more complete sequence.

Ophiolites of the Cordilleran type are generally found in the western Pacific and Cordilleran region in North America and are primarily Paleozoic to Mesozoic in age (Dilek, 2003b). These typically show no definitive relationship with old continental crust and are often associated with tectonic (accretionary) mélanges with high grade metamorphics and extrusive volcanic rocks of island arcs (Moores et al., 2000). Spaggiari et al. (2003) describe these as displaying "disrupted upper oceanic crustal" rocks.

At many conferences in the 1990's, emerging experts laid out various other 'types' of ophiolites. The Mediterranean-type occur in the eastern Mediterranean region including Troodos and Oman, two of the more well-known sequences. These are typically complete Penrose sequences as described previously, and were emplaced onto passive continental margins and there does not seem to be any particular formation setting that uniquely defines these types (Dilek, 2003a and 2003b). Sierran-type ophiolites are typically found on the Pacific Rim particularly the Cordillera of the Americas as well as Japan and the Philippines. These are generally arc-related complexes and exhibit sheeted dike swarms (Dilek, 2003a).

Dilek et al. (1998) described two types of ophiolites by the differences between fast and slow spreading ridges. Fast spreading centers generally demonstrate a complete ophiolite sequence whereas slow spreading ridges typically reveal an incomplete and highly faulted zone with a highly serpentinized exposed surface.

1.3 Organization of the Ophiolites for this Study

One of the principal questions addressed by this research is: what are the temporal and spatial patterns of ophiolite formation and obduction? Ophiolite data was collected to test whether the formation and obduction of ophiolites was random, uniform or episodic. Random patterns, if found, could indicate ophiolites occur with no discernable pattern in space and time. Episodic ophiolite events occur at uneven intervals and could indicate a link to some geologic or tectonic events. Lastly, the data

compiled in this study might show a uniform trend where ophiolites occur regularly throughout time. In Chapter 2, the author describes the database that was compiled to test these three models. The results are described in Chapter 6.

Another question to be addressed is: what does the spatial-temporal pattern of ophiolite formation and obduction imply about plate tectonic processes? Other researchers have suggested (Dilek, 2003b; Ishiwatari, 1999a) that the emplacement of ophiolites occurs during times of global plate reorganization, or that ophiolites are obducted primarily during continental collisions or the collapse of backarc basins. Chapter 6 presents a discussion of the question of tectonic setting.

The results of this research study are organized into three chapters (Chapters 3, 4, and 5) that describe the 280 ophiolites. The discussion of the ophiolites is presented in chronological sequence (oldest to youngest). Chapter 3 presents ophiolites that were emplaced primarily in Europe, Arabia, Africa, and Russia during the Precambrian and Paleozoic Eras. Chapter 4 presents ophiolites emplaced generally along the Cordillera and Europe during the Mesozoic Era. In the final detailed ophiolite discussion section, Chapter 5, ophiolites are shown to have been emplaced along the India-Tibet collision zone, Europe, the Caribbean, the Southwest Pacific, and Southeast Asia during the Cenozoic Era and are discussed in detail. There are three appendices for this report as well: Appendix A is the ophiolite database, Appendix B is a list of the references for each of the ophiolite localities, and Appendix C is the paleogeographic maps with associated ophiolite locations in full color fold out form.

Notations in Chapters 3, 4, and 5 use the ophiolite reference numbers given in [brackets] as found in the column "Ophiolite #" in Appendix A. Example: [5.35] refers to the Troodos ophiolite noted in the database shown in Appendix A and are unique to this research as a means to simplify the references to the ophiolites. The reference to millions of years in the database is noted in this paper using the abbreviation "Ma" which is from an old Latin form of *million anno* meaning millions of years.

CHAPTER 2

METHODS OF DATA ACQUISITION AND ASSEMBLY

Recent ophiolite researchers (Dilek, 2003; Abbate, 1985) have published information about ophiolites and have assessed the distribution over geologic time. In these past studies, the data has been amalgamated and combined in ways that make it difficult to assess the contribution and validity of each individual ophiolite locality. This work also discusses the plate tectonic framework in which the ophiolites formed and were emplaced. This chapter describes in depth the methods of data acquisition and map making.

2.1. Ophiolite Data Acquisition and Assimilation

This chapter describes: 1) the structure of the ophiolite database (Appendix A), 2) how the information that comprises this database was acquired, and 3) the GIS techniques that were used to plot the ophiolites on paleogeographic maps.

2.1.1 The Ophiolite Data Table Structure

An Excel spreadsheet was used in this study to collect information about worldwide ophiolite localities. The information in the spreadsheet was then plotted on

paleogeographic maps based on the emplacement age of the ophiolites. The structure of the database was designed so that the ophiolite localities could be easily transferred to a Geographic Spatial Information System (ArcGIS by ESRI). Appendix A is a complete listing of the ophiolite locality database.

2.1.1.1 Fields for Ophiolite Location

The database has five major sections or headings: Location, Formation, Emplacement, Miscellaneous, and Reliability. The first section of fields titled 'Location' is general information, which includes the name of the ophiolite and its modern geographic location. The "Ophiolite #" is the first subheading or field in this section and its purpose is to uniquely identify each ophiolite. This identifier comprises a number from one to eight followed by a decimal and a two-digit number. The first number represents the general geographic region of the world in which the ophiolite is located. The number following the decimal is simply an incremental acquisition number. No attempt was made to organize the data into sub-regions. The unique identification number was used primarily as a map label to identify each ophiolite locality. Table 2.1 lists the regions of the world and associated tectonic or geologic features.

The second field "Map #" is the field used to identify the map on which the ophiolite locality is plotted (See Appendix C). The ophiolites were plotted on the map that most closely matched the time of ophiolite emplacement. An ophiolite with no plate number listed in this column had no age data to use for plotting on

paleogeographic maps but was still considered noteworthy for understanding the geologic and tectonic framework of this study. Table 2.2 lists the map intervals, age in millions of years, and some of the important tectonic events that took place during that time using the Geological Society of America 1999 timescale. The separation of the data into the different map and time groupings was based on a general knowledge of tectonic events throughout geologic time.

The next field "Name" is the name of the ophiolite complex. Assigning a unique name was difficult at times because often ophiolite names are interchanged with regions or renamed when thought to be a different suite of ophiolitic rocks. The names used in this database represent the most commonly used name for the ophiolite complex. The next field is "Country" and is the country where the rocks currently are found or the country associated with the oceanic region in which the ophiolite is found. The next field is "Region" and is used to further specify the location of the ophiolite. In some cases, it is a heading such as north or south, and in other cases, it may be a city, mountain range or other geographic feature that is often associated with the ophiolite.

Table 2.1 Ophiolite Regions

Ophiolite Regions	Geographic Area
1	Arabian-Nubian Shield Egypt Northwestern Africa
2	Caledonides Appalachians Eastern Canada Europe
3	Koryak Mountains Urals Russia Baykal
4	Cordillera Western Americas Alaska
5	Zagros Southern Mediterranean Europe Iran Turkey
6	Himalayas Pakistan Tibet India China Tianshan
7	Caribbean region Cuba Guatemala
8	Southwest Pacific Southeast Asia Australia Indonesia Japan

Table 2.2 GIS Map Number Correlation to Geologic Events or Times

Ophiolite Maps and Associated Times				
Map	**Geologic Period**	**Age in Millions of Years**	**Age of Paleogeographic Map**	**Significant Geologic Events**
11	Modern	all	0	
10	Late Cenozoic	0-50	20	SW Pacific Islands
9	Late Cretaceous to Early Cenozoic	50 - 100	70	Himalayas & Tibet, Greater Antilles, Cuba, North America, South America
8	Mid Cretaceous	100 - 140	100	Himalayas, Tibet, Alps, Zagros, Rockies
7	Mid to Late Jurassic	140 - 190	160	Rockies & Alaska
6	Triassic to Early Jurassic	190 - 250	220	
5	Late Carboniferous to Permian	250 - 310	280	
4	Early Carboniferous	310 - 360	340	Tasman Orogen, Urals and Mongolian Island Arcs
3	Ordovician, Silurian, Devonian	360 - 500	440	Tasman Orogen, Urals and Mongolian Island Arcs
2	Cambrian	500 - 545	520	Iapetus
1	Neoproterozoic	545 - 1100+	750	Pan African

"Longitude" and "Latitude" describe the location of the ophiolite within 1/10 of a degree. All values are given in decimal degrees. The convention +N, -S, +E, -W was also used. The Federal Communications Commission has a conversion website http://www.fcc.gov/mb/audio/bickel/DDDMMSS-decimal.html for a useful online calculator that converts degrees-minutes-seconds to decimal degrees. The last field in this section is "Area" which represents the area extent of the ophiolite complex. In

most cases, this information was not cited in the literature; therefore, there are relatively few data points that actually have this information.

2.1.1.2 Fields for Ophiolite Formation

The second group of fields describes the age of 'Formation' of the ophiolite. The 'age of formation' refers to the time when the oceanic crust that comprises the ophiolite was formed, usually at some type of extensional plate boundary (i.e. mid-ocean ridge, back arc basin spreading center). The "Plate" field identifies the tectonic plate on which the oceanic crust that makes up the ophiolite formed. If the plate was given in the literature then it was included; if the plate was not given, then it was inferred by geographic location from the plate tectonic reconstructions.

The next field "Stratigraphic Age" is the stratigraphic age of origin or formation, with the notations coded as acronyms (see Table 2.3). In some cases, the literature only noted a general geological time such as 'Late Jurassic.' The stratigraphic age was converted to the numerical values using the Geological Society of America 1999 time scale.

The next two fields "Old Age" and "Young Age" are an estimate of the age range during which the oceanic crust that makes up the ophiolite formed. In these columns, the values are given in millions of years. An age range was used because often the dating techniques did not give a precise age, or more than one age was cited from different literature sources.

Table 2.3 Ophiolite Age Stratigraphic Abbreviations

Stratigraphic Codes			
Code	Description		
e	Early		
m	Middle		
l	Late		
		Old (Ma)	Young (Ma)
Ceno	Cenozoic	65	0.01
Meso	Mesozoic	248	65
Paleo	Paleozoic	543	248
PC	Precambrian	3400+	543
Q	Quaternary	1.8	0.01
T	Tertiary	65	1.8
Ng	Neogene	23.8	1.8
Pg	Paleogene	65	23.8
Plio	Pliocene	5.3	1.8
Mioc	Miocene	23.8	5.3
Olig	Oligocene	33.7	23.8
Eoc	Eocene	54.8	33.7
Paleoc	Paleocene	65	54.8
K	Cretaceous	144	65
Jur	Jurassic	206	144
Tr	Triassic	248	206
Perm	Permian	290	248
Carb	Carboniferous	354	290
Dev	Devonian	417	354
Sil	Silurian	443	417
Ord	Ordovician	490	443
Camb	Cambrian	543	490
NP	Neoproterozoic	900	543
MP	Mesoproterozoic	1600	900
PP	Paleoproterozoic	2500	1600
Arch	Archean	3400+	2500

The "Best Estimate" column is simply the numerical average of the total age range or $\frac{(OldAge + YoungAge)}{2}$. The next field, "Difference Between Old & Young Ages," is the difference between the ophiolite "Old Age" and "Young Age" and was used as a rough indicator of reliability. This field was particularly useful for ophiolites described in literature sources as 'dating from Triassic to Cretaceous.' That difference is so large that the data, theoretically, could have spanned four different maps and should be considered less reliable. Every effort was made to narrow down the date to a reasonable time interval; however, in some cases precise age information was not found.

The field "Reliability of Age" is where the reliability of the data was noted. A code of one, two, or three was used to denote a reliability of age based on the difference between the old and young age. An entry of '1' was considered a reliable age (difference is ≤ 20 Ma), an entry of '2' is a moderately reliable age (difference > 20 but ≤ 40 Ma) and an entry of '3' is considered a less reliable age (difference > 40 Ma). As the geologic age goes further back in time (i.e. Precambrian), it is noteworthy that the gaps become larger due to the lack of reliable rock dating methods. An entry of '0' correlates to no data being present to assess the reliability.

The last field for the formation section is "Tectonic Environment" and was the field used to enter the type of tectonic environment in which the oceanic crust that makes up the ophiolite formed. Table 2.4 describes the codes used for the tectonic environments.

Table 2.4 Ophiolite Tectonic Environment Codes

Extensional Environments	
Code	Description
PCM	passive continental margin
MOR	mid-ocean ridge
PMOR	proto-mid-ocean ridge
ICR	intra-continental rift
AUL	aulocogen (failed arm)
IMP	impactogen
PAB	pull apart basin
Mid-Ocean Ridge Environments	
Code	Description
OPL	oceanic plateau
MOI	mid-ocean island (hot spot)
SMT	seamount, guyot, submerged mid-ocean island
Strike-Slip Environments	
Code	Description
OFZ	oceanic fracture zone
CSS	continental strike slip zone
Convergent Environments	
Code	Description
AND	Andean margin
ARC	island arc
ACP	accretionary prism
FAB	forearc basin
IAB	intra-arc basin
BAB	backarc basin
Collisional Environments	
Code	Description
ACC	island arc-continent collision
AAC	island arc-island arc collision
BAC	back-arc basin collapse
CCC	continent-continent collision

The tectonic environment of ophiolite formation, and obduction, can be somewhat difficult to explain. As mentioned in chapter 1, there are many possibilities for ophiolite formation and obduction (Figure 1.5) and often the ophiolite was emplaced shortly after the formation making the environments somewhat overlap. The back arc basin is a common example where an ophiolite can form and then shortly thereafter, in geologic time, is emplaced within the back arc basin as it collapses. Examples of this situation are the Iranshar [5.06] and Fanuj [5.07] ophiolites located in southeastern Iran. Another example is an ophiolite that forms within an island arc and then is accreted onto continental lithosphere shortly after. An example of this situation occurs within the Koryak Mountains [3.10] of Siberia.

2.1.1.3 Fields for Ophiolite Emplacement

This section describes evidence concerning the obduction or emplacement of ophiolites. The emplacement age, as mentioned previously, is the time at which the ophiolite was obducted. The same fields, which were used to describe the ophiolite formation, have also been used to describe the emplacement age and tectonic setting. In this case, however, the ages refer to the obduction date rather than the age of formation of the oceanic crust that makes up the ophiolite. In many cases, one or more values are missing. The data was left empty if the specific age of emplacement was not reported in literature sources. In a few cases, where no definitive age of emplacement is known, the ophiolite is plotted on the modern map, Figure 1.1, but has not been plotted on any reconstruction. Tectonic environment is included for emplacement as well and is

similar to the tectonic environment of formation. The possible environments are different from that of ophiolite formation and are listed in Table 2.4. The last field, "Difference in Formation and Emplacement Age," was calculated by subtracting the emplacement age from the formation age. Some geoscientists have proposed that the difference in age of formation and emplacement of an ophiolite is generally about 20 million years (Hacker, 1994; Cox et al., 1999; Ping et al., 2005). This field was included to address that hypothesis.

2.1.1.4 Fields for Ophiolite Reliability and Completeness

The last section in the database focuses on the reliability of the data. The "Obduction Complex" field is used to describe the name of the obducted complex. In some cases, the names are different from the name of the ophiolite complex given in the "Name" field due to regional, tectonic, or other geologic formations. This field was useful in cases where other literature was needed to further refine the data and allowed for broader search descriptors when researching the ophiolite localities. The next field of this section is "Overlying Sediment Name" which describes the formation or group named in the literature that overlies the ophiolite unit.

The last field, titled Completeness, describes the rocks within the ophiolite suite. The ophiolite reliability is an important section used to determine if the sequence was complete, had been disrupted through tectonic processes, or subjected to high-grade metamorphism. The typical Penrose definition was used for the categories of this group. These next seven fields titled: "Mantle," "Moho," "Cummulates," "Gabbro,"

"Dikes," "Pillows," and "Sediments," were used to indicate if these were lithologically present in the ophiolite sequence. A "1" indicates that the subunit was present and a "0" indicates that it was absent. If no information was available, the field was left empty.

The next field is the "Completeness Score." The completeness score is the sum of the seven-subunit rocks that are present in the ophiolite complex. A score of seven indicates that all of the typical Penrose subunits are present. The issue of reliability and completeness of an ophiolite complex is an important factor because some geoscientists think that the term ophiolite has been "overused" and that some rock suites are not necessarily of ophiolitic origin despite the designation as such (Coleman, 1977 and Dilek, 2003a).

2.1.2 Ophiolite Data Collection Procedures

Attempts were made by the author to make this compilation as comprehensive as possible. The key sources of data were Dilek and Newcomb, 2003; Coleman, 1977; Gass et al., 1984; Dilek et al, 2000; Dilek and Robinson, 2003; Panayiotou, 1980; and Peters et al., 1990 as well as many individual journal articles. At times, the author would find an ophiolite citation and try to find the original referenced article. The World Wide Web is a wonderful research tool but is limited to what is made available on the websites. The author, in some instances, would find reference to an article but it was too old to access in full (i.e. only abstracts available) on any public or University authorized websites. Therefore the author made extensive use of the ophiolite reference

resource website http://earth.s.kanazawa-u.ac.jp/ishiwata/searche.htm created by Dr. Akira Ishiwatari. Dr. Ishiwatari is a Professor of Geology and Petrology in the Department of Earth Sciences from Kanazawa University in Kakuma-machi Japan, is one of the editors-in-chief of "The Island Arc" journal, and has a primary research interest in ophiolites.

2.1.3 The Significance of Errors in the Data

Errors are inherent in many scientific research projects and are undoubtedly part of the process. This study has made every effort to avoid errors; however, there may be some unavoidable assumptions included in this report. When an ophiolite was located, the longitude and latitude were entered as precisely as possible. In many cases, the literature source included a map with the longitude and latitude graticule; in these cases, the values entered are as precise as the original map source. In other cases, reference material did not include numerical values of latitude and longitude and the location was researched using the (2003) "Hammond Atlas of the World" and located as precisely as possible. In some cases, the reference source cited a city or region near the ophiolite locality. Another source for latitudinal and longitudinal information was the website http://www.earthsearch.net/ that is an international searchable database that includes geographical features, as well as, city and country information. There were instances when an ophiolite could not be located by source information or from an atlas; in some of those cases this website provided better information. This website combines information from the USGS, NASA, NGA (National Geospatial-Intelligence Agency),

and other geographical data repositories to create a searchable site to find many obscure geographical locations.

Another source of possible error is the age bracketing within the stratigraphic codes; the 1999 Geological Society of America Geologic Time Scale was used throughout this study. Ophiolites are often noted in the literature as "occurring in the Late Cretaceous" and for these situations, the "Old Age" would have been entered as 99 Ma and the "Young Age" would be entered as 65 Ma. If the literature made no other more specific mention of an age for the ophiolite then the 99 to 65 Ma time constraint was used. These would also have been the values used for the further calculations of "Best Estimate" and "Difference" as mentioned in the previous section. The distinction of "Late Cretaceous" could then theoretically have a wider margin of error than dates for ophiolites obtained by radiometric dating techniques. In many cases the age of the metamorphic sole of the ophiolite complex was used for the emplacement age; this could be a source of error if the time of metamorphism does not strictly correlate to the age of obduction.

2.2 Ophiolite Data Rotation in ArcGIS

After the ophiolite data was compiled, the next step was to prepare the data for plotting in ArcGIS. The ArcGIS software was used in the Windows environment and was compatible with Access documents. The following section describes how the data was translated in ArcGIS.

2.2.1 The Use and Incorporation of GIS with the Data

Each ophiolite entry was assigned a spatial location, latitude, and longitude, which generated a point shapefile for further use in ArcGIS. Files must first be translated into a format that the GIS program can read; however since this database was designed as an Excel spreadsheet, the data was converted to comma delimited/comma separated values, or a CSV file and then imported into ArcGIS. This shapefile data was then joined with attributes that described the plate on which the ophiolite had traveled. Using the 'Plate Tracker' program written by C. R. Scotese and P. Featherstone (Shell Oil Co.), the point data was reconstructed and plotted on paleogeographic maps through Geologic time with its associated geological plate.

Once the data was sorted by the geologic times listed in Table 2.2, the data was reconstructed to the appropriate Geologic time by using the in the ArcObjects script called 'Plate Tracker,' that Scotese and Featherstone created for ArcGIS. After the "Age" Plate Tracker script is enabled at the chosen age, the plates are rotated and the GIS software then allows editing the layers. The plate rotation models are based on the tectonic and paleogeographic interpretations of Scotese and the PALEOMAP Project

reconstructions. The edits are saved, and a new layer is then created for the specified time period. Rotating the point data with the plates is useful for correlation of past geologic and tectonic events associated with these ophiolites. The GIS program and Plate Tracker script visually enhance the data on a map in such a way that an ordinary data table could not demonstrate. This allows maps with reconstructions of geologic events and with the ophiolite data to be viewed for interpretation.

Twelve maps (see Appendix C) portray paleo-plates, paleo-coastlines, paleogeography, and paleo- plate boundaries as well as the ophiolite data. Each map depicts the ophiolites as they traveled with the plates. One of the maps seen in Figure 1.1 is the modern map, which displays all the present-day ophiolite locations. The layers of plates, coastlines, and paleogeography are from Scotese; the plate boundaries were drawn by the author in GIS from Scotese's tectonic and paleoreconstructions; and the ophiolite data comes from the author's database. Annotation of the ophiolite numbers from the "Ophiolite #" field were scripted using Visual Basic (VB) code in the GIS platform by the author.

2.2.2 Problems Encountered with the use of GIS

The ability to manipulate data is a key benefit of a GIS approach. One problem encountered in working with the Plate Tracker program in ArcGIS was with the initial 'plates2' layer. If the data and plates2 layer are located in the same folder in the computer filing system, the Plate Tracker program would overwrite the existing modern plates file with the data that had been reconstructed to the specified time period.

Another problem encountered was writing the formula to isolate the time intervals. The requirements for the formula are exacting and if not done properly then an error message will appear and will not allow the selecting function to work.

As mentioned previously, the data is annotated, or labeled, on the map and this was a source of a slight problem as well. In ArcGIS, the use of shapefiles and geodatabases is common; however, the functionality can be different for each type depending on the needs of the user and the data. Geodatabases are useful for large expansive datasets because they allow for relationships between fields to be established; these can be useful in data for citywide information plotted on GIS maps. In this study, only shapefiles were utilized; using a geodatabase was too extensive for this small dataset. This posed a slight problem when trying to annotate the labels for the ophiolites on the GIS maps. A geodatabase allows for much easier use of labels but the shapefile does not. The shapefile writes all of the labels directly over the data point; this posed an enormous problem as many of the ophiolite locations around the world are clustered together in a geographically small area. Even when zoomed in, the labels were not discernable. The labels were not movable or editable, which created a bit of confusion as the GIS program cut off "extraneous' zeros from the data points i.e. the data point 5.10 was truncated to 5.1 by the program. Nevertheless, the problem was overcome with the author incorporating the VB script and creating the annotation labels for the ophiolites and the labels became movable and editable.

CHAPTER 3

PROTEROZOIC AND PALEOZOIC OPHIOLITES

In this chapter, as well as in chapters 4 and 5, the ophiolite localities are plotted on a summary introductory figure and are individually listed in a summary table with ages given in millions of years. Each ophiolite has a unique identification number as mentioned in the previous section. For more information about each ophiolite, see the ophiolite database (Appendix A). The ophiolites are presented by region in chronological order based on the age of obduction.

This chapter analyzes the global distribution and the tectonic setting of formation and emplacement of Late Precambrian (Middle to Late Proterozoic) and Paleozoic ophiolites. These ophiolite localities are plotted on Figure 3.2 and individually listed in Table 3.1 and Figure 3.1 shows a legend for all paleogeographic maps presented in this paper. Thirty Proterozoic ophiolites are described in this study from Africa, Eurasia, North America, and Australia. Thirty-nine ophiolites are described from the Cambrian through Devonian. These ophiolites are found in the Russian Urals, Scandinavian Caledonides, Norway, Newfoundland, and Quebec as well as a few in Europe, China, and Australia. There are four ophiolite localities in the Early Carboniferous, three in Eurasian areas and one in China. Seven ophiolites of late Carboniferous to Permian age occur in Australia, New Zealand, Russia, and the United States of America.

3.1 Proterozoic

3.1.1 Proterozoic Ophiolites

The controversy over ophiolites older than 1100 Ma and their tectonic environments is one topic still debated with Geology researchers today (Stern et al, 2004; Moores & Twiss, 1995). Most geoscientists believe that plate tectonics, and the processes which produce ophiolites, were different in the Archean. The main basis for this argument is that the ophiolites formed before the Late Proterozoic are lacking the ultramafic tectonic boundary typically seen in Phanerozoic ophiolite sequences (Moores & Twiss, 1995). This paper presents only a few examples of these older ophiolites (see Figure 3.2 and Table 3.1). The presence of pre-late Proterozoic ophiolites cannot be denied; however, the inferences that we derive from them concerning ancient tectonic environments are very uncertain (Moores & Twiss, 1995).

3.1.1.1 Arabian-Nubian Ophiolites

Ophiolites in the Arabian-Nubian Shield during the Late Precambrian tend to show a general trend from north-south to northeast-southwest. Most seem to show moderate amounts of displacement during this period and many tend to be highly dismembered although still recognizable (Berhe, 1990; Ren & Abdelsalam, 2005).

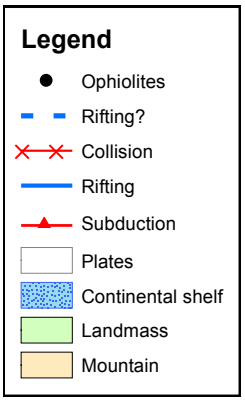

Figure 3.1 Legend for paleogeographic reconstruction maps seen in chapters 3, 4, and 5

Table 3.1 Neoproterozoic and Older Ophiolites

			Age of Formation			Age of Obduction		
Map #	Name	Country	Old Age	Young Age	Best Estimate	Old Age	Young Age	Best Estimate
1	Marlborough	Australia	560.00	560.00	560.00			
1	Balkan-Carpathian	Bulgaria, Serbia, Romania	568.00	558.00	563.00			
1	Purtuniq 1	Canada	2000.00	1960.00	1980.00			
1	Purtuniq 2	Canada	2000.00	1960.00	1980.00			
1	Purtuniq #3	Canada	2000.00	1960.00	1980.00			
1	Outokumpu	Finland	1970.00	1970.00	1970.00			
1	Jormua	Finland	1956.00	1950.00	1953.00			
1	Dongwanzi	China	2507.20	2502.80	2505.00			
1	Kunlun	China	900.00	543.00	721.50			
1	Itmurunda zone	Russia	820.00	775.00	797.50			
1	Northern Baykal	Russia	1400.00	800.00	1100.00			
1	Sharyzhalgay	Russia	2500.00	2400.00	2450.00			
1	Fawakhir	Egypt	900.00	800.00	850.00	800.00	780.00	790.00
1	Wadi Ghadir	Egypt	765.00	726.00	745.50	746.00	727.00	736.50
1	Quift Quseir	Egypt	810.00	790.00	800.00	800.00	780.00	790.00
1	Quseir Marsa Alam	Egypt	800.00	780.00	790.00	800.00	780.00	790.00
1	Meatiq Dome	Egypt	596.00	594.00	595.00	589.00	587.00	588.00
1	Wadi Hafafit	Egypt	900.00	700.00	800.00			
1	Wadi Lawi - Wadi Lawai	Egypt	900.00	543.00	721.50			
1	Wadi 'Allaqi-Heiani	Egypt	710.00	710.00	710.00			
1	Yubdo	Ethiopia			0.00	800.00	800.00	800.00
1	Abdola-Moyale	Ethiopia-Kenya	700.00	700.00	700.00			
1	Baragoi	Kenya	796.00	796.00	796.00	609.00	609.00	609.00
1	Halaban-Ithilal	Saudi Arabia	699.00	689.00	694.00	690.00	543.00	616.50
1	Jabal Wask-Jabal Ess	Saudi Arabia	834.00	810.00	822.00	782.00	767.00	774.50
1	Bir Umq	Saudi Arabia	848.00	828.00	838.00	720.00	640.00	680.00
1	Al Amar	Saudi Arabia	702.00	686.00	694.00	663.00	660.00	661.50
1	Onib & Gerf	Sudan	822.00	794.00	808.00	762.00	720.00	741.00
1	Nakasib	Sudan	840.00	760.00	800.00	760.00	700.00	730.00
1	Onib Sol Hamed	Sudan	735.00	735.00	735.00			

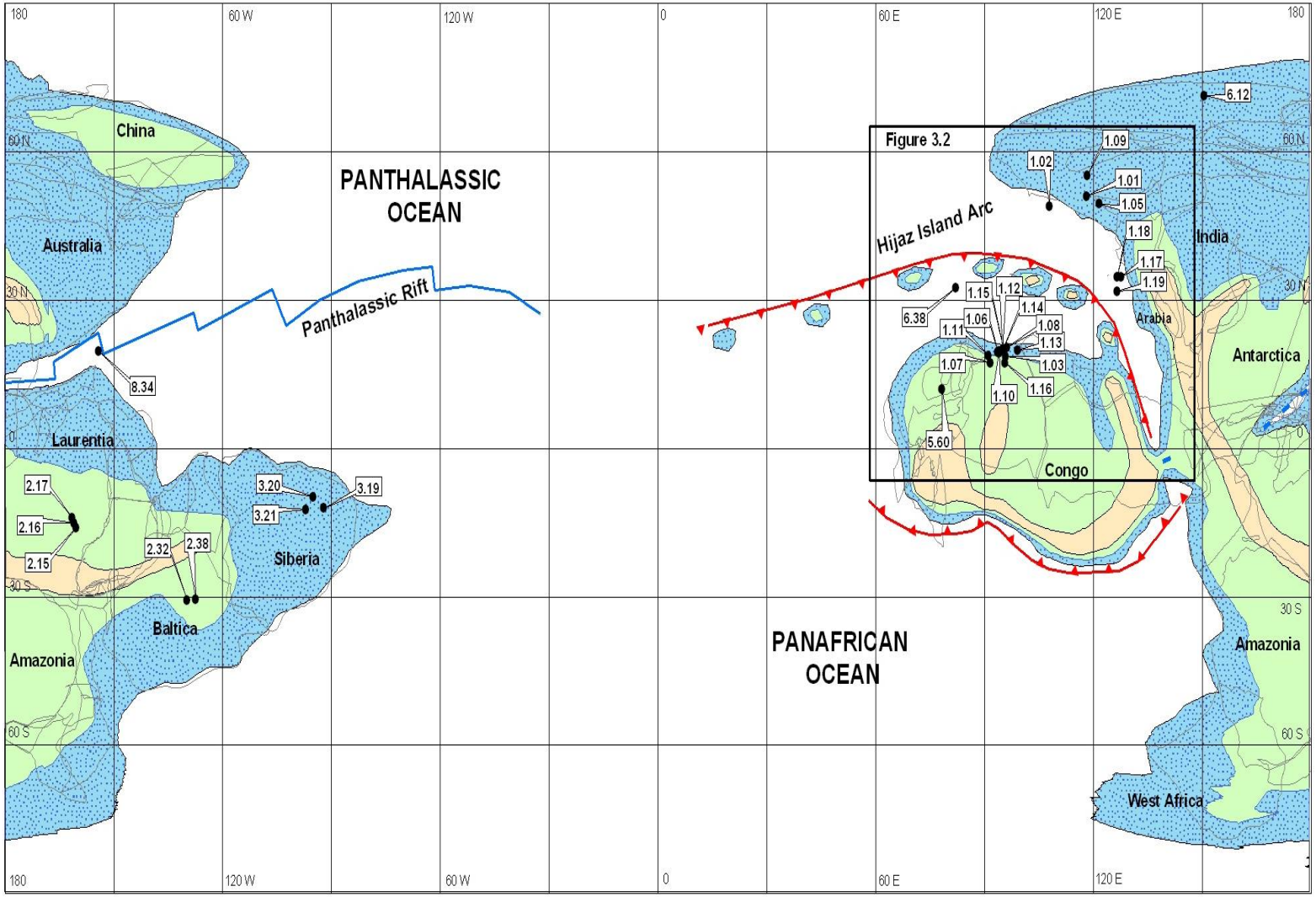

Fig 3.2 Proterozoic ophiolite locations plotted on a 750 Ma paleogeographic reconstruction (Scotese, 2004)

The Halaban-Ithilal ophiolite complex [1.01] part of the Al-Amar-Idas suture in Saudi Arabia formed in the Late Proterozoic between 699 and 689 Ma (Coleman, 1984; Stacey & Stoeser, 1983). This complete complex is thought to be a continental accretion of an island arc onto the Arabian plate around 690 to 543 Ma (Coleman, 1984).

Figure 3.3 shows many of the ophiolites in the Arabian-Congo area. On the western coast of Saudi Arabia, the Jabal Wask-Jabal Ess ophiolite [1.02] formed around 834 to 810 Ma and obducted onto the Arabian continental margin around 782 to 767 Ma. The tectonic environment for this complex is an intra-ocean system related to island arcs and marginal basins (Kemp et al., 1980; Coleman, 1984).

Blasband et al., (1997; 2000) and Berhe, (1990) describe the Al Amar ophiolite [1.09] in Saudi Arabia which falls along the Al Amar suture zone. This ophiolite is a complete ophiolitic sequence, with a completeness score of 6, forming around 702 to 686 Ma and was obducted onto the Arabian plate around 663 to 660 Ma.

Bir Umq [1.05], another Late Proterozoic ophiolite in northwest Saudi Arabia, formed around 848 to 828 Ma and was obducted around 720 to 640 Ma. This virtually complete ophiolite sequence, with a completeness score of 5, is part of the Proterozoic cratonization and backarc basin of the Arabian plate (Kemp et al., 1980; Al-Shanti & Roobol, 1979; Coleman, 1984).

Fawakhir, an Egyptian ophiolite complex [1.03], also formed during the Late Proterozoic around 900 to 800 Ma. It was emplaced onto the continental margin shortly after formation around 800 to 780 Ma (El-Sayed et al., 1999; Coleman, 1984).

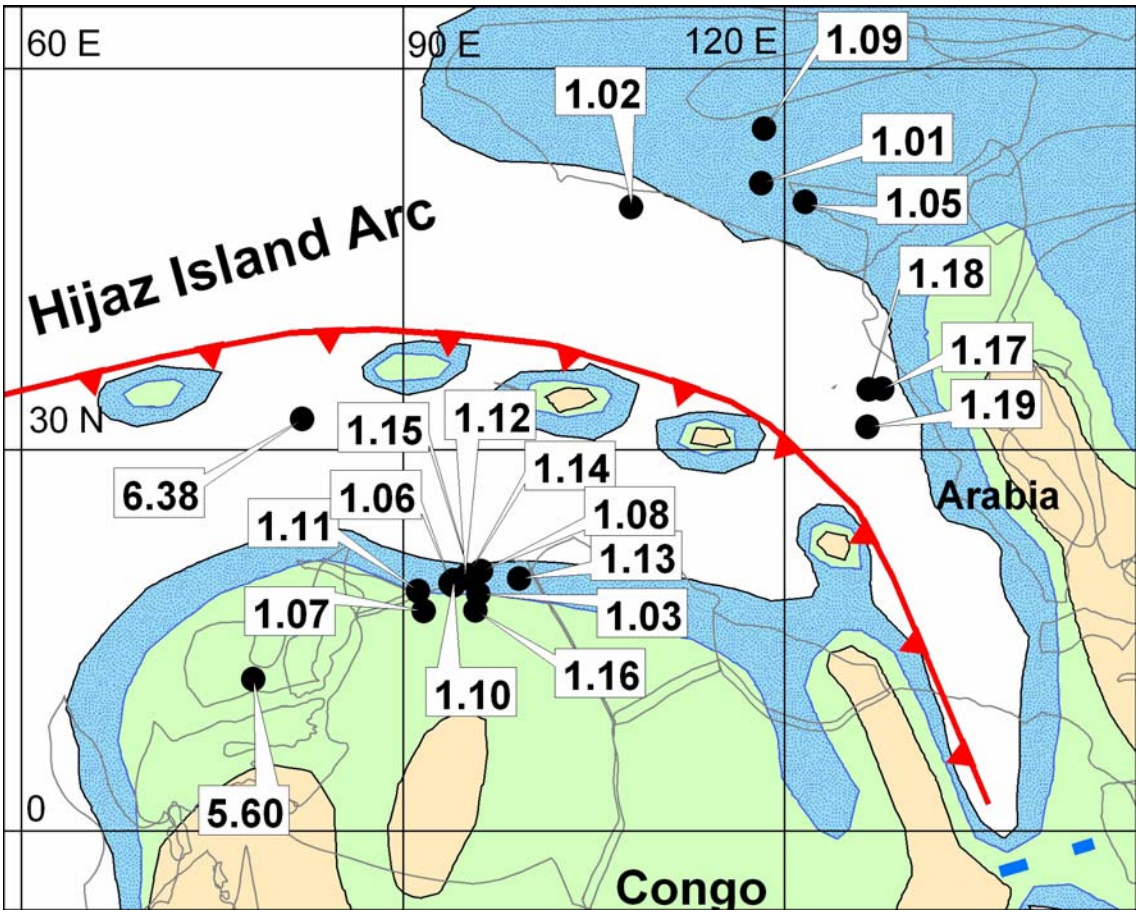

Figure 3.3 Proterozoic ophiolite locations along the Congo and Arabian region plotted on a 750 Ma paleogeographic reconstruction (Scotese, 2004)

Wadi Ghadir [1.06], another Egyptian ophiolite currently in the Central Eastern Desert, formed around 765 to 726 Ma. This ophiolite was obducted around 746 to 727 Ma onto the continental margin of the east African plate (Kröner, 1985, 1992; El Akhal, 1993; Blasband et al., 2000).

Blasband et al. (1997; 2000) along with Pallister et al. (1988) and Claesson et al. (1984) also report that the Quift Quseir Ophiolite [1.07] in Egypt was formed around

800 ±10 Ma. This ophiolite was emplaced shortly after forming at 790 ±10 Ma along the eastern side of the African plate.

Ries et al. (1983) describe the Quseir Marsa Alam ophiolite [1.10] in the Central Eastern Desert of Egypt as mostly complex suite forming around 800 to 780 Ma as part of the African plate. Although the emplacement age is not implicitly known, it can be inferred that it was emplaced in the Late Precambrian (Ries et al. 1983; Blasband et al., 2000).

The Meatiq Dome ophiolite [1.11] in Egypt formed around 589 to 587 Ma. It was emplaced sometime during the Late Precambrian onto the east African continental margin (Sturchio et al., 1983; Loizenbauer et al., 2001; Greiling et al., 1994; Blasband et al., 1997, 2000).

The Wadi Hafafit ophiolite [1.12] in Egypt is known to be part of an island arc system and formed around 800 ±100 Ma. The emplacement age is not known but can be inferred to have obducted onto the African continental margin in the Late Proterozoic (Greiling et al., 1994; Blasband et al., 1997; Blasband et al., 2000).

The Wadi Lawi - Wadi Lawai ophiolite [1.15], part of the Wadi-Lawai Ophiolite Mélange in Egypt, is a rather poorly understood sequence thought to be formed in the Late Proterozoic around 900 to 543 Ma. It is thought to have formed as a result of the Hijaz island arc and to have been obducted onto the African plate in the Late Precambrian (Ahmed et al., 2001).

Another Egyptian ophiolite is the Wadi 'Allaqi-Heiani complex [1.16] which lies in the southern regions of Egypt. Ren and Abdelsalam (2005) report it to have

formed around 710 Ma and was obducted onto the continental margin sometime during the Late Precambrian.

The Onib and Gerf ophiolite [1.08] in Sudan along the Onib and Gerf suture zone are dated with formation age of around 822 to 794 Ma. It was obducted onto the African plate around 762 to 720 Ma (Stern et al., 1990; Kröner et al., 1987; Blasband et al., 2000).

Another ophiolite in Sudan, the Nakasib ophiolite [1.13], formed along the Nakasib suture in an arc – arc environment around 840 to 760 Ma. It was emplaced onto the continental margin with arc – continental collision around 760 to 700 Ma (Abdelsalam, 1994; Abdelsalam & Stern, 1996; Schandelmeier et al., 1994; Blasband et al., 2000).

The Onib Sol Hamed ophiolite complex [1.14], also in Sudan, formed in a back arc basin around 735 Ma. It is thought to have emplaced during the Late Cambrian due to arc-arc collision (Bishady et al., 1994; Shackleton, 1994).

The Baragoi complex [1.19], a complete and typical Penrose sequence in Kenya, formed at around 796 Ma. It was emplaced around 609 Ma and is thought to have a tectonic affinity for mid-ocean ridge and a suprasubduction zone based on the ophiolite complex. This sequence reflects crustal shortening in Sudan and Kenya and shows evidence of nappe-folds and thrusts as part of the emplacement structure (Berhe, 1990).

The Abdola-Moyale ophiolite complex [1.17] in Kenya and Ethiopia is a mostly complete ophiolite sequence, a completeness score of 5, with the formation dating

around 700 Ma. It is thought to be a part of the mid-ocean ridge or island arc accretion (Berhe, 1990).

The Yubdo Complex [1.18] in Ethiopia yields an emplacement age of 800 Ma. Though the formation age is not known, it is reported to show evidence of arc-arc collision (Berhe, 1990).

In the Balkans, the Balkan-Carpathian ophiolite [5.60] outcrops in parts of Bulgaria, Serbia, and Romania and has been reported to have a formation age of about 568 to 558 Ma forming along a mid-ocean ridge. Although an exact emplacement age is not known, it is thought to have been emplaced along the Tracian suture during the Late Precambrian. Along with many of the other European ophiolites in places such as the Eastern Alps, Turkey, and the Arabian-Nubian shield, it has been proposed that these sequences represent the Proto-Tethys (Savov, 1999; Savov et al., 2001).

3.1.1.2 Laurentian and Siberian Ophiolites

The Purtuniq complex [2.15-2.17] in northern Quebec, Canada is composed of three ophiolites that date from the early Proterozoic (2000 to 1960 Ma). More research is needed to more accurately pinpoint the age of emplacement for this ophiolite. Scientists agree that it was emplaced sometime during the Late Precambrian (Scott et al., 1991; 1992).

The Outokumpu complex [2.32] in eastern Finland is another Proterozoic ophiolite with a formation date of around 1970 Ma and is possibly of mid-ocean origin. This ophiolite is also thought to have been emplaced during the Late Precambrian

although a precise emplacement age is not known (Anderson et al., 1990; Zhou, 1996; Koistinen, 1981).

The Jormua ophiolite [2.38] in northeastern Finland is thought to have formed along a slow spreading center around 1956 to 1950 Ma. The formation age of the ophiolite was obtained by using U-Pb zircon dating techniques with a sample of the gabbroic rock that cut across the mantle tectonite. The emplacement age is not known, but Furnes et al. (2005) suggest that is was obducted sometime during the Late Precambrian. (Peltonen et al., 2003).

There are a few Precambrian ophiolites from Russia. In the northern Baykal (also known as Baikal) Mountains [3.20], Grudinin and Demin (1994) report ophiolites of Riphean age (1400 to 800 Ma). In the southwest Baykal Mountains, the Sharyzhalgay Block [3.21] yields somewhat questionable Proterozoic ages for ophiolites dated at 2500 to 2400 Ma (Gornova & Petrova, 1999). The Itmurunda zone [3.19], part of southern Kazakhstan, yields zircon formation ages of around 820 to 775 Ma. Although the exact emplacement age is not well understood, it is thought that this ophiolite was part of the extensive rifting events in Siberia (Avdeev, 1984; Koralenko et al., 1994).

3.1.1.3 Other Notable Late Proterozoic Ophiolites

The Dongwanzi ophiolite [6.12] lies just north of the Great Wall in the North China Craton near Quinlong (Li et al., 2002). This ophiolite is Archean in age as reported by Kusky et al. (2001) dating to around 2505±2.2 Ma. This extremely old

ophiolite, controversial as mentioned previously, is reported to be part of a dismembered ophiolite in the greenstone belt by Kusky et al. (2001) and is corroborated by Li et al. (2000).

In eastern China, a few ophiolites are reported from the Kunlun Mountains. The ophiolite sequence [6.38] along the eastern section of the mountains has an age of formation in the Late Proterozoic around 900 to 543 Ma. As the orogeny continued northward, other ophiolites were formed and emplaced at younger geologic times (Laurent-Charvet et al., 2005).

In Marlborough, Australia near the northeastern coastline, an ophiolite sequence [8.34] with an age of formation of 560 Ma has been reported (Spaggiari et al., 2004). Spaggiari et al. suggest that it may have formed along a spreading ridge and was emplaced along the continental margin during the latest Precambrian (Spaggiari et al., 2004; Bruce & Niu, 2000).

3.1.2 Proterozoic Tectonics

After the break up of Rodinia in the Late Proterozoic (750 Ma), new ocean basins were formed and old ocean basins began to close providing for both the formation and emplacement of ophiolites. Many locations in the Arabian-Nubian Shield [1.01, 1.02, 1.03, 1.05 – 1.19, 5.60, 6.38, and likely 6.12] represent the closing ocean and back arc basins that were thrust onto adjacent continental margins (Kröner et al., 1992). Many of the Egyptian-Arabian ophiolites were likely emplaced along the Hijaz suture between the Arabian-Nubian Shield and East Gondwana around 800 to 700

Ma (Ren & Abdelsalam, 2005). In the Precambrian as Siberia, Laurentia, and Baltica rifted apart, sea floor spreading created new ocean floor which would later become ophiolites [2.15, 2.16, 2.17, 2.32, 2.38, 3.19, 3.20, and 3.21] (Laurent, 1980). As the Panthalassic Ocean rifted Laurentia from Australia and Antarctica, the Marlborough ophiolite [8.34] formed (Spaggiari et al., 2004; Bruce & Niu, 2000).

Undoubtedly, Ren and Abdelsalam's (2005) model of the tectonic evolution of this area during the Precambrian is not the only accepted hypothesis. Claesson et al. (1984) believe there is Pb isotopic data to provide evidence for repeated Archean rifting events that yielded formation and closure of several small ocean basins (Berhe, 1990).

3.2 Cambrian ~545 – 500 Ma

3.2.1 Cambrian Ophiolites

The Cambrian was a relatively quiet time for the production and emplacement of ophiolites. Figure 3.4 and Table 3.2 depict the two locations identified in this study. Further research is still needed in this time period to uncover any other ophiolite localities during the Cambrian.

The Primorye ophiolite [3.17] currently sits on the border of Manchuria and eastern Siberia along the remnants of the Sikhote – Alin mountains. Vyosotsky (1994) reports the ophiolite was formed in the early to middle Cambrian (543 – 512 Ma) and implies it was emplaced shortly after its origin (Vyosotsky, 1994; Ishiwatari & Tsujimori, 2003).

The Tyennan-Delamerian ophiolite [8.35] lies on the northwestern outskirts of the Great Diving Range in southwest Australia. The Great Diving Range, part of the Tasman Fold Belt, is a series of plateaus and mountains that roughly parallels the eastern and southeastern coast of Australia. This ophiolite is reported to have formed between 530 and 515 Ma in a forearc setting above an island arc subduction zone. The emplacement of the Tyennan-Delamerian ophiolite is thought to have been emplaced sometime in the mid to late Cambrian after 515 Ma (Audet et al., 2004; Spaggiari et al., 2004).

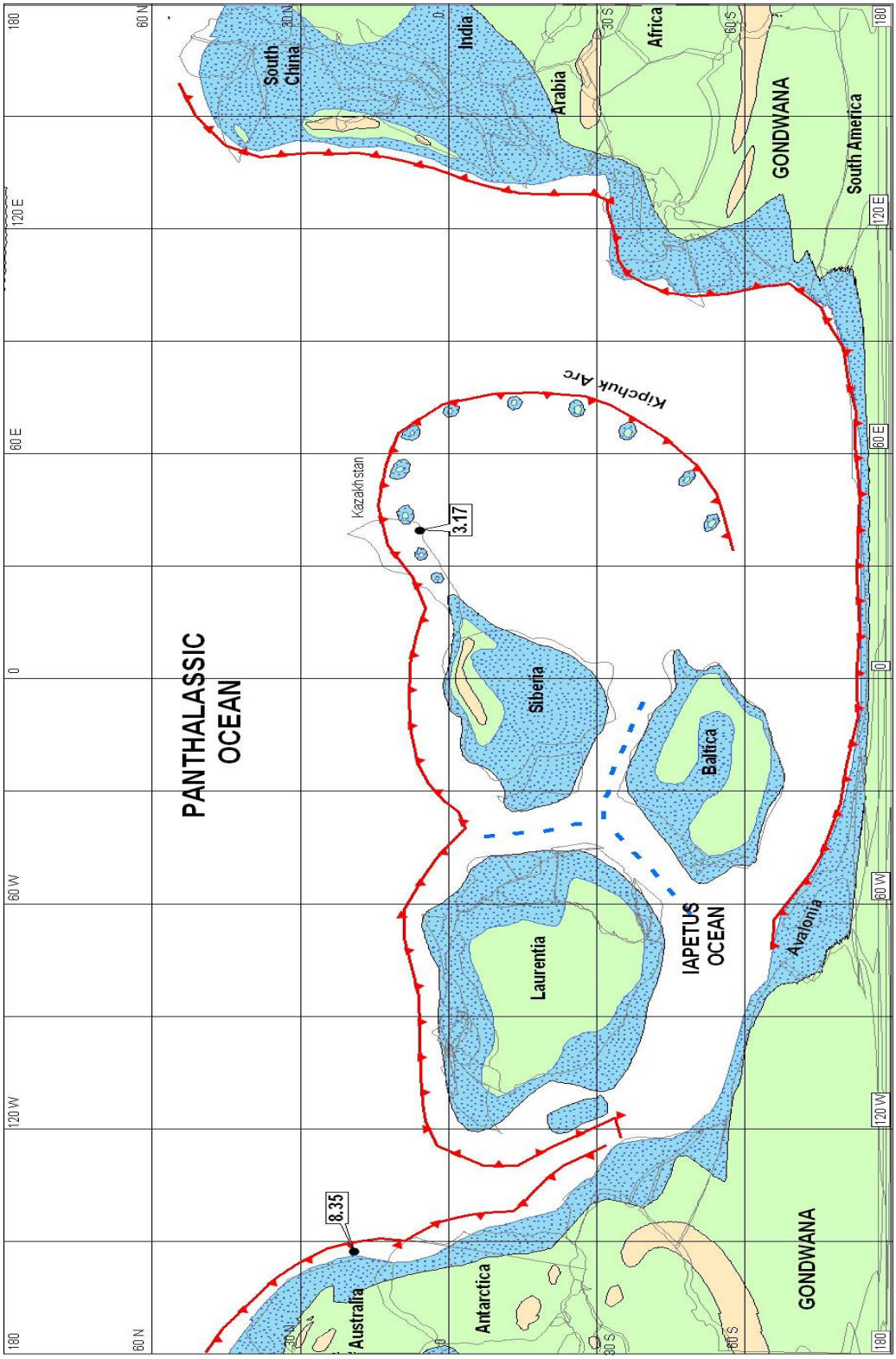

Figure 3.4 Cambrian ophiolite locations plotted on a 520 Ma paleogeographic reconstruction (Scotese, 2004)

Table 3.2 Cambrian Ophiolites

				Age of Formation			Age of Obduction		
Ophiolite ID#	Map #	Name	Country	Old Age	Young Age	Best Estimate	Old Age	Young Age	Best Estimate
8.35	2	Tyennan - Delamerian	Australia	530.00	515.00	522.50	515.00	515.00	515.00
3.17	2	Primorye	Russia	543.00	512.00	527.50			

3.2.2 Cambrian Tectonics

The Tyennan – Delamerian ophiolite probably formed in an early Cambrian back arc basin along the eastern margin of the Australia craton. The ophiolite was obducted soon after it was formed, presumably as a consequence of the collapse of the back arc basin. This event produced some uplift from repeated fault block reactivation and allowed for basement rocks to be exhumed (Comacho et al., 2002).

The Primorye ophiolite [3.17] is juxtaposed between younger (Late Paleozoic to Early Mesozoic) ophiolitic sequences. Recent research suggests that the ophiolites formed within a collisional zone along the eastern extension of the Kipchuk arc. This region of eastern Mongolia consists of the island arc, back arc basin material, and accreted crustal and mantle sequences (Ishiwatari & Tsujimori, 2003).

3.3 Early Ordovician to Late Devonian ~500 – 360 Ma

3.3.1 Early Ordovician to Late Devonian Ophiolites

The thirty-seven ophiolites described in this section are located in two principal areas; the Laurentian borders and the Urals. These ophiolites, shown in Figure 3.5, are emplaced as a result of tectonic events along regions of the circum-Iapetus, the Urals, Russia, Australia, Canada, and Europe.

3.3.1.1 Ordovician to Devonian Ophiolites of the Urals

Ophiolites of the Urals were emplaced during the Ordovician to Devonian. In the southern Urals several complete ophiolitic sequences make up an allocthonous ophiolitic belt. This area represents the collision zone between the Russian platform to the west and the Uralides to the east. The ages given by Savelieva et al. (1997) come from conodonts that occur in the lavas and sediments intercalated with the ophiolites.

The somewhat incomplete sequence of the Nurali ophiolite [3.01] is thought to have formed at 472 to 443 Ma. The emplacement of the Nurali ophiolite occurred between 410 and 348 Ma. This ophiolite is closely related to the Main Uralian Fault or suture zone (Savelieva et al., 1997; Pertsev et al., 1997; Ruzhentsev & Samygin, 1979).

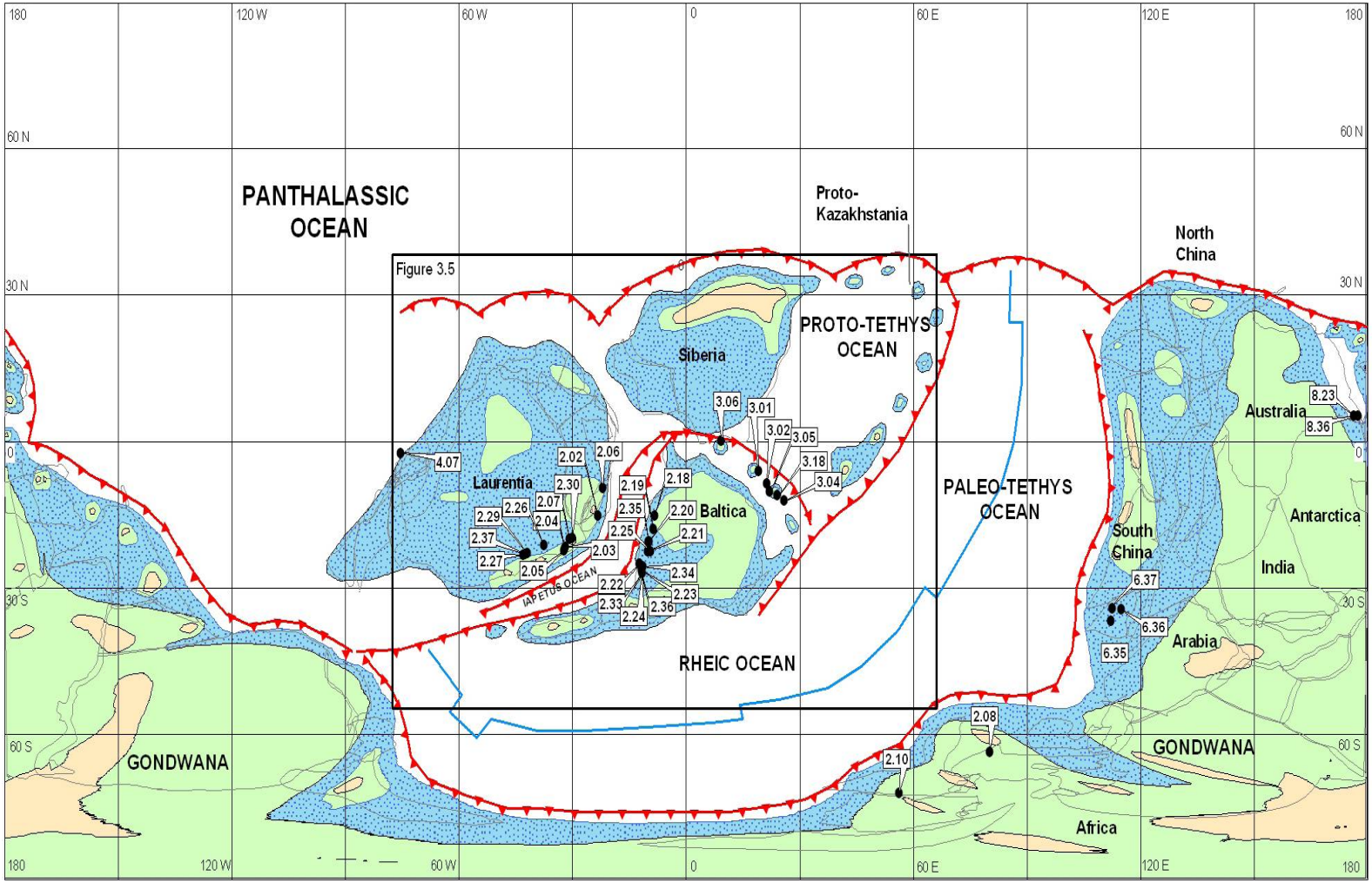

Figure 3.5 Early Ordovician to Late Devonian ophiolite locations plotted on a 440 Ma paleogeographic reconstruction (Scotese, 2004)

Table 3.3 Ordovician, Silurian, and Devonian Ophiolites

				Age of Formation			Age of Obduction		
Ophiolite ID#	Map #	Name	Country	Old Age	Young Age	Best Estimate	Old Age	Young Age	Best Estimate
2.18	3	Scandinavian Caledonides 1	Norway	443.00	443.00	443.00	443.00	428.00	435.50
2.19	3	Scandinavian Caledonides 2	Norway	437.00	437.00	437.00	443.00	428.00	435.50
2.20	3	Scandinavian Caledonides 3	Norway	497.00	497.00	497.00	443.00	428.00	435.50
2.21	3	Scandinavian Caledonides 4	Norway	478.00	478.00	478.00	443.00	428.00	435.50
2.22	3	Scandinavian Caledonides 5	Norway	443.00	443.00	443.00	425.00	425.00	425.00
2.23	3	Scandinavian Caledonides 6	Norway	485.00	485.00	485.00	443.00	428.00	435.50
2.24	3	Scandinavian Caledonides 7	Norway	485.00	485.00	485.00	443.00	428.00	435.50
2.25	3	Scandinavian Caledonides 8	Norway	466.50	466.50	466.50	443.00	428.00	435.50
2.33	3	Karmøy	Norway	500.00	489.00	494.50			
2.34	3	Gullfjellet	Norway	492.00	486.00	489.00			
2.35	3	Leka	Norway	499.00	495.00	497.00			
2.36	3	Solund-Stavfjord	Norway	446.00	440.00	443.00	426.00	400.00	413.00
2.07	3	Hare Bay	Canada	488.00	479.00	483.50	471.80	464.00	467.90
2.26	3	Mt. Albert	Canada	460.00	456.00	458.00			
2.27	3	Mt. Orford	Canada	480.00	460.00	470.00			
2.29	3	Thetford Mines	Canada	494.00	478.00	486.00	482.00	472.00	477.00
2.30	3	St. Anthony	Canada	488.00	479.00	483.50	471.80	464.00	467.90
2.37	3	Asbestos	Canada	480.00	460.00	470.00	377.00	377.00	377.00
6.35	3	Hongguleleng	China	443.00	418.00	430.50			
6.36	3	Tianshan	China	443.00	418.00	430.50			
6.37	3	Mishigou	China	458.00	419.00	438.50	391.00	354.00	372.50
2.03	3	Bay of Islands 1	Newfoundland	515.00	475.00	495.00	485.00	454.00	469.50
2.04	3	Bay of Islands 2	Newfoundland	508.00	504.00	506.00	469.00	469.00	469.00
2.05	3	Bay of Islands 3	Newfoundland	489.00	486.00	487.50	469.00	463.00	466.00
2.10	3	Limousin	France	440.00	400.00	420.00			
2.08	3	Hoch Grossen	Austria	545.00	455.00	500.00			
3.01	3	Nurali	Russia	472.00	443.00	457.50	400.00	400.00	400.00
3.02	3	Mindyak	Russia	415.00	410.00	412.50			
3.04	3	Kempersay Massif	Russia	470.00	428.00	449.00	423.00	391.00	407.00
3.05	3	Sakmara Massif	Russia	490.00	470.00	480.00	428.00	391.00	409.50
3.06	3	Voykar	Russia	417.00	391.00	404.00	391.00	380.00	385.50
3.18	3	Khabarny	Russia	490.00	430.00	460.00			
2.02	3	Ballantrae	Scotland	487.00	479.00	483.00	482.00	474.00	478.00
2.06	3	Gibbs Islands	Scotland	479.00	465.00	472.00			
8.36	3	Lachlan	Australia	505.00	495.00	500.00			
8.23	3	Tasmania	Tasmania	512.00	490.00	501.00	500.00	490.00	495.00
4.07	3	Trinity	USA	480.00	450.00	465.00	470.00	443.00	456.50

The more complete section of the Mindyak ophiolite [3.02] in the Southern Urals formed around 415 to 410 Ma. Savelieva et al. (1997) and Ruzhentsev & Samygin (1979) suggest that the ophiolite was emplaced between 410 and 348 Ma. This ophiolite is part of the Serpentinite Mélange zone on the Eastern European paleocontinental margin (Pertsev et al. 1997).

The Kempersay Massif [3.04] in the Urals consists of ophiolitic material formed at around 470 to 428 Ma. Like the Mindyak ophiolite, it is reported to have been emplaced onto the Russian margin between 410 and 348 Ma (Savelieva et al., 1997; Ruzhentsev & Samygin, 1979).

Voykar [3.06] is another Russian Uralide complex that has a formation date of 417 to 391 Ma. It is reported to have been emplacement at around 391 to 380 Ma during an early phase of Mountain building in the northern Urals (Saveliev et al., 1999; Sharkov et al., 1999).

The Khabarny ophiolite [3.18] in the southern Urals of Russia is a complete ophiolitic sequence formed around 490 to 430 Ma (Savelieva et al., 1997). The Sakmara complex [3.05] also in the Urals, formed at around 490 to 470 Ma. The emplacement for Sakmara dated between 410 and 348 Ma. All of the ophiolites in this Uralide belt seem to have formed in the Early to middle Ordovician (490 – 430 Ma) and were obducted in the Devonian and Early Carboniferous (410 -348 Ma) (Savelieva et al., 1997; Ruzhentsev & Samygin, 1979).

3.3.1.2 Ophiolites of the Iapetus Ocean

Ophiolites are found on both sides of the Iapetus Ocean, Figure 3.6. On the east coast of Iapetus, ophiolites were emplaced along the length of the Scandinavian Caledonides as a result of several island arcs forming above eastward and westward dipping subduction zones. These ophiolites likely represent remnants of those island arcs and the ocean basins between them (Furnes et al., 2003).

Solund-Stavfjord complex [2.36] in Norway formed between 495 and 440 Ma. The area is suspected to be an island arc subduction zone that was obducted during the closure of the Iapetus Ocean (Furnes et al, 2003; Andersen et al., 1990).

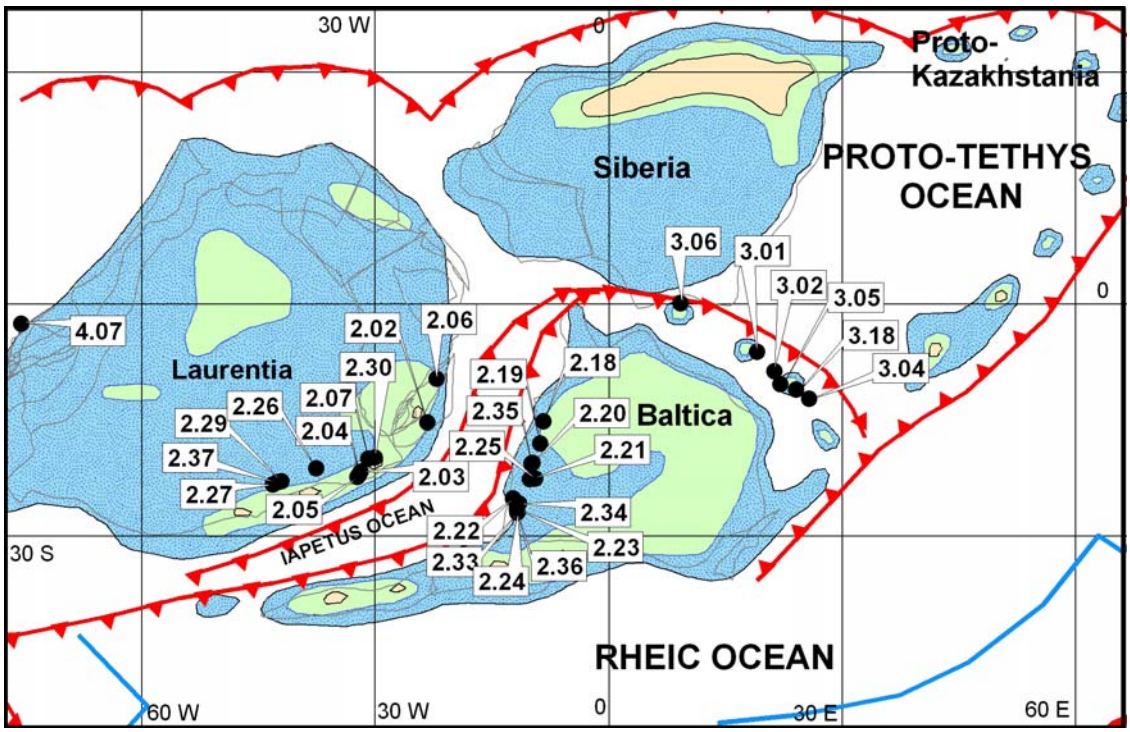

Figure 3.6 Laurentian, Baltic, and Siberian ophiolites from the Ordovician to Devonian plotted on a 440 Ma paleogeographic reconstruction (Scotese, 2004)

The Karmøy ophiolite [2.33], also in Norway, formed between 495 and 440 Ma. This ophiolite is also thought to be a result of the rifting of Laurentia and Baltica. It was emplaced during the closure of the Iapetus as portions of the down going slab of Baltica were accreted in the late Silurian (Andersen et al., 1990; Zhou, 1996). The Leka ophiolite [2.35] along with the Gullfjellet ophiolite [2.34] is part of the Sunnfjord Mélange in Norway (Prestvik, 1980). These ophiolites have oceanic lithosphere, which formed between 495 and 440 Ma along the Iapetus mid-ocean ridge (Andersen et al., 1990; Boyle, 1980; Mason, 1980; Pedersen & Malpas, 1984; Sturt et al., 1979).

The Scandinavian Caledonides in Norway have many ophiolites [2.18–2.25] that document the opening during the early Paleozoic and closure of the Iapetus Ocean during the Late Silurian. The formation ages range from 497 to 437 Ma and emplacement ages range from 436 to 425 Ma. All of these outcrops appear to be part of the Solund-Stavfjord Complex and are overlain by pelagic sediments from the Herland group (Sturt et al., 1984; Sturt & Roberts, 1991; Furnes et al., 2001; Furnes et al., 1982; Andersen et al., 1984).

The Mt. Orford [2.27] Canadian ophiolite formed as part of Laurentia. This ophiolite is reported to have a formation age of around 480 to 450 Ma and was emplaced as the Iapetus Ocean basin closed (Van Staal, 2005; Dunning et al., 1986; Dunning & Krough 1985; Lux, 1986; Coish & Sinton, 1992). Thetford Mines ophiolite [2.29] also formed as part of Laurentia. The Thetford Mines ophiolite formed around 480 to 450 Ma and is thought to have been emplaced as a result of the basin closure (Feininger, 1981; Van Staal, 2005; Dunning et al., 1986; Lux, 1986; Schroetter et al.,

2005; Coish & Sinton, 1992). The Asbestos complex [2.37], near the Thetford Mines, has a formation age around 480 to 460 Ma and an emplacement age of 377 Ma based on (Van Staal, 2005).

Mt. Albert [2.26] ophiolite located in the Gaspé Peninsula of Quebec, Canada formed as part of Laurentia. This sequence is dated to have formed around 480 to 450 Ma (Dunning et al., 1986; Lux, 1986; MacGregor et al., 1979; Gagnon & Jamieson, 1985; Coish & Sinton, 1992).

Eastern Canada has another suite of ophiolites in the Bay of Islands area. Elthon, et al. (1982) notes three ophiolite sections [2.03-2.05], which are part of the Lewis Hills massif as tectonically associated with mid-ocean ridge systems and date formation between 506 and 488 Ma. Obduction dates show to be Early Ordovician, around 470 to 466 Ma (Girardeau & Mevel, 1982; Dallmeyer & Williams 1975; McCaig, 1983; Suhr & Cawood, 2001; Casey & Dewey, 1984).

The St. Anthony complex [2.30] in Canada formed around 488 to 479 Ma. This ophiolite was obducted onto the North American continental margin at about 472 to 464 Ma. This ophiolite is also thought to be a result of the Northern Appalachian orogeny as the Iapetus Ocean basin closed (Girardeau & Nicolas, 1981; Jamieson, 1980).

The Hare Bay ophiolite [2.07] complex in Newfoundland was formed in an arc or ocean floor around 488 to 479 Ma. This ophiolite was obducted around 472 to 464 Ma as a result of the closure of Iapetus and emplacement onto the continental margin (Dunning & Krough, 1985; Talkington and Malpas, 1980; Malpas et al., 1973; Cawood, 1989).

The Ballantrae Complex [2.02] in Southwest Scotland formed in an arc and/or ocean floor environment around 487 to 479 Ma. It was emplaced around 482 to 474 Ma along the continental margin (Bluck et al., 1980; Thirwall & Bluck, 1984). Gibbs Island ophiolite complex [2.06] on the Shetland Islands of Scotland formed around 479 to 465 Ma along the mid-ocean ridge (Spray, 1984; DeWit et al., 1977).

3.3.1.3 Other Notable Ophiolites of the Ordovician to Devonian

Austria's Hochgrössen ophiolite [2.08] has a formation date around 545 to 455 Ma. This ophiolite is thought to be part of the Speik Complex (east of the Tauern Window), which is thought to be a fragment of the Variscan oceanic lithosphere subducted under Baltica (Ageed et al., 1980; Crowley et al., 2000; Faryad and Hoinkes, 2004).

The Limousin ophiolite [2.10] in the western French Massif dates from Late Ordovician to Early Silurian. This ophiolite location is found along the Bohemian massif embedded along the mélange (Crowley et al., 2000; Girardeau et al., 1986; Berger et al., 2005).

Laurent-Charvet et al., (2005) report several the Chinese Tianshan ophiolites resulting from the Bogeda Arc. Research has shown these ophiolites to be of Ordovician to Silurian age in the north and east and Permian in the southern regions. The Tianshan orogen separates the Tarim and Junngar blocks and with the ophiolitic rock sequences and their ages implies a northward deformation event in central Asia. The southern region Tianshan ophiolite [6.36] was formed between 443 and 418 Ma

and likely emplaced during the Permian. The Hongguleleng ophiolite [6.35] in Xinjiang Uygur eastern region of Tianshan, was formed in the Silurian around 443 and 418. The ophiolite was likely emplaced during the Permian as a result of multiple accretions onto the Asian continental margin North of Paleo-Tethys (Peng et al., 1995; Laurent-Charvet et al., 2005). The Mishigou ophiolite [6.37] the third and most central location for the Tianshan Range is the oldest ophiolite forming around 458 and 419 Ma. Laurent-Charvet et al., (2005) report it was likely emplaced in the Devonian to Early Carboniferous between 391 and 354 Ma.

The Tasmanian ophiolite [8.23] in the Dundas trough was formed sometime during the middle to Late Cambrian as part of a continental rift. This ophiolite was obducted in the Late Cambrian as a result of collision of the backarc along the continental margin (Brown et al., 1988).

The Lachlan ophiolite [8.36] in Australia also formed during the Late Cambrian around 505 to 495 Ma. Although no explicit emplacement age is known, obduction is thought to have resulted from forearc – backarc collapse (Fergusson & Coney, 1992; Audet et al., 2004).

The Trinity ophiolite [4.07] lies within the Klamath Mountains in Northern California. This sequence was thought to have formed between 480 and 450 Ma. Although no metamorphic sole age is known, it is thought to have been emplaced along the continental (Davies et al., 1965, Spray, 1984, Wright & Wyld, 1986, and Wallin et al., 1988).

3.3.2 Early Ordovician to Late Devonian Tectonics

Laurentia and Baltica rifted apart in the latest Precambrian generating ocean floor that would later become ophiolites as the Iapetus Ocean closed during the late Silurian to early Devonian. These ophiolites are preserved in the northern Appalachians and Scandinavian Caledonides [2.02 – 2.07, 2.26, 2.27, 2.29, 2.30, 2.37]. It is interpreted that the Avalonian terrane of the Canadian Appalachians was accreted to Laurentia after it rifted away from the North African margin of Gondwana (Furnes et al., 2001, Coish et al., 1991, and Van Staal, 2005). The Urals also began to form during this time interval. The ophiolite belt [2.18 – 2.25, 2.34 – 2.36, 3.01 – 3.06, and 3.18] likely formed as a consequence of island arc collision and the collapse of back arc basins along the eastern margin of the Russian platform (Baltica) (Furnes et al., 2001, Ivanov et al., 1990, and Van Staal, 2005).

As the Paleo-Tethys subducted along the northern and eastern coast of Gondwana a few other remnants of the ocean were preserved as ophiolites [2.08, 2.10, 6.35, 6.36, and 6.37]. Ophiolites along the eastern margin of Australia [8.23 and 8.36] were probably formed in marginal back arc basins that collapsed during the Tasman orogeny during the Silurian and Devonian (Fergusson & Coney, 1992; Audet et al., 2004).

3.4 Late Devonian to Early Carboniferous ~360 – 310 Ma

3.4.1 Late Devonian to Early Carboniferous Ophiolites

Although this time seems to be a tectonically quiet time period, there are a few ophiolites worth mentioning (Figure 3.8 and Table 3.4). In England, the Lizard ophiolite [2.11] was formed in a back arc basin during the Devonian (403 to 350 Ma). This ophiolite is reported by Clark et al. (1998) to be part of the Rhenohercynian zone of the External Variscides. It is thought to have been emplaced along the collision zone between Euramerica and North Africa during the early Carboniferous (377 to 337 Ma). Clark et al. (1998) used zircon U – Pb dating to corroborate previously published dates for the Lizard ophiolite (Green, 1964; Styles & Kirby, 1980; Clark et al., 1998; Barnes & Andrews, 1984).

The Munchberg Gneiss Complex [2.14] in Germany has a formation date of around 525 Ma. This ophiolite has an emplacement age of Famennian (about 380 to 336 Ma) and was likely formed near a slow spreading ridge and obducted during the collision of Euramerica and North Africa (Franke et al., 1993; Clark et al., 1998).

The Kraka ophiolite [3.03] in Russia formed during the Ordovician (490 to 417 Ma). The Kraka ophiolite is thought to be part of an allocthonous ophiolite belt in the Southern Uralides. It was emplaced along the southeast continental margin of the Russian platform in the Late Devonian between 348 and 410 Ma (Savelieva et al., 1997; Ruzhentsev & Samygin, 1979).

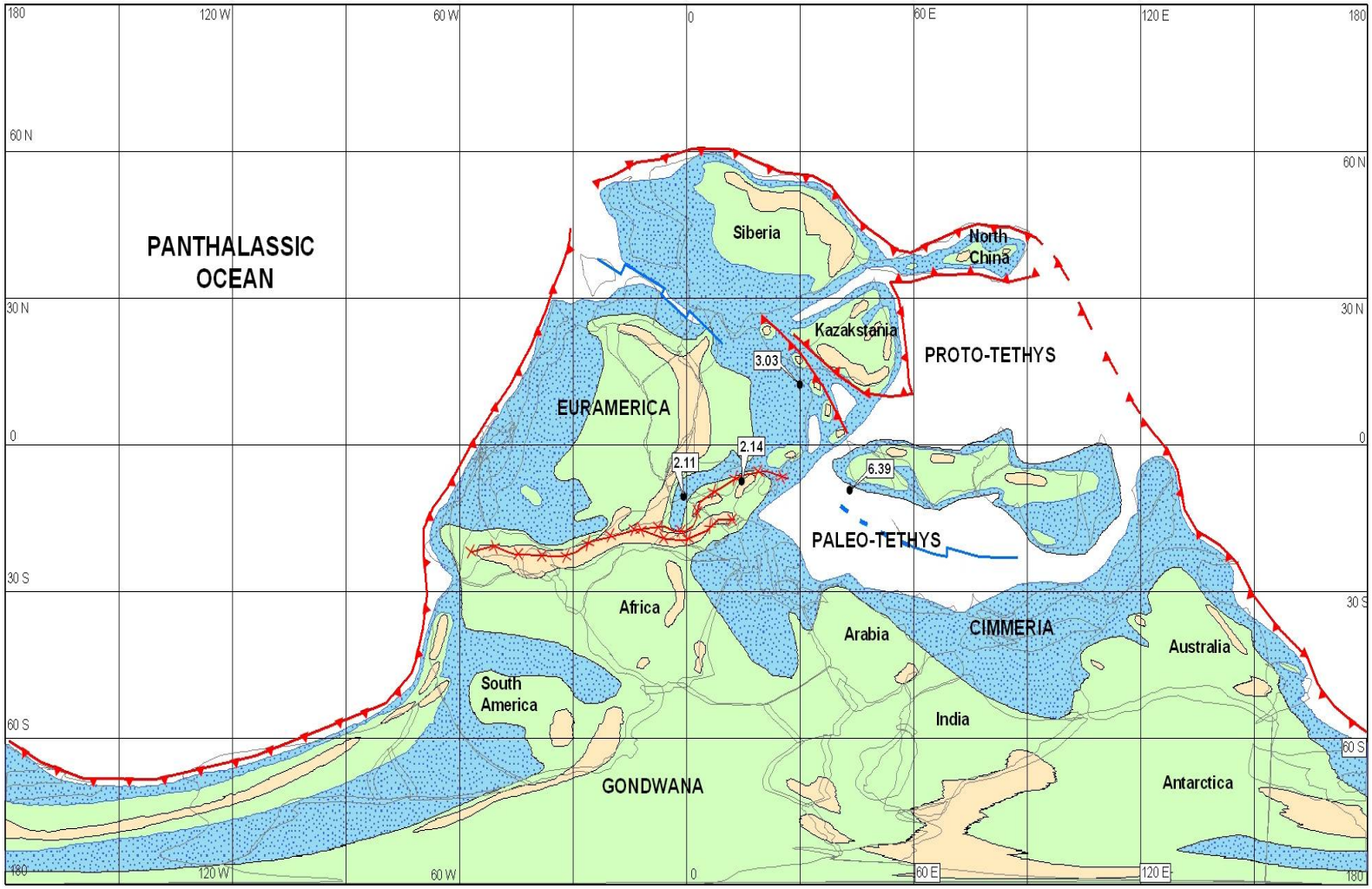

Figure 3.7 Late Devonian to Early Carboniferous ophiolite locations plotted on a 340 Ma paleogeographic reconstruction (Scotese, 2004)

Table 3.4 Early Carboniferous Ophiolites

				Age of Formation			Age of Obduction		
Ophiolite ID#	Map #	Name	Country	Old Age	Young Age	Best Estimate	Old Age	Young Age	Best Estimate
6.39	4	Kunlun	China	354.00	327.00	340.50			
2.11	4	Lizard	England	403.00	350.00	376.50	377.00	337.00	357.00
2.14	4	Munchberg	Germany	525.00	525.00	525.00	380.00	336.00	358.00
3.03	4	Kraka	Russia	490.00	417.00	453.50	370.00	327.00	348.50

In China's south Kunlun block, the northern section of ophiolite [6.39] formed around 354 to 327 Ma. This ophiolite probably formed in Paleo-Tethys Ocean that separated the Cathaysian continents of North and South China from the Cimmerian continents (Turkey, Iran, Afghanistan, Tibet, Lhasa, Burma, and Qiantang) that were adjacent to the Indo-Australian margin of northern Gondwana. Although no precise emplacement age is known, this ophiolite may have been emplaced during the Early Carboniferous orogenic event described by Laurent-Charvet et al., (2005) and Yuan et al. (2003).

3.4.2 Late Devonian to Early Carboniferous Tectonics

As Gondwana collided with Euramerica, the super continent of Pangea began to assemble. This collision is characterized by tectonic mélanges, and obducted ophiolites such as the Lizard complex [2.11] in southwestern England and the Munchberg site [2.14] in Germany (Clark et al., 1998).

Early and Middle Ordovician ophiolites (Kraka) that originally formed in volcanic back arc basins associated with the Magnitogorsk island arc, were emplaced during the late Devonian as the back arc basin collapsed against the eastern margin of

the Russian platform (Puchkov, 1997; Savelieva et al., 1997; Ruzhentsev & Samygin, 1979).

The Kunlun Range ophiolite [6.39] is interpreted to be part of the Tarim and Kunlun blocks (Yuan et al., 2003). This region may have undergone rifting during the separation of Cathaysia from Cimmeria (Laurent-Charvet et al., 2005).

3.5 Late Carboniferous to Permian ~310 – 250 Ma

3.5.1 Late Carboniferous to Permian Ophiolites

By the late Carboniferous – early Permian, the western half of Pangea had assembled (Figure 3.9). The seven ophiolites described in this section encircle Pangea and are part of the circum-Panthalassic subduction zone (Table 3.5).

3.5.1.1 Late Carboniferous to Permian Southwest Pacific Ophiolites

The Yarras ophiolite [8.09] in the New England Fold belt of Australia formed during the Late Devonian – Early Carboniferous (Aitchison et al., 1994) and was emplaced around 290 to 248 Ma (Offler & Shaw, 2006; Kawachi, 1991).

The Attunga ophiolite [8.10] in the Great Serpentine Belt of Australia (Peel-Manning fault) formed sometime during the Middle to Late Devonian. It was obducted sometime during the Permian as the Lachlan Fold Belt was overthrust with the New England fold belt during collision with the continental margin (Aitchison et al., 1994).

The Port Macquarie ophiolite [8.11], also in the Great Serpentine Belt of Australia, formed sometime between Middle to Late Devonian. This ophiolite is reported to be part of the serpentinite matrix mélange formed along the Peel-Manning fault system. The Port Macquarie ophiolite was obducted sometime during the Permian and appears to be a dismembered sequence (Aitchison et al., 1994).

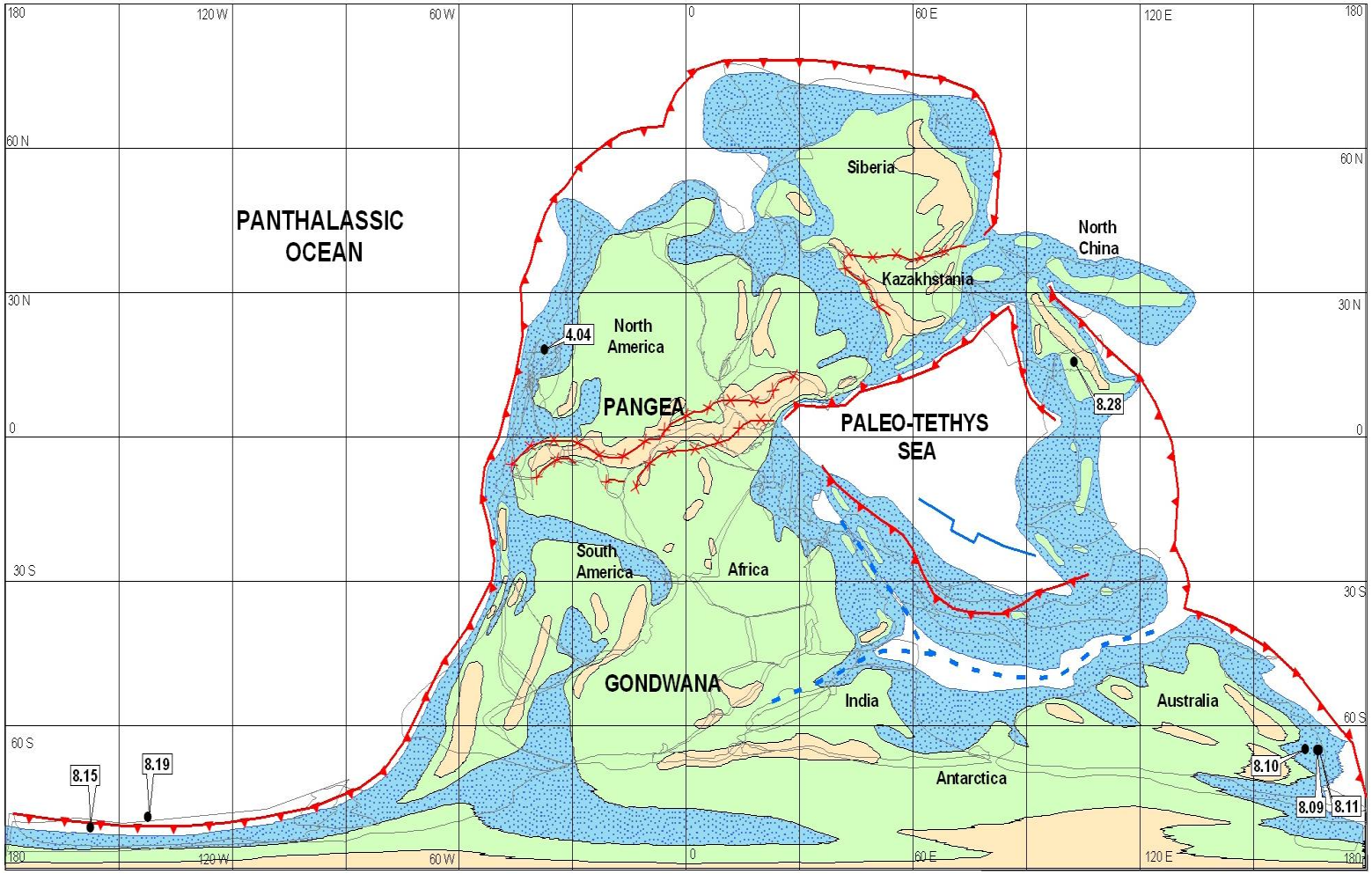

Figure 3.8 Late Carboniferous to Permian ophiolite locations plotted on a 280 Ma paleogeographic reconstruction (Scotese, 2004)

Table 3.5 Late Carboniferous to Permian Ophiolites

				Age of Formation			Age of Obduction		
Ophiolite ID#	**Map #**	**Name**	**Country**	**Old Age**	**Young Age**	**Best Estimate**	**Old Age**	**Young Age**	**Best Estimate**
8.09	5	Yarras	Australia	391.00	354.00	372.50	290.00	248.00	269.00
8.10	5	Attunga	Australia	391.00	290.00	340.50	290.00	248.00	269.00
8.11	5	Port Macquarie	Australia	370.00	323.00	346.50	290.00	248.00	269.00
8.28	5	Yakuno	Japan	426.00	409.00	417.50	287.00	280.00	283.50
8.15	5	Dun Mt	New Zealand	290.00	256.00	273.00	256.00	248.00	252.00
8.19	5	Red Hills	New Zealand	280.00	280.00	280.00	256.00	248.00	252.00
4.04	5	Canyon Mt	USA	278.00	265.50	271.75			

The Dun Mountain ophiolite [8.15] in New Zealand includes the Lee River Group and Red Hills ultramafic body, each having distinct tectonic affinities. This sequence was formed between 290 and 256 Ma (Late Carboniferous – Early Devonian) along a mid-ocean ridge or back-arc basin and was emplaced during the late Permian (256 and 248 Ma) (Coombs et al., 1976).

The Red Hills ultramafic complex [8.19], also part of the Dun Mountain ophiolite and Lee River Group in New Zealand, was formed around 280 Ma (Early Permian). This ophiolite sequence was emplaced during the Late Permian in an island arc environment (Sano et al., 1997; Coombs et al., 1976).

Herzig et al. (1997) reports that the Yakuno ophiolite [8.28] in Japan formed between 426 and 409 Ma (Silurian – early Devonian) based on Rb-Sr, K-Ar, and Sm-Nd dating methods. The emplacement age from Koide et al. (1987) reported by Rb-Sr whole rock dating is 287 to 280 Ma. This early Permian date is corroborated by U-Pb zircon dating by Herzig et al. (1997). The tectonic environment for the Yakuno

ophiolite is consistent with transitional type MORBs and immature island arc oceanic crust (Ishiwatari, 1985; Ishiwatari, 1990a; 1990b; Sano, 1992; Herzig et al., 1997).

3.5.1.2 Other Notable Late Carboniferous to Permian Ophiolites

In North America, the mostly complete Canyon Mountain ophiolite sequence [4.04] occurs in eastern Oregon around the Blue Mountains Baker terrane is reported to be a dismembered complex, which was uplifted during subduction. This ophiolite was likely formed from an island arc between 278 and 265 Ma and emplaced as a result of intra-oceanic subduction (Nicolas, 1989).

3.5.2 Late Carboniferous to Permian Tectonics

The circum-Panthalassic subduction zone of the Late Carboniferous to Permian likely facilitated emplacing the ophiolites discussed in this section. The Dun Mountain and Red Hills [8.15 and 8.19] ophiolites are thought to have formed and been emplaced in collapsing back arc basins along the continental margin of Australia. These arc – continent collisions formed the New England Fold Belt and the other Australian ophiolites [8.09, 8.10, and 8.11] that were emplaced at this time (Coombs et al., 1976).

In Japan, the Sangun-Renge Terrane and the Maizuru Terrane ophiolite [8.28] likely formed as the Panthalassic plate was subducted westward beneath North and South China (Ishiwatari, 1990a & 1990b).

In North America, the Baker Terrane which formed the Canyon Mountain ophiolite likely formed in a far traveled terrane that collided with the North American plate (Nicolas, 1989).

The ophiolites of the Proterozoic and Paleozoic are evidence that there was tectonic activity that reorganized the plates. The lack of the ultramafic boundary is evidence that there may have been different dynamics, which fostered this movement and is a principal debate among modern researchers of these rocks. However, these ophiolites are still considered a part of the story that ophiolites tell us about the tectonic history of the earth.

CHAPTER 4

MESOZOIC OPHIOLITES

Late Mesozoic ophiolites (Late Jurassic and Cretaceous) are more abundant than Early Mesozoic ophiolites (Triassic and Early – Middle Jurassic). This chapter investigates seventy ophiolites: three ophiolites from the Triassic to Early Jurassic, fifty ophiolite locations from the Middle to Late Jurassic, and seventeen ophiolites from the Middle Cretaceous. These Mesozoic ophiolites occur primarily in Coastal California, in the East Siberian Koryak Mountains, and throughout the Eastern Mediterranean and Middle Eastern regions.

4.1 Triassic to Early Jurassic ~250 – 190 Ma

The ophiolites described in the Triassic to Early Jurassic are found in Iran and the Kunlun Mountains of China. These ophiolites are plotted on Figure 4.1 and individually listed in Table 4.1 and described in detail within this section.

4.1.1 Triassic to Early Jurassic Ophiolites

The Mashad [5.04] ophiolite lies near the Shahr-Babak ophiolite in northeast Iran. This ophiolite formed sometime before the late Triassic (210 Ma) and is thought

to have originated in a small ocean basin between the Lut block and the adjacent continent, probably Afghanistan or Central Iran (Ghazi & Hassanipak, 2000b). Another hypothesis, suggested by Chatterjee and Scotese (2000), proposes that the Lut block originally occupied a location adjacent to Northern Somalia and southeastern Arabia. In this case, the Mashad and Shahr–Babak ophiolites may have formed in pull-apart basins related to the rifting of India away from East Africa in the middle Jurassic.

The Rasht ophiolite [5.15] is located in the northwestern part of Iran near the Caspian Sea. This ophiolite is located along the Nain fault Zone and lies within the Alborz Belt. The ophiolite is of pre-Jurassic age forming sometime before 210 Ma. No emplacement age is known; it is thought to have been emplaced along the collision zone between the Cimmerian continent and the southern Caspian region (Ghazi & Hassanipak, 2000a).

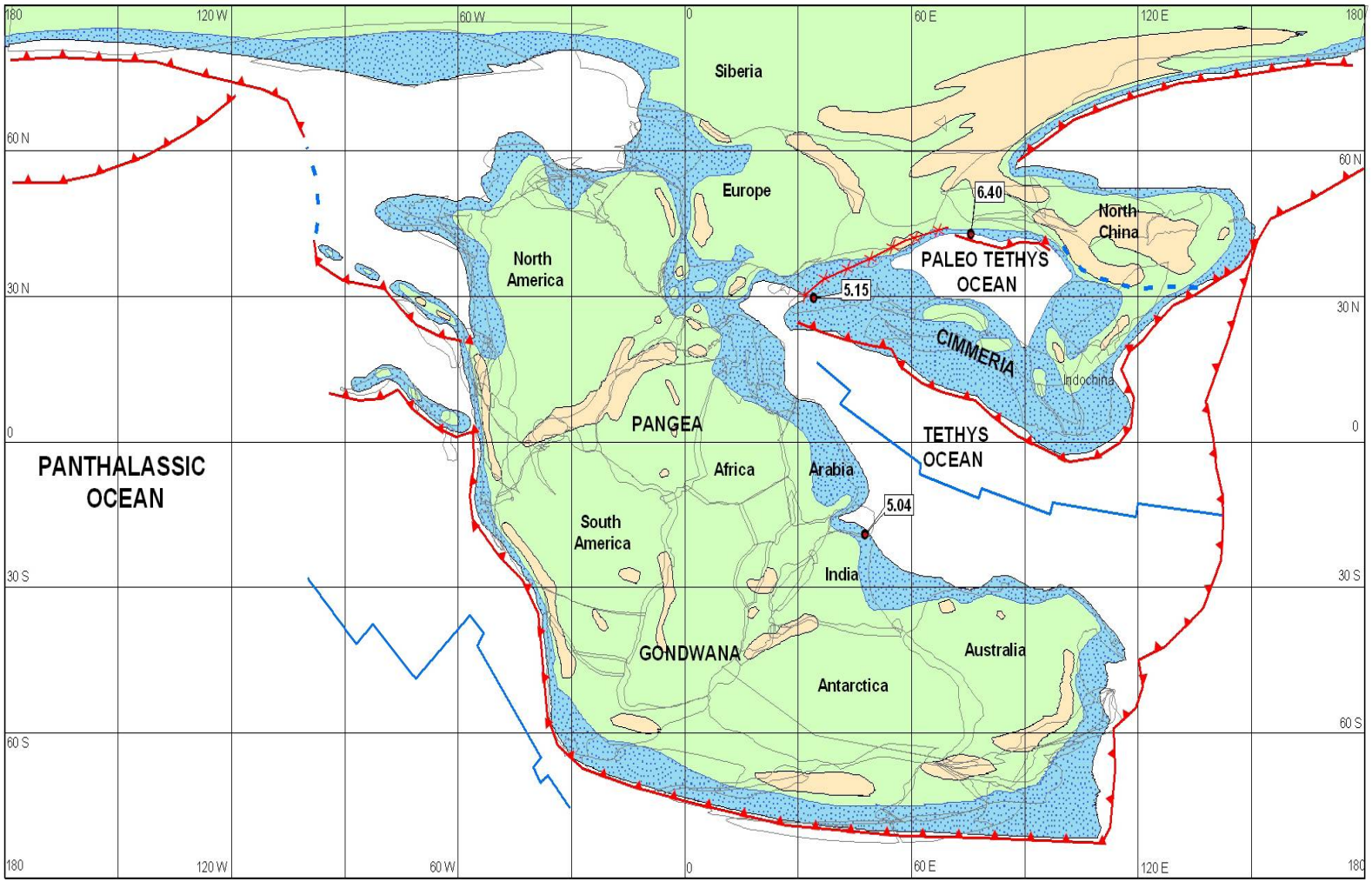

Figure 4.1 Triassic to Early Jurassic ophiolite locations plotted on a 220 Ma paleogeographic reconstruction (Scotese, 2004)

Table 4.1 Triassic to Early Jurassic Ophiolites

				Age of Formation			Age of Obduction		
Ophiolite ID#	Map #	Name	Country	Old Age	Young Age	Best Estimate	Old Age	Young Age	Best Estimate
6.40	6	Kunlun	China	260.00	227.00	243.50			
5.04	6	Mashod	Iran	210.00	210.00	210.00			
5.15	6	Rasht	Iran	210.00	210.00	210.00			

A Triassic to Early Jurassic ophiolite sequence [6.40] is formed along the southern part of the Kunlun Mountains in western China. This ophiolite is thought to be part of the Tarim craton and is separated from the Tibetan Plateau by the Altyn Tagh fault. Formed during the late Paleozoic or Early Triassic (260 to 227 Ma), this ophiolite started as an island chain, hot spot or volcanic arc. This ophiolite was likely emplaced during the Triassic as the Paleo-Tethys was subducted beneath Central Asia (Figure 4.1) (Yuan et al., 2003; Laurent-Charvet et al., 2005).

4.1.2 Triassic to Early Jurassic Tectonics

The Paleo-Tethys Ocean separating the Cimmerian continent from south-central Asia closed during the Triassic and Early Jurassic. The Rasht and Kunlun ophiolites were probably formed in Paleo-Tethys and were emplaced during the piece-wise collision of Cimmeria with Asia during the early Mesozoic. The Rasht and Mashad ophiolites, though not far apart today, represent different ocean basins, and were once widely separated. The original location of the Lut block is not known. Various reconstructions place it somewhere along the Indo-Arabian margin of Gondwana. This

ocean basin, however, had closed by the early Cretaceous (McCall, 1997; Şengör, 1990; Yuan et al., 2003).

4.2 Middle to Late Jurassic and Earliest Cretaceous ~190 – 140 Ma

This section describes fifty ophiolites, which are reported to have been emplaced during the middle to late Jurassic. The main areas of emplacement were the North American western continental margin, the Apennines, and the Alps.

4.2.1 Middle to Late Jurassic Ophiolites

4.2.1.1 North American and South American Middle and Late Jurassic Ophiolites

Most of the Middle and Late Jurassic ophiolites of western North America are found in California. These ophiolites can be divided into five groups, which from west to east are: 1) the Franciscan Complex, 2) the Round Mountain Serpentinite Mélange, 3) the Coast Range ophiolites, 4) the Great Valley forearc province, and 5) the Sierra Nevada Foothills.

The Franciscan Complex, the northern section of the Coast Range Ophiolites, is an accretionary prism, which formed the Sierra Nevada foothills. It is one of the best-known subduction complexes (Saha et al., 2005; Coleman, 2000). This sequence has several dismembered ophiolites: New Idria, Burro Mountain, Cazadero, and Red Mountain.

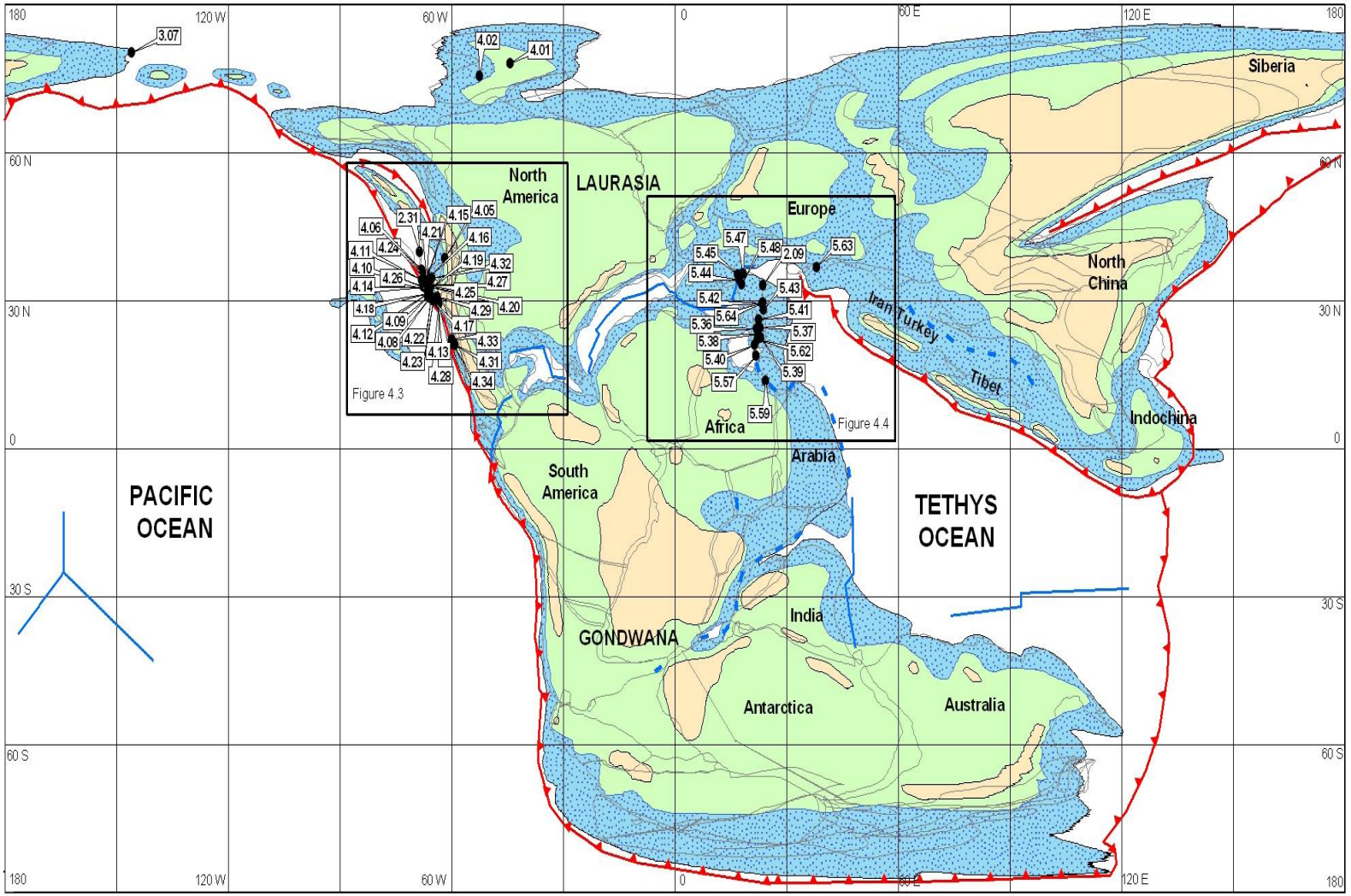

Figure 4.2 Middle to Late Jurassic ophiolite locations plotted on a 160 Ma paleogeographic reconstruction (Scotese, 2004)

Table 4.2 Middle to Late Jurassic Ophiolites

				Age of Formation			Age of Obduction		
Ophiolite ID#	Map #	Name	Country	Old Age	Young Age	Best Estimate	Old Age	Young Age	Best Estimate
4.01	7	NW Alaska	USA	180.00	144.00	162.00			
4.02	7	Brooks Range	USA	186.00	168.00	177.00	169.00	163.00	166.00
4.05	7	Sparta	USA			0.00	157.00	157.00	157.00
4.06	7	Josephine (Smith River)	USA	180.00	162.00	171.00			
4.08	7	Franciscan New Idria	USA	180.00	159.00	169.50	140.00	140.00	140.00
4.09	7	Franciscan Burro Mt	USA	180.00	159.00	169.50	140.00	140.00	140.00
4.10	7	Franciscan Cazadero	USA	180.00	159.00	169.50	140.00	140.00	140.00
4.11	7	Franciscan Red Mt	USA	180.00	159.00	169.50	140.00	140.00	140.00
4.12	7	Coast Range Del Puerto	USA	168.00	154.00	161.00	140.00	140.00	140.00
4.13	7	Coast Range Point Sal	USA	159.00	144.00	151.50			
4.14	7	Coast Range Black Mountain	USA	164.00	154.00	159.00			
4.15	7	Coast Range Stonyford	USA	172.00	166.00	169.00	161.00	161.00	161.00
4.16	7	Coast Range Paskenta	USA	163.00	159.00	161.00	161.00	161.00	161.00
4.17	7	Coast Range Llanada	USA	170.00	164.00	167.00	161.00	161.00	161.00
4.18	7	Coast Range Hospital Canyon	USA	170.00	170.00	170.00	161.00	161.00	161.00
4.19	7	Great Valley Cuesta Ridge	USA	151.00	144.00	147.50			
4.20	7	Great Valley 2	USA	151.00	144.00	147.50			
4.21	7	Great Valley 3	USA	151.00	144.00	147.50			
4.22	7	Great Valley 4	USA	151.00	144.00	147.50			
4.23	7	Great Valley 5	USA	151.00	144.00	147.50			
4.24	7	Sierra Nevada Foothills 1	USA	162.00	156.00	159.00	150.00	140.00	145.00
4.25	7	Sierra Nevada Foothills 2	USA	162.00	156.00	159.00	150.00	140.00	145.00
4.26	7	Sierra Nevada Foothills 3	USA	162.00	156.00	159.00	150.00	140.00	145.00
4.27	7	Sierra Nevada Foothills Smartville	USA	162.00	156.00	159.00	150.00	140.00	145.00
4.28	7	Stanley Mountain	USA	168.00	164.00	166.00			
4.29	7	Sierra Nevada Foothills Kings River	USA	165.00	155.00	160.00	150.00	140.00	145.00
4.32	7	Elder Creek	USA	172.00	165.00	168.50			
4.31	7	Baja Alta Terrane	Mexico	221.00	220.00	220.50	156.00	135.00	145.50
4.33	7	Cedros Island	Mexico	175.00	171.00	173.00	156.00	135.00	145.50
4.34	7	Vizcaino	Mexico	223.00	219.00	221.00	156.00	135.00	145.50

Table 4.2 *Continued*

				Age of Formation			Age of Obduction		
Ophiolite ID#	**Map #**	**Name**	**Country**	**Old Age**	**Young Age**	**Best Estimate**	**Old Age**	**Young Age**	**Best Estimate**
5.41	7	Albania-Brezovica	Albania	227.00	180.00	203.50	174.00	160.00	167.00
2.09	7	Kraubath	Austria	354.00	327.00	340.50	175.00	175.00	175.00
5.57	7	Cretan Nappe	Crete	156.00	140.00	148.00			
5.59	7	Mamonia	Cyprus	248.00	210.00	229.00	208.00	104.00	156.00
5.45	7	Montgenevre	France	200.00	180.00	190.00	190.00	180.00	185.00
5.36	7	Pindos	Greece	176.00	168.00	172.00	168.00	163.00	165.50
5.37	7	Vourinos	Greece	180.00	164.00	172.00	175.00	167.00	171.00
5.38	7	Othris	Greece	180.00	160.00	170.00	180.00	160.00	170.00
5.39	7	Euboea	Greece	180.00	159.00	169.50	180.00	160.00	170.00
5.40	7	Agelona	Greece	227.00	210.00	218.50	180.00	160.00	170.00
5.62	7	Hellinic	Greece	208.00	144.00	176.00			
5.47	7	Zermatt-Saas-Fee	Italy	166.70	161.70	164.20	161.00	152.00	156.50
5.48	7	Internal Liguride (Ligurian)	Italy	178.00	150.00	164.00	159.00	145.00	152.00
5.44	7	Corsican	Italy/France	187.00	175.00	181.00	181.00	165.00	173.00
5.42	7	Krivaja-Kanjuh	Yugoslavia	180.00	159.00	169.50	180.00	145.00	162.50
5.43	7	Zlatibor	Yugoslavia	180.00	159.00	169.50	180.00	145.00	162.50
5.64	7	Dinaride (Central Zone)	Yugoslavia	206.00	144.00	175.00			
3.07	7	Chersky	Russia	430.00	370.00	400.00	174.00	170.00	172.00
5.63	7	Kure	Turkey	208.00	144.00	176.00			
2.31	7	Shulaps	Canada	242.00	121.00	181.50			

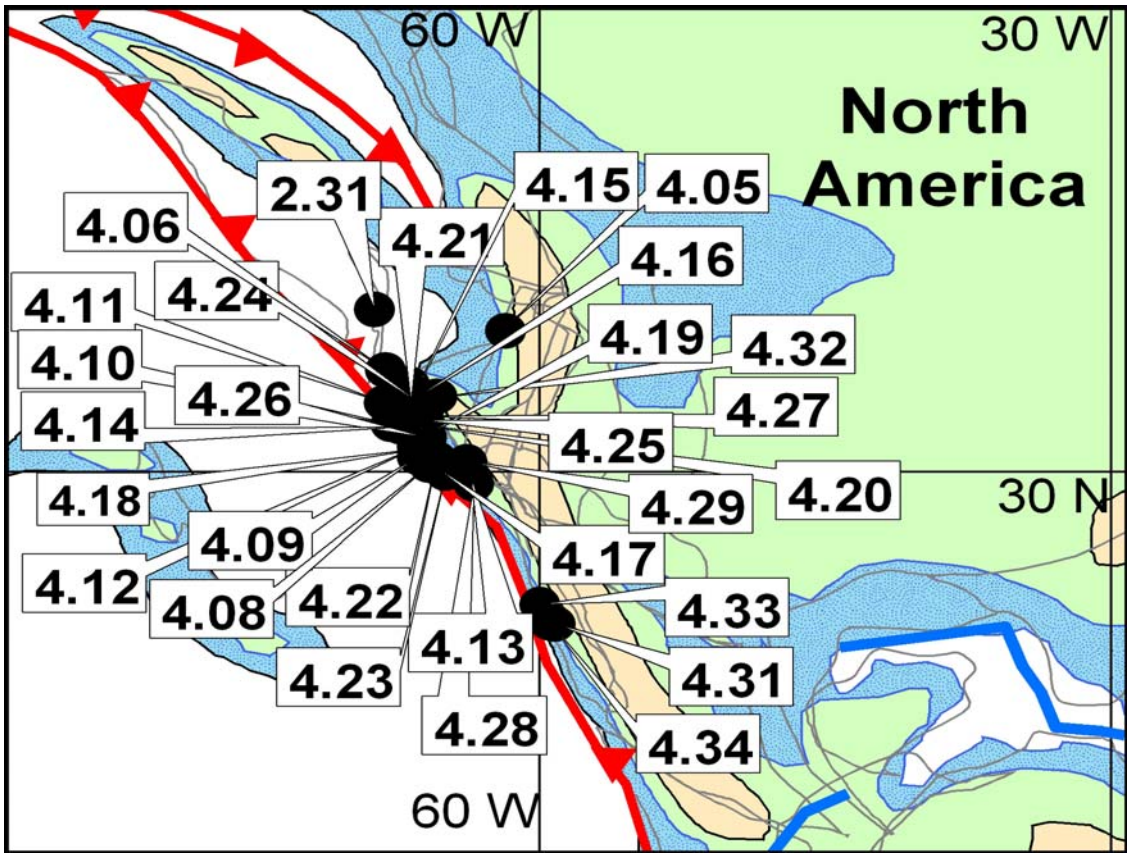

Figure 4.3 Middle to Late Jurassic ophiolite locations in North America plotted on a 160 Ma paleogeographic reconstruction (Scotese, 2004)

As depicted in Figure 4.3, the New Idria [4.08] ophiolite is made up of oceanic crust that formed in the Middle Jurassic (180 to 159 Ma) in an early stage island arc setting (Shervais et al., 2005). This sequence yields an obduction age of around 140 Ma and was emplaced as a result of subduction beneath the North American continental margin (Saha et al., 2005; Coleman, 2000). Burro Mountain [4.09], another ophiolite form the Franciscan complex, was also formed in an island arc setting. Saha et al. (2005), Shervais et al. (2005), and Coleman (2000) report that the Burro Mountain ophiolite formed between 180 to 159 Ma and was obducted around 140 Ma as a result

of subduction of the island arc. The Cazadero ophiolite [4.10] is another ophiolitic suite of the Franciscan complex, which formed during the Middle Jurassic (180 to 159 Ma) (Shervais et al., 2005). This sequence yields an obduction age of around 140 Ma and is reported to have been a result of accretion due to subduction along the continental margin (Saha et al., 2005; Coleman, 2000). Red Mountain [4.11], the last Franciscan ophiolite noted in this study, formed around 180 to 159 Ma (Shervais et al., 2005). This sequence also yields an obduction age of around 140 Ma. Most of the geologic ages of the ophiolites were determined using $^{40}Ar/^{30}Ar$ radiometric and U-Pb zircon age dating methods in recent work. These studies imply emplacement was due to accretion from subduction along the margin of North America (Shervais et al., 2005; Saha et al., 2005; Coleman, 2000).

The Coast Range Ophiolite complex in California is closely related to the Franciscan complex. It is reported by Shervais et al. (2005) that the Coast Range ophiolites are thought to be a part of oceanic lithosphere formed at the mid-ocean ridge that was obducted as a whole slab onto the North American continental margin. Del Puerto [4.12] formed at a mid-ocean ridge during the middle Jurassic (168 to 154 Ma). This ophiolite was obducted during the earliest Cretaceous (140 Ma) as an oceanic plate was subducted under the continental margin (Shervais et al., 2005; Coleman, 2000).

The Josephine ophiolite (or Smith River) [4.06] in northern California, has a formation age of 180 to 162 Ma and may have formed within the back arc basin as part of the Coast Range ophiolites (Gillis & Banerjee, 2000; Harper, 1984). Radiolarian data from Pessango et al. (1993) also dated the pelagic sediment which overlays the

sequence to mid-Oxfordian (157 Ma). Although no emplacement age is given, it is thought to have been emplaced in the Middle to Late Jurassic (Gillis & Banerjee, 2000).

The Point Sal ophiolite [4.13], another Coast Range ophiolite, formed at a mid-ocean ridge during the late Jurassic. This sequence was obducted onto the continental margin sometime during the late Jurassic (Shervais et al., 2005; Coleman, 2000). The Black Mountain ophiolite [4.14], also part of the Coast Range ophiolites, formed at a mid-ocean ridge around 164 to 154 Ma. This sequence was obducted onto the continental margin sometime shortly after formation during the late Jurassic (Shervais et al., 2005; Coleman, 2000). Stonyford [4.15], an ophiolite complex in the northern region of California's Coast Range ophiolite, formed at a mid-ocean ridge during the middle Jurassic (172 to 166 Ma). It is thought that this less complete sequence was emplaced due to the collision and subduction along the margin of California around 161 Ma (Shervais et al., 2005; Coleman, 2000).

The Elder Creek ophiolite [4.32] sequence is one of the best preserved ophiolites in the Coast Ranges of northern California (Shervais et al. 2005). The oceanic lithosphere, which formed the complex, was formed between 172 and 165 Ma. Geochemical data from the serpentinite matrix mélange, suggest an arc environment for emplacement for the Elder Creek ophiolite. Stanley Mountain ophiolite [4.28], also part of the southern Coast Range ophiolites, formed during the middle Jurassic (168 to 164 Ma) and is thought to have been emplaced at the same time as many other ophiolitic sequences during the Middle to Late Jurassic (Shervais et al., 2005).

The Paskenta ophiolite [4.16] of the Coast Range complex formed at the mid-ocean ridge around 172 to 164 Ma. It is reported to have been obducted around 161 Ma as a result of subduction along the continental margin during the Nevadan orogeny (Shervais et al., 2005; Coleman, 2000). The Llanada ophiolite [4.17], another Coast Range ophiolite, formed at the mid-ocean ridge around 170 to 164 Ma. This ophiolite was also obducted around 161 Ma onto the continental margin (Shervais et al., 2005; Coleman, 2000). Another ophiolite from the Coast Range complex is Hospital Canyon ophiolite [4.18], which formed at the mid-ocean ridge around 170 Ma. This ophiolite was obducted around 161 Ma along the continental margin as a result of subduction and the orogenic processes during the Middle to Late Jurassic (Shervais et al., 2005; Coleman, 2000).

The Great Valley forearc province [4.20–4.23] of California is thought to be the basement of the Coast Range sequence and yields a mid-Jurassic ophiolite. These ophiolites are thought to have been emplaced due to the same subduction processes that emplaced the Coast Range ophiolites (Shervais et al., 2005).

A sequence of the incomplete Great Valley ophiolites includes the Cuesta Ridge ophiolite [4.19], which has a formation date of around 151 to 144 Ma. This ophiolite is also thought to have been emplaced in the Middle to Late Jurassic as a result of subduction of the Farallon plate beneath western North America (Shervais et al., 2005).

The Sparta complex [4.05] on the northern edge of the Great Valley sequence, was likely formed in a mid-ocean ridge. This ophiolite was emplaced as a consequence

of the subduction along the North American continent around 157 Ma (Phelps & Ave' Lallemant, 1980).

The Sierra Nevada Foothills has several unnamed ophiolite complexes [4.24-4.26] that yield mid-Jurassic ages. The ophiolites in this area formed around 162 to 156 Ma along the mid-ocean ridge that was west of the continental margin of North America. These were subsequently emplaced sometime between 150 and 140 Ma (Day & Bickford, 2004; Saleeby et al., 1989). The Smartville complex [4.27] also part of the Sierra Nevada Foothills, formed around 162 to 156 Ma. This ophiolite was emplaced along the continental margin of North America at around 150 to 140 Ma (Day and Bickford, 2004; Beard, 1998; Saleeby et al., 1989). Another ophiolite from the Sierra Nevada Foothills is the Kings River complex [4.29]. This ophiolite also formed around 165 to 155 Ma and was emplaced sometime between 150 and 140 Ma (Day and Bickford, 2004; Saleeby et al., 1989).

The Baja Alta Terrane in Mexico and southern California has produced a few ophiolites dating back to the Late Triassic (Busby, 2004). The Cedros Island ophiolite [4.33], also known as the Gran Canon Formation, formed in the backarc basin during the middle Jurassic (175 to 171 Ma) and was obducted around 156 to 135 Ma (Kimbrough & Moore, 2003; Moore & Kimbrough, 2005; Busby, 2004).

The oceanic lithosphere which formed the Baja Alta ophiolite [4.31] has been dated at 221 to 220 Ma using zircon U-Pb data. The Baja Alta ophiolite is thought to have formed in a backarc basin during the Middle to Late Jurassic (Busby, 2004).

The Vizcaino Peninsula ophiolite [4.34] dates from 223 to 219 Ma and was obducted during the Late Jurassic (Busby, 2004). The Vizcaino Peninsula ophiolite is interpreted by Moore (1985) and Kimbrough (1984) to have formed in an intra-arc or backarc environment. This ophiolite is also part of the southern sequence of California's Coast Range ophiolites (Kimbrough & Moore, 2003).

The Shulaps ophiolite [2.31] near Bridge River in southwestern British Columbia, is part of the Canadian Cordillera, see Figure 4.2. It lies between Yalakom fault and the Insular superterranes at the southern end of the Stikine terrane. This ophiolite formed around 242 to 121 Ma in an ocean basin that collapsed prior to the collision of the Stikine terrane with North America. It was probably emplaced as a result of the subduction event along the western margin of North America sometime during the middle Jurassic to late Cretaceous (Potter, 1983; Calon et al., 1989).

4.2.1.2 European – Arabian Middle to Late Jurassic Ophiolites

As seen in Figure 4.4, the Kraubath Massif [2.09] is an ophiolite in the Eastern Alps of Austria and is thought to have formed around 354 to 327 Ma. This ophiolite has an emplacement age from Ar-Ar data of 175 Ma, and is part of the Speik Complex (east of the Tauern Window and Hochgrössen), which is thought to be a fragment of the Variscan oceanic lithosphere originally subducted under Baltica during the Devonian (Ageed et al., 1980; Crowley et al., 2000; Faryad and Hoinkes, 2004).

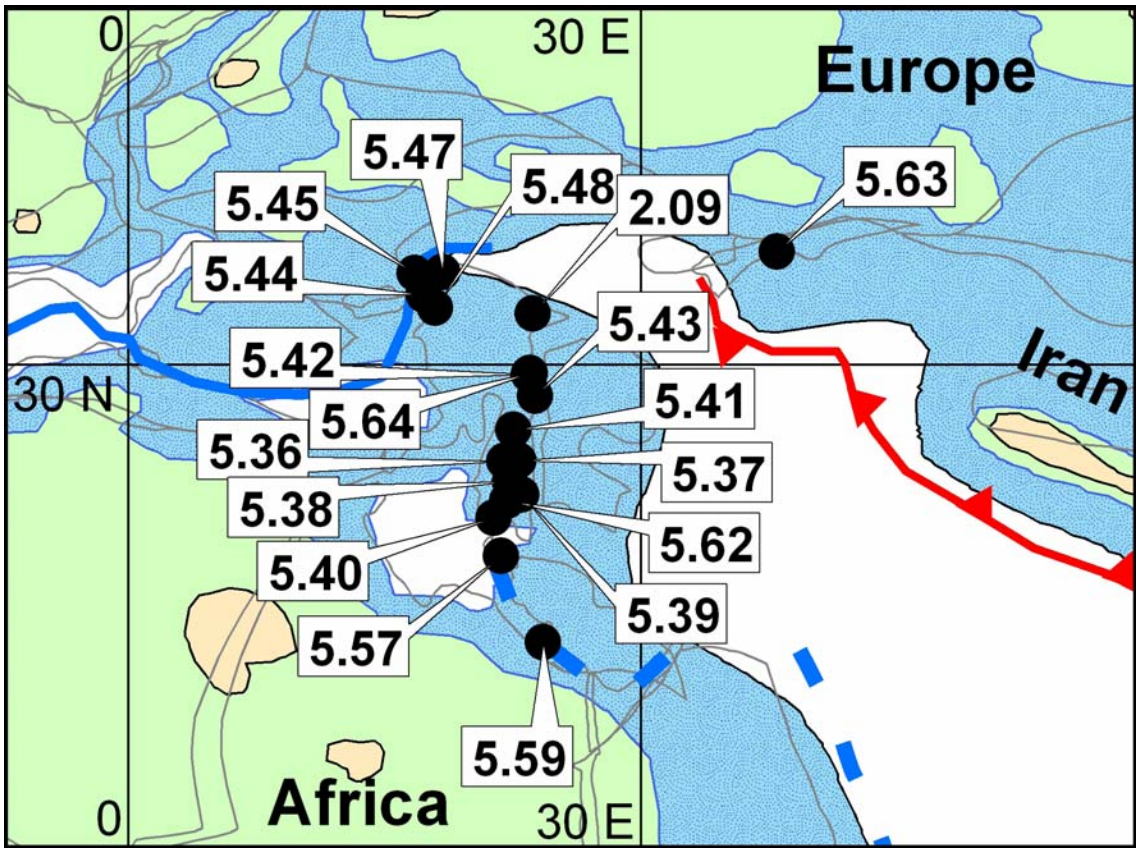

Figure 4.4 Middle to Late Jurassic ophiolite locations around the European-African Paleo-Mediterranean plotted on a 160 Ma paleogeographic reconstruction (Scotese, 2004)

In Greece the dismembered Agelona ophiolite [5.40] formed sometime between 227 and 210 Ma along a mid-ocean ridge in western Tethys. This complex is a part of the Hellenic Alpine orogenic belt within the Hellenides. It is reported to have been emplaced during subduction along the continental margin of Europe around 180 to 160 Ma (Danelian et al., 2000).

The Hellinic ophiolite in the Grecian Alps [5.62] was formed sometime between 208 and 144 Ma along a mid-ocean ridge. This ophiolite is thought to have been

emplaced along a subduction zone sometime shortly after formation (Dilek & Flower, 2003; Spray et al., 1984).

Greece has several fairly complete ophiolites that formed during the middle to late Jurassic. The Pindos ophiolite in northern Greece [5.36] formed in a backarc basin during the Middle Jurassic (176 to 168 Ma). This sequence was emplaced into an accretionary prism mélange around 168 to 163 Ma (Jones et al., 1991; Rassios & Smith, 2000). The Vourinos ophiolite [5.37] in Northern Greece formed between 180 and 164 Ma. It is reported to have been emplaced along the southern margin of the Eurasian plate around 175 to 167 Ma (Rassios & Smith, 2000).

The Othris ophiolite [5.38] in central Greece, formed around 180 to 160 Ma. This ophiolite was emplaced immediately along the continental margin as a result of subduction (Rassios & Smith, 2000). The Euboea ophiolite [5.39] in southern Greece also formed during the Middle Jurassic (180 to 159 Ma). This sequence is also believed to have been obducted shortly after forming as a result of subduction along the continental margin of Eurasia (Marinos, 1980).

The Cretan Nappe ophiolite [5.57] in Crete has been interpreted to be a slab of oceanic lithosphere that formed around 156 to 140 Ma. This ophiolite sequence is reported to have formed in an island arc and was emplaced along the continental margin of Eurasia shortly after they were created (Borradaile & Lucas, 2003).

The Mamonia ophiolite [5.59] in western Cyprus (south of the Troodos site), is thought to have formed around 248 to 210 Ma as a result of Triassic rifting in the Tethys-Mediterranean region. This ophiolite is reported to have been emplaced

sometime during the Jurassic to Early Cretaceous (Borradaile & Lucas, 2003; Dietrich, 1979).

The Corsican ophiolite [5.44] of Italy, formed sometime around 181±6 Ma. This ophiolite was obducted between 181 and 165 Ma onto the margin of Corsica (Desmons, 1989). The Internal Liguride (or Ligurian) ophiolite in northern Italy [5.48] formed along a mid-ocean ridge approximately 178 to 150 Ma. This complex was emplaced between 159 to 145 Ma in the accretionary prism that now makes up part of the Northern Apennines (Borsi et al., 1996; Rampone et al., 1998; Rampone & Piccardo, 2000).

The Zermatt-Saas-Fee ophiolite complex [5.47] is dated by Rubatto et al. (1998) to be 166.7 to 161.7 Ma and is thought to have formed at the same time as the opening of the Atlantic. The obduction age is controversial and ranges from 161 to 152 Ma (Rubatto et al., 1998) to 40 Ma or younger based on eclogite zircon dating (Amato et al., 1999). These Tethyan ophiolites are thought to be part of the Jurassic oceanic lithosphere created in the Mediterranean that was later largely destroyed during the Alpine Orogeny (Miller & Cartwright, 2000).

The European Alpine–Apenninic area as well as Albania, Yugoslavia, and Austria has produced many outcrops of ophiolites for scientists to study over the last several decades. The Dinaride ophiolite in Yugoslavia, which is part of the Central Zone of Ophiolites, [5.64] formed in an island arc environment between 208 and 144 Ma. This sequence was emplaced sometime during the Late Jurassic (Pamić, 1977; Dilek & Flower, 2003).

The Brezovica ophiolite [5.41] in north-central Albania formed along a Tethyan mid-ocean ridge around 227 to 180 Ma. It was emplaced as part of an accretionary mélange onto the continental margin of Europe around 174 to 160 Ma (Vergely et al., 1998; Robertson & Shallo, 2000).

The Krivaja-Kanjuh ophiolite [5.42] in southwest Yugoslavia lies within the Krivaja ultramafic massif and formed during the middle Jurassic around 180 to 159 Ma. It was emplaced shortly there after (180 to 145 Ma) and is thought to have been thrust onto the Dinaride massif (Pamić et al., 1998; Okrusch & Seidel, 1978). The Zlatibor ophiolite [5.43] in Yugoslavia also formed in the early-middle Jurassic. It is reported to have been emplaced around 180 to 145 Ma as part of the fold and thrust belt that developed in the northeastern Adriatic as a result of the collision of the Apulian prong along the southern margin of Europe (Pamić et al., 1998; Okrusch & Seidel, 1978).

The Montgenevre ophiolite [5.45] in Eastern France formed sometime between 200 and 180 Ma. This ophiolite was obducted shortly thereafter, around 190 to 180 Ma (Costa & Caby, 2001).

4.2.1.3 Other Notable Middle to Late Jurassic Ophiolites

Alaska also has several ophiolite belts in its northwestern, central, and southern regions. The Brooks Range [4.02] ophiolite Alaska, as reported by Wirth et al. (1993) and Moore (1997), yields formation ages around 186 to 168 Ma. This ophiolite formed in the Augayucham Ocean of the Chukotka-Arctic Alaska block and lies within the Hammond Subterrane and Arctic Alaska Superterrane (Wirth et al, 1993). These blocks

are believed to have collided with the continental margin of the North Slope block and resulted in subduction and accretion of the ophiolitic rocks. The emplacement of the Brooks Range ophiolite dates from the middle Jurassic (169 to 163 Ma) (Moore et al., 1997).

In northwest Alaska, an ophiolite [4.01] lies within the Misheguk Mountains. This ophiolite is closely related to the Brooks Range ophiolite and has a formation age around 180 to 144 Ma. It is thought to have been emplaced shortly after formation, sometime during the Middle to Late Jurassic (Foley, 1992).

The Kure ophiolite [5.63] in northeastern Turkey formed between 208 and 144 Ma. This complex lies within the Central Pontides and is thought to have been emplaced sometime during the Middle to Late Jurassic at the same time as many of the other Tethyan ophiolites (Bortolotti & Principi, 2005).

The Chersky complex [3.07] lies within Yakutia in northeastern Russia and was derived from backarc basin and oceanic crustal fragments around 430 to 370 Ma. This complex was obducted around 174 to 170 Ma during the collision of the Omolon Terrane (Oxman et al., 1995).

4.2.2 Middle to Late Jurassic Tectonics

During the middle to late Jurassic, Pangea divided into the three main regions (Laurasia, East Gondwana, and West Gondwana). The Pacific plate, Gulf of Mexico and Mediterranean basin also formed during the middle to late Jurassic. Other important tectonic events during the middle to late Jurassic were the start of the North

America Rockies (Nevadan orogeny), the formation of the Greater Antilles (Cuban) island arc, and the closure of the Armurian (Asian) seaway (Fonsec et al., 1985; Nekrasov et al., 1989). As a result of these diverse tectonic events, many ophiolites were formed and emplaced during the middle to late Jurassic. Subduction of the Farallon plate beneath the western coast of the North American resulted in the emplacement of many of the Californian and Alaskan ophiolites (Shervais et al., 2005; Dietrich, 1979; Moore & Kimbrough, 2005; Zhou et al., 2001; Busby, 2004). The Coast Range Ophiolites [4.12-4.18], Franciscan ophiolites [4.08-4.11 and 4.32], Sierra Nevada Foothills [4.24-4.27], and Great Valley ophiolites [4.19-4.23] all formed at mid-ocean ridges and were emplaced along the western margin of North American as a result of east dipping subduction (Miller, 1985; Saha et al., 2005). The Great Valley province represents a forearc basin and the Franciscan region represents an accretionary zone characterized by a chaotic tectonic mélange (Shervais et al., 2005). The granites of the Sierra Nevadas represent the batholiths beneath the continental volcanic arc along the western margin of North America. The Sierra Nevada foothills ophiolites were emplaced as a result of the subduction of the Farallon plate under the Coast Range and squeezing up some of the lighter lithospheric material. Further south in the Baja Alta region, ophiolites [4.31, 4.33, 4.34] were also formed as a result of the Farallon plate subducting under the North American plate. In Alaska, subduction beneath the southern margin of the North Slope block resulted in the emplacement of ophiolites [4.01 and 4.02] (Busby, 2004; Moore et al., 1997).

In the Mediterranean region, the western Tethys Ocean was developing as a result of the breakup of Pangea. As the Tethys began to close the seaward Alpine ophiolites [2.09, 5.36-5.48, 5.57, 5.59, and 5.62,] were emplaced in a successively younger pattern from the northwest (Alps, Apennines, and Dinarides) to southeast (Taurides, Zagros, Himalayas) (Schuster & Kurz, 2005; Spray et al., 1984; Pamić et al., 1979; Dilek & Flower 2003).

4.3 Early Cretaceous ~140 – 100 Ma

4.3.1 Early Cretaceous Ophiolites

This section presents seventeen ophiolites which were emplaced during the middle Cretaceous. These middle Cretaceous ophiolites are primarily located in the regions of the Siberian Koryak Mountains, a few in Europe, and a few in the Caribbean region. These ophiolites can be seen on Figure 4.5 and are listed individually in Table 4.3.

4.3.1.1 Siberian Cretaceous Ophiolites

Several complexes of ophiolites are exposed in the Koryak Mountains of northeast Siberia. The Mainitis Zone [3.08] in the central Koryak Mountain region seems to have formed in an island arc environment between 159 to 121 Ma and was emplaced around 144 to 99 Ma (Palandzhjan, 1986).

The Ust'–Belaya ophiolite section [3.09] in the northern region of the Koryak Mountains formed during the middle Paleozoic (417 to 323 Ma). This sequence was

emplaced much later in the early Cretaceous (137 to 132 Ma) as a result of accretion along the continental margin of northeastern Siberia (Palandzhjan, 1986).

The Uga-Murugal ophiolite complex on Porotory Cape [3.14] also lies within the Koryak Mountains in northern Siberia. This complex was formed around 129 Ma and was emplaced shortly there after (Palandzhjan et al., 1999).

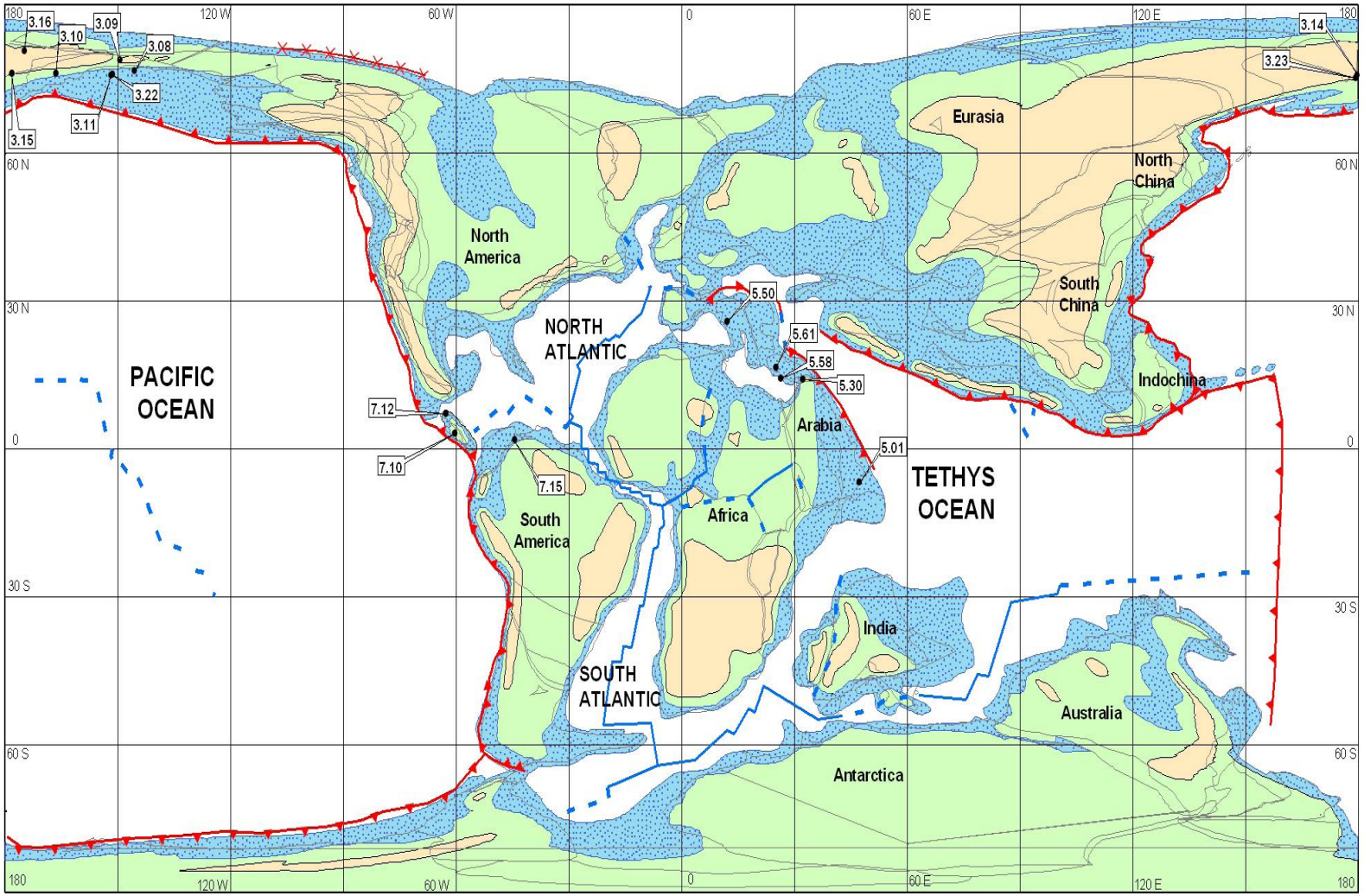

Figure 4.5 Cretaceous ophiolite locations plotted on a 100 Ma paleogeographic reconstruction (Scotese, 2004)

Table 4.3 Early Cretaceous Ophiolites

				Age of Formation			Age of Obduction		
Ophiolite ID#	Map #	Name	Country	Old Age	Young Age	Best Estimate	Old Age	Young Age	Best Estimate
5.58	8	Akamas	Cyprus	144.00	65.00	104.50			
5.50	8	Tuscany	Italy	156.00	148.00	152.00	144.00	65.00	104.50
5.01	8	Masirah	Oman	158.00	124.00	141.00	132.00	121.00	126.50
5.30	8	Ispendere-Komurhan	Turkey	144.00	65.00	104.50			
5.61	8	Honaz	Turkey	144.00	65.00	104.50			
3.08	8	Mainitis Zone	Russia	159.00	121.00	140.00	144.00	99.00	121.50
3.09	8	Ust' - Belaya Mts	Russia	417.00	323.00	370.00	137.00	132.00	134.50
3.10	8	Kuyul Mélange	Russia	155.00	121.00	138.00	121.00	99.00	110.00
3.11	8	Upper Khatyrka	Russia	248.00	206.00	227.00	144.00	112.00	128.00
3.14	8	Porotory Cape	Russia	159.00	99.00	129.00			
3.15	8	Elistratova Complex	Russia	210.00	144.00	177.00	121.00	99.00	110.00
3.16	8	Aluchin	Russia	374.00	231.00	302.50	144.00	112.00	128.00
3.22	8	Koryak	Russia	144.00	121.00	132.50	121.00	99.00	110.00
3.23	8	Taigonos Peninsula (Uga-Murugal)	Russia	129.00	129.00	129.00			
7.12	8	Bermeja	Puerto Rico	146.00	142.00	144.00	112.00	99.00	105.50
7.10	8	Cordillera Central	Hispaniola	137.00	132.00	134.50	112.00	99.00	105.50
7.15	8	Siquisique	Venezuela	176.00	164.00	170.00	159.00	99.00	129.00

Taigonos Peninsula [3.23], another ophiolite found in the Koryak Mountains, formed as part of an island arc around 129 Ma. It was emplaced onto the continental margin due to subduction and accretion probably in the late Cretaceous (Palandzhjan et al., 1999).

In Russia, the Aluchin ophiolite [3.16] or Anyui ophiolite, part of the Northeast margin of the Kolyma Omolon Block is believed to have formed sometime during the Permian to Triassic (374 to 231 Ma) (Ishiwatari et al., 1999). Sokolov et al., (2002)

report that the oceanic basin that this ophiolite formed in was at one time connected to the Polar Urals basin and the Taimyr basin. This ophiolite was emplaced during the Early Cretaceous as a result of the continental collision along the South Anyui suture (Sokolov et al., 2002; Lychagin, 1985; Chekhovich et al., 1999). The Upper Khatyrka ophiolite complex [3.11] in the Koryak Mountains of northeastern Siberia is Middle Triassic in age (248 to 206 Ma). This ophiolite is thought to have formed as a result of sea floor spreading in a forearc setting. The accreting island arcs were emplaced onto the continental margin of Siberia sometime in the Early Cretaceous (Palandzhjan, 1986; Sokolov et al., 2002; Chekhovich et al., 1999). The Kuyul Mélange [3.10] is part of the Kuyul massif in the Koryak Mountains of Siberia. It formed in an island arc environment around 155 to 121 Ma. It is reported to have been emplaced during the early to mid-Cretaceous (121 to 99 Ma) (Palandzhjan, 1986).

The Elistratova complex [3.15] is a complete ophiolite sequence found in the Taigonos Peninsula of the Koryak Mountains, formed sometime during the Jurassic (210 to 144 Ma) in an island arc environment. This ophiolite was emplaced as part of an accretion complex between 121 and 99 Ma (Ishiwatari et al., 1998).

In the Northeast region of the Koryak Mountains, another ophiolite [3.22] has been described by Palandzhjan (1986) that yields ages of 144 to 121 Ma for formation. It appears to have been emplaced around 121 to 99 Ma as the result of the accretion of an island arc.

4.3.1.2 European – Arabian Cretaceous Ophiolites

The tectonic evolution of Iran and Turkey during the middle to Late Jurassic is complex. Oman has many well-studied ophiolite complexes that date from the middle to late Jurassic. A complete ophiolite sequence, the Masirah Island [5.01] complex, in eastern Oman formed on the Indian plate between 158 and 124 Ma at a mid-ocean ridge. It is reported to be made up of two nappe structures and was obducted onto the Arabian continental margin during the early Cretaceous (132 to 121 Ma) (Gealey, W.K., 1977; Gnos & Perrin, 1996; Marquer et al., 1998; Peters & Mercolli, 1997).

The southeastern area of Turkey has many ophiolites that formed during the mid-Cretaceous. The Ispendere-Komurhan ophiolite [5.30] probably formed during the early Cretaceous and was obducted onto the continental margin around 92 to 90 Ma (Dilek et al., 1999; Yilmaz, 1993; Juteau et al., 1980). The Honaz ophiolite [5.61] in the Lycian regions of Turkey was also formed during the Cretaceous. It is also reported to have been obducted shortly after formation (Dilek & Flower, 2003).

The Tuscany ophiolite [5.50] in central Italy formed around 156 to 148 Ma along the mid–ocean ridge. It was emplaced during the Cretaceous along the continental margin of Italy (Tribuzio et al., 2000). The Akamas ophiolite [5.58] in western Cyprus, is thought to have formed sometime during the Cretaceous. This ophiolite is also part of the Troodos Complex in Western Cyprus. It is reported to stratigraphically lie atop the Troodos sequence and implies that it was emplaced in one of the last thrust sheets. Many researchers link the Mamonia, Troodos, and Akamas ophiolites to the same series of tectonic events (Borradaile & Lucas, 2003).

4.3.1.3 Caribbean Cretaceous Ophiolites

The Siquisque ophiolite [7.15] in western Venezuela was formed around 176 to 164 Ma. It is though to be formed as a part of the spreading event that opened up the proto-Caribbean and Atlantic during this time. It is believed to have been emplaced in the Late Jurassic to Early Cretaceous, as the proto-Caribbean was subducted beneath the Greater Antilles island arc (Bartok et al., 1985).

The Cordillera Central ophiolite [7.10] in central Hispaniola, is thought to have formed between 137 and 132 Ma. It was emplaced between 112 and 99 Ma (Wadge et al., 1984; Haldemann et al., 1980).

The Bermeja ophiolite [7.12] in southwest Puerto Rico was formed in 146 to 142 Ma. It is thought to have been emplaced around 112 to 99 Ma as the Proto-Caribbean ocean floor was subducted beneath the overriding Greater Antilles Arc (Mattson, 1974).

4.3.2 Cretaceous Tectonics

During the Middle Cretaceous western and eastern Gondwana divided, South America separated from Africa as well as India and Madagascar separated from Australia and Antarctica. Pangea also continued to break apart in the Middle Cretaceous around 120 Ma as the Proto-Caribbean was forming (Scotese, 2001). The rifting of the Caribbean formed ophiolites such as the Central in Hispaniola and the Bermeja in Puerto Rico (Wadge et al., 1984). The Akamas, Honaz, and Ispendere-

Komurhan were the ophiolites produced in the region of Turkey as Anatolia subducted onto the continental margin (Dilek & Flower, 2003).

The Koryak Mountains, the Mainitis, Taigonos Peninsula, Ust'- Belaya, and Porotory Cape ophiolites formed as a result of the accretion along the southeastern continental margin of Northeast Siberia (Ishiwatari et al., 1999). Most of the rocks of these ophiolites indicate that the Koryak and Taigonos Peninsula were formed in subduction zones (Ishiwatari et al., 1999). The subduction beneath the Siberian and the North American margin of the circum-Panthalassic "ring of fire" likely resulted in the Aluchin ophiolite [3.16] (Sokolov, 2002; Lychagin, 1985). In the Northeast Pacific, subduction of Panthalassic ocean floor beneath northeast Asia continued through the Triassic and Jurassic. The Upper Khatyrka ophiolite also found in the Koryak mountain range in northeastern Siberia probably formed in a small ocean basin that separated the Olutorsky island arc from northeast Asia (Morozov et al. 2004). The Koryak region (Siberia) was undergoing subduction along the continental margin which likely resulted in the Kuyul, Elistratova, and Koryak complexes to be emplaced (Ishiwatari et al., 1998).

As the Indian and African plates moved northward, the Tethys Ocean began to close and allow for mid-ocean rifting events to form new crustal sequences. In this environment, the Masirah ophiolite of Oman is thought to have formed (Gnos & Perrin, 1996; Gealey, 1977).

The Mesozoic ophiolites described in this section clearly illustrate the active movement of the plates and the role ophiolites portray in understanding those

movements. From North America to Siberia and the Mediterranean, the ophiolites depict the active tectonics during periods of global reorganization.

CHAPTER 5

LATE CRETACEOUS AND CENOZOIC OPHIOLITES

This chapter is divided into two sections. The first section covers the late Cretaceous and early Cenozoic (Paleocene). For this time period, sixty-four ophiolites are found emplaced in the regions of the Caribbean and in the Indo-Arabian-European zone. In the second half of this chapter, fifty-two ophiolite localities are described that range in age from Eocene to Miocene. These ophiolites are found in Southwest Pacific and India-Indonesia regions.

5.1 Late Cretaceous and Early Cenozoic ~100 – 50 Ma

There are sixty-four ophiolites presented in this section. These ophiolites are primarily located in Iran, Turkey, Eastern Europe, Pakistan, and the Middle Americas Caribbean region. This section discusses 14 Caribbean ophiolites and 43 Tethyan ophiolites with sub-regions discussed in each section along with ophiolites at eight other localities.

5.1.1 Late Cretaceous and Early Cenozoic Ophiolites

5.1.1.1 Late Cretaceous to Paleocene Ophiolites of North America and South America

The fourteen ophiolites in this section are located primarily in three sub regions of North America and South America: Cuba, Central America, and the remainder of North America and South America. These ophiolites are the result of the collision of the Cuban island arc with the Bahamas platform, the collapse of the Chortis backarc basin, and the advance of the Caribbean plate into the Central Atlantic.

The Western Belt ophiolite [7.06] in central Cuba formed during the Aptian (112 Ma) and were emplaced during the Paleocene to mid-Eocene (65 to 34 Ma). The ophiolite is a result of the collision of Cuban island arc with the Bahamas platform (Wadge et al., 1984; Fonsec et al., 1985; Mossakovskiy & Albear, 1978).

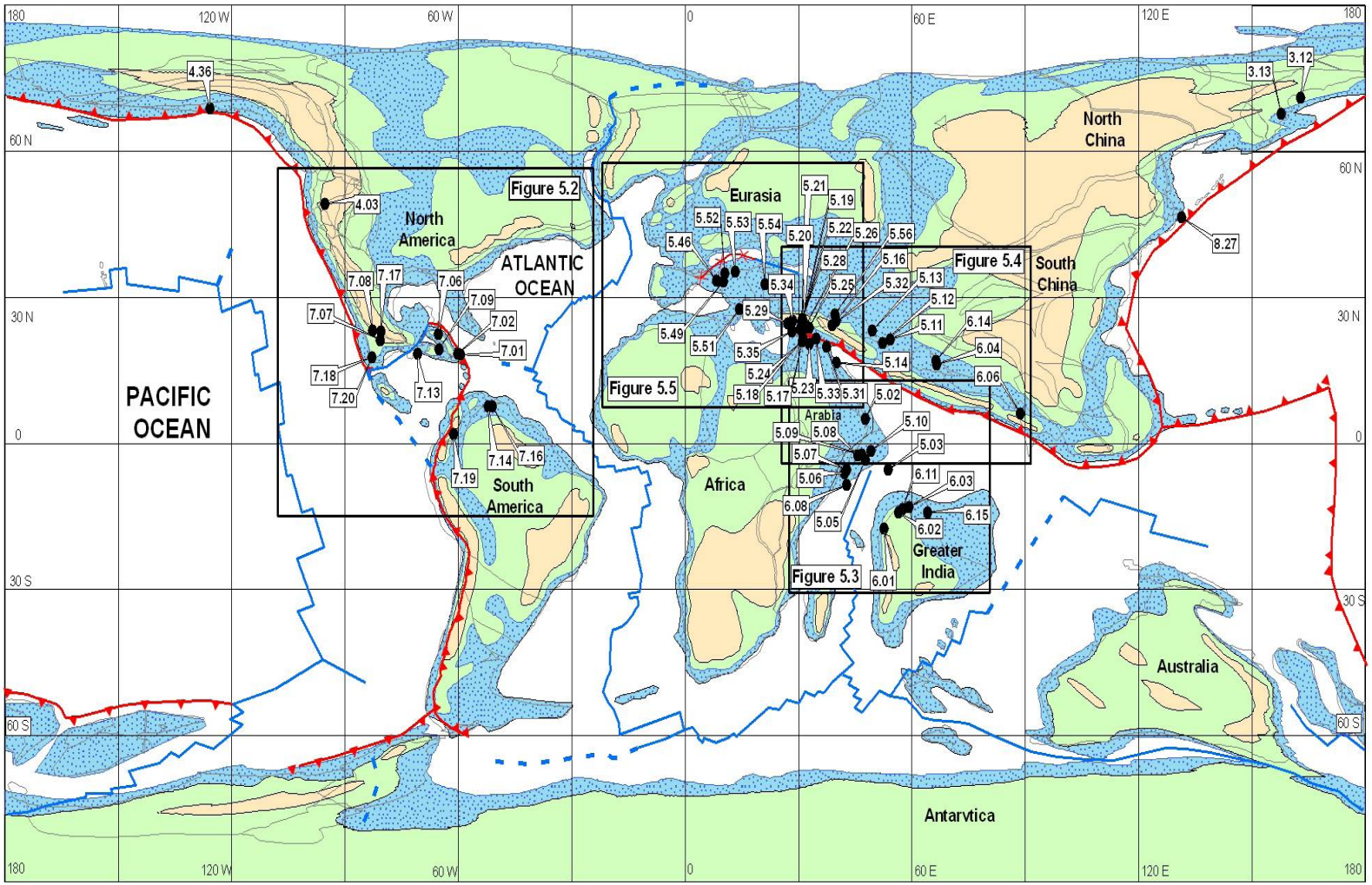

Figure 5.1 Late Cretaceous and Early Cenozoic ophiolite locations plotted on a 70 Ma paleogeographic reconstruction (Scotese, 2004)

Table 5.1 Late Cretaceous and Early Cenozoic Ophiolites

Ophiolite ID#	Map #	Name	Country	Age of Formation			Age of Obduction		
				Old Age	Young Age	Best Estimate	Old Age	Young Age	Best Estimate
7.14	10	Tinaquillo	Venezuela	89.00	85.80	87.40	85.00	65.00	75.00
7.16	10	Villa de Cura	Venezuela	100.00	100.00	100.00	99.00	55.00	77.00
7.19	10	Rio Calima	Columbia	112.00	66.00	89.00			
7.20	10	Esperanza	Costa Rica	99.00	83.50	91.25	84.00	84.00	84.00
7.18	10	Matapolo	Costa Rica	164.00	93.50	128.75	84.00	84.00	84.00
7.02	10	Nipe-Cristal	Cuba				65.00	61.00	63.00
7.01	10	Purial	Cuba				65.00	54.80	59.90
7.06	10	Western Belt	Cuba	112.00	112.00	112.00	65.00	50.00	57.50
7.08	10	Sierra de Las Minas	Guatemala	132.00	112.00	122.00	85.80	65.00	75.40
7.07	10	Sierra de Santa Cruz	Guatemala	132.00	99.00	115.50	83.50	65.00	74.25
7.09	10	North Coast	Hispaniola	93.50	89.00	91.25	65.00	55.00	60.00
7.13	10	Blue Mountains	Jamaica	83.50	71.30	77.40	71.00	55.00	63.00
7.17	10	Xolopa	Mexico	165.00	128.00	146.50	99.00	33.70	66.35
5.02	10	Semail	Oman	97.90	93.50	95.70	95.00	90.00	92.50
5.03	10	Sabzevar	Iran	99.00	65.00	82.00	65.00	65.00	65.00
5.05	10	Tchehel Kureh	Iran	99.00	65.00	82.00	65.00	65.00	65.00
5.06	10	Iranshahr	Iran	99.00	65.00	82.00	65.00	65.00	65.00
5.07	10	Fanuj Maskutan	Iran	99.00	65.00	82.00	65.00	65.00	65.00
5.08	10	Kahnuj	Iran	144.00	121.00	132.50	89.00	66.00	77.50
5.09	10	Esfandagheh	Iran	99.00	65.00	82.00	65.00	65.00	65.00
5.10	10	Shahr-Babak	Iran	144.00	65.00	104.50	65.00	65.00	65.00
5.11	10	Baft	Iran	99.00	65.00	82.00	65.00	65.00	65.00
5.12	10	Neyriz	Iran	95.00	93.00	94.00	89.00	89.00	89.00
5.13	10	Nain	Iran	144.00	65.00	104.50	65.00	65.00	65.00
6.08	10	Makran	Pakistan	95.00	95.00	95.00	93.50	89.00	91.25
5.14	10	Kermanshah	Iran				71.00	65.00	68.00
5.16	10	Khoy	Iran	103.00	98.00	100.50	96.00	95.00	95.50
5.17	10	Baër-Bassit	Syria	144.00	65.00	104.50	100.00	86.00	93.00
5.18	10	Kizildag	Turkey	99.00	74.00	86.50	86.00	65.00	75.50
5.19	10	Mersin	Turkey	96.00	91.50	93.75	90.00	61.00	75.50
5.20	10	Aladaj	Turkey	99.00	93.50	96.25	93.50	89.00	91.25
5.21	10	Kiziltepe	Turkey	92.00	90.00	91.00	78.30	65.00	71.65
5.22	10	Ali Hoca	Turkey	152.00	132.00	142.00	90.00	87.00	88.50
5.23	10	Yuksekova	Turkey	248.00	144.00	196.00	68.00	55.00	61.50
5.24	10	Yayladag	Turkey	248.00	144.00	196.00	68.00	55.00	61.50
5.25	10	Berit	Turkey	248.00	65.00	156.50	68.00	55.00	61.50
5.26	10	Pozanti-Karsanti	Turkey	94.00	70.00	82.00	78.30	65.00	71.65
5.28	10	Sarikaramn	Turkey	93.50	90.00	91.75	85.80	80.00	82.90
5.29	10	Antalya-Tekirova	Turkey	144.00	65.00	104.50	92.00	90.00	91.00
5.31	10	Cilo	Turkey	248.00	65.00	156.50	99.00	65.00	82.00
5.32	10	Gevas	Turkey	248.00	65.00	156.50	68.00	55.00	61.50
5.33	10	Guleman	Turkey	144.00	65.00	104.50	99.00	55.00	77.00
5.34	10	Beysehir	Turkey	144.00	65.00	104.50	95.00	80.00	87.50
5.56	10	Lesser Caucasus	Turkey	208.00	159.00	183.50	99.00	86.00	92.50

Table 5.1 *Continued*

Ophiolite ID#	Map #	Name	Country	Age of Formation			Age of Obduction		
				Old Age	Young Age	Best Estimate	Old Age	Young Age	Best Estimate
6.01	10	Bela	Pakistan	70.00	65.00	67.50	66.00	64.00	65.00
6.02	10	Muslim Bagh	Pakistan	87.00	65.00	76.00	70.00	65.00	67.50
6.03	10	Waziristan	Pakistan	115.00	100.00	107.50	70.00	68.00	69.00
6.11	10	Zhob	Pakistan	150.00	65.00	107.50	70.00	65.00	67.50
6.15	10	Dras Sangeluma	Pakistan	99.00	55.00	77.00			
5.35	10	Troodos	Cyprus	92.00	90.00	91.00	75.00	65.00	70.00
5.46	10	Monviso	Italy	206.00	144.00	175.00	99.00	65.00	82.00
5.49	10	External Liguride (Piedmont)	Italy	185.00	145.00	165.00	84.00	65.00	74.50
5.51	10	Calabria	Italy	206.00	144.00	175.00	106.00	65.00	85.50
5.52	10	Platta	Switzerland	206.00	144.00	175.00	99.00	65.00	82.00
5.53	10	Tauern	Austria	206.00	144.00	175.00	99.00	65.00	82.00
5.54	10	Apuseni (Romario)	Romania	206.00	180.00	193.00	144.00	55.00	99.50
6.04	10	Spontang	Ladakh	99.00	65.00	82.00	68.00	55.00	61.50
6.06	10	Tuensang	India				99.00	55.00	77.00
6.14	10	Shyok	Pakistan	144.00	99.00	121.50	99.00	15.00	57.00
4.36	10	Resurrection Peninsula	USA				57.00	57.00	57.00
4.03	10	Ingalls Complex	USA	180.00	144.00	162.00	99.00	99.00	99.00
8.27	10	Poroshiri	Japan	100.00	100.00	100.00			
3.13	10	Goven Peninsula	Russia	83.00	65.00	74.00			
3.12	10	Vyvenka	Russia	95.15	95.15	95.15			

The Purial [7.01] ophiolite of southeastern Cuba is reported by Wadge et al. (1984) to have been emplaced around 65 to 54.8 Ma. This complex was emplaced in thrust sheets that formed during the collision of the Cuban island arc with the Bahamas platform (Cobiella, 1978; Cobiella et al., 1977).

Nipe-Cristal [7.02] ophiolite, which is part of the Placetas Belt of southeastern Cuba, formed during the rifting event of the proto-Caribbean. It is reported by Wadge et al. (1984) to have been emplaced around 65 to 54.8 Ma (Cobiella et al., 1977; Cobiella, 1978; Bortolotti & Principi, 2005).

Figure 5.2 shows the Blue Mountains ophiolite [7.13] of eastern Jamaica that formed in an island arc system between 83.5 and 71.3 Ma. This ophiolite was obducted between 71 to 55 Ma and was emplaced as part of the Jamaica-Nicaragua Rise subduction complex (Wadge et al., 1982; Draper, 1986).

The North Coast ophiolite [7.09], in Hispaniola was formed between 93.5 and 89 Ma. This complex was emplaced as a result of transgressive strike-slip motion between Cuba and Hispaniola between 65 and 55 Ma (Wadge et al., 1984).

The Esperanza ophiolite [7.20] that is part of the Nicoya complex in northwestern Costa Rica was formed between 99 and 83.5 Ma (Bortolotti & Principi, 2005) and was emplaced around 84 Ma (Bourgois et al., 1982). The Matapolo ophiolite [7.18] in northwest Costa Rica was formed on the Farallon plate around 164 to 93.5 Ma and was emplaced onto the Caribbean plate during the Upper Santonian about 84 Ma (Bourgois et al., 1982; Wadge et al., 1984).

The Sierra de Las Minas ophiolite [7.08] in southeastern Guatemala was formed in a back arc basin between 132 and 112 Ma. It was emplaced as a result of the collapse of that back arc basin around 85.8 and 65 Ma (Muller, 1979; Williams, 1975; Wadge et al., 1984). The Sierra de Santa Cruz ophiolite in Guatemala [7.07] lies along the Montagua fault. It was formed, around 132 to 99 Ma, in a Cretaceous back arc basin. This complex was emplaced between 83.5 to 65 Ma (Rosenfeld, 1981; Wadge et al., 1984). The Xolopa ophiolite [7.17] in Southern Mexico formed sometime between 165 to 128 Ma. This complex was obducted sometime around the Late Cretaceous to Early Tertiary around 99 to 33.7 Ma (Nelson & Ratschbacher, 1994).

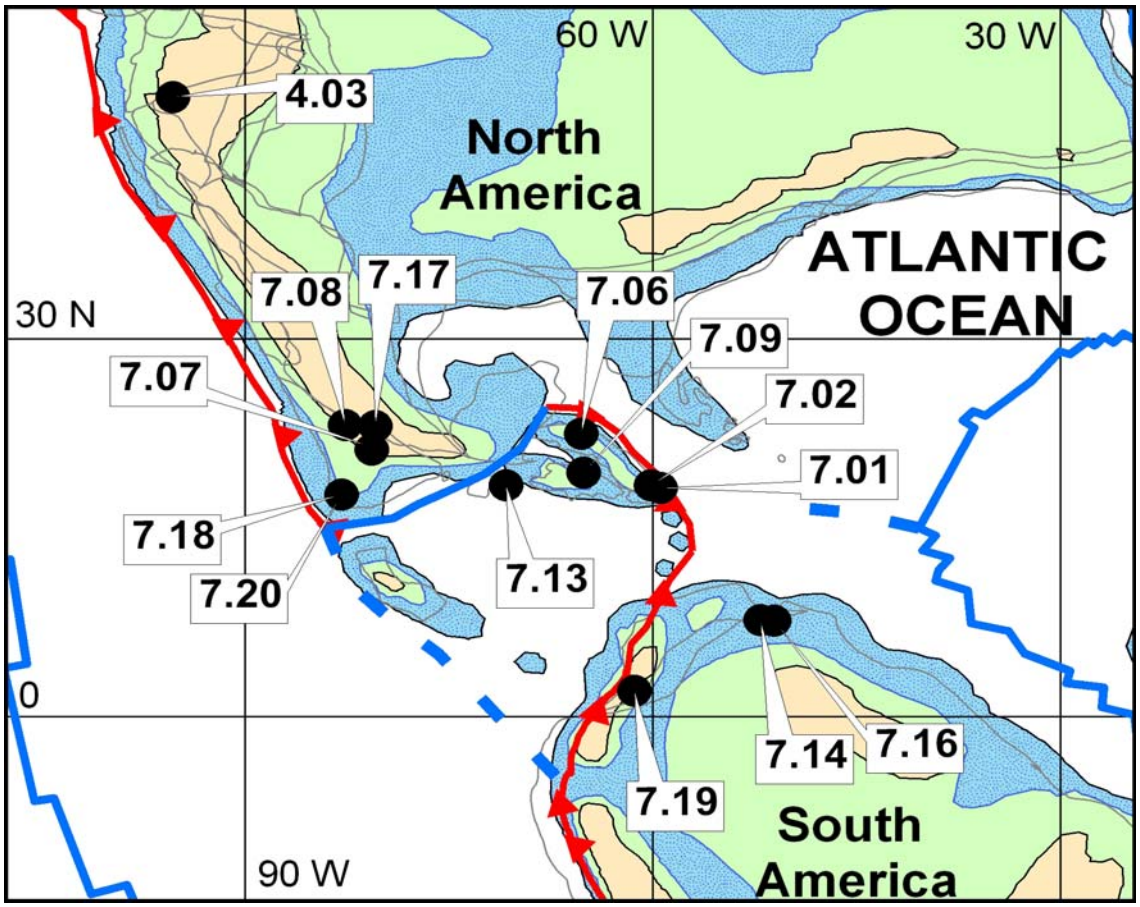

Figure 5.2 North American and South American ophiolites plotted on a 70 Ma paleogeographic reconstruction (Scotese, 2004)

The Tinaquillo ophiolite [7.14] in the Cojedes region of northern Venezuela formed between 89 and 85.8 Ma. It is reported to have been obducted around 85 to 65 Ma onto the South American continental margin (Seyler, et al., 1998 and Mackenzie, 1960). The Villa de Cura ophiolite [7.16] in eastern Venezuela formed around 100 Ma. This ophiolite was emplaced around 99 to 55 Ma onto the South American margin due to the eastward motion of the Caribbean plate (Gealey, 1980).

The Rio Calima [7.19] is part of the Buga-Buenaventura transverse in the Western Cordillera in western Columbia. This Andean ophiolite formed sometime between Albian and Maastrichtian time (112 to 66 Ma). This ophiolite complex is reported to have been obducted onto the South American plate sometime during the Paleocene (Bourgois et al., 1982).

5.1.1.2 Late Cretaceous to Paleocene Ophiolites of the Central Iran and India Regions

There are many ophiolitic complexes of Late Cretaceous and Early Cenozoic age in Iran and the surrounding regions (Figure 5.3). The Shahr-Babak [5.10] complex in central Iran was formed sometime between 144 and 65 Ma and obducted around the end of the Cretaceous (65Ma) (Ghazi & Hassanipak, 2000a).

In Iran, the Kahnuj ophiolite [5.08] is a well-studied complete ophiolite sequence with a completeness score of 6. The complex formed around 144 to 121 Ma along the mid-ocean ridge and was emplaced along the passive continental margin between 89 and 66 Ma (Kananian et al., 2001).

Esfandagheh [5.09] an ophiolite in south-central Iran formed around 99 to 65 Ma. It is was emplaced shortly before the Paleocene, around 65 Ma, when the small ocean basin around the Lut block closed as the Central Iranian microcontinent and the Sanandaj-Sirjan block collided (Ghazi & Hassanipak, 2000a; Pamić et al. 1979).

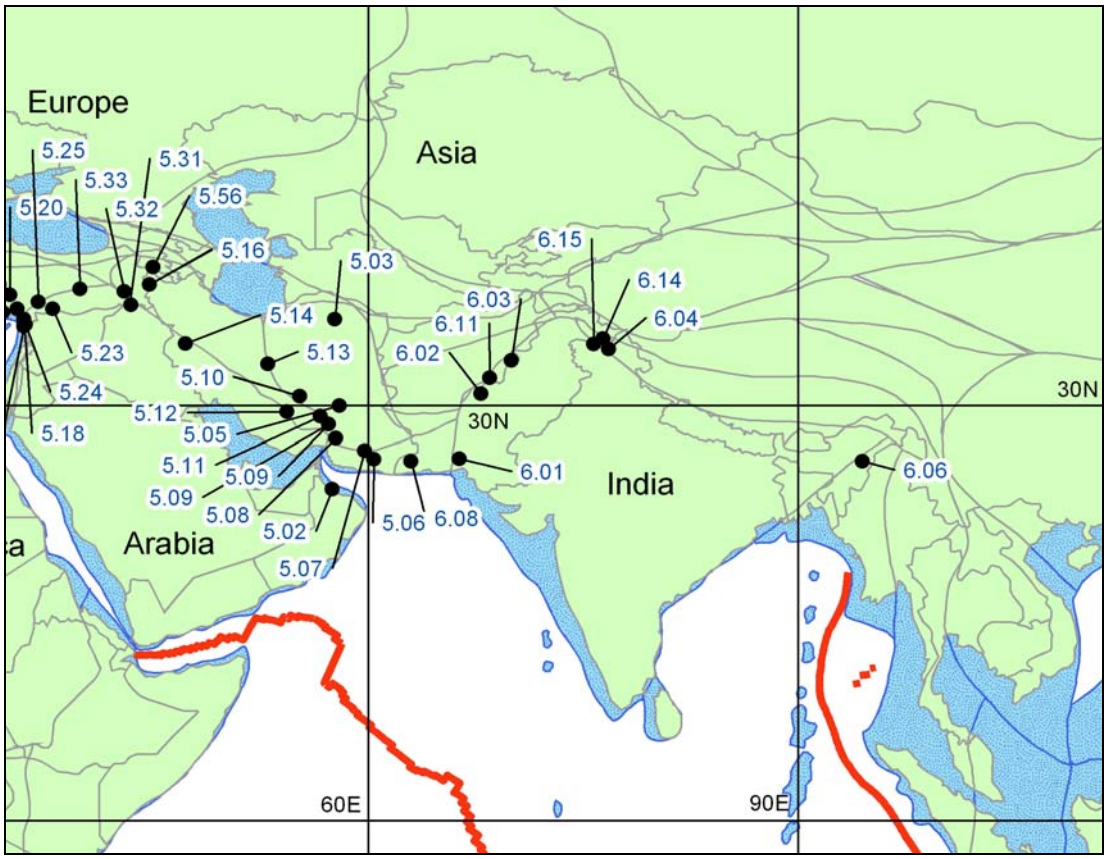

Figure 5.3 Ophiolites from the India and Central Iran regions illustrated on a modern map

The Sabzevar [5.03] ophiolite in northeast Iran formed around 99 to 65 Ma and was emplaced shortly before the Paleocene around 65 Ma. This ophiolite is thought to be a result of the ocean basin forming between the Lut block of Iran and the southern terranes of Afghanistan. It is suggested to have traveled northward as the block was emplaced during the late Paleocene as part of the Sanandaj-Sirjan micro-continental block (Ghazi & Hassanipak, 2000a; Pamić et al. 1979).

Oman has some of the best examples of obducted ophiolites in the world and the Semail ophiolite complex [5.02] in Oman is one of the more thoroughly studied

ophiolite sequences. This sequence formed at a fast spreading mid-ocean ridge around 97.9 to 93.5 Ma (Nicolas, 1989) and was obducted along the passive continental margin between 95 and 90 Ma (Cox et al., 1999; Nicolas & Boudier, 2000; Gray et al., 2000).

Tchehel Kureh [5.05] an ophiolite in eastern Iran, formed around 99 to 65 Ma. It is thought to have been emplaced shortly before the Paleocene around 65 Ma as a result of the ocean basin closing between the Lut block and Asia north of the Tethyan subduction zone (Ghazi & Hassanipak, 2000a; Pamić et al. 1979).

The Fanuj Maskutan [5.07] ophiolite in southeastern Iran formed around 99 to 65 Ma. It is reported to have been emplaced shortly before the Paleocene around 65 Ma as a result of the collapse of a backarc basin (Ghazi & Hassanipak, 2000a; Pamić et al. 1979).

A few ophiolite sequences are also found in western Pakistan. The Iranshar [5.06] ophiolite in the Makrãn Range of southern Pakistan formed around 99 to 65 Ma. It is reported to have been emplaced shortly before the Paleocene around 65 Ma as a result of the collapse of a backarc basin along the southern margin of Asia, prior to the collision of India (Ghazi & Hassanipak, 2000a; Pamić et al. 1979).

The Makrãn ophiolite [6.08] is located in the Central Makrãn Range in southern Pakistan along the Makrãn coast. It was formed in a spreading center around 95 Ma and was obducted onto the continental margin shortly thereafter, between 93.5 to 89 Ma (McCormick, 1991).

The Bela ophiolite [6.01] in Pakistan was emplaced between 70 and 65 Ma as part of a thrust sheet with Eurasia preceding the collision of India and is thought to have

formed along a spreading center. It was emplaced within the accretionary prism of the Sunaro Massif around 66 to 64 Ma in the North-South Axial zone of the Sulaimãn Range (Gnos et al., 1998; Ahmed & Ernst, 1999; Sarwar, 1992; Zaigham & Mallick, 2000; McCormick, 1991).

Muslim Bagh [6.02] is another ophiolite located in the Central Makrãn Range of Pakistan. This sequence also formed at the Cretaceous-Tertiary boundary as a result of the subduction event (McCormick, 1991; Gnos et al., 1998).

The Waziristan ophiolite [6.03] is located in the Sulaimãn Range of Pakistan. It formed at a spreading center around 115 to 100 Ma. This complex was emplaced around 70 to 68 Ma along the North-South Axial Zone (Moores et al., 1980; Shah & Khan, 1999).

The Zhob ophiolite [6.11] lies within the Sulaimãn Range in Pakistan. It is reported to have formed between 150 and 65 Ma in the backarc basin. This ophiolite was accreted around 70 to 65 Ma onto the western Indian margin before India's collision with Tibet (Gnos et al., 1997).

The Dras Sangeluma ophiolite [6.15] lies in the Great Himalaya Range of Pakistan. This ophiolite formed between 99 and 55 Ma and is part of the Indus Yarlung Zangbo suture (Robertson & Degnan, 1994).

The Shyok ophiolite [6.14] near the Nanga Parbat in northeastern Pakistan lies in the Great Himalaya Range. This complex was formed in a mid-ocean ridge around 144 to 99 Ma and was obducted onto the continental margin during the Eocene (Pêcher et al., 2002). The Spontang ophiolite [6.04] in Ladakh (western Himalayas) along the

Pakistan Zanskar zone formed around 99 to 65 Ma as part of the Tethyan ocean crust in a forearc basin and was obducted along the Dras island arc near the continental margin around 68 to 55 Ma (Mahmood et al., 1995; Searle & Stevens, 1980).

The Nagaland (Tuenshang) ophiolite [6.06] in India was obducted sometime during the Late Cretaceous to earliest Paleocene. It was obducted when the Indian plate collided with the Burmese plate (Agrawal & Kacker, 1980).

5.1.1.3 Late Cretaceous to Paleocene Ophiolites of Western Iran and Eastern Turkey

As seen in Figure 5.4, the Baft [5.11] ophiolites in south central Iran formed around 99 to 65 Ma within a mid-ocean ridge. It is reported to have been emplaced shortly before the Paleocene around 65 Ma as a result of the closing of a small ocean basin around the Lut block as the Central Iranian microcontinent and the Sanandaj-Sirjan block collided (Ghazi & Hassanipak, 2000a; Pamić et al. 1979).

The Neyriz complex [5.12] is located in the Zagros region of Southern Iran. This ophiolite formed between 95 and 93 Ma and was obducted around 89 Ma. It is thought to have been emplaced as part of the Central Iranian microcontinent collided with the Sanandaj-Sirjan block (Adib & Pamić, 1980; Pamić et al., 1979; Ghazi & Hassanipak, 2000a).

The Nain complex [5.13] in Iran lies within the eastern outskirts of the Zagros range. It formed sometime during the Cretaceous (144 – 65 Ma) and was obducted at the end of the Cretaceous period, 65 Ma (Ghazi & Hassanipak, 2000a).

The southeastern region of Turkey has many outcrops of ophiolites. The Kizildağ ophiolite [5.18] with a completeness score of six, formed on the Afro-Arabian plate along the mid-ocean ridge around 99 to 74 Ma. It was obducted between 86 and 65 Ma onto the continental margin (Dilek & Delaloye, 1992).

The Kermanshah ophiolite [5.14] in the Zagros region of western Iran was obducted around 71 to 65 Ma. It is thought to have been emplaced as a result of the Central Iranian microcontinent and the Sanandaj-Sirjan block colliding after being separated by a small ocean basin (Ghazi & Hassanipak, 1999; Ghazi & Hassanipak, 2000a).

The Baër-Bassit ophiolite [5.17] is located along the coastline in western Syria. It formed sometime between 144 and 65 Ma and was emplaced around 100 to 86 Ma. It is reported that sections of the oceanic crust began to slice off as the plate was emplaced onto the Arabian margin (Thuizat et al., 1981).

The Cilo ophiolite [5.31] in the Anatolia region of Turkey has been loosely dated as forming sometime from the Triassic to Cretaceous (248 to 65 Ma) (Dilek & Flower, 2003). An obduction age is reported by Yilmaz (1993) as between 99 and 65 Ma.

The Guleman ophiolite [5.33] lies within the Güneydogu Toraslar range of the Zagros Mountains. It formed during the Cretaceous and was obducted around 92 to 90 Ma onto the margin as the Arabian plate (Dilek et al., 1999; Yilmaz, 1993; Juteau et al., 1980).

The Yuksekova ophiolite [5.23] is located in the south-central region of Turkey and is part of the Southern section of the Taurus Mountains. It formed in an island arc environment around 248 to 144 Ma and was obducted onto the Arabian platform between 68 and 55 Ma (Yilmaz, 1993).

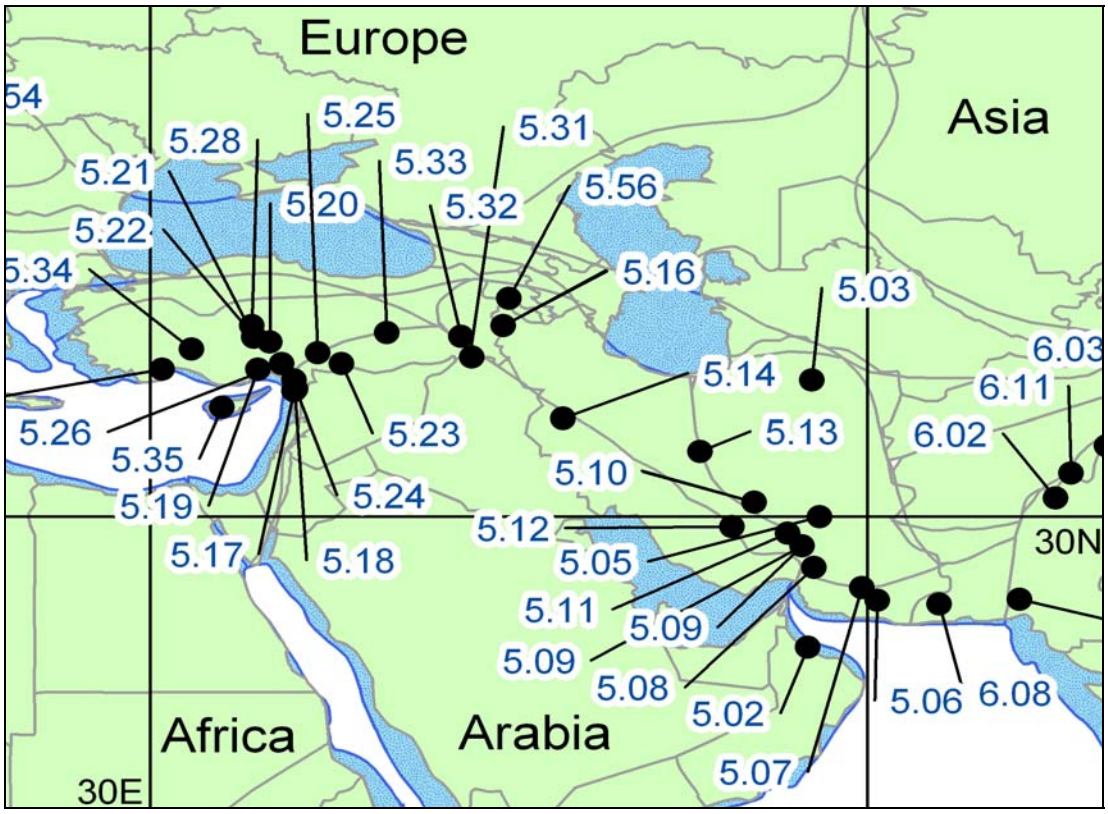

Figure 5.4 Ophiolites from the Arabian region illustrated on a modern map

The Yayladağ ophiolite [5.24] lies on the south central coastline of Turkey very near the border to Syria. This sequence formed around 248 to 144 Ma and was emplaced around 68 to 55 Ma (Yilmaz, 1993).

Gevas ophiolite [5.32] in eastern Turkey is part of the Anatolian orogenic belt. The ophiolite is near Lake Van in the Güneydogu Toraslar region of the belt. The formation of this sequence dates loosely between Triassic and Cretaceous (248 to 65 Ma) (Dilek & Flower, 2003). Yilmaz (1993) dates obduction at around 68 to 55 Ma and considers it part of the nappe within the orogenic belt.

The Lesser Caucasus ophiolite [5.56] lies within the Lesser Caucasus mountain range along the eastern Turkey border. It formed around 208 to 159 Ma and was emplaced between 99 and 86 Ma as the Afro-Arabian and Eurasian plates collided. This complex is considered a nappe sequence that has been thrust over the island arc along the Sevano-Akera zone (Knipper, 1991).

The Khoy ophiolite [5.16], in northwestern Iran, is located near the Bitlis-Zagros suture zone. It formed between 103 to 98 Ma obducted between 96 and 95 Ma. This is a complete sequence that likely formed at a spreading center as the Central Iranian microcontinent later combined with the southern Sanandaj-Sirjan block (Hassanipak & Ghazi, 2000b).

One of the well-studied sites in southern Turkey is the Ali Hoca ophiolite [5.22] formed between 152 and 132 Ma. This sequence lies along the Taurus Mountains and was obducted around 90 to 87 Ma (Alabaster et al., 1982; Dilek & Whitney, 1997).

The Berit ophiolite [5.25] in south-central Turkey lies in the southern regions of the Taurus Mountains. It has been given a more broad range of formation ages from 248 to 65 Ma. A more precise age for emplacement is reported to be of Paleocene age, between 65 and 55 Ma (Yilmaz, 1993).

The Antalya–Tekirova ophiolite [5.29] in southwestern Turkey lies along the coastline near the city of Antalya. It formed around 144 to 65 Ma and was obducted around 92 to 90 Ma along the continental margin. This ophiolite suite is unique in that it represents several sequences piled on top of one another (Juteau et al., 1980; Dilek et al., 1999; Yilmaz, 1993).

The Beysehir ophiolite [5.34] is located in the central region of Anatolia of Turkey. It formed during the Cretaceous and was obducted around 92 to 90 Ma as a result of the collision of the Arabian and Eurasian plates (Dilek et al., 1999; Yilmaz, 1993; Juteau et al., 1980).

The Troodos ophiolite [5.35] in Cyprus is probably one of the better-studied complete ophiolite sequences with a completeness score of 7. This ophiolite formed during the Late Cretaceous (92 to 90 Ma) and was emplaced around 75 to 65 Ma in a collapsing back-arc basin (Borradaile & Lucas, 2003; Robinson et al., 1983; Robertson & Woodcock, 1980).

The Mersin ophiolite [5.19] lies in the southern region of the Taurus Mountains along the coast of south-central Turkey. This is a fairly complete sequence, with a completeness score of four. It formed around 96 to 91.5 Ma. It was emplaced between 90 and 61 Ma as a consequence of the collision of the Arabian and Eurasian plates (Parlak & Delaloye, 1999).

The Kiziltepe ophiolite [5.21] formed along the northern region of the Taurus Mountains in central Turkey. The age of formation is around 92 to 90 Ma. It was emplaced around 78.3 to 65 Ma along the intra-oceanic subduction zone in the eastern

Mediterranean (Dilek & Whitney, 1997). The Aladaj ophiolite [5.20] is located near the Kiziltepe ophiolite in Turkey. This suite of ophiolitic rocks formed around 99 to 93.5 Ma and was emplaced around 93.5 to 89 Ma because of the Arabian and Eurasian plate collision (Dilek & Whitney, 1997). The Pozanti-Karsanti ophiolite [5.26], also in the Taurides of Turkey, formed around 94 to 70 Ma in a forearc environment. It was emplaced around 78.3 to 65 Ma along the subduction zone as Arabia collided with southern Turkey (Palat et al., 1996). The Sarikaramn ophiolite [5.28] in central Turkey formed around 93.5 to 90 Ma in the oceanic lithosphere. It was emplaced around 85.8 to 80 Ma along the subduction zone as the Arabian plate was pushed northward (Yaliniz et al., 2000).

5.1.1.4 Late Cretaceous to Paleocene Ophiolites of the Alpine Belt

As seen in Figure 5.5, there are many Eurasian ophiolites that formed during the Late Cretaceous and Paleocene. Some of these ophiolites have been instrumental in defining the classic ophiolite suite. There are six ophiolite locations in this sub-region.

The Monviso ophiolite [5.46] in northwestern Italy is reported by Lombardo et al. (1978) to be of Jurassic formation age (Figure 5.5). This ophiolite sequence has it's origin in the ocean to the north of the formation of the Apennine terrane and was obducted in the Late Cretaceous onto Alpine Europe (Rampone et al., 1998). The External Liguride (or Piedmont) ophiolite [5.49] in Italy formed between 185 and 145 Ma along a slow oceanic spreading center as the Mediterranean opened between the Eurasian plate and Africa. This suite of rocks was obducted sometime in the Late

Cretaceous (84 to 65 Ma) as the Adria plate thinned along the continental margin (Borsi et al. 1996; Marroni et al. 1998; Rampone & Piccardo, 2000).

The Platta ophiolite [5.52] in southeastern Switzerland located in the Lepontine region of the Alps. This suite formed along the slow spreading center sometime during the Jurassic. It is reported to have been obducted in the Late Cretaceous (Desmons, 1989). The Tauern Window complex [5.53] lies within the Hohe Tauern range in southwestern Austria. It is part of the Lower Austroalpine nappe system in the along the rim of the Penninic Tauern region. This complex formed in the Jurassic around 206 to 144 Ma. It was obducted sometime between 99 and 65 Ma along the continental margin as the crust began to thin (Desmons, 1989; Zimmerman et al., 1994; Raith et al. 1977).

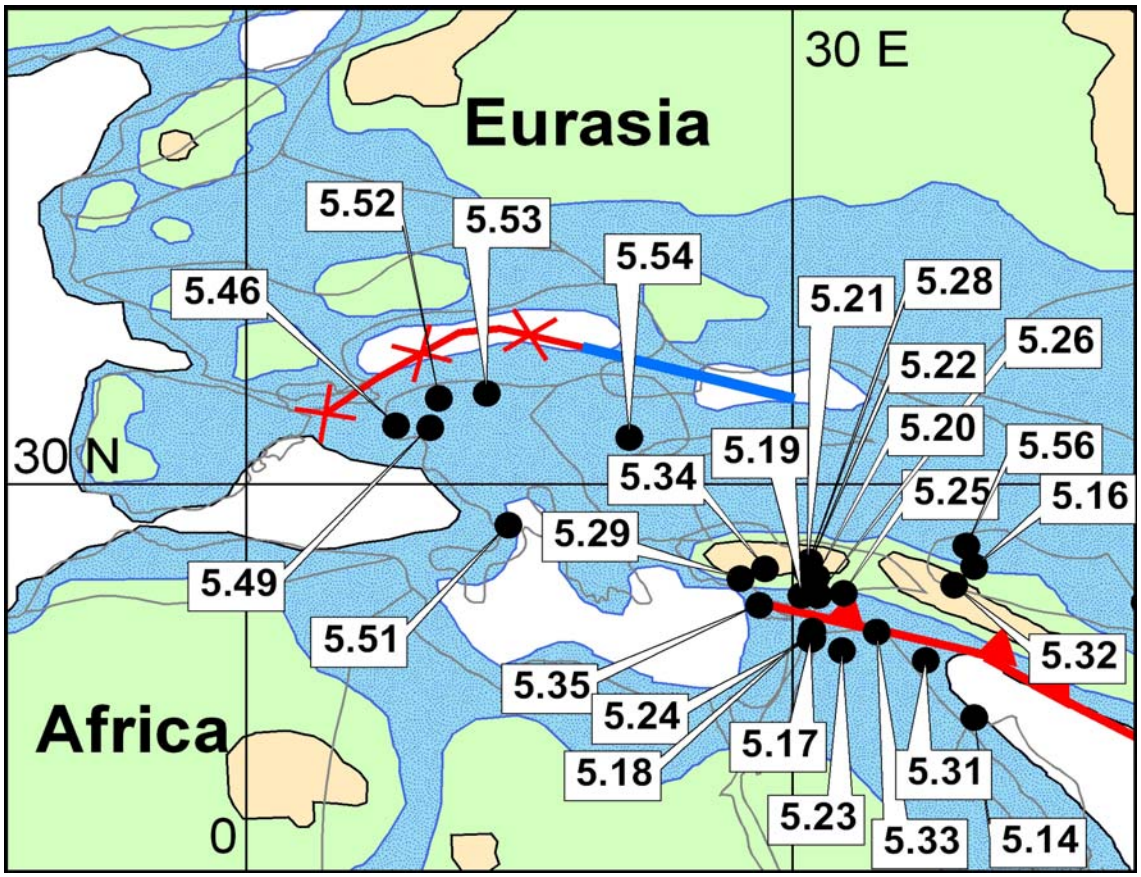

Figure 5.5 Ophiolites from the regions of Western Iran, Eastern Turkey, and Nujiang-Co plotted on a 70 Ma paleogeographic reconstruction (Scotese, 2004)

The Apuseni (Romario) ophiolite [5.54] in central Romania lies on the northern edge of the Transylvanian Alps. It was formed around 206 to 180 Ma due to the rifting event and was obducted onto the Eurasian continental margin sometime during the Cretaceous (Herz and Savu, 1974; Nicolae & Saccani, 2003).

The Calabria ophiolite [5.51] in central Italy is in the southern end of the Apennine belt. It formed sometime in the Jurassic also likely as a result of the rifting

event. It was obducted in the Late Cretaceous as part of the collisional event with the Eurasian margin (Beccaluva et al. 1980; Desmons, 1989).

5.1.1.5 Other Notable Later Cretaceous to Early Cenozoic Ophiolites

In Alaska, the Kenai Peninsula (also called the Resurrection Peninsula) an ophiolite [4.36] is reported by Cole et al. (2006) to have been emplaced between 70 and 57 Ma. This complex lies along the Sanak-Baranof belt as part of the Kula-Resurrection ridge and was emplaced due to the Aleutian megathrust accreted terrane (Cole et al., 2006; Kusky et al., 1997; Kusky & Young, 1999).

In North America, the Ingalls Complex [4.03] forms a belt around the southern region of Mount Stuart Batholith in the North Cascades of Washington. It was formed around 180 to 144 Ma at a spreading ridge. This ophiolite was accreted onto the continental margin of North America around the Navaho Divide fault in the Middle Cretaceous (99 Ma) (Nicolas, 1989; Miller & Mogk, 1987; Southwick, 1974; Miller, 1985).

The Poroshiri ophiolite [8.27] in Hokkaido Japan formed around the Albian Cenomanian boundary (99Ma). This ophiolite is a complete complex, completeness score of 7, and is part of the nappe structure and mélange of Northeastern Japan and is reported to have been obducted in an island arc-marginal basin environment as the Pacific plate subducted beneath the Eurasian plate (Ishiwatari, 1990a; 1990b).

The Vyvenka ophiolite [3.12] in the Koryak Mountains of Russia formed around 95 Ma. This ophiolite has no emplacement age but is assumed to have been

emplaced along the margin as a result of subduction beneath northeast Siberia (Suren, 1986; Palandzhjan, 1986). The Goven Peninsula ophiolite [3.13], also in the Koryak Mountains, formed in the Campanian between 83 and 65 Ma. This ophiolite is part of the East Kamchatka Belt and is assumed to have been accreted sometime in the late Paleocene (Suren, 1986; Palandzhjan, 1986).

5.1.2 Late Cretaceous to Paleocene Tectonics

Most of the ophiolites described in this section were formed in the western part of Tethys and were emplaced as Tethys closed. The five principle tectonic events in western Tethys were: 1) the collision of the Apulian prong, (Greece and Turkey with Northern Europe), 2) the collision of an island arc with Northern and Eastern Arabia (the Oman ophiolites), 3) the rifting and collapse of back arc basins around the Central Iranian micro-continent, 4) the collision of India with the island arcs fringing south-central Asia, and 5) the collapse of the Bangong–Nujiang–Co back arc basin along the southern margin of Eurasia.

As Arabia collided with Eurasia and Tethys closed, modern-day Greece and Turkey also collided with the Balkans resulting in the Hellenides and Dinarides Mountains, which resulted in many ophiolitic emplacements (Pamić, 1977). Ophiolites [5.46, 5.49, 5.51 – 5.54] formed during the subduction zone that resulted from the Balkan collision (Dilek & Flower, 2003; Scotese, 2001). Further south as Arabia collided with Iran [5.11 – 5.14, 5.16 – 5.26, 5.28, 5.29, 5.31 – 5.35, and 5.56]. These

were emplaced due to subduction and accretion onto Eurasia along the Zagros and Taurus Mountains (Hassanipak and Ghazi, 2000b).

The other group of ophiolites described in this chapter is associated with Late Cretaceous to early Cenozoic tectonic events in the circum-Caribbean regions. These tectonic events include: 1) the collision of Cuba with the Bahamas platform, 2) the collapse of the Chortis back arc basin, and the 3) emplacement of ophiolites along the northern margin of South America as a consequence of the intrusion of the Caribbean plate and subduction of the proto-Caribbean. The ophiolites [7.01, 7.02, 7.06 – 7.09, 7.13, 7.14, 7.16 – 7.20, and 4.03] are expressions of these tectonic events (Pindell et al., 1982; Wadge et al., 1984).

In the Late Cretaceous, the Izangi plate was subducting under the eastern margin of Northeast Siberia. The remnant ophiolites [8.27 in Japan, 3.12 and 3.13 in Russia], were emplaced during this tectonic episode (Lytwyn et al., 1997).

5.2. Middle to Late Cenozoic ~50 – 0 Ma

5.2.1 Eocene, Oligocene, and Miocene Ophiolites

During the Miocene, Oligocene and Eocene, ophiolites (Figure 5.6 and Table 5.2) were obducted primarily in three regions: 1) the Southwest Pacific and Southeast Asia with twenty-three localities, 2) India and Tibet with twenty-two localities, and 3) seven other localities worldwide.

5.2.1.1 Indian – Tibetan Collisional Ophiolites

The Indus Yarlung Zangbo suture zone is well known for the numerous ophiolites that occur along the coliision zone between India and Tibet. In this study, 17 of ophiolite localities stretch along the Himalayan front from 75° E to 92° E. Eight ophiolites [6.23-6.25, 6.27-6.31] are described as being part of the southern range in the Himalayas. These were obducted along the suture zone (Dupuis et al., 2005) that closed in the mid-Tertiary, 65 to 34 Ma (Rowley, 1996 & 1998). The age of the ocean floor that makes up these ophiolites is more difficult to pinpoint but the best age range, is late Jurassic to early Cretaceous (178 to 123 Ma and 163 to 150 Ma) (Dupuis et al., 2005; Rowley, 1996).

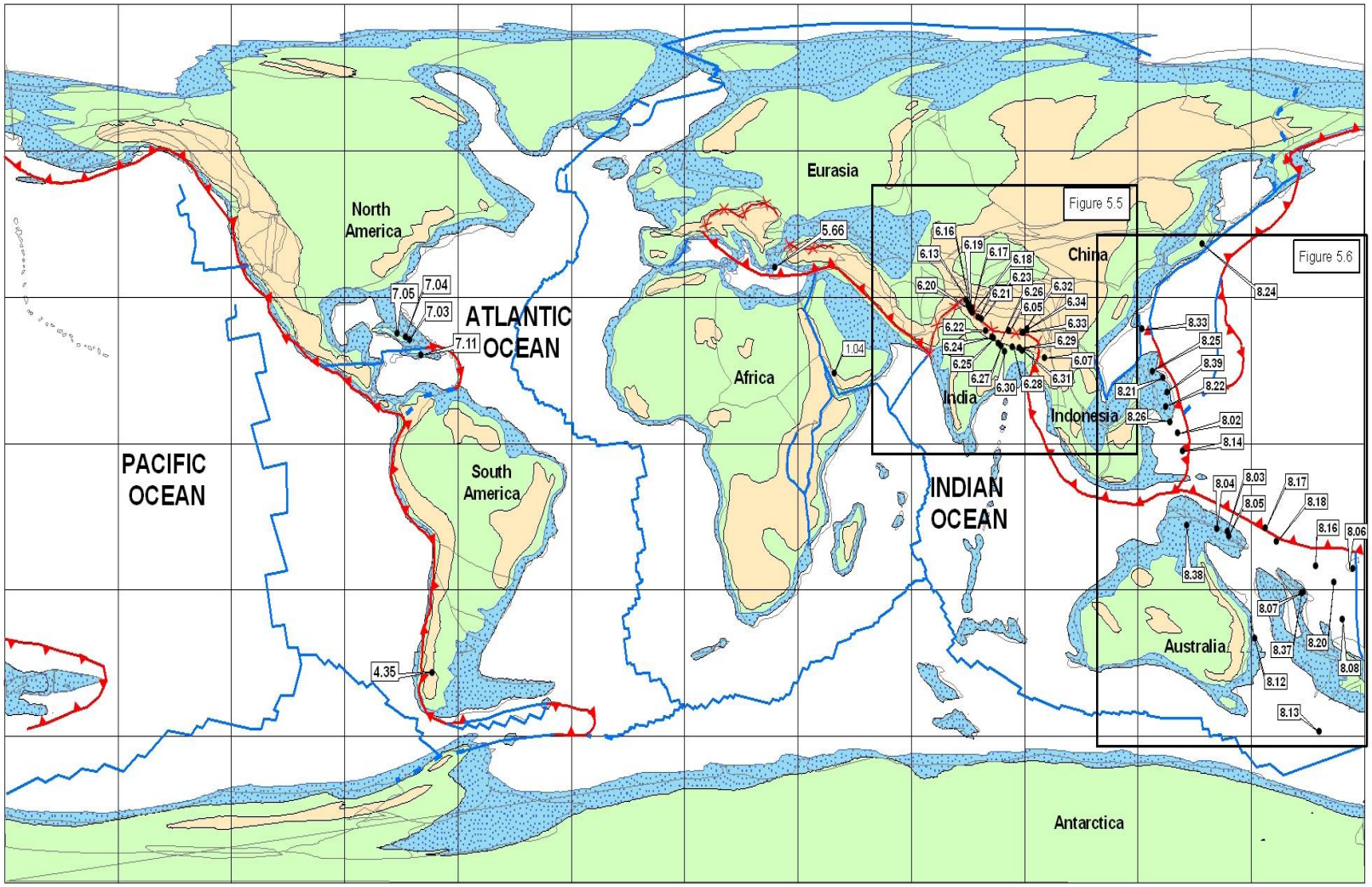

Figure 5.6 Cenozoic ophiolite locations plotted on a 20 Ma paleogeographic reconstruction (Scotese, 2004)

Table 5.2 Eocene, Oligocene, and Miocene Ophiolites

				Age of Formation			Age of Obduction		
Ophiolite ID#	Map #	Name	Country	Old Age	Young Age	Best Estimate	Old Age	Young Age	Best Estimate
6.16	10	Indus - Yarlung Zangbo	China	130.00	110.00	120.00	65.00	34.00	49.50
6.17	10	Indus - Yarlung Zangbo	China	130.00	110.00	120.00	65.00	34.00	49.50
6.18	10	Indus - Yarlung Zangbo	China	130.00	110.00	120.00	65.00	34.00	49.50
6.19	10	Indus - Yarlung Zangbo	China	130.00	110.00	120.00	65.00	34.00	49.50
6.20	10	Indus - Yarlung Zangbo	China	130.00	110.00	120.00	65.00	34.00	49.50
6.21	10	Indus - Yarlung Zangbo	China	130.00	110.00	120.00	65.00	34.00	49.50
6.22	10	Indus - Yarlung Zangbo	China	130.00	110.00	120.00	65.00	34.00	49.50
6.23	10	Indus - Yarlung Zangbo	China	163.00	150.00	156.50	65.00	34.00	49.50
6.24	10	Indus - Yarlung Zangbo	China	163.00	150.00	156.50	65.00	34.00	49.50
6.25	10	Indus - Yarlung Zangbo	China	163.00	150.00	156.50	65.00	34.00	49.50
6.26	10	Indus - Yarlung Zangbo	China	163.00	150.00	156.50	65.00	34.00	49.50
6.27	10	Indus - Yarlung Zangbo	China	163.00	150.00	156.50	65.00	34.00	49.50
6.28	10	Indus - Yarlung Zangbo	China	163.00	150.00	156.50	65.00	34.00	49.50
6.29	10	Indus - Yarlung Zangbo	China	178.00	123.00	150.50	65.00	34.00	49.50
6.30	10	Indus - Yarlung Zangbo	China	178.00	123.00	150.50	65.00	34.00	49.50
6.31	10	Indus - Yarlung Zangbo	China	178.00	123.00	150.50	65.00	34.00	49.50
6.32	10	Indus - Yarlung Zangbo	China	178.00	123.00	150.50	65.00	34.00	49.50
6.33	10	Indus - Yarlung Zangbo	China	178.00	123.00	150.50	65.00	34.00	49.50
6.34	10	Indus - Yarlung Zangbo	China	178.00	123.00	150.50	65.00	34.00	49.50
6.07	10	Moreh	India	85.00	75.00	80.00	49.00	42.00	45.50
6.13	10	Nanga Parbat	Pakistan	144.00	65.00	104.50	23.00	6.00	14.50
6.05	10	Xigaze Dagzhuka	Tibet	110.00	100.00	105.00	50.00	40.00	45.00
4.35	10	Taitao	Chile	11.20	5.30	8.25			
7.11	10	Southern Peninsula	Hispaniola	93.50	71.30	82.40	55.00	5.00	30.00
7.04	10	Camaguey	Cuba	112.00	112.00	112.00	54.80	41.30	48.05
7.03	10	Holguin-Gibara	Cuba	121.00	121.00	121.00	54.80	41.30	48.05
7.05	10	Las Villas	Cuba	112.00	112.00	112.00	49.00	34.00	41.50
1.04	10	Tihama - Asir	Saudi Arabia	24.00	20.00	22.00			
5.66	10	Cyclades (Evia)	Greece	99.00	65.00	82.00	25.00	17.00	21.00

Table 5.2 *Continued*

				Age of Formation			Age of Obduction		
Ophiolite ID#	**Map #**	**Name**	**Country**	**Old Age**	**Young Age**	**Best Estimate**	**Old Age**	**Young Age**	**Best Estimate**
8.12	10	Baryulgil	Australia	65.00	34.00	49.50	34.00	23.80	28.90
8.13	10	Macquarie Island	Australia	12.00	9.50	10.75	5.00	0.00	2.50
8.38	10	Cyclops	E Indonesia	43.00	29.00	36.00	23.00	5.00	14.00
8.06	10	Fiji	Fiji	33.70	23.80	28.75	14.00	7.00	10.50
8.14	10	Obi (E Indonesia)	Indonesia	99.00	33.70	66.35	25.00	25.00	25.00
8.22	10	Izu Bonin	Izu Bonin	41.80	40.80	41.30			
8.24	10	Hayama Mineoka	Japan	65.00	24.00	44.50			
8.37	10	Koniambo Massif	New Caledonia	54.00	42.00	48.00	49.00	34.00	41.50
8.07	10	New Caledonia	New Caledonia	65.00	55.00	60.00	37.00	34.00	35.50
8.08	10	Northland Allochthon	New Zealand	144.00	65.00	104.50	40.00	20.00	30.00
8.20	10	Tonga	New Zealand	49.00	41.30	45.15			
8.03	10	April Ultramafic	Papua New Guinea	54.80	33.70	44.25	33.00	24.00	28.50
8.04	10	Marum	Papua New Guinea	121.00	65.00	93.00	37.00	17.00	27.00
8.05	10	Papua Ultramafic Belt	Papua New Guinea	144.00	65.00	104.50	55.00	34.00	44.50
8.17	10	Solomon Islands 1	Papua New Guinea	54.80	33.70	44.25	37.00	34.00	35.50
8.18	10	Solomon Islands 2	Papua New Guinea	54.80	33.70	44.25	37.00	34.00	35.50
8.39	10	Palawan	Philippines	248.00	144.00	196.00	23.00	5.00	14.00
8.25	10	Zambales	Philippines	37.00	33.70	35.35			
8.21	10	East Sulawesi	Sulawesi	144.00	65.00	104.50	65.00	23.80	44.40
8.33	10	Taiwan Ophiolite	Taiwan	5.00	1.80	3.40	1.80	1.00	1.40
8.02	10	E Timor Island	Timor				8.00	5.00	6.50
8.26	10	W Timor Island	Timor	23.00	1.80	12.40	11.00	0.10	5.55
8.16	10	New Hebrides	Vanuatu	54.80	33.70	44.25	37.00	34.00	35.50

Another section of the Indus-Yarlung Zangbo complex [6.16-6.22] Lies along the Karakorum Range of the Himalayas along the northwestern collision zone between India and Tibet. They are reported to have formed in a back arc tectonic environment (Rowley, 1996) and are reported by Dupuis et al. (2005) to have formed around 130 to 110 Ma for the locations at 90° E to 94° E. These ophiolites were obducted sometime during the Paleocene to Eocene (Hébert et al., 2003; Dupuis et al., 2005).

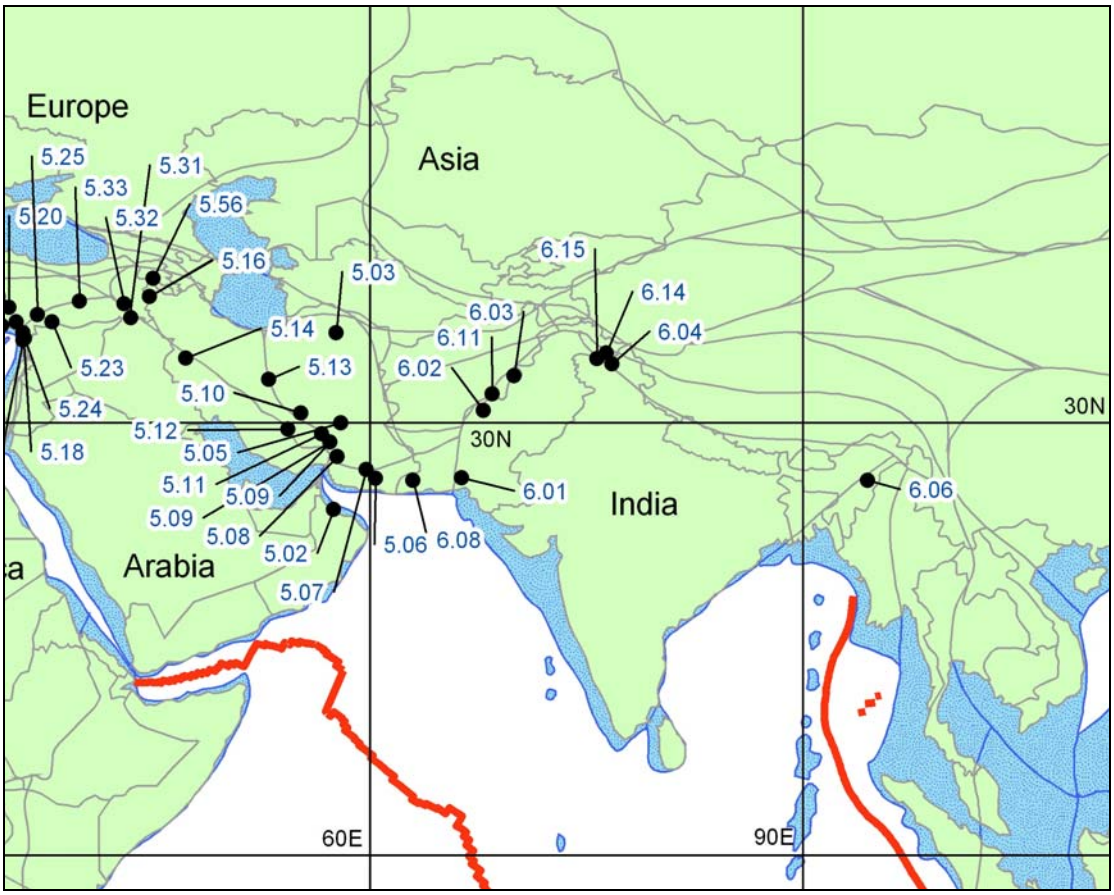

Figure 5.7 Late Cenozoic ophiolites along the Tibet – India collision zone illustrated on a modern map

Ophiolites, that are not formally named, occur along the Indus-Yarlung Zangbo suture (Figure 5.7). These ophiolites were obducted as a result of the Indian and Eurasian plate collision during the Cretaceous, as previously mentioned. The Xigaze Dagzhuka ophiolite [6.05] in Tibet lies along the Himalayan suture within the Lhasa block of Tibet. It formed in a forearc basin sometime between 110 and 100 Ma. This sequence was obducted around 50 to 40 Ma as a result of collision of the Indian plate and the Eurasian plate (Hébert et al., 2003; Nicolas, 1989).

Another section of ophiolites [6.26, 6.32-6.33] is a result of the collision of India and Eurasia and lies within the Himalayas. This section of ophiolites was formed between 178 and 123 Ma as a result of the rifting in a Jurassic ocean basin. These ophiolites were emplaced sometime during the Paleocene to Eocene (65 – 34 Ma) as a result of the Himalayan suture (Dupuis et al., 2005).

In Pakistan, the Nanga Parbat ophiolite [6.13] part of the Himalayan region of Ladakh, formed sometime during the Cretaceous. This sequence was one of the more recent ophiolites emplaced, sometime during the Early Miocene, because of the India-Tibet collision (Pêcher et al., 2002).

The Manipur, or Moreh, ophiolite [6.07] in the Ukhrul region of India appears in the Arakan Mountain range. It is reported by Vidyadharan et al. (1989) to have formed around 85 to 75 Ma in an ocean basin. The suite was obducted onto Burma in the mid-Eocene around 49 to 42 Ma during the collision of the Indian plate and Tibetan region (Morely, 2001; Vidyadharan et al., 1989).

5.2.1.2 Middle to Late Cenozoic Ophiolites of Southeast Asia and the Southwest Pacific

In eastern Sulawesi, or Celebes, Indonesia, an ophiolite [8.21] has been reported by Rangin et al. (1990) to have formed in a spreading center during the Cretaceous. It was emplaced as part of the island arc sometime during the Paleogene to Early Miocene (Rangin et al., 1990; Parkinson et al., 1998).

The Island of Timor has two ophiolitic locations. The West Timor Island ophiolite [8.26] is associated with the subduction zone that includes the Banda Arc.

This ophiolite sequence formed sometime during the Miocene and was emplaced in the last few million years (Pleistocene) (Sopaheluwakan et al., 1989). The formation date for the East Timor ophiolite [8.02] is still debated and questions have been raised as to whether it is really a true ophiolite. The "ophiolitic sequence" on East Timor does follow the typical Oman-type sequence but some features are not analogous. What is clear is that the East Timor ophiolite was emplaced along the Australian continental margin around 8 to 5 Ma as the southern part of the Banda arc (Harris & Long, 2000).

The Zambales ophiolite [8.25] in the Philippines lies along the western margin of Luzon Island. It is a two-part complete sequence consisting of the Coto Block and Acoje Block and comprises the Masinloc Massif, the Cabangan Massif, and the San Antonio Massif. This suite formed during the Late Eocene as part of an island-arc-back-arc system. It was obducted in the very recent geologic past (Zhou et al. 2000).

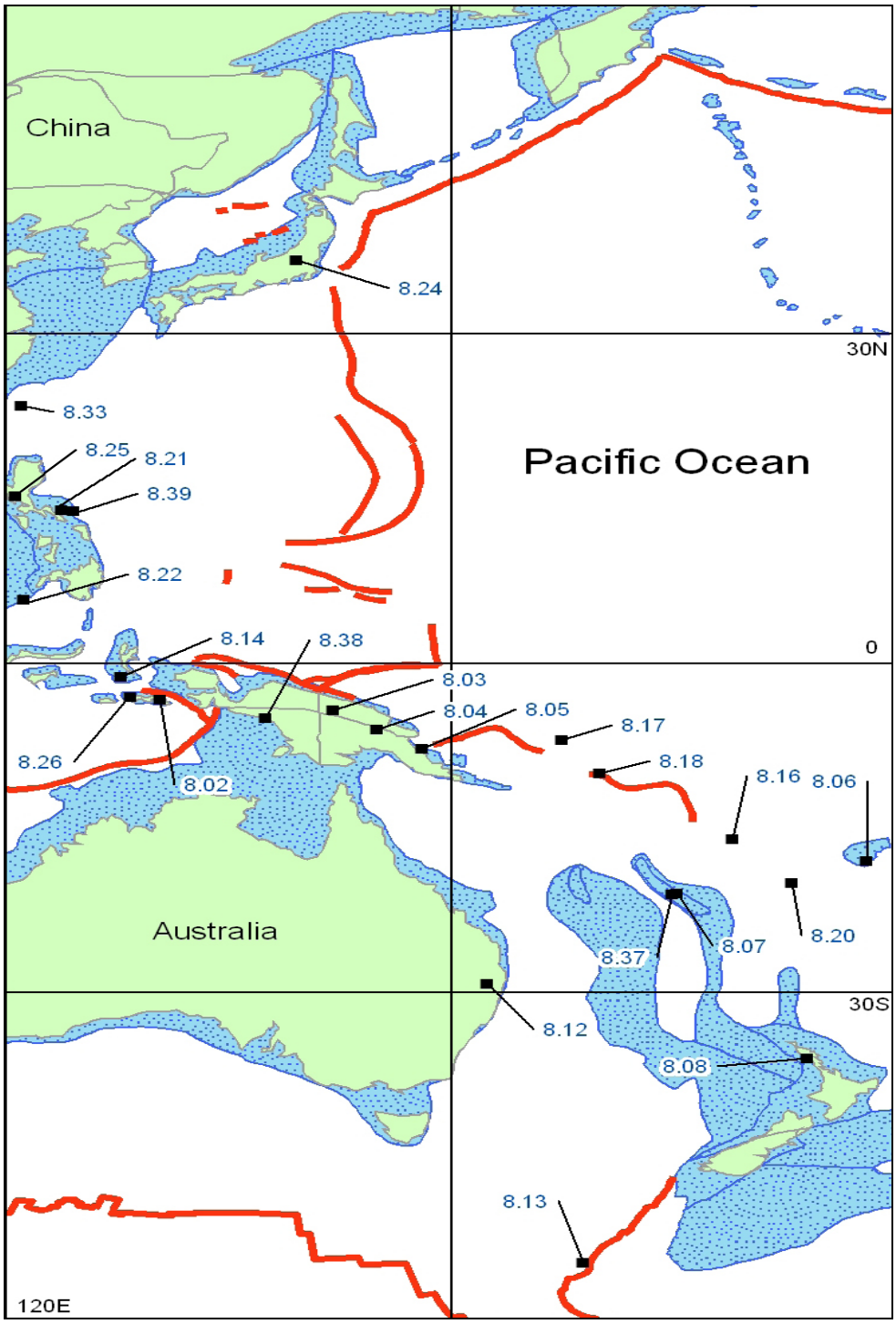

Figure 5.8 Southwest Pacific late Cenozoic ophiolites illustrated on a modern map

The April Ultramafic ophiolite [8.03] in the western Sepik plains of Papua New Guinea is an incomplete complex, missing the mafic component, with a completeness score of 4. It is reported to have formed during the Eocene and was emplaced during the Oligocene as a consequence of the arc-continental collision of the Bismark arc with the Australian plate (Milsom, 1984; 2003).

Closely related to the April Ultramafic complex is the Marum ophiolite [8.04], of the Maoke Mountains of Papua New Guinea. Marum is a mostly complete sequence, with a completeness score of five, which formed around 121 to 65 Ma. This suite was emplaced as part of the Bismark arc – Australian collision in the Late Eocene to Early Miocene (Milsom, 1984).

The Cyclops ophiolite [8.38] in Indonesian Irian Jaya lies in between Australia's northeastern border and the New Guinea Islands. This complex formed between 43 and 29 Ma in the backarc basin environment. It was emplaced between 23 to 5 Ma along the Australian continental margin (Gnos & Peters, 1997).

The Southwest Pacific ophiolite referred to as the Papua Ultramafic Belt [8.05] lies within the Owen Stanley Range. These rocks formed sometime during the Cretaceous as a result of seafloor spreading in the Woodlark basin. These were emplaced during the Eocene arc collision with New Guinea (Spray, 1984).

The Solomon Islands have two ophiolite locations [8.17 & 8.18], which lie, along the southern region of the Ontong-Java plateau. These were later emplaced in the Late Eocene (37 to 34 Ma) (Coleman, 1966; Parrot & Dugas, 1980).

The ophiolite found in New Caledonia [8.07], which lies off the northeastern coast of Australia, is part of the nappe system of the Massif du Sud. It was formed around 60±5 Ma in the Paleocene backarc basin. It was emplaced along the subduction zone around 37 to 34 Ma as part of Tangihua complex (Audet et al., 2004; Nicholson et al., 2000a; Prinzhofer et al., 1980).

The Koniambo massif in New Caledonia [8.37] lies in the northern region of the Norfolk ridge. It formed between 54 and 42 Ma in a backarc basin environment. It was emplaced along the subduction zone between 49 and 34 Ma (Audet et al., 2004).

The Fiji ophiolite [8.06] in Viti Levu was formed sometime around 33.7 to 23.8 Ma in the south Fiji backarc basin. It was emplaced sometime between 14 and 7 Ma in the arc. Colley (1984) reports paleomagnetic data suggests that the Fiji ophiolite rotated 180-degrees during the interval between formation and obduction.

The New Hebrides ophiolite [8.16] in Vanuatu was formed between 54.8 and 33.7 Ma during the Eocene. It was emplaced between 37 and 34 Ma along the arc as the plate subducted under the Pacific (Coleman, 1970; Parrot & Dugas, 1980).

The Tonga ophiolite [8.20] lies in the Southwest Pacific Tonga Trench. It was formed sometime between 49 and 41.3 Ma in a forearc environment, and is thought to have been emplaced as a result of subduction (Fisher & Engel, 1968; Banerjee et al., 2000).

Several theories have been proposed to explain the Northland ophiolite [8.08] in New Zealand (Malpas et al., 1992). Whattam et al. (2005) date formation of this ophiolite, with $^{206}Pb/^{238}U$ ages obtained from zircon analysis, between 29 and 26 Ma

with emplacement occurring shortly thereafter. A very different date is given by Davis (1971) who dates the ophiolite forming between 144 and 65 Ma with emplacement in the Oligocene around 30 Ma. It is also not clear what the tectonic environment of formation for the Northland ophiolite was. Hopper & Smith (1996) and Whattam (2005) suggest the Northland ophiolite forming in a suprasubduction, or island arc subduction, environment whereas Cande & Kent (1995) suggest that it formed along an oceanic spreading center. On the other hand, Nicholson et al. (2000b) used zircon from diorite to analyze the suite of rocks, and suggested that the ophiolite may have formed in a back-arc basin environment, 32 to 28 Ma. With eastern Gondwana undergoing extension and fragmentation during the Late Cretaceous (Hall, 2002) it is possible both of these theories are correct and that there may have been multi-phase ophiolite formation in this region.

The Baryulgil ophiolite [8.12] in eastern Australia lies along the Great Dividing Range. This suite was formed sometime during the Early to Middle Paleogene and was obducted during the Oligocene around 33.7 to 23.8 Ma, although the mechanism of emplacement is not clear (Aitchison et al., 1994).

An ophiolite [8.13] occurs on Macquarie Island, south of New Zealand that has dated at 12 to 9.5 Ma. It is thought to have formed as a result of the spreading between the Australian and Pacific plate. The emplacement occurred around 5 Ma and likely contributed to the formation of the island itself (Hopper & Smith, 1996, Malpas et al., 1994, and Varne et al., 2000).

The Obi ophiolite [8.14] in eastern Indonesia along the Sorong fault formed on the Philippine plate as part of an intra-ocean-arc around Late Cretaceous to Paleogene. This sequence was emplaced during the Banda arc-continent collision with Australia around 25 Ma (Hall, 2002).

The Philippines Palawan ophiolite [8.39] is reported by Gealey (1980) to have formed between 248 and 144 Ma. It was emplaced around 23 to 6 Ma as fragments of the Asian continent collided with a forearc in the South China Sea.

The Izu-Bonin ophiolite [8.22] in the Pacific lies along the convergent plate margin. It is part of the Izu-Bonin-Mariana system and was formed between 41.8 and 40.8 Ma as part of the forearc of these islands. This region is reported to be a result of the rapid growth of the plates in the last 50 million years (Taylor, 1992).

The Taiwan ophiolite [8.33] is an example of an ophiolite that has formed very recently (in the last 5 million years). This ophiolite is suggested to have been emplaced between 1 and 2 million years ago (Bor-ming, 1996; Sopaheluwakan et al., 1989).

In central Japan, the Hayama Mineoka ophiolite [8.24] was formed between 65 and 24 Ma. It is thought to be emplaced as a result of the subduction event along the continental margin of northeast Eurasia (Ogawa & Taniguchi, 1987).

5.2.1.3 Other Notable Middle to Late Cenozoic Ophiolites

South America and Cuba have a few ophiolites that likely formed during the Early Cretaceous and were emplaced later during the Eocene. The Camaguey ophiolite [7.04] in Cuba formed during Pre-Aptian time (112 Ma). It was emplaced during the

Paleocene to mid-Eocene. The ophiolite was carried by mélange-bearing thrusts onto the Bahamas platform around 65 to 34 Ma as the Caribbean plate collided with the southern margin of North America (Wadge et al., 1984; Mossakovskiy & Albear, 1978).

The Southern Peninsula ophiolite [7.11] in southern Hispaniola was formed around 93.5 to 71.3 Ma. It was part of thrusted slabs that were emplaced during Caribbean subduction sometime during the Eocene to Miocene (Wadge et al., 1984 and Maurasse et al., 1979).

The Holguin-Gibara ophiolite [7.03] in southeastern Cuba formed sometime before the Aptian (121 Ma). It was emplaced as imbricated recumbent thrusts over the Bahamas platform around 54.8 to 41.3 Ma (Kozary, 1968; Wadge et al., 1984).

The Las Villas ophiolite complex [7.05] was also formed Pre-Aptian (112 Ma) was emplaced during the Paleocene to Mid Eocene (65 to 34 Ma). This sequence is thought to have a mélange at the base and to have been emplaced in thrust sheets that overlay the Bahamas platform (Wadge et al., 1984; Mossakovskiy & Albear, 1978).

In Chile, the Taitao sequence [4.35] yields formation ages of 11.2 to 5.3 Ma. The data indicates that it formed in a forearc rift above the ridge along the western margin of the South American plate. It was eventually obducted as the Pacific plate subducted beneath the South American plate (Nelson et al., 1993).

The Cyclades [5.66] is ophiolitic mélange, in Evia, Greece, which formed during the Upper Cretaceous in an oceanic basin. It is part of the Attic-Cycladic Massif in Southern Evia, which was derived from protoliths of Mesozoic age. This sequence

was emplaced in the Late Oligocene to Early Miocene due to accretion during subduction events of the Eocene (Katzir et al., 2000; Dilek & Flower, 2003).

Tihama – Asir [1.04], an ophiolite complex near Jizar, Saudi Arabia along the eastern coastal plains of the Red Sea, was formed in the Neogene around 22 to 20 Ma. It is thought to be the result of tectonic crustal attenuation between the Arabian plate and the African plate as the Red Sea opened (Schmidt & Brown, 1982; Coleman, 1984).

5.2.2 Eocene, Oligocene, and Miocene Tectonics

The tectonics of the Late Cenozoic in Southeast Asia and the Southwest Pacific is complex and a coherent plate tectonic model has yet to be proposed (Milsom, 2003). However, there are good regional models describing the tectonic evolution of Southeast Asia (Rangin et al, 1990; Hall, 2002) and the southwest Pacific (Pubellier et al., 1999). No single model unites all these regional models in one grand synthesis.

This chapter gives a review of the ophiolites that formed and were emplaced in four principal regions. First, the collision of India with Tibet (Eurasian plate) just before 50 Ma is likely to have been the nursery grounds for the formation of the Indus-Yarlung-Zangbo suture and many of the noted ophiolites [6.05, 6.07, 6.13, and 6.16 – 6.34] (Nicolas, 1989; Laurent-Charvet et al., 2005). The Indus Yarlung Zangbo suture formed as the Northwest Himalayas began to form and the Tethys subducted with Eurasia, (Gnos et al., 1997; Nicolas, 1989).

The second principal region of ophiolites was reported for the collision of Australia with Southeast Asia [8.03 – 8.08, 8.12, 8.13, 8.16 – 8.18, 8.20, and 8.37]. The

third region was the assembly of the Philippines and its collision with Southeast Asia [8.02, 8.14, 8.22, and 8.26]. The last region described was the recent back arc basin formation in the Western Pacific [8.21, 8.24, 8.25, 8.33, and 8.39] (Hall, 2002; Scotese, 2001; Rangin, 1990; Dilek, & Flower, 2003).

Other Cenozoic ophiolites from other parts of the world include the Tihama-Asir ophiolite in Saudi Arabia, and are a result of the Arabian plate rifting with the African Plate and the continued opening of the Red Sea (Coleman, 1984). The Taitao ophiolite in Chile was a result of the Pacific plate subducting beneath the South American plate (Nelson et al., 1993)

The Cenozoic ophiolites portray the active tectonics of the earths recent past. The Southwest Pacific region has been particularly active during the Cenozoic and the complex nature of its origin and tectonics has been the focus of much modern research in the Geoscience community. The evidence clearly shows that there is much more research yet to be done to understand the complex nature of global reorganization even from the earths recent Cenozoic past.

CHAPTER 6

DISCUSSION AND CONCLUSIONS

If I have seen farther than others, it is because I was standing on the shoulder of giants...
-Sir Isaac Newton

The final chapter of this thesis discusses the temporal pattern of ophiolite formation and emplacement. Not all ophiolite localities are equivalent. In order to eliminate errors due to poor age constraints or geographic clustering, several filtering and resampling techniques were used to remove unreliable or redundant data. The questions raised in the first chapter will be revisited; namely: 1) what are the temporal and spatial patterns of ophiolite formation and obduction? and 2) what does the spatial-temporal pattern of ophiolite formation and obduction imply about plate tectonic processes? The data collected from this study indicates that the temporal pattern of ophiolite formation and obduction have followed global reorganization of the plates and that Peak ophiolite formation and emplacement events occurred during the Ordovician, Jurassic, and Late Cretaceous. This chapter will present the evidence that supports this conclusion.

6.1 Introduction to Ophiolite Analysis Methods

The following section presents several methods of analysis to understand the ophiolite data and their pattern through time. These are separated into two subsections, Paleozoic and Mesozoic - Cenozoic, with each section having separate discussions on formation data and emplacement data.

The ophiolite data compiled in these sections are presented as histograms with frequency along the vertical axis and ophiolite age along the horizontal axis. This presentation of the data is in raw form with no biases removed. This raw data set is useful for comparison to the filtered and declustered results, as well as presenting a comparison to other research in the literature. The data was then filtered by removing age data that was poorly constrained. After presentation of the filtered data, the ophiolite frequency histogram is shown by removing the geographic clusters. Next is a discussion of tectonic environments. Lastly, there is a combined analysis, which includes the filtered and declustered methods.

Table 6.1 shows a synthesis of the information contained within the ophiolite database. A total of 280 ophiolite localities described in this study. However, only 92% had an age of formation and 71% had an age of emplacement, with 14 localities with no verifiable age of formation or emplacement. As previously mentioned, this study included as many ophiolites as could be found at the time of this research.

The reliability of data is key to interpreting the validity of the maps for this study. As seen in Table 6.1 the data can be filtered in many ways and assumptions and

conclusions can be made from those statistics. As the data is filtered, there are fewer localities that comprise each filtered set; yet the data becomes more accurate after removing the bias. The data was sorted to depict an accurate illustration of the geologic events in which the ophiolites were forming and being emplaced. Within these filters, the statistics speak for themselves.

Table 6.1 Summary of Distribution of Ophiolites

Summary of Ophiolite Data				
	Formation		Emplacement	
Category	Number	Percentage	Number	Percentage
Ophiolites with Age Data	258	92%	198	71%
Ophiolites with Reliability of 1	135	20%	132	67%
Ophiolites with Reliability of 2	60	23%	44	22%
Ophiolites with Reliability of 3	63	24%	22	11%
Ophiolites with Tectonic Environment Data	177	69%	138	70%
Filtered Ophiolites	180	70%	123	62%
Declustered Ophiolites	165	64%	122	62%
Combined 'Refined' Data	121	47%	84	42%

Category	Number	Percentage
Difference Between Formation and Emplacement age <20 MA	72	27%
Difference Between Formation and Emplacement age >20 and <41 MA	34	13%
Ophiolites with Completeness Score of 6-7	28	25%
Ophiolites with Completeness Score of 4-5	58	51%
Ophiolites with a Completeness Score 3 or less	28	25%
Ophiolites with no Specific Rock Reference for Completeness Score	166	59%
Ophiolites with No Age Data	14	5%
Total Number of Ophiolites Found for this study	280	100%

6.2 Analysis of Raw Ophiolite Data

6.2.1 Combining Ophiolite Mean Ages Using Variable Time Intervals

In order to visually determine how robust the temporal patterns of ophiolite formation and emplacement are, the mean ophiolite ages of formation and emplacement were resampled using time windows of five and ten million years (Figures 6.1, 6.2, 6.3, 6.4). There is inherent bias in the raw data in the form of an over abundance of data in certain well studied geographic locations such as California. In addition, some of the age data may be considered less reliable; some literature sources cited a wide range for ophiolite age of formation or emplacement depending on the various dating techniques. This yielded large differences in the maximum and minimum age estimates, especially among Paleozoic and Precambrian ophiolites. Some ophiolite data may be considered less reliable if the ophiolite is an incomplete sequence, see 'Completeness Score' field in Appendix A. Only ophiolites for which there were assigned ages of formation and or emplacement were included in this resampling method. In the following section, the Paleozoic ophiolite data is reviewed in the next section as well as the ophiolite data for the Mesozoic and Cenozoic.

6.2.2 Temporal Distribution of Paleozoic Ophiolites

6.2.2.1 Paleozoic Ages of Ophiolite Formation

The temporal distribution of 54 Paleozoic ophiolite locations, defined by the formation age, is shown in Figures 6.1 and 6.2. These data display a few marked peaks. The peaks noted as 4 and 5 in Figures 6.1 and 6.2 are likely to be ophiolites that formed in association with the breakup of the late Proterozoic Pangea, Pannotia, and the opening of the Iapetus Ocean during the Cambrian as seen in Figure 3.4. The group of peaks including those marked 2 and 3 are likely due to the basins forming in the Proto-Tethys, Paleo-Tethys, Rheic Oceans as noted in Figure 3.5. The Early Carboniferous, peak 1, is likely to be ophiolites, which resulted from the Paleo-Tethys opening, and the separation of Siberia and Euramerica as noted on Figure 3.8. Figure 6.2 shows the same distribution of data, which has been filtered at 10 million year intervals, and yields peaks at the same geologic times. Comparison of these two figures shows there is very little change in the overall pattern of the distribution of the ophiolite formation ages over time when sorted either at 5 million or 10 million intervals. Of the 54 ophiolites, 35 occur between 510 and 435 Ma comprising about 65% of the Paleozoic ophiolites.

Figures 6.1 and 6.2 illustrate that there are several ‘quiet’ times in which there is a lack of ophiolite data, namely the late Carboniferous and Permian (340 to 255 Ma). There are also significantly less ophiolites forming in the Early Carboniferous and Devonian when compared to the Ordovician and Silurian.

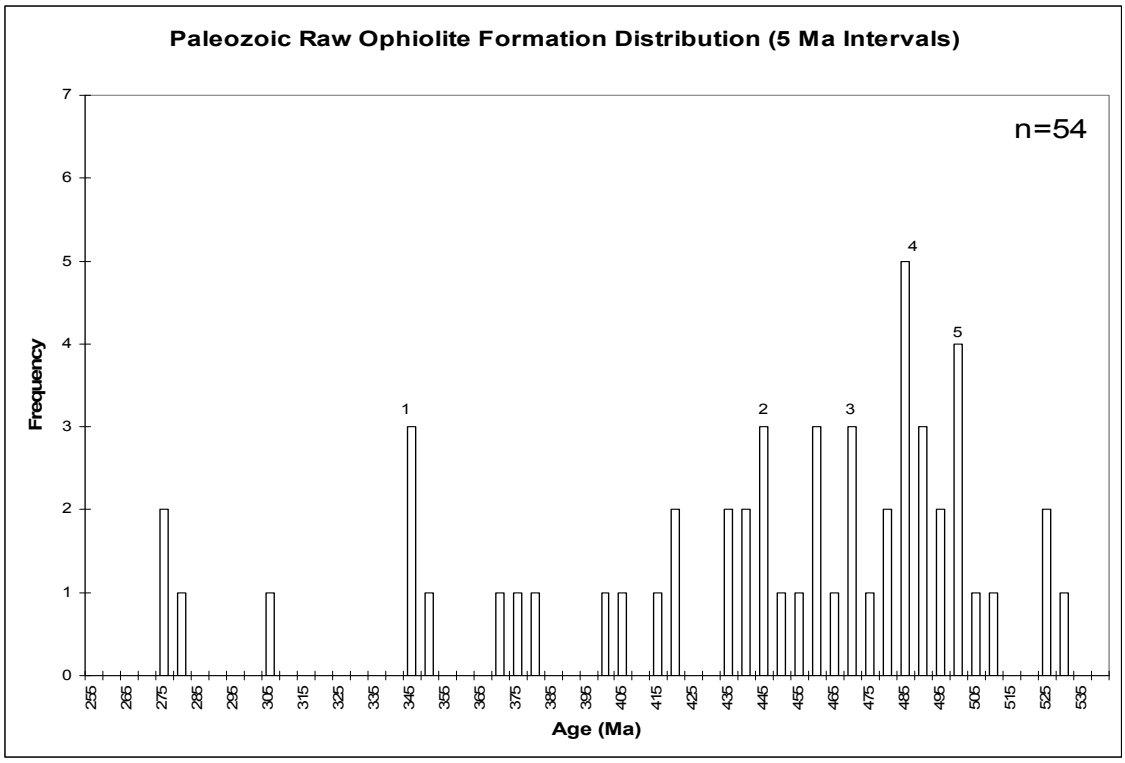

Figure 6.1 Paleozoic ophiolite formation raw data (5 Ma)

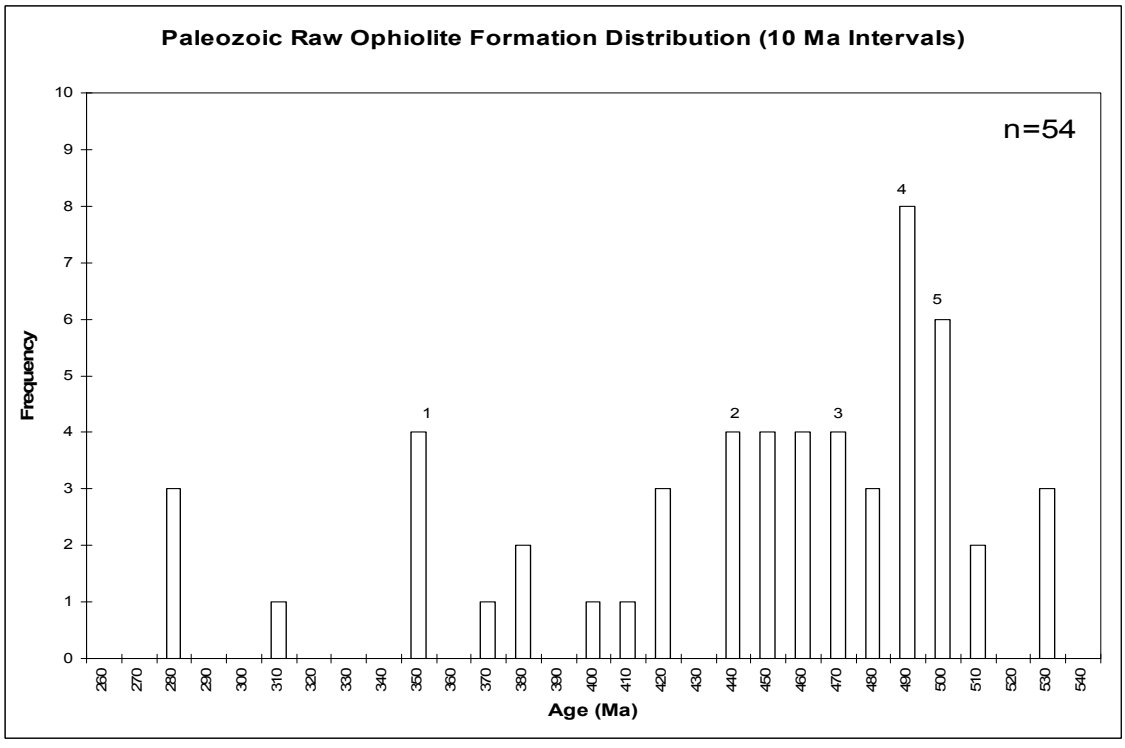

Figure 6.2 Paleozoic ophiolite formation raw data (10 Ma)

6.2.2.2 Paleozoic Ages of Ophiolite Emplacement

The temporal distribution of the age of emplacement of 34 Paleozoic ophiolites is depicted in Figures 6.3 and 6.4. The peaks noted as two and three in Figure 6.3 generally depict the Caledonian ophiolites which were emplaced as a result of the subduction events along the eastern margin of Laurentia and the western borders of Baltica, as well as the subduction between the Proto-Tethys and the northern margin of Baltica occurring during the early Ordovician through late Devonian. The ophiolites emplaced during the peak, marked as one in Figure 6.3, are Permian ophiolites which were emplaced during the formation of Pangea. These Paleozoic ophiolites show an average rate of emplacement at about two ophiolites per 5 million years. Notable times of an absence of Paleozoic ophiolite emplacement occur during most of the Carboniferous (350 to 295 Ma). This is unusual because this was the time during which western Pangea was being assembled and more evidence of ophiolite obduction would have been expected

Figure 6.4 depicts the same obduction events grouped in 10 million year intervals. 26 of the 34 Paleozoic ophiolite emplacement ages are similar when plotted at either 5 million or 10 million year intervals. In addition, 50% of Paleozoic emplacement events occur during a relatively brief 60 million year time interval during the Ordovician and Silurian. Obduction events between 480 and 350 Ma making up about 76% of all of the Paleozoic ophiolites that were emplaced in the raw data set.

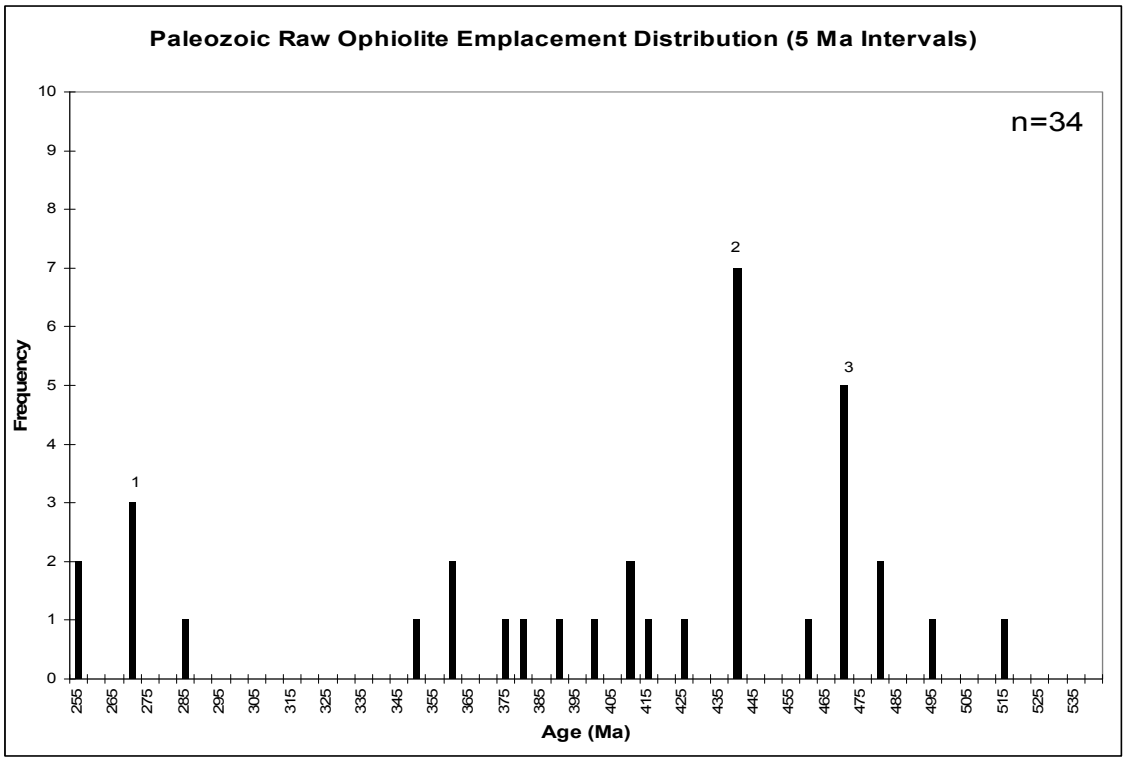

Figure 6.3 Paleozoic ophiolite emplacement raw data (5 Ma)

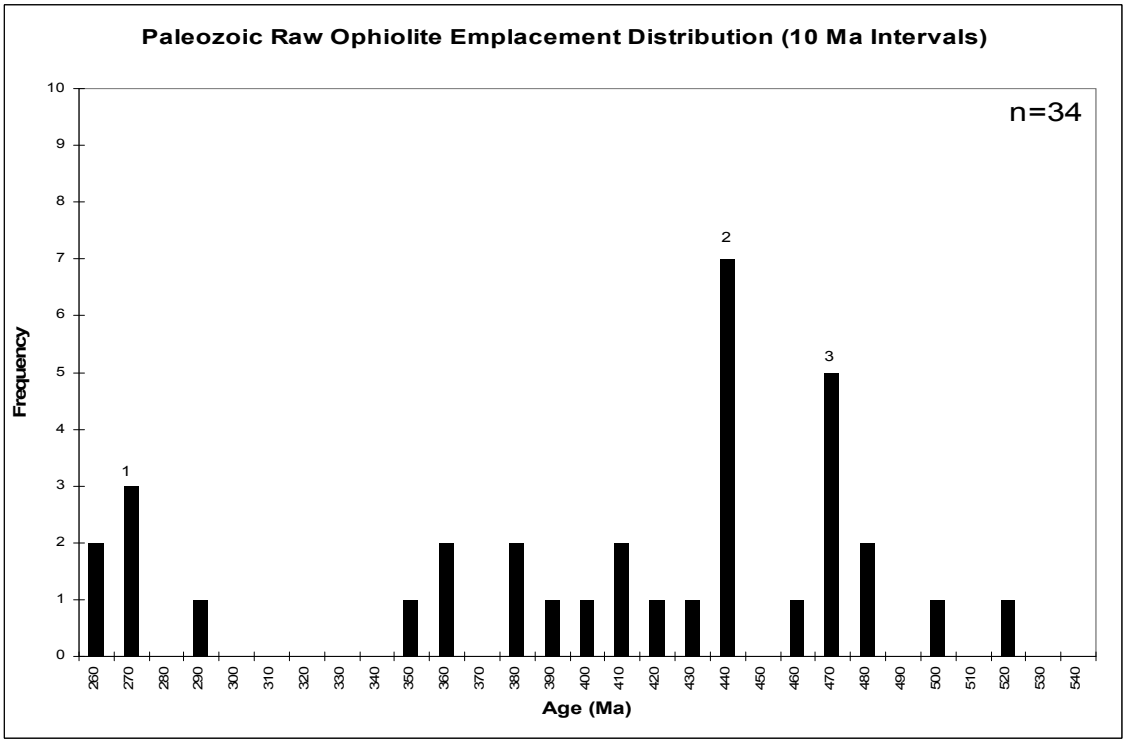

Figure 6.4 Paleozoic ophiolite emplacement raw data (10 Ma)

6.2.3 Temporal Distribution of Mesozoic and Cenozoic Ophiolites

6.2.3.1 Mesozoic and Cenozoic Ages of Ophiolite Formation

Figures 6.5 and 6.6 show the distribution of 175 ophiolites which formed during the Mesozoic and Cenozoic. The pattern of ophiolite formation is distinctly bimodal with broad peaks centered on 165 million years, 105 million years, and to a lesser degree 45 million years. The ophiolites, which are noted at peaks 6, 7, and 8 on Figure 6.5, formed in the Pacific Ocean basin during the middle to late Jurassic. Peak 5 represents ophiolites that formed during the Early Cretaceous in the Pacific Ocean, as well, within the ocean floor in the Tethys Ocean, north of India. Peaks 2, 3, and 4 are from a diverse set of regions and tectonic environments. Many, however, are associated with the closure of back arc basins that formed around the perimeter of the Tethys and Pacific Oceans. Figure 6.6 shows the same general trend in the data with a few areas where the data have been amalgamated. Notable pauses in ophiolite formation are the near present (35 to 0 Ma) and 55 to 75 Ma.

Mesozoic ophiolites formed at an average rate of 7 ophiolites per 10 million year interval. The ophiolites from 130 to 70 Ma, mostly Cretaceous, seen in peaks 2 – 5 of Figure 6.5 and peaks 2 – 4 in Figure 6.6, comprise 68 of the 175 ophiolites. This translates to approximately 39% of the total raw data plotted for ophiolite formation in the Mesozoic to Cenozoic. Between the times of 180 to 140 Ma, earliest Cretaceous to Late Jurassic, there are 72 ophiolites that comprise about 41% of the total 175 ophiolites.

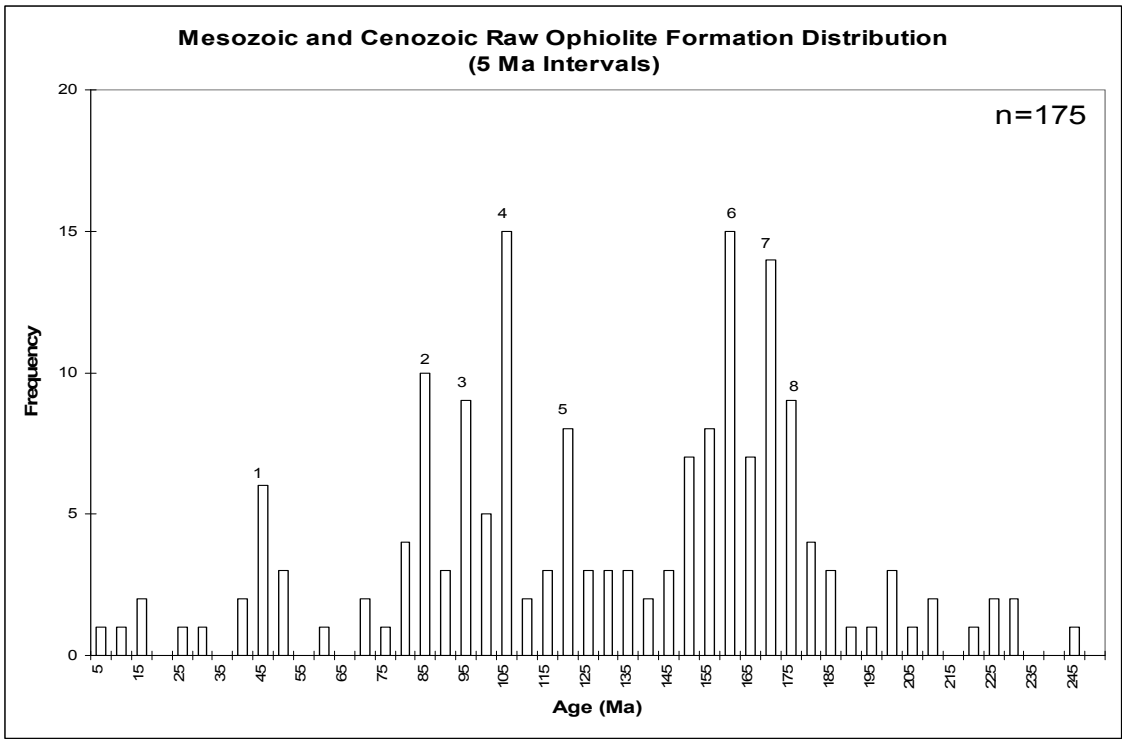

Figure 6.5 Mesozoic – Cenozoic ophiolite formation raw data (5 Ma)

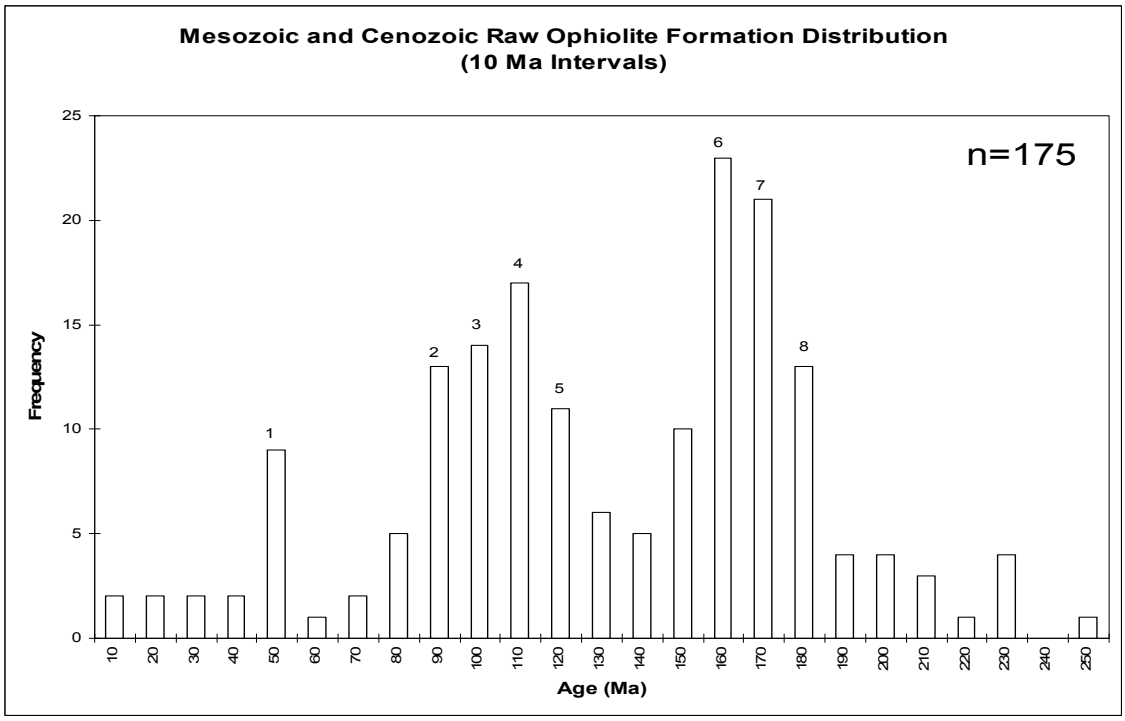

Figure 6.6 Mesozoic – Cenozoic ophiolite formation raw data (10 Ma)

6.2.3.2 Mesozoic and Cenozoic Ages of Ophiolite Emplacement

Figures 6.7 and 6.8 show 151 raw ophiolite emplacement dates for the Mesozoic through Cenozoic. These ophiolites show a consistent average rate of emplacement of about 5 ophiolites emplaced every 5 million years. The ophiolite emplacement data for the Mesozoic and Cenozoic yields two distinct peaks in Figure 6.7. One peak occurs at 50 million years and the other at 65 million years. Of the 151 ophiolites referenced for this chart, 21% occur between 40 and 55 Ma and 21% are from the interval of 60 and 75 therefore making the Eocene, Paleogene, and late Cretaceous significant time events in the emplacement of Mesozoic ophiolites. The 10 million year interval chart depicts the same distribution with a heavy emphasis on the late Cretaceous and early Cenozoic. In addition, two notable gaps in ophiolite emplacement occur at the interval between 115 and 125 million years and a longer gap between 250 and 190 million years.

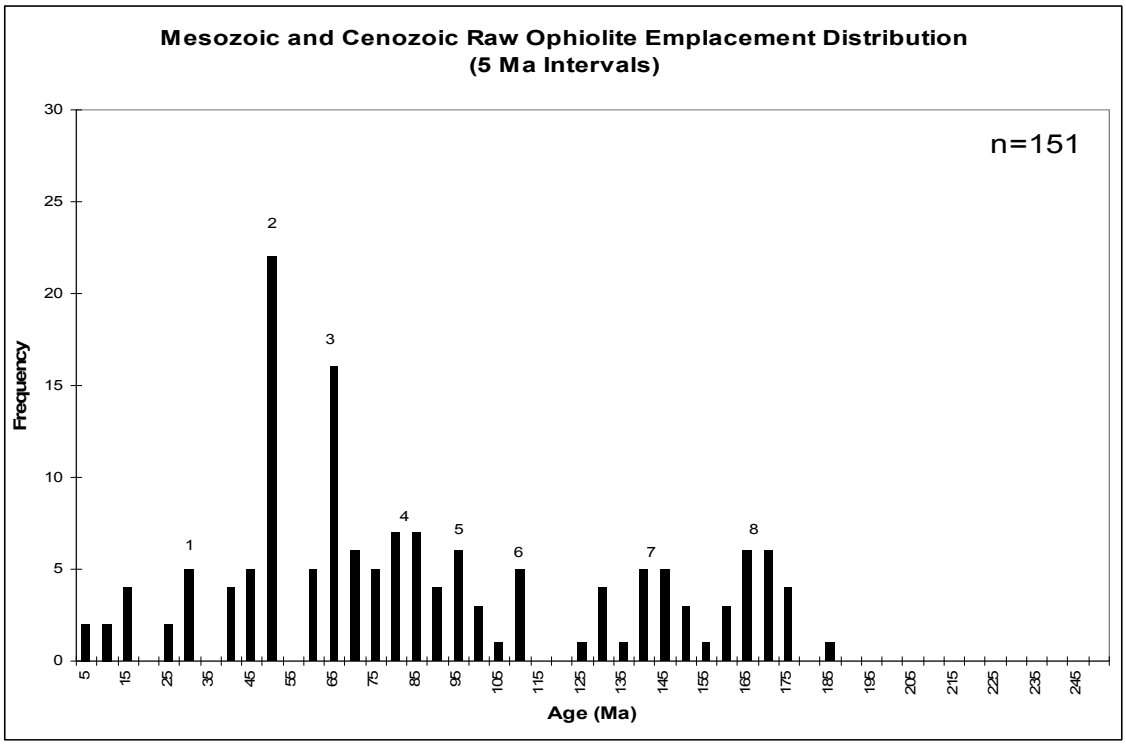

Figure 6.7 Mesozoic – Cenozoic ophiolite emplacement raw data (5 Ma)

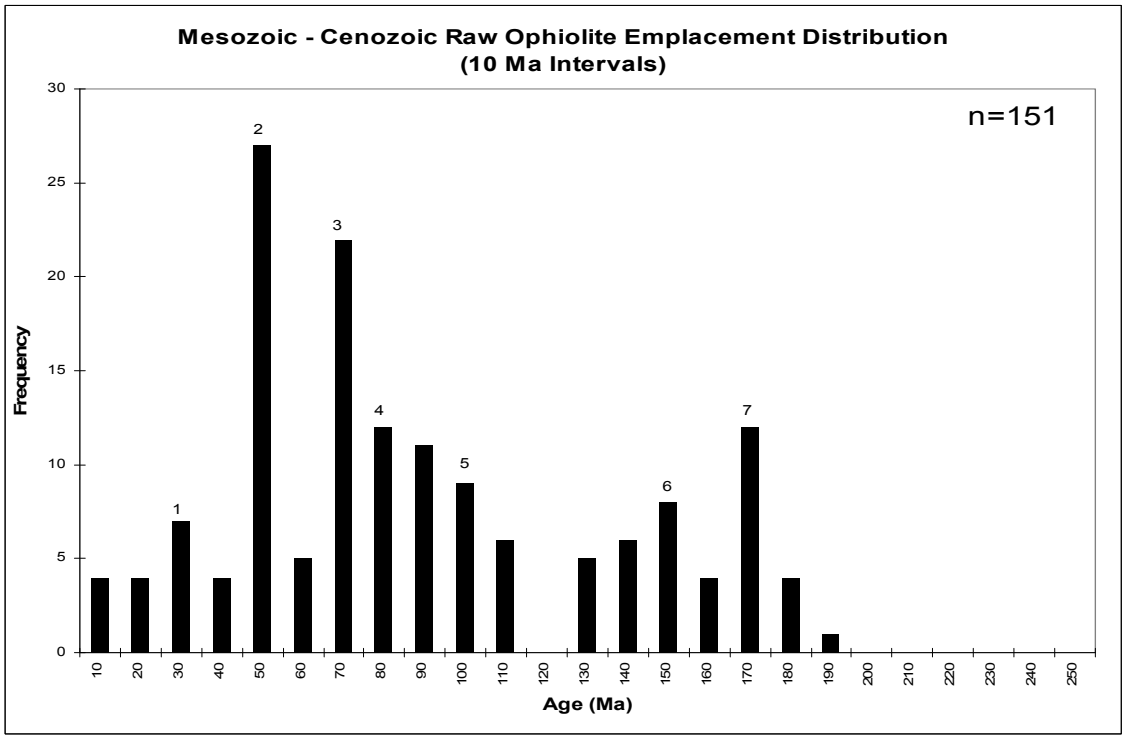

Figure 6.8 Mesozoic – Cenozoic ophiolite emplacement raw data (10 Ma)

6.2.3.3 Combined Paleozoic, Mesozoic, and Cenozoic Ophiolite Ages of Formation and Emplacement

Figure 6.9 depicts the combined analysis of the distribution of the raw formation and emplacement data. Obvious peak events of both formation and emplacement occur at 50 and 180 Ma, as well as a large cluster of formation and emplacement during the middle Jurassic and middle and late Cretaceous. Other peak events appear in the Paleozoic with less intensity, likely due to the reduction of data available for that time period. As previously mentioned, the evidence for an ophiolite sequence can get recycled and is likely the cause for the fewer number of Paleozoic localities. A noticeable gap of ophiolite data appears at the interval between 340 and 220 Ma. As previously reported, this is likely due to the quiescence of tectonic activity during this time and the reorganization of Pangea.

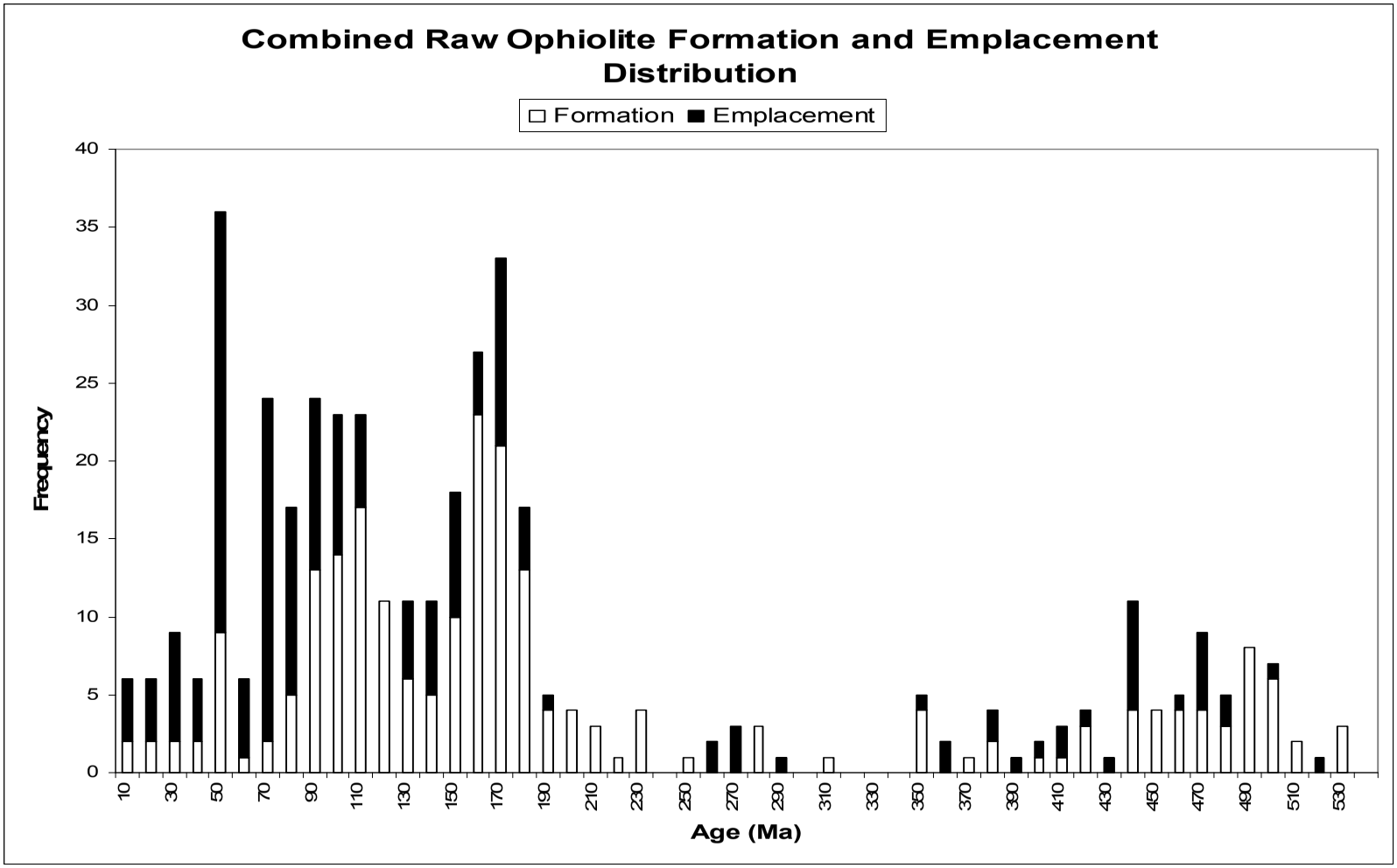

Figure 6.9 Combined Cenozoic, Mesozoic, and Paleozoic ophiolite formation and emplacemen raw data, distributed at 10 million year intervals

6.3 Analysis of Ophiolite Data by Removing Bias

The following section presents several techniques that have been used to reduce geographical and temporal bias. To reduce geographical bias a "declustering" technique was used to eliminate temporal bias a filtering technique was used which eliminated poorly dated ophiolites.

6.3.1 Temporal Distribution of Declustered Ophiolites

This section of analysis describes the declustering method used to improve the quality of the data. This method is an attempt to eliminate the geographic bias found in regions such as California where many ophiolites with the same geologic age of formation and emplacement were geographically clustered tightly together. The data was analyzed manually on the maps, seen in Appendix C, and any tightly clustered geographic data, which represented similar geologic and or tectonic events, were reduced in number. For example, in Region 4 of California and the Caribbean, there are 36 ophiolites in the raw dataset for this region and time period but with the declustering method; this number was reduced to 19 ophiolites. Table 6.2 shows the declustered data and lists the ophiolite localities that were combined to form new localities. This method reduced the raw ophiolite data from 280 locations to 165. The following discussion is the analysis of the declustered dataset.

Table 6.2 Data from Decluster Analysis of Ophiolites

Map #	Cluster Group #	Name	Group Ophiolite Represents	Best Estimate Formation (Ma)	Best Estimate Emplacement (Ma)
1	1l	Halaban-Ithilal	1.01	694.00	616.50
1	1i	Jabal Wask-Jabal Ess	1.02	822.00	774.50
1	1q	Fawakhir	1.03, 1.16	850.00	790.00
10	10h	Tihama - Asir	1.04	22.00	
1	1m	Bir Umq	1.05	838.00	680.00
1	1o	Wadi Ghadir	1.06, 1.08, 1.10, 1.12, 1.14, 1.15	745.50	736.50
1	1p	Quift Quseir	1.07, 1.11	800.00	790.00
1	1j	Al Amar	1.09	694.00	661.50
1	1t	Meatiq Dome	1.11	595.00	588.00
1	1r	Nakasib	1.13	800.00	730.00
1	1n	Abdola-Moyale	1.17, 1.18	700.00	
1	1s	Baragoi	1.19	796.00	609.00
3	3m	Ballantrae	2.02	483.00	478.00
3	3o	Bay of Islands 1	2.03, 2.04, 2.05	495.00	469.50
3	3l	Gibbs Islands	2.06	472.00	
3	3n	Hare Bay	2.07, 2.30	483.50	467.90
3	3b	Hoch Grossen	2.08	500.00	
7	7i	Kraubath	2.09	340.50	175.00
3	3a	Limousin	2.10	420.00	
4	4b	Lizard Ophiolite	2.11	376.50	357.00
4	4c	Munchberg gneiss	2.14	525.00	358.00
1	1b	Purtuniq	2.15, 2.16, 2.17	1980.00	
3	3k	Scandinavian Caledonides 1	2.18	443.00	435.50
3	3j	Scandinavian Caledonides 2	2.19	437.00	435.50
3	3i	Scandinavian Caledonides 3	2.20, 2.21, 2.25, 2.35	497.00	435.50
3	3h	Scandinavian Caledonides 5	2.22, 2.23, 2.24, 2.33, 2.34, 2.36	443.00	425.00
3	3p	Mt. Albert	2.26	458.00	
3	3g	Mt. Orford	2.27, 2.29, 2.37	470.00	
7	7d	Shulaps	2.31	181.50	
1	1c	Outokumpu	2.32, 2.38	1970.00	
3	3r	Nurali	3.01	457.50	400.00
3	3s	Mindyak	3.02	412.50	
4	4d	Kraka	3.03	453.50	348.50
3	3v	Kempersay Massif	3.04	449.00	407.00
3	3t	Sakmara Massif	3.05	480.00	409.50
3	3q	Voykar	3.06	404.00	385.50
7	7a	Chersky	3.07	400.00	172.00
8	8k	Ust' - Belaya Mts	3.09	370.00	134.50
8	8l	Kuyul Mélange	3.10	138.00	110.00
8	8j	Upper Khatyrka	3.11	227.00	128.00
9	9c	Vyvenka	3.12	95.15	
9	9d	Goven Peninsula	3.13	74.00	
8	8n	Elistratova Complex	3.15	177.00	110.00
8	8m	Aluchin	3.16	302.50	128.00

Table 6.2 *Continued*

Map #	Cluster Group #	Name	Group Ophiolite Represents	Best Estimate Formation (Ma)	Best Estimate Emplacement (Ma)
2	2b	Primorye	3.17	527.50	
3	3u	Khabarny	3.18	460.00	
1	1d	Itmurunda	3.19	797.50	
1	1e	Northern Baykal	3.20	1100.00	
1	1f	Sharyzhalgay	3.21	2450.00	
8	8i	Koryak	3.08, 3.22	132.50	110.00
8	8o	Taigonos Peninsula (Uga-Murugal)	3.14, 3.23	129.00	
7	7c	NW Alaska	4.01	162.00	
7	7b	Brooks Range	4.02	177.00	166.00
9	9b	Ingalls Complex	4.03	162.00	99.00
5	5f	Canyon Mt	4.04	271.75	
7	7e	Sparta	4.05		157.00
7	7z	Josephine (River)	4.06	171.00	
3	3w	Trinity	4.07	465.00	456.50
7	7y	Franciscan Burro Mt	4.08, 4.09, 4.18	169.50	140.00
7	7r	Coast Range Point Sal	4.13	151.50	
7	7s	Coast Range Black Mountain	4.14	159.00	
7	7v	Coast Range Paskenta	4.16, 4.12	161.00	161.00
7	7q	Great Valley 3	4.19, 4.20, 421	147.50	
7	7t	Sierra Nevada Foothills Smartville	4.24, 4.25, 4.26, 4.27	159.00	145.00
7	7w	Stanley Mountain	4.17, 4.28	166.00	
7	7u	Sierra Nevada Foothills Kings River	4.29	160.00	145.00
7	7f	Baja Alta Terrane	4.31, 4.33, 4.34	220.50	145.50
7	7x	Elder Creek	4.32, 4.10, 4.11, 4.15	168.50	
10	10b	Taitao	4.35	8.25	
9	9a	Resurrection Peninsula	4.36		57.00
8	8h	Masirah	5.01	141.00	126.50
9	9y	Semail	5.02	95.70	92.50
9	9z	Sabzevar	5.03	82.00	65.00
6	6b	Mashod	5.04	210.00	
9	9gg	Tchehel Kureh	5.05	82.00	65.00
9	9ee	Iranshahr	5.06, 5.07	82.00	65.00
9	9ff	Kahnuj	5.08, 5.09	132.50	77.50
9	9hh	Shahr-Babak	5.10	104.50	65.00
9	9v	Baft	5.11	82.00	65.00
9	9u	Neyriz	5.12, 5.13	94.00	89.00
9	9t	Kermanshah	5.14		68.00
6	6c	Rasht	5.15	210.00	
9	9ll	Mersin	5.19, 5.20, 5.21, 5.22, 5.26, 5.28	93.75	75.50
9	9ii	Yayladağ	5.24, 5.23, 5.17, 5.18	196.00	61.50

Table 6.2 C*ontinued*

Map #	Cluster Group #	Name	Group Ophiolite Represents	Best Estimate Formation (Ma)	Best Estimate Emplacement (Ma)
9	9mm	Berit	5.25	156.50	61.50
8	8g	Ispendere-Komurhan	5.30	104.50	
9	9s	Cilo	5.31	156.50	82.00
9	9jj	Guleman	5.33	104.50	77.00
9	9kk	Troodos	5.29, 5.34, 5.35	91.00	70.00
7	7o	Pindos	5.36, 5.37, 5.38	172.00	165.50
7	7p	Albania-Brezovica	5.41	203.50	167.00
7	7j	Krivaja-Kanjuh	5.42, 5.43, 5.64	169.50	162.50
7	7k	Zermatt-Saas-Fee	5.45, 5.47	164.20	156.50
7	7l	Internal Liguride (Ligurian)	5.48, 5.44	164.00	152.00
9	9n	External Liguride (Piedmont)	5.46, 5.49	165.00	74.50
8	8d	Tuscany	5.50	152.00	104.50
9	9q	Calabria	5.51	175.00	85.50
9	9o	Tauern	5.52, 5.53	175.00	82.00
9	9p	Apuseni (Romario)	5.54	193.00	99.50
9	9r	Lesser Caucasus	5.56, 5.16, 5.32	183.50	92.50
7	7m	Cretan Nappe	5.57	148.00	
8	8f	Akamas	5.58	104.50	
7	7h	Mamonia	5.59	229.00	156.00
1	1h	Balkan-Carpathian	5.60	563.00	
8	8e	Honaz	5.61	104.50	
7	7n	Hellinic	5.62, 5.40, 5.39	176.00	
7	7g	Kure	5.63	176.00	
10	10g	Cyclades (Evia)	5.66	82.00	21.00
9	9aa	Bela	6.01	67.50	65.00
9	9bb	Muslim Bagh	6.02, 6.03, 6.11	76.00	67.50
9	9w	Spontang	6.04, 6.14	82.00	61.50
10	10dd	Xigaze Dagzhuka	6.05	105.00	45.00
9	9x	Tuensang	6.06		77.00
10	10gg	Moreh	6.07	80.00	45.50
9	9dd	Makran	6.08	95.00	91.25
1	1k	Dongwanzi	6.12	2505.00	
10	10y	Nanga Parbat	6.13, 6.16 - 6.21	104.50	14.50
9	9cc	Dras Sangeluma	6.15	77.00	
10	10aa	Indus - Yarlung Zangbo	6.22	120.00	49.50
10	10z	Indus - Yarlung Zangbo	6.23	156.50	49.50
10	10bb	Indus - Yarlung Zangbo	6.24, 6.25	156.50	49.50
10	10cc	Indus - Yarlung Zangbo	6.26, 6.27, 6.30	156.50	49.50
10	10ee	Indus - Yarlung Zangbo	6.28, 6.29, 6.31	156.50	49.50
10	10ff	Indus - Yarlung Zangbo	6.32, 6.33, 6.34	150.50	49.50
3	3c	Hongguleleng	6.35	430.50	
3	3d	Tianshan	6.36	430.50	
3	3e	Mishigou	6.37	438.50	372.50
1	1g	Kunlun	6.38	721.50	
4	4a	Kunlun	6.39	340.50	
6	6a	Kunlun	6.40	243.50	

Table 6.2 *Continued*

Map #	Cluster Group #	Name	Group Ophiolite Represents	Best Estimate Formation (Ma)	Best Estimate Emplacement (Ma)
9	9h	Purial	7.01, 7.02		59.90
10	10e	Holguin-Gibara	7.03	121.00	48.05
10	10c	Camaguey	7.04	112.00	48.05
10	10f	Las Villas	7.05	112.00	41.50
9	9i	Western Belt	7.06	112.00	57.50
9	9k	Sierra de Santa Cruz	7.07, 7.13	115.50	74.25
9	9m	Sierra de Las Minas	7.08, 7.17	122.00	75.40
9	9j	North Coast	7.09	91.25	60.00
8	8b	Cordillera Central	7.10	134.50	105.50
10	10d	Southern Peninsula	7.11	82.40	30.00
8	8a	Bermeja	7.12	144.00	105.50
9	9g	Tinaguilla	7.14, 7.16	87.40	75.00
8	8c	Siquisique	7.15	170.00	129.00
9	9l	Matapolo	7.18, 7.20	128.75	84.00
9	9f	Rio Calima	7.19	89.00	
10	10o	East Timor	8.02, 8.21, 8.26		6.50
10	10q	April Ultramafic	8.03, 8.04, 8.05, 8.12	44.25	28.50
10	10u	Fiji	8.06	28.75	10.50
10	10w	New Caledonia	8.07. 8.37	60.00	35.50
10	10a	Northland Allochthon	8.08	104.50	30.00
5	5a	Yarras	8.09, 8.11	372.50	269.00
5	5b	Attunga	8.10	340.50	269.00
10	10x	Macquarie Island	8.13	10.75	2.50
10	10l	Obi (E Indonesia)	8.14	66.35	25.00
5	5d	Dun Mt	8.15	273.00	252.00
10	10v	New Hebrides	8.16	44.25	35.50
10	10r	Solomon Islands 1	8.17	44.25	35.50
10	10s	Solomon Islands 2	8.18	44.25	35.50
5	5e	Red Hills	8.19	280.00	252.00
10	10t	Tonga	8.20	45.15	
10	10k	Izu Bonin	8.22	41.30	
3	3f	Tasmania	8.23, 8.36	501.00	495.00
10	10i	Hayama Mineoka	8.24	44.50	
10	10n	Zambales	8.25	35.35	
9	9e	Poroshiri	8.27	100.00	
5	5c	Yakuno	8.28	417.50	283.50
10	10j	Taiwan Ophiolite	8.33	3.40	1.40
1	1a	Marlborough	8.34	560.00	
2	2a	Tyennan - Delamerian	8.35	522.50	515.00
10	10p	Cyclops	8.38	36.00	14.00
10	10m	Palawan	8.39	196.00	14.00

6.3.1.1 Temporal Distribution of Paleozoic Declustered Ophiolites

Figures 6.10 illustrates the Paleozoic ophiolite formation data from the decluster analysis with 39 ophiolite values used. Figure 6.11 depicts the temporal distribution of the 23 Paleozoic ophiolite emplacement events.

The notable events in both of these distributions occur during the early Silurian to Ordovician as also seen in the raw dataset. A significant ophiolite pulse of formation occurred during the middle to late Ordovician followed by peaks of emplacement around 20 million years later during the early to late Silurian. Another significant lapse in ophiolite formation occurs at the intervals of 250 to 280 million years and again at 290 to 340 million years.

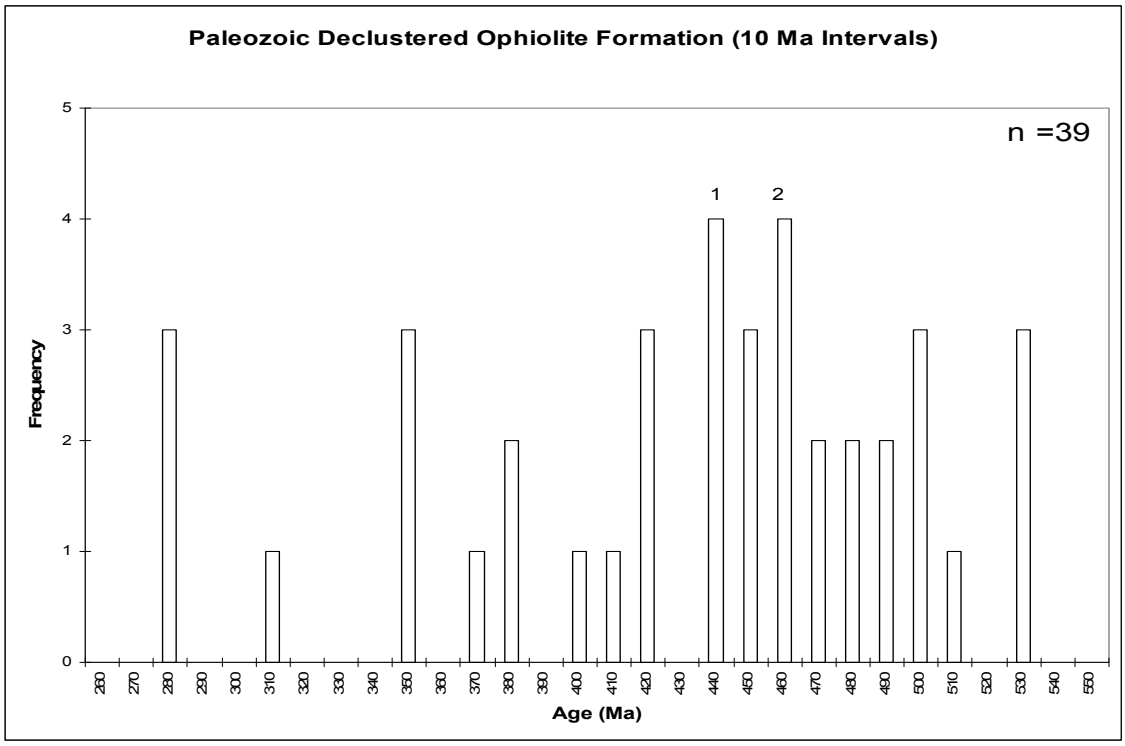

Figure 6.10 Decluster analysis of Paleozoic ophiolite formation (10 Ma)

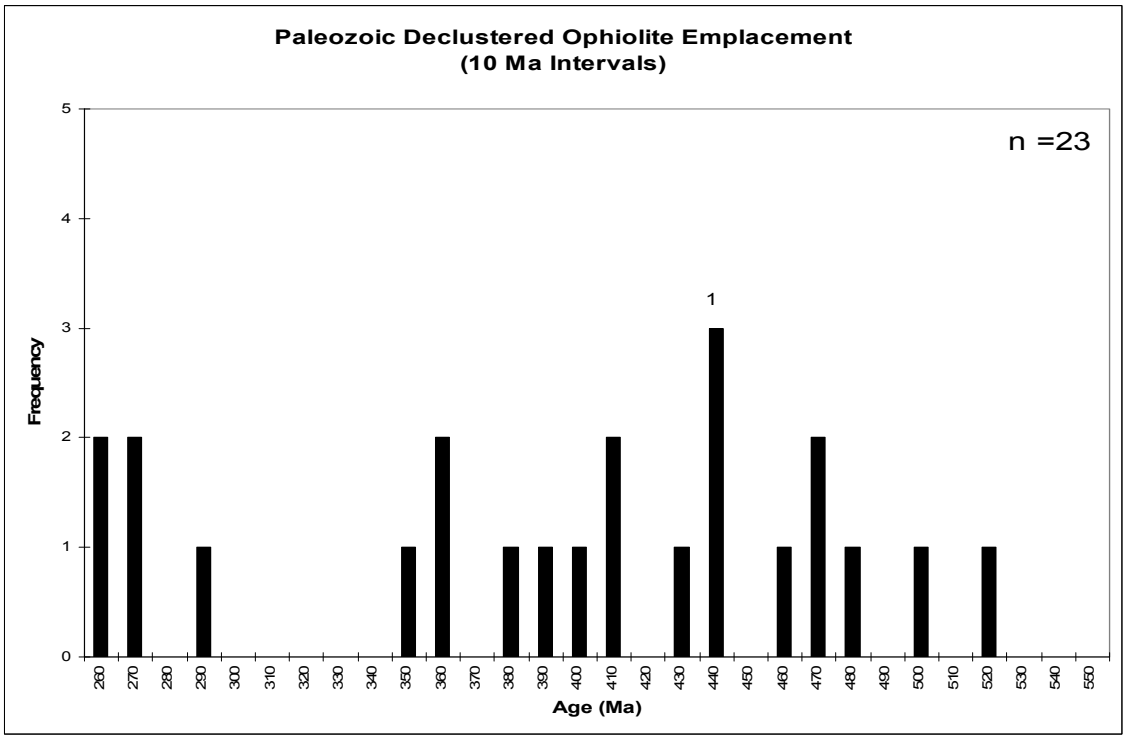

Figure 6.11 Decluster analysis of Paleozoic ophiolite emplacement (10 Ma)

6.3.1.2 Temporal Distribution of Mesozoic and Cenozoic Declustered Ophiolites

Figures 6.12 and 6.13 illustrate the Mesozoic and Cenozoic pattern of declustered ophiolites. There are 87 ophiolite emplacement events and 106 ophiolite formation events. The peak formation events occurred during the middle to early Jurassic and Late Cretaceous to Albian. A noteworthy lapse in ophiolite formation occurs at the intervals after 210 million years. Notable peaks of emplacement, Figure 6.12, occurred at 110, 70, and 50 Ma. It is noticeable that the distribution of ophiolite emplacement compared to formation shows an offset of 20 to 30 million years from formation to emplacement, which might imply that most ophiolites emplaced, began 20 million years after formation. Figure 6.13 shows significant emplacement events occurring at 50 and 70 Ma. A noticeable absence of ophiolite emplacements began at 190 Ma.

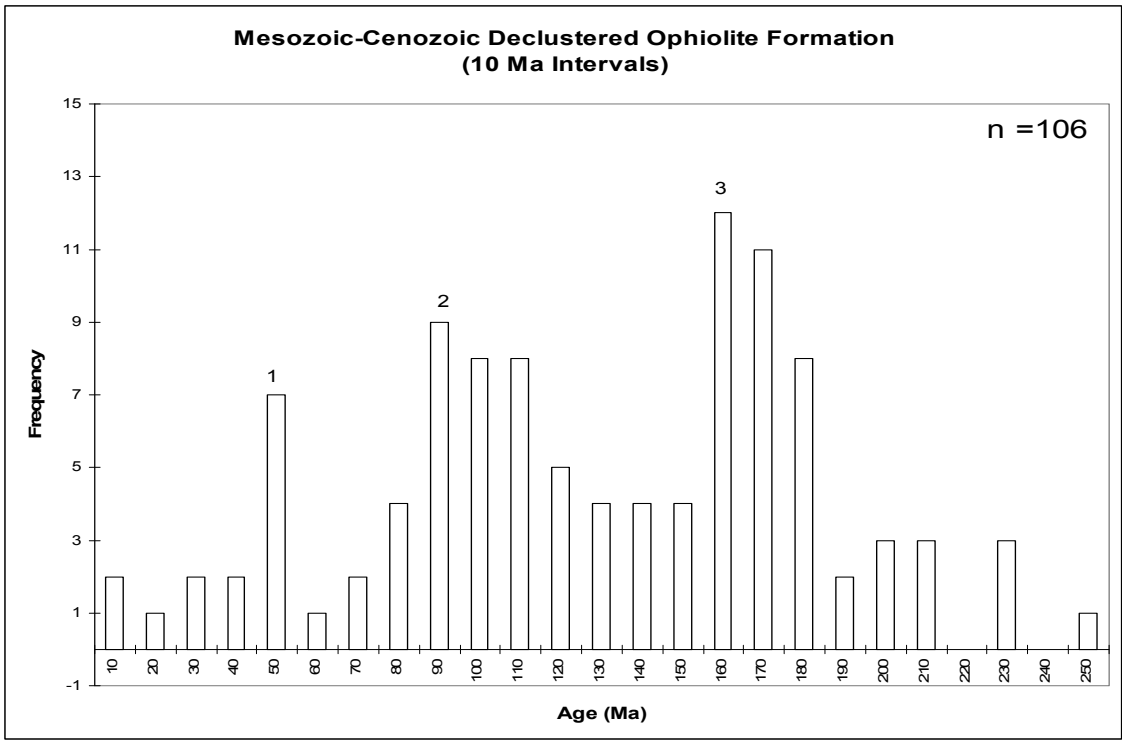

Figure 6.12 Mesozoic and Cenozoic declustered ophiolite formation (10 Ma)

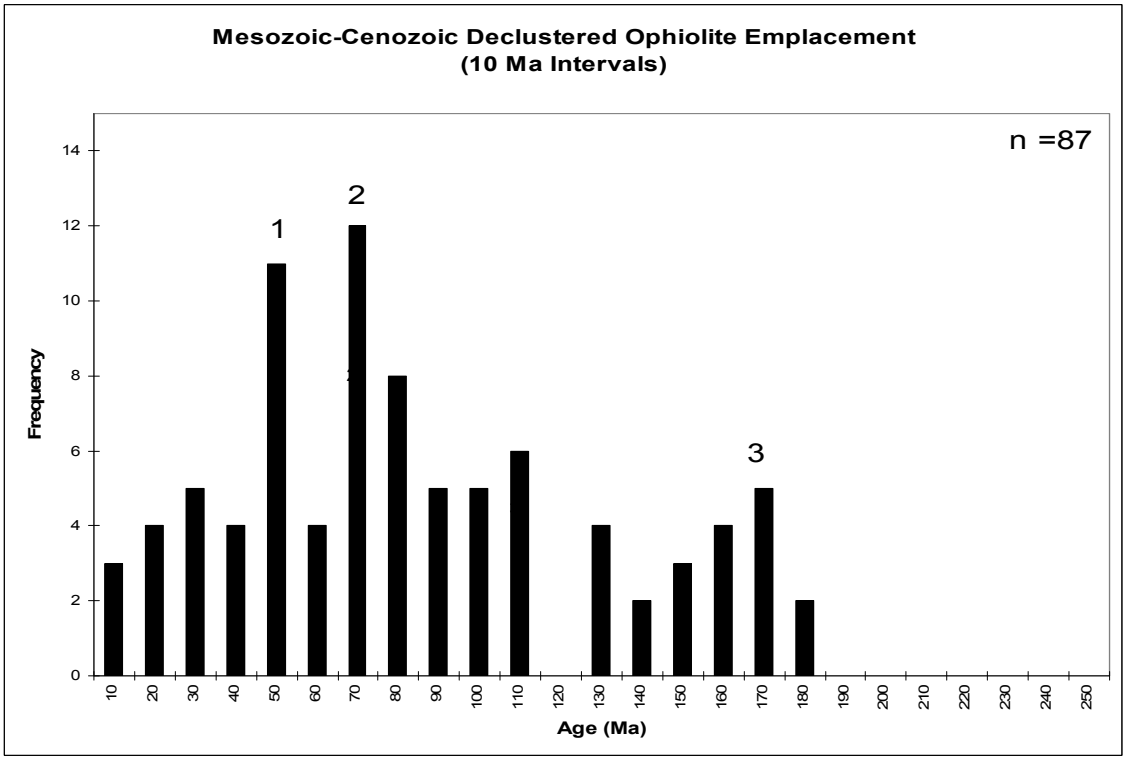

Figure 6.13 Mesozoic and Cenozoic declustered ophiolite emplacement (10 Ma)

6.3.1.3 Combined Declustered Ophiolite Analysis

Figure 6.14 depicts the decluster analysis for ophiolites from the Cenozoic through the Paleozoic. Noticeable peak events are visible at 50, 70 – 100, 160 – 180, and 440 Ma. It is also noteworthy that there is a significant gap between 190 to 340 Ma. Figure 6.9 (raw data) has also been included for visual comparison with the declustered data.

The declustered ophiolite data is combined into one illustration seen in Figure 6.23 with Cenozoic, Mesozoic and Paleozoic ophiolite formation and emplacement shown. The noteworthy peak events seen in the raw data, Figure 6.9, also appear in the declustered data. The peak events of ophiolite formation and emplacement during the Cretaceous, Jurassic, and Silurian-Devonian is evident in the declustered data in figure 6.23 but compared to the raw data is more evenly distributed during the peak events. This analysis clearly illustrates the formation episodes followed by emplacement episodes particularly in the interval between 180 and 90 million years. The declustered data is clearly a more accurate representation of ophiolite formation and emplacement during the Cenozoic, Mesozoic, and Paleozoic.

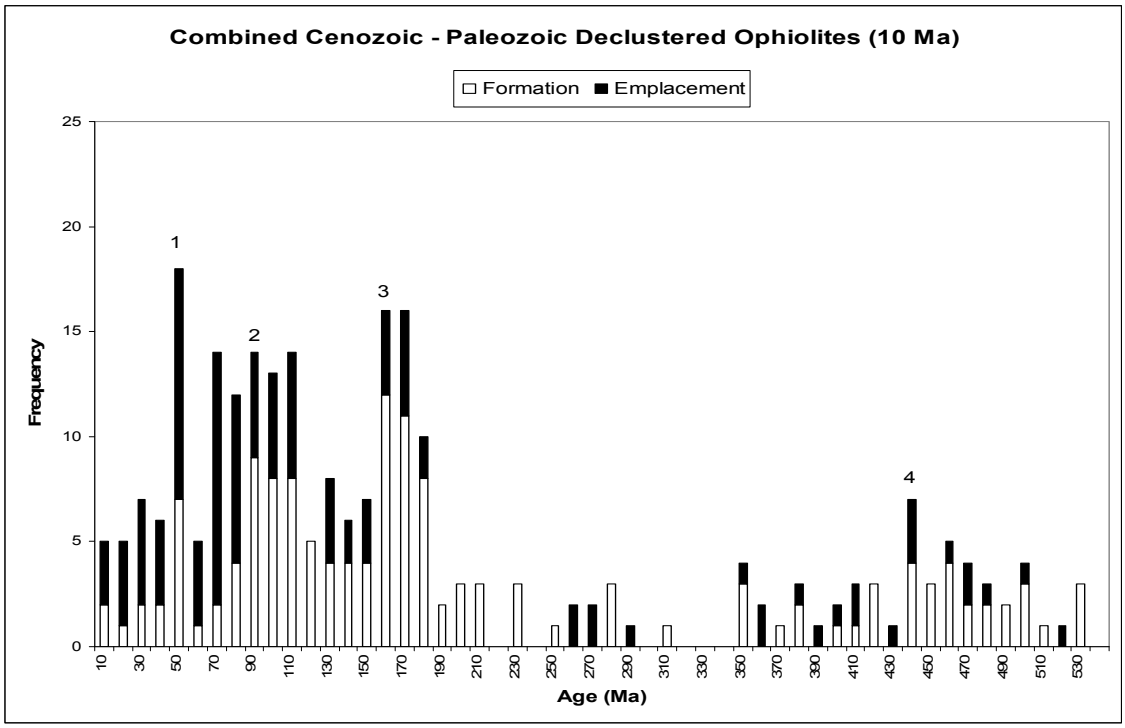

Figure 6.14 Combined Declustered Ophiolites (10 Ma)

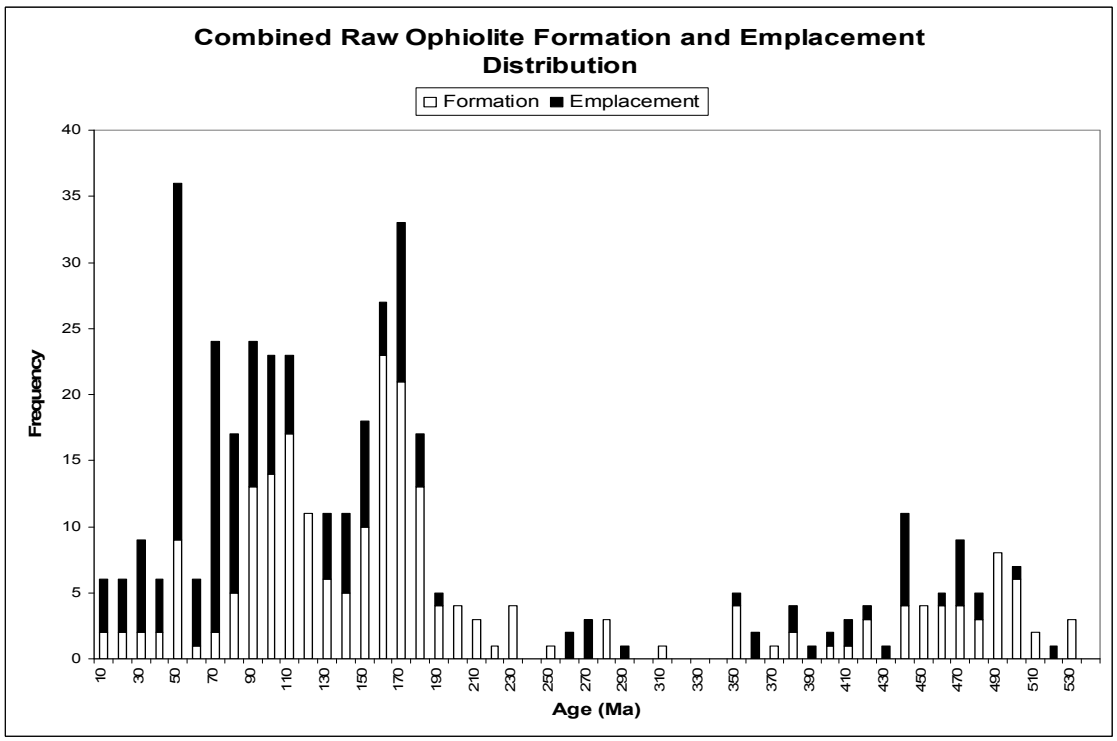

Figure 6.9 (repeated) Combined Cenozoic, Mesozoic, and Paleozoic ophiolite formation and emplacement raw data, distributed at 10 million year intervals

6.3.2 Temporal Distribution of Filtered Ophiolites

The reliability of an ophiolite description is most clearly correlated with the precision of its age assignment. It should be noted that for each ophiolite locality, an attempt was made to define both the oldest possible age and the youngest possible age of both ophiolite formation and emplacement (Appendix A). The "Best Age Estimate" is the average of these two ages. In this study, on average, the age of formation was known to within ±35 million years, and the age of emplacement, on average, was known to within ±19 million years. In order to improve the quality of the dataset, the data was filtered by the precision of the 'Best Estimate' age assignment. Any ophiolites with an uncertainty in the age of formation greater than ±35 million years, was rejected from the database. Similarly, an ophiolite with an uncertainty in the age of emplacement greater that ±19 million years was rejected from the database. After applying this filter, the number of ophiolite localities used to describe the age of formation was reduced from 258 to 180. Similarly, the number of ophiolite localities used to describe the ages of emplacement was reduced from 198 to 123.

6.3.2.1 Paleozoic Filtered Ophiolite Formation and Emplacement

Paleozoic formation and emplacement of ophiolites is generally more sparse than the data for the Mesozoic and Cenozoic. Figure 6.15 and 6.16 show the Paleozoic distribution of ophiolites based on formation and emplacement ages after the application of the age filter. It is notable that there are more emplacement events during the Ordovician, whereas, formation appears to be more distributed through the time interval 510 and 430 Ma. A significant peak event occurs at 490 Ma for formation and 440 and 470 Ma for emplacement. It is also noticeable that these peak events for formation are earlier when compared to emplacement (20 to 30 million years). This is more or less the expected pattern as noted by many ophiolite researchers. Noteworthy gaps also occur in the formation of ophiolites during the interval from early Permian to Devonian (260 to 400 Ma). Similarly, there is a gap in emplacement of ophiolites during the interval from 260 to 370 Ma. The ophiolites, which formed during the interval from 440 to 510 Ma makeup in 73% of the 40 ophiolites, formed during the Paleozoic. In the same way, of the 23 ophiolites that were emplaced during the interval from 440 to 480 Ma comprise 65% of the dataset.

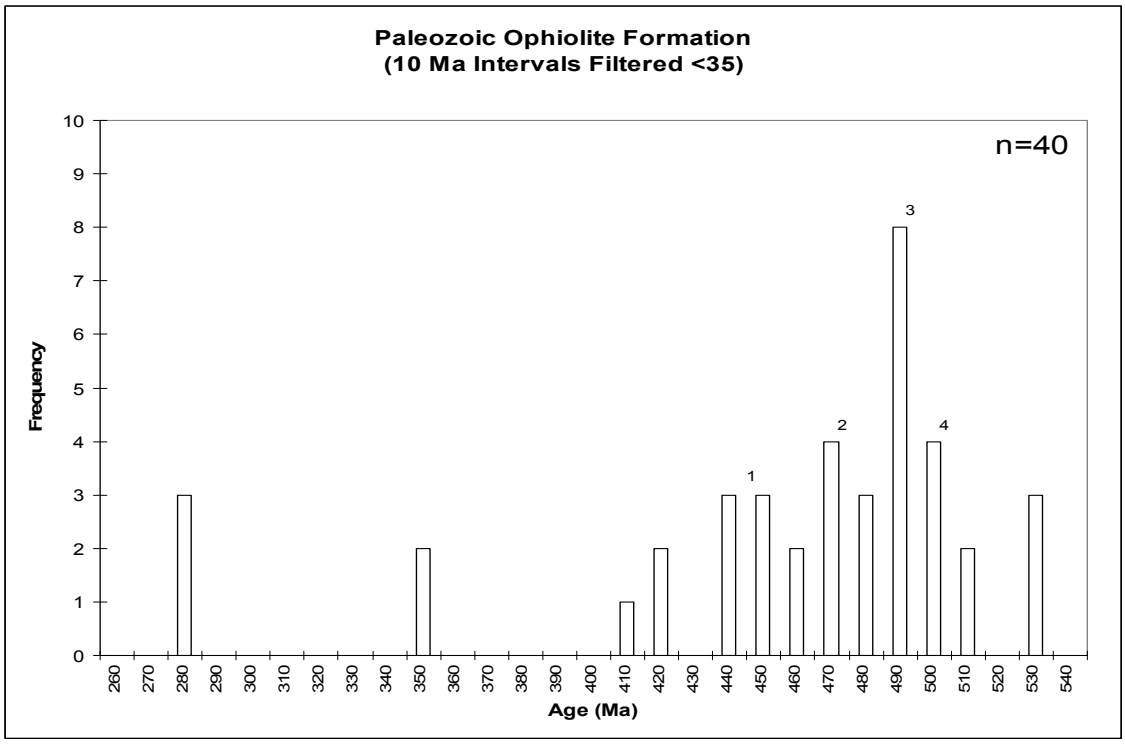

Figure 6.15 Paleozoic filtered ophiolite formation data (10 Ma)

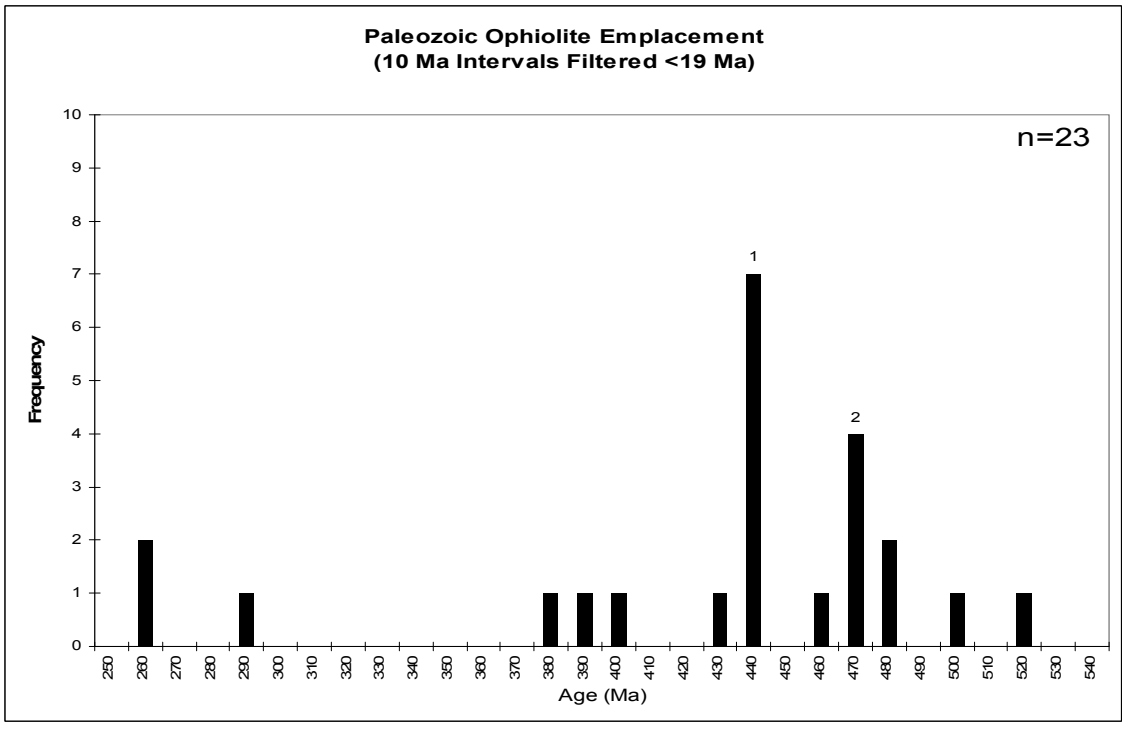

Figure 6.16 Paleozoic filtered ophiolite emplacement data (10 Ma)

6.3.2.2 Mesozoic and Cenozoic Filtered Ophiolite Formation and Emplacement

The Mesozoic and Cenozoic data was filtered using the same criteria described in section 6.3.2.1. In Figure 6.17, 123 ophiolite formation localities are noted. The peaks labeled 5–7 depict the ophiolites, which formed during the Middle to Late Jurassic, peaks 2–4 depict Cretaceous ophiolites, and peak 1 depicts Eocene ophiolites. The interval from 120 to 80 Ma includes 42 ophiolites, approximately 34% of the filtered ophiolites. The interval from 50 to 40 Ma consists of 10 out of the 123 ophiolites and corresponds to about 8% of the Mesozoic and Cenozoic filtered ophiolites. Significantly less ophiolite formation occurs before 190 Ma.

There were 94 ophiolites emplaced during the Mesozoic and Cenozoic. Figure 6.18 shows the temporal distribution of these ophiolites. In figure 6.17, peaks 5 – 7 occur during the Middle to Late Jurassic, and peaks 2 – 4 comprise Cretaceous ophiolites. In Figure 6.18, there are 25 ophiolites from 180 to 140 Ma, or 27%, and there are 20 ophiolites noted in the interval from 110 to 80 Ma, which equates to 21% of the total used in this analysis. The interval from 70 to 60 Ma yields 25 ophiolites, also 27%, and the interval from 50 to 40 Ma shows 10 ophiolites which make up about 11% of the total. Few ophiolites were emplaced before 200 Ma and the same 20 to 30 million-year shift in the age of formation followed by emplacement, is notable.

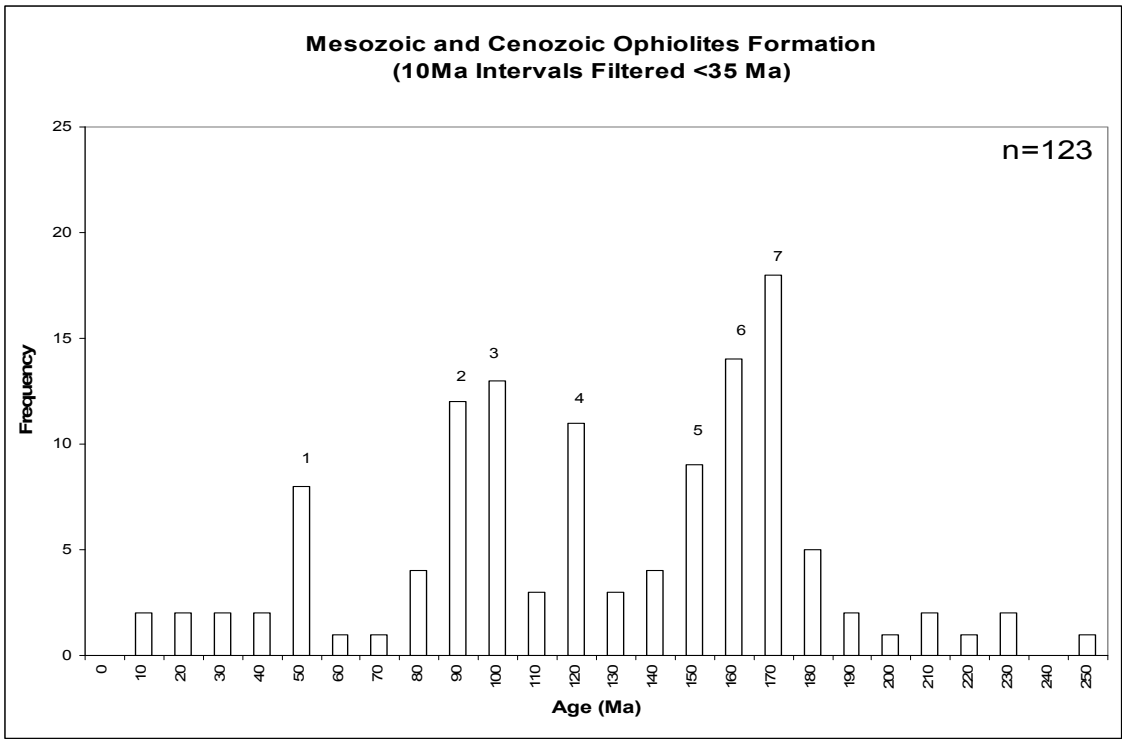

Figure 6.17 Mesozoic and Cenozoic filtered ophiolite formation data (10 Ma)

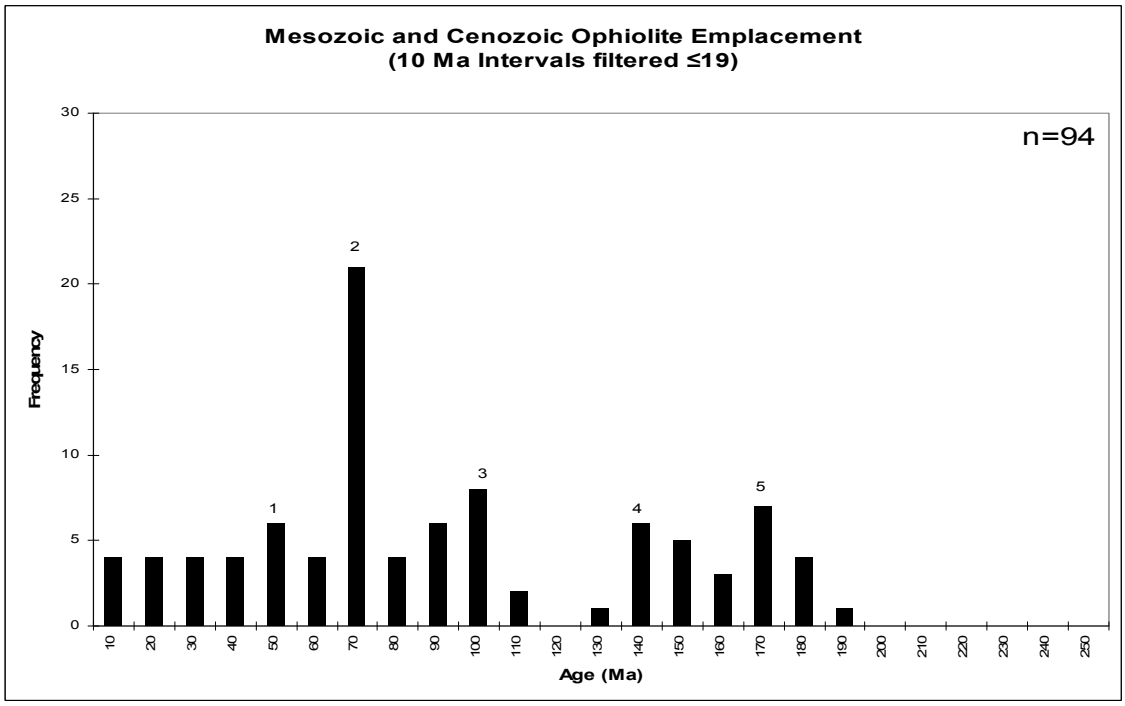

Figure 6.18 Mesozoic and Cenozoic filtered ophiolite emplacement data (10 Ma)

6.3.2.3 Combined Filtered Ophiolite Distributions

The ophiolite data that was filtered by age precision has been plotted together to in combined formation and emplacement diagrams (Figures 6.19). The distribution, Figure 6.19, depicts the same ophiolite formation and emplacement trends as previously mentioned in the raw and clustered datasets. A significant lack of formation and emplacement takes place during the Permian to late Devonian, as seen in the previous methods of analysis. In Figure 6.19, there is notable formation at the time interval of 120 Ma when there is an apparent lack of ophiolite emplacement. Another obvious difference is at the interval of 70 Ma in which many ophiolites were emplaced and yet had few forming. Likely, this is a result of the multitude of ophiolites that formed from 120 to 80 Ma that were finally coming to their 'resting' place. As previously mentioned, there is a lapse of formation and emplacement during the interval from 200 Ma and older. Figure 6.9 (raw dataset) was included again for comparison purposes.

Figures 6.1 – 6.9 depict the ophiolite data as raw resampled data over 5 and 10 million year intervals. Figure 6.19 shows the filtered ophiolite data combined with formation and emplacement as well as including all for Cenozoic, Mesozoic and Paleozoic data. Figure 6.19 compares to Figure 6.9 and it is evident that the filtered data represents a more concise representative dataset. With much of the age error removed in Figure 6.19 it is still clear that there is significant ophiolite formation and emplacement occurring during the late Cretaceous, Jurassic, and Silurian Devonian. Removing the bias did not shift any of the peak events although it is clear that there is a more even distribution over the Cretaceous and Jurassic in the filtered data. The filtered

data and illustration is preferable over the raw dataset as it depicts a more accurate representation of the overall distribution of ophiolite formation and emplacement since the Precambrian.

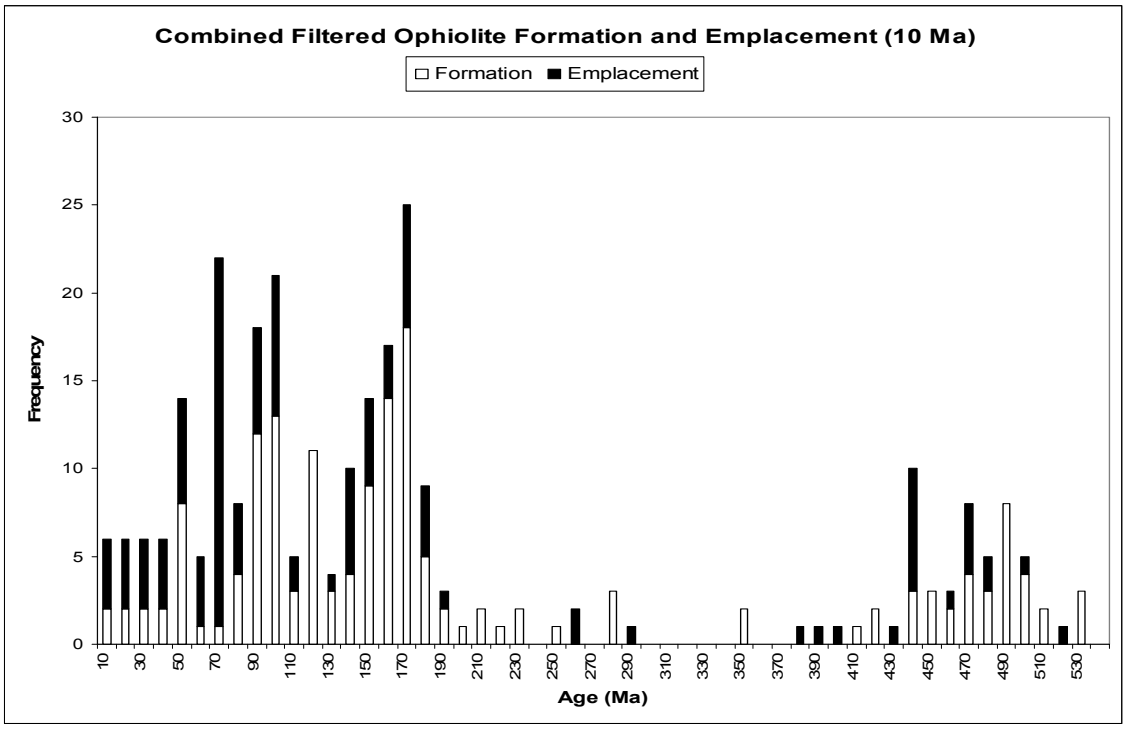

Figure 6.19 Combined Cenozoic, Mesozoic, and Paleozoic filtered ophiolites (10 Ma)

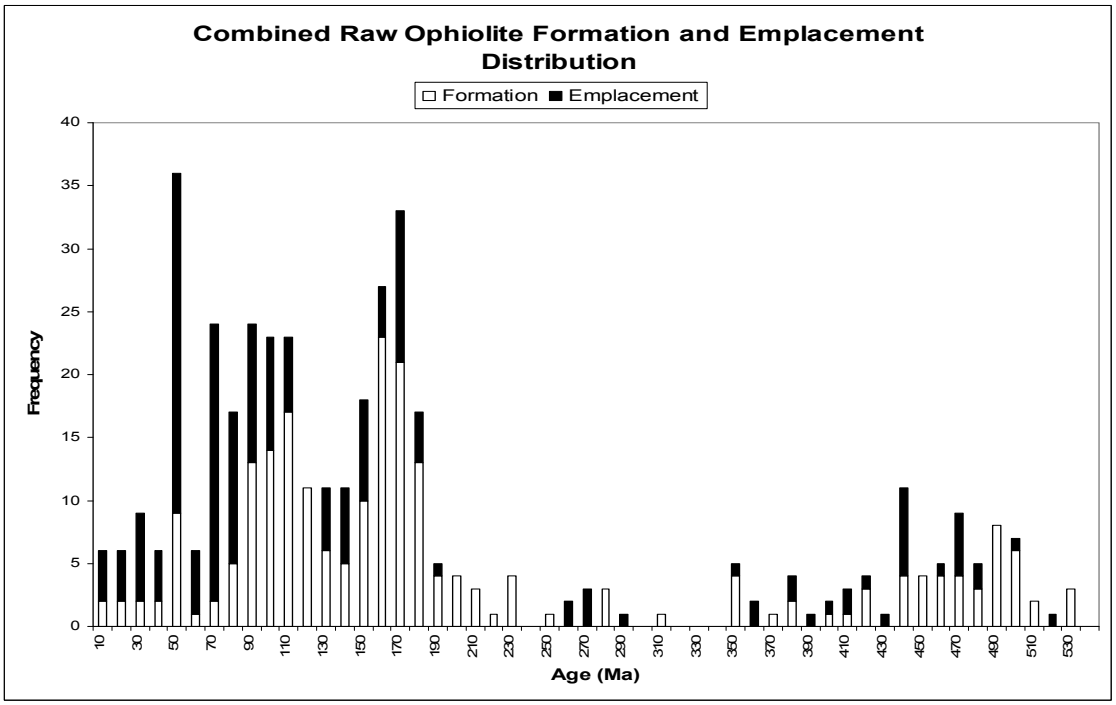

Figure 6.9 (repeated) Combined Cenozoic, Mesozoic, and Paleozoic ophiolite formation and emplacement raw data, distributed at 10 million year intervals

6.4 Refined Ophiolite Data

After individually reviewing the raw, declustered, and filtered data, the ophiolites were combined into a 'refined' dataset that utilized ophiolite data that had geographical "declustered" and temporally filtered (Figure 6.20). The data from the declustered method was used to start this refined analysis. The data was then temporally filtered and data with differences between old and young ages of formation (>35) and emplacement (>19), were removed from the decluster dataset. This combining of the two resampling techniques resulted in a new dataset, which is called the 'refined' data. 121 ophiolites localities used for formation and 84 being used for emplacement met both sampling criteria. The data shows a more or less shifted pattern of formation and emplacement occurring at approximately 20 to 30 million year intervals. The previously mentioned lapse in formation and emplacement of ophiolites is apparent in this illustration as well. Figure 6.9 (raw dataset) was included again for comparison purposes.

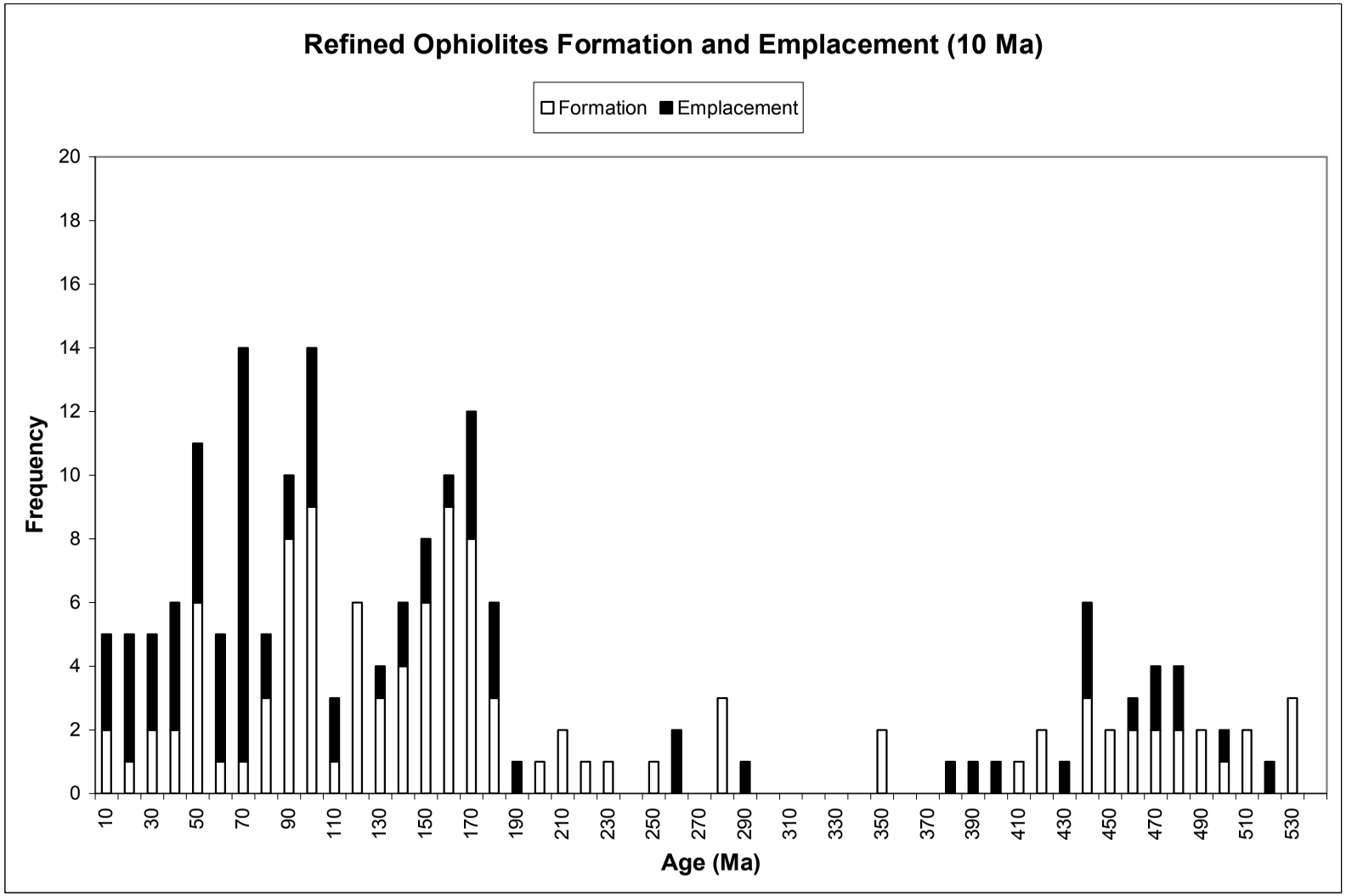

Figure 6.20 Refined ophiolite distribution plotted at 10 Ma intervals

6.5 Comparison of Ophiolite Analysis Methods

The ophiolite distributions in this study have been analyzed from raw data, filtered data, and declustered data. The analysis methods were then combined resulting in a refined dataset. A comparison of these various results is discussed in this section.

6.5.1 Comparison of Refined Ophiolites with Raw, Filtered, and Declustered

The analysis of the ophiolites formation and emplacement for this study was comprehensive and it is notable to compare the different techniques. Figures 6.9, 6.21, 6.22, and 6.23 are all useful for comparison of the analysis methods. The raw distribution, Figure 6.9, is obviously biased yet still depicts a useful representation of the overall distribution of ophiolite formation and emplacement. Comparing the raw data in Figure 6.9 to the filtered data in Figure 6.22 and declustered data in Figure 6.23, it is clear that the removal of bias put the ophiolite data into a more accurate illustration of temporal distributions over time. However, the declustered method is preferable when compared to the raw and filtered analysis datasets. The declustered analysis shows more clearly the trend of formation followed by 20 to 30 million year later emplacement and illustrates the episodic events that seem apparent in the data. In the declustered analysis, Figure 6.23, the formation events occur at the intervals of 90 to 180 Ma followed by the formation events.

The refined dataset also illustrates, Figure 6.21, this same event with an even more accurate dataset. Clearly, the refined data illustrates the episodic events of the ophiolite formation and emplacement events over the last 540 million years and is the

best representation of the trends therein. The ophiolite formation and emplacement events are obviously episodic and seem to be tied to global plate reorganization.

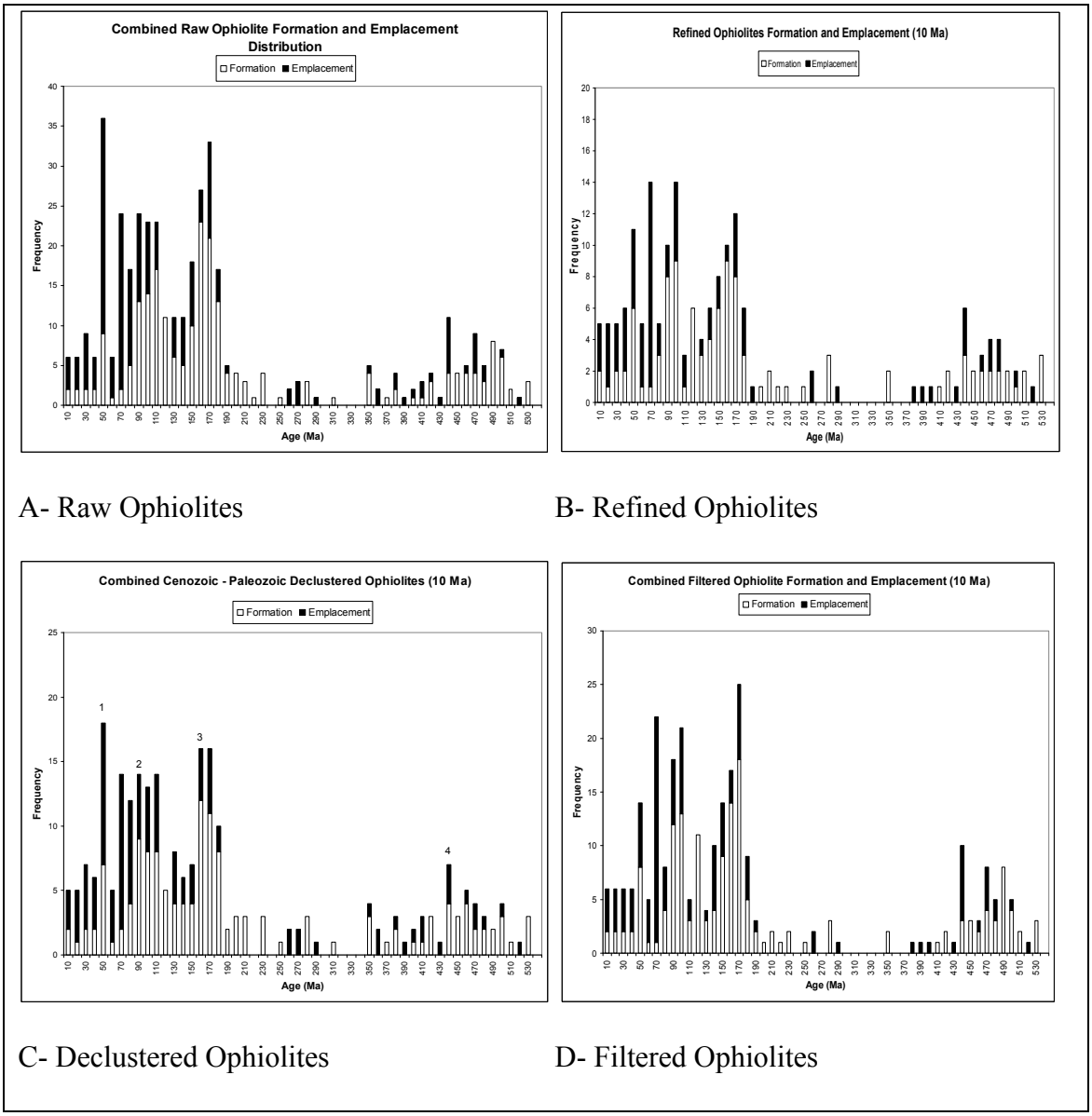

A- Raw Ophiolites

B- Refined Ophiolites

C- Declustered Ophiolites

D- Filtered Ophiolites

Figure 6.21 Comparison of ophiolite distributions based on analysis

6.6 Ophiolite Tectonic Environments

The tectonic environments of formation and emplacement for the ophiolites in this study have distinctly characteristic percentages. Figures 6.22 and 6.23 are pie charts showing the percentages of the known environments (see Table 2.4 for the complete list) found in the literature for these ophiolites. In the ophiolite formation data (Figure 6.1), there are seven main environments that were found in the literature. Out of the 280 ophiolites cited, 140 of the locations had verifiable tectonic environments of formation cited in the literature (summary in Table 6.2). In this study mid-ocean ridge, island arc, and back-arc basin make up the largest percentage of types of geologic and tectonic environments in which the ophiolites form, yielding 34%, 22.7%, and 23.4 % respectively. This observation parallels what many geoscientists already know; that the rocks which make up the ophiolite suites are generally present at mid-ocean ridges, back-arc basins, and island arcs. These are typically identified by the rocks and mineral assemblages, as well as any structures within them. These assemblages have been identified by many petrologists (Coleman, 1977) as belonging to certain tectonic environments and will not be covered in this paper as that extends beyond the scope of the study.

Table 6.3 Ophiolite Tectonic Environments

Formation Environment	**Number**	**Percentage**
Island Arc (ARC)	30	17%
Mid-Ocean Ridge (MOR)	100	57%
Intra-continental Rift (ICR)	2	1%
Back-arc Basin (BAB)	24	14%
Forearc Basin (FAB)	12	7%
Intra-arc Basin (IAB)	3	2%
Andean (AND)	1	1%
Continental Strike Slip Zone (CSS)	1	1%
Mid-Ocean Island-Hotspot (MOI)	2	1%
total	175	63%
null	105	38%
Emplacement Environment	**Number**	**Percentage**
Island Arc-Island Arc Collision (AAC)	3	2%
Island Arc-Continent Collision (ACC)	27	21%
Continent-Continent Collision (CCC)	30	23%
Accretionary Prism (ACP)	41	32%
Back-arc Basin Collapse (BAC)	20	15%
Intra-Arc Basin (IAB)	3	2%
Andean Margin (AND)	2	2%
Passive Continental Margin (PCM)	3	2%
Pull Apart Basin (PAB)	1	1%
total	130	46%
null	150	54%

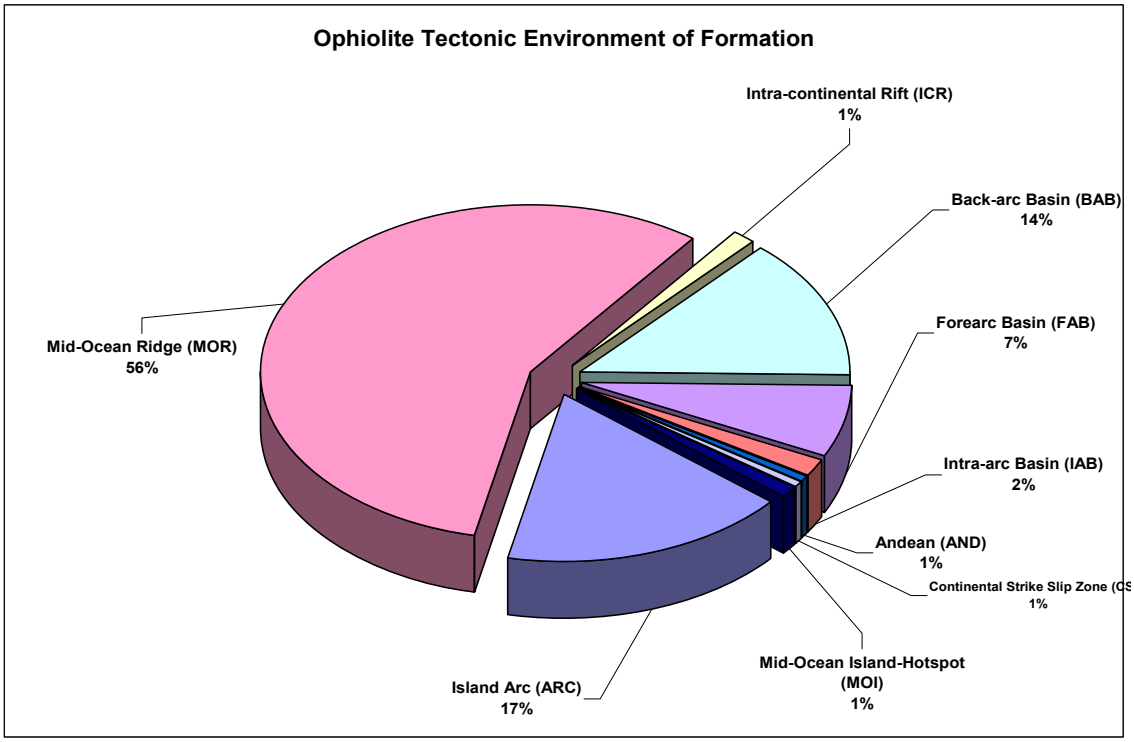

Figure 6.22 Tectonic environments of ophiolite formation

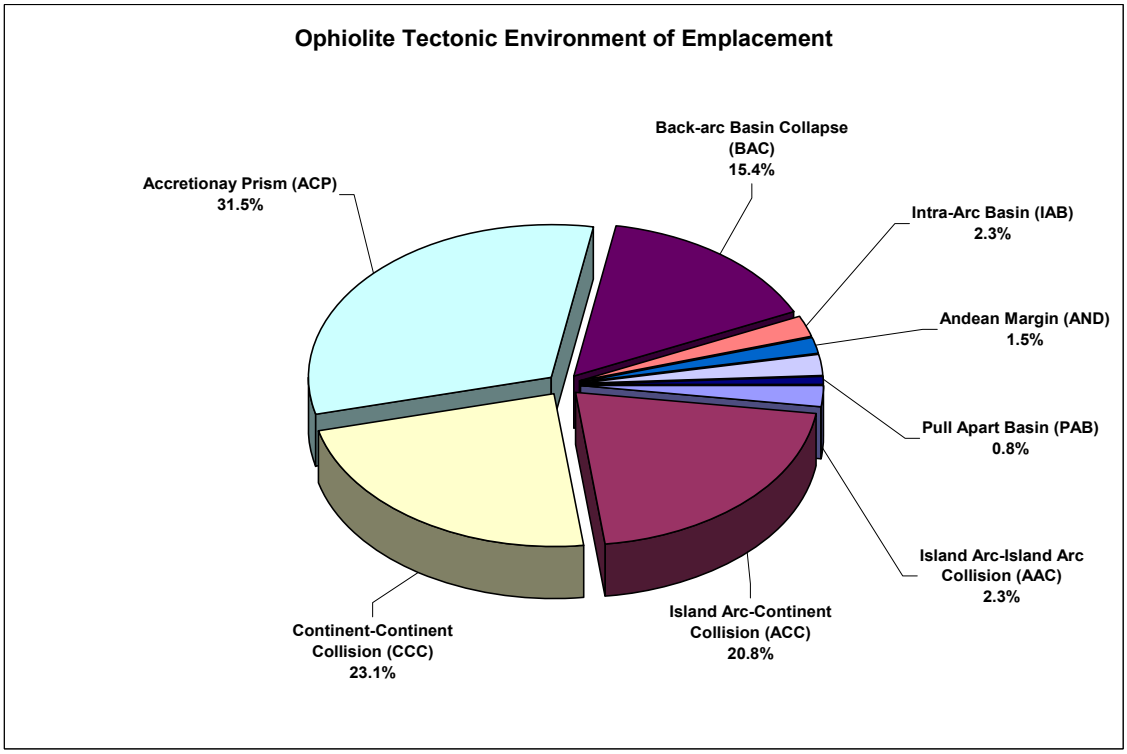

Figure 6.23 Tectonic environments of ophiolite emplacement

In the ophiolite emplacement environments, Figure 6.34, there are only 70 of the 280 ophiolite locations that cited the tectonic environments. These are typically more ambiguous in ascertaining as the rocks become metamorphosed and structurally dismembered over time. The major environments noted here (Figure 6.2) are continent-continent collision, island arc-continent collision, and accretionary prism which yield 36.8%, 20.6%, and 11.8% respectively. These emplacement environments are the expected result most researchers agree in which ophiolites are emplaced.

6.7 Conclusions

It is clear from the three different methods of analysis of the ophiolite data presented in this study, it is clear that there have been several significant formation and emplacement events. The data shows that the Paleozoic had greater tectonic activity during the Devonian through Cambrian and the Mesozoic and Cenozoic Eras had increased formation during the early Jurassic, early Cretaceous, and early Cenozoic. Dilek (2003b) presented a similar study on the distribution of ophiolites and when compared to the raw formation data in this study is an almost identical frequency distribution seen in Figures 6.26 and 6.27.

It is also clear that the ophiolite distribution though the geologic record is tied to major orogenic events, at least in the last 540 million years. Dilek's illustration is

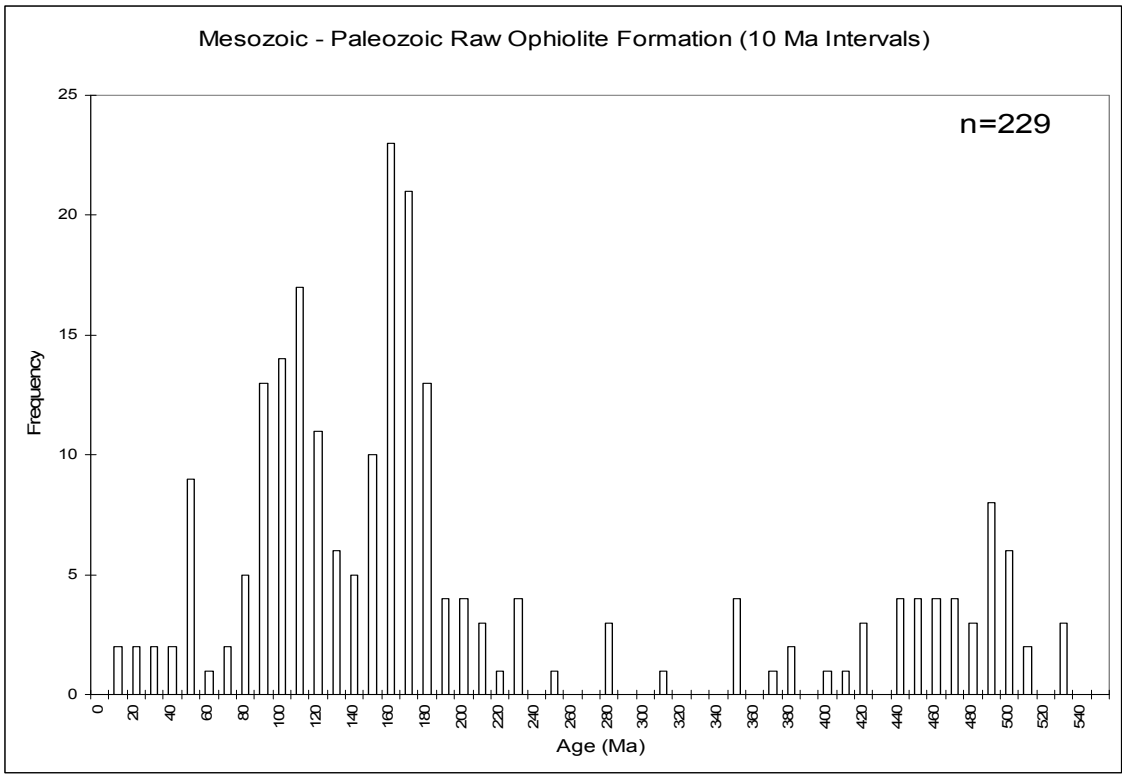

Figure 6.24 Ophiolite formation distributions over Mesozoic, Cenozoic, and Paleozoic

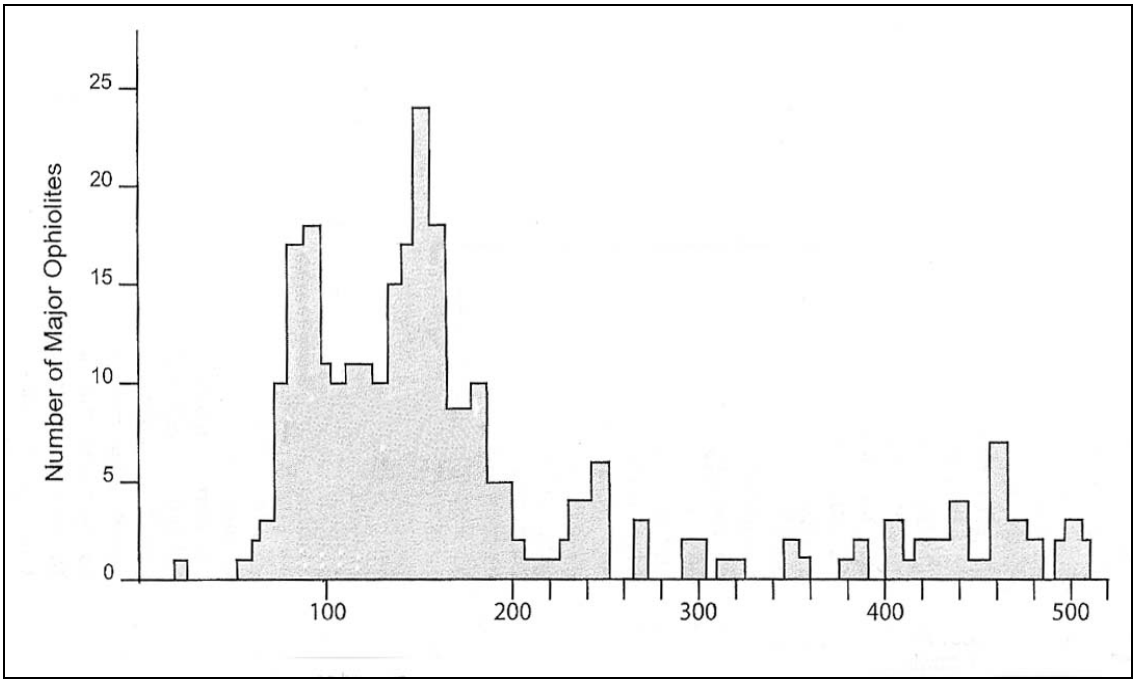

Figure 6.25 Major ophiolite occurrences (modified from Dilek, 2003b)

intended to be more of an overview of the pulses of ophiolitic events through time. Dilek suggests the link between the Wilson cycle and the stages of ocean sea floor spreading is a key factor to ophiolite formation (Dilek, 2003b) while Ishiwatari (1999a) links ophiolite pulses to major orogenic belts.

Abbate et al. (1985) also discussed the topic of ophiolite distribution over time and came to the same general conclusions with increased ophiolites occurring during the Jurassic and Ordovician due to general tectonic events. It is clear from the work of Dilek (2003b), Ishiwatari (1999a), and Abbate et al. (1985) as well as this thorough study of formation and emplacement that raw formation data is useful for general assumptions but more rigorous analysis present the specific distributions by region, time and type of environments. The best analysis, which depicts the trend of episodic ophiolite formation and emplacement, is the refined data seen in Figure 6.21. The modern world map with ophiolites, Figure 1.1 or Plate 11 in Appendix C, shows these events as they are continuing to be studied today.

APPENDIX A

OPHIOLITE DATABASE

Note: All ophiolite ages, mean ages, and differences in ages are given in millions of years (Ma). All Latitude and Longitude values are in decimal degrees. For further descriptions, see chapter two describing the structure of the database

Ophiolite #	Map #	Name	Country	Region	Longitude	Latitude	Area	Plate F
1.01	1	Halaban-Ithilal	Saudi Arabia	Al-Amar-Idas Suture	44.83	23.33		Saudi Arabia
1.02	1	Jabal Wask-Jabal Ess	Saudi Arabia	Western Coast (N of Al Hadina	37.83	25.83		Saudi Arabia
1.03	1	Fawakhir	Egypt	Central Eastern Desert	34.30	22.83	300 km 2	Egypt
1.04	10	Tihama - Asir	Saudi Arabia	Jizar, Eastern coastal plains of Red Sea	43.00	17.33		Saudi Arabia
1.05	1	Bir Umq	Saudi Arabia	NW Saudi Arabia	23.00	23.83		Sudan
1.06	1	Wadi Ghadir	Egypt	Central Eastern Desert	35.00	25.00		Egypt
1.07	1	Quift Quseir	Egypt	Central Eastern Desert	32.33	26.75		Egypt
1.08	1	Onib & Gerf	Sudan	Oniband Gerf Suture Zone (E. Coast)	36.25	22.83		Sudan
1.09	1	Al Amar	Saudi Arabia	Al Amar Suture zone	47.70	26.75		Saudi Arabia
1.10	1	Quseir Marsa Alam	Egypt	Central Eastern Desert	35.25	24.83		Egypt
1.11	1	Meatiq Dome	Egypt	Central Eastern Desert	34.00	27.33		Egypt
1.12	1	Wadi Hafafit	Egypt	Central Eastern Desert	35.55	24.00		Egypt
1.13	1	Nakasib	Sudan	Nakasib Suture zone (E coast)	36.00	20.00		Sudan
1.14	1	Onib Sol Hamed	Sudan		35.83	23.83		Sudan
1.15	1	Wadi Lawi - Wadi Lawai	Egypt	South of Eastern Desert	34.82	24.78		Egypt
1.16	1	Wadi 'Allaqi-Heiani	Egypt	S Egypt	32.90	22.90		Egypt
1.17	1	Abdola-Moyale	Ethiopia-Kenya	S-NE	39.07	3.52		Ethiopia
1.18	1	Yubdo	Ethiopia	W	38.35	4.00		Ethiopia
1.19	1	Baragoi	Kenya		36.50	1.70		Kenya
1.20		Ingessana Complex	Sudan		34.02	11.50		Sudan
2.01		Addie-Webster	USA	N. Carolina	-83.16	35.41		
2.02	3	Ballantrae	Scotland	SW Scotland	-4.80	55.20		UK
2.03	3	Bay of Islands 1	Newfoundland	W. Newfoundland	-58.00	49.40		Canada
2.04	3	Bay of Islands 2	Newfoundland	W. Newfoundland	-58.25	49.00		Canada
2.05	3	Bay of Islands 3	Newfoundland	W. Newfoundland	-58.50	48.70		Canada

Ophiolite #	Stratigraphic Age F	Old Age F	Young Age F	F Best Estimate	Difference Between Old Young Age F	Reliability Age F	Tectonic Environment F	Plate E	Stratigraphic Age E	Old Age E	Young Age E	E Best Estimate
1.01	NP	699.00	689.00	694.00	10.00	1	ARC	Saudi Arabia	NP	690.00	543.00	616.50
1.02	NP	834.00	810.00	822.00	24.00	2	IAB	Saudi Arabia	NP	782.00	767.00	774.50
1.03	NP	900.00	800.00	850.00	100.00	3		Egypt	NP	800.00	780.00	790.00
1.04	e Mioc	24.00	20.00	22.00	4.00	1	MOR					0.00
1.05	NP	848.00	828.00	838.00	20.00	1	BAB	Sudan	NP	720.00	640.00	680.00
1.06	NP	765.00	726.00	745.50	39.00	2		Egypt	NP	746.00	727.00	736.50
1.07	NP	810.00	790.00	800.00	20.00	1		Egypt	NP	800.00	780.00	790.00
1.08	NP	822.00	794.00	808.00	28.00	2		Sudan	NP	762.00	720.00	741.00
1.09	NP	702.00	686.00	694.00	16.00	1		Saudi Arabia	NP	663.00	660.00	661.50
1.10	NP	800.00	780.00	790.00	20.00	1		Egypt	NP	800.00	780.00	790.00
1.11	NP	596.00	594.00	595.00	2.00	1		Egypt	NP	589.00	587.00	588.00
1.12	NP	900.00	700.00	800.00	200.00	3	ARC					0.00
1.13	NP	840.00	760.00	800.00	80.00	3	ARC	Sudan	NP	760.00	700.00	730.00
1.14	NP	735.00	735.00	735.00	0.00	1	BAB	Sudan				0.00
1.15	NP	900.00	543.00	721.50	357.00	3	ARC	Egypt				0.00
1.16	NP	710.00	710.00	710.00	0.00	1						0.00
1.17	NP	700.00	700.00	700.00	0.00	1	MOR	Ethiopia				0.00
1.18				0.00	0.00	0	ARC	Ethiopia	NP	800.00	800.00	800.00
1.19	NP	796.00	796.00	796.00	0.00	1	MOR	Kenya	NP	609.00	609.00	609.00
1.20				0.00	0.00	0	ARC					0.00
2.01				0.00	0.00	0						0.00
2.02	e Ord	487.00	479.00	483.00	8.00	1	ARC	UK	e Ord	482.00	474.00	478.00
2.03	Camb	515.00	475.00	495.00	40.00	2	MOR	Canada	e - l Ord	485.00	454.00	469.50
2.04	Camb	508.00	504.00	506.00	4.00	1	MOR	Canada	m Ord	469.00	469.00	469.00
2.05	e Ord	489.00	486.00	487.50	3.00	1	MOR	Canada	m Ord	469.00	463.00	466.00

Ophiolite #	Difference Between Old Young Age E	Reliability Age E	Tectonic Environment E	Difference Formation Emplacement Age	Obduction Complex	Overlying Sediment Name	Mantle	Moho	Cummulates	Gabbro	Dikes	Pillows	Sediments	Completeness Score
1.01	147.00	3	ACP	77.50	Halaban-Ithilal		1	0	0	1	1	1	1	5
1.02	15.00	1	AAC	47.50	Jabal Wask-Jabal Ess		1	1	1	1	1	0	1	6
1.03	20.00	1		60.00	Fawakhir		1	0	1	1	0	0	0	3
1.04	0.00	0		22.00	Tihama - Asir		1	0	0	1	1	0	1	4
1.05	80.00	3		158.00	Bir Umk		0	0	1	1	1	1	1	5
1.06	19.00	1		9.00	Wadi Ghadir		0	0	1	1	1	1	1	5
1.07	20.00	1		10.00	Quift - Quseir		1	0	1	1	1	1	1	6
1.08	42.00	3		67.00	Onib and Gerf		0	0	1	1	1	1	0	4
1.09	3.00	1		32.50	Al Amar		1	0	1	1	1	1	1	6
1.10	20.00	1		0.00	Quseir Marsa Alam		1	0	1	1	1	1	0	5
1.11	2.00	1		7.00	Meatiq		0	0	0	0	0	0	1	1
1.12	0.00	0		800.00	Wadi - Hafafit									0
1.13	60.00	3	ACC	70.00	Nakasib		0	0	1	1	0	0	1	3
1.14	0.00	0	AAC	735.00			1	1	1	1	1	1	1	7
1.15	0.00	0	ACC	721.50	Wadi Lawi - Wadi Lawai Melange		0	0	1	1	0	0	0	2
1.16	0.00	0		710.00										0
1.17	0.00	0	ACP	700.00			0	1	1	1	0	1	1	5
1.18	0.00	1	AAC	-800.00			0	1	1	1	0	1	0	4
1.19	0.00	1		187.00			1	1	1	1	1	1	1	7
1.20	0.00	0		0.00			0	1	1	1	1	1	1	6
2.01	0.00	0		0.00										0
2.02	8.00	1		5.00										0
2.03	31.00	2		25.50	Lewis Hills Massif									0
2.04	0.00	1		37.00	Lewis Hills Massif									0
2.05	6.00	1		21.50	Lewis Hills Massif									0

Ophiolite #	Map #	Name	Country	Region	Longitude	Latitude	Area	Plate F
2.06	3	Gibbs Islands	Scotland	Shetland Islands	-1.30	60.50		UK
2.07	3	Hare Bay	Canada	Newfoundland	-56.80	51.20		Canada
2.08	3	Hoch Grossen	Austria		14.20	47.40		Austria
2.09	7	Kraubath	Austria		14.80	47.30		Austria
2.10	3	Limousin	France		-2.00	45.50		France
2.11	4	Lizard Ophiolite	England		-5.20	49.90		UK
2.12		Massif Central	France		4.50	45.50		
2.13		Massif Amoricain	France		-3.00	48.40		
2.14	4	Munchberg gneiss	Germany		11.80	50.20		Germany
2.15	1	Purtuniq 1	Canada	N Quebec	-73.00	62.00	5 sq deg	Canada
2.16	1	Purtuniq 2	Canada	N Quebec	-75.50	62.00	5 sq deg	Canada
2.17	1	Purtuniq 3	Canada	N Quebec	-78.00	62.00	5 sq deg	Canada
2.18	3	Scandinavian Caledonides 1	Norway	N Scandinavian Caledonides	20.00	69.70		Norway
2.19	3	Scandinavian Caledonides 2	Norway	N Scandinavian Caledonides	16.20	67.20		Norway
2.20	3	Scandinavian Caledonides 3	Norway	N Scandinavian Caledonides	12.00	65.10		Norway
2.21	3	Scandinavian Caledonides 4	Norway	N Scandinavian Caledonides	10.00	63.20		Norway
2.22	3	Scandinavian Caledonides 5	Norway	N Scandinavian Caledonides	4.80	61.10		Norway
2.23	3	Scandinavian Caledonides 6	Norway	N Scandinavian Caledonides	5.25	59.75		Norway
2.24	3	Scandinavian Caledonides 7	Norway	N Scandinavian Caledonides	5.25	59.25		Norway
2.25	3	Scandinavian Caledonides 8	Norway	N Scandinavian Caledonides	11.50	63.10		Norway
2.26	3	Mt. Albert	Canada	Quebec	-66.20	48.92		Canada
2.27	3	Mt. Orford	Canada	Quebec	-72.40	45.33		Canada
2.29	3	Thetford Mines	Canada	Black Lake	-71.30	46.10		Canada
2.30	3	St. Anthony	Canada		-55.58	51.37		Canada
2.31	7	Shulaps	Canada	Bridge River	-120.30	50.80	180 km2	Canada

Ophiolite #	Stratigraphic Age F	Old Age F	Young Age F	F Best Estimate	Difference Between Old Young Age F	Reliability Age F	Tectonic Environment F	Plate E	Stratigraphic Age E	Old Age E	Young Age E	E Best Estimate
2.06	e - m Ord	479.00	465.00	472.00	14.00	1	MOR					0.00
2.07	e Ord	488.00	479.00	483.50	9.00	1	MOR	Canada	e - m Ord	471.80	464.00	467.90
2.08	Camb-Ord	545.00	455.00	500.00	90.00	3						0.00
2.09	e Carb	354.00	327.00	340.50	27.00	2	MOR	Austria	m Jur	175.00	175.00	175.00
2.10	e Sil - e Dev	440.00	400.00	420.00	40.00	2						0.00
2.11	e Dev - e Carb	403.00	350.00	376.50	53.00	3	BAB	UK	m Dev - e Carb	377.00	337.00	357.00
2.12				0.00	0.00	0						0.00
2.13				0.00	0.00	0						0.00
2.14	Camb	525.00	525.00	525.00	0.00	1	MOR	Germany	m Dev - e Carb	380.00	336.00	358.00
2.15	PP	2000.00	1960.00	1980.00	40.00	2						0.00
2.16	PP	2000.00	1960.00	1980.00	40.00	2						0.00
2.17	PP	2000.00	1960.00	1980.00	40.00	2						0.00
2.18	e Sil	443.00	443.00	443.00	0.00	1	MOR	Norway	e Sil	443.00	428.00	435.50
2.19	e Sil	437.00	437.00	437.00	0.00	1	MOR	Norway	e Sil	443.00	428.00	435.50
2.20	Camb	497.00	497.00	497.00	0.00	1	MOR	Norway	e Sil	443.00	428.00	435.50
2.21	e Ord	478.00	478.00	478.00	0.00	1	MOR	Norway	e Sil	443.00	428.00	435.50
2.22	e Sil	443.00	443.00	443.00	0.00	1	MOR	Norway	e Sil	425.00	425.00	425.00
2.23	e Ord	485.00	485.00	485.00	0.00	1	MOR	Norway	e Sil	443.00	428.00	435.50
2.24	e Ord	485.00	485.00	485.00	0.00	1	MOR	Norway	e Sil	443.00	428.00	435.50
2.25	m Ord	466.50	466.50	466.50	0.00	1	MOR	Norway	e Sil	443.00	428.00	435.50
2.26	m Ord	460.00	456.00	458.00	4.00	1						0.00
2.27	e - m Ord	480.00	460.00	470.00	20.00	1		Canada				0.00
2.29	Camb - e Ord	494.00	478.00	486.00	16.00	1		Canada	e Ord	482.00	472.00	477.00
2.30	e Ord	488.00	479.00	483.50	9.00	1		Canada	e - m Ord	471.80	464.00	467.90
2.31	m Tr - e K	242.00	121.00	181.50	121.00	3	ARC					0.00

Ophiolite #	Difference Between Old Young Age E	Reliability Age E	Tectonic Environment E	Difference Formation Emplacement Age	Obduction Complex	Overlying Sediment Name	Mantle	Moho	Cummulates	Gabbro	Dikes	Pillows	Sediments	Completeness Score
2.06	0.00	0		472.00										0
2.07	7.80	1	BAC	15.60										0
2.08	0.00	0		500.00										0
2.09	0.00	1	BAC	165.50	Speik									0
2.10	0.00	0		420.00	Variscan French Massif		1	1	1	1	0	0	0	4
2.11	40.00	2	CCC	19.50			0	1	1	1	1	0	1	5
2.12	0.00	0		0.00										0
2.13	0.00	0		0.00										0
2.14	44.00	3	CCC	167.00										0
2.15	0.00	0		1980.00										0
2.16	0.00	0		1980.00										0
2.17	0.00	0		1980.00										0
2.18	15.00	1	BAB	7.50	Solund - Stavfjord	Herland group							1	1
2.19	15.00	1	BAB	1.50	Solund - Stavfjord	Herland group							1	1
2.20	15.00	1	BAB	61.50	Solund - Stavfjord	Herland group							1	1
2.21	15.00	1	BAB	42.50	Solund - Stavfjord	Herland group							1	1
2.22	0.00	1	BAB	18.00	Solund - Stavfjord	Herland group	0	1	0	1	1	1	1	5
2.23	15.00	1	BAB	49.50	Solund - Stavfjord	Herland group	0	1	0	1	1	1	1	5
2.24	15.00	1	BAB	49.50	Solund - Stavfjord	Herland group	0	1	0	1	1	1	1	5
2.25	15.00	1	BAB	31.00	Solund - Stavfjord	Herland group							1	1
2.26	0.00	0		458.00										0
2.27	0.00	0	BAC	470.00			0	1	1	1	1	1	0	5
2.29	10.00	1	BAC	9.00			1	1	1	1	1	1	0	6
2.30	7.80	1		15.60										0
2.31	0.00	0		181.50			0	0	1	1	1	1	1	5

Ophiolite #	Map #	Name	Country	Region	Longitude	Latitude	Area	Plate F
2.32	1	Outokumpu	Finland	East	29.01	62.43		Finland
2.33	3	Karmøy	Norway		5.25	59.25		Norway
2.34	3	Gullfjellet	Norway		6.00	60.40		Norway
2.35	3	Leka	Norway		11.70	65.10		Norway
2.36	3	Solund-Stavfjord	Norway		4.80	61.10		Norway
2.37	3	Asbestos	Canada	near Thetford	-71.90	45.80		Canada
2.38	1	Jormua	Finland	NE	29.00	64.50		Finland
2.39		Buck Creek	USA	N Carolina	-83.50	35.00		
3.01	3	Nurali	Russia	S Urals	59.70	54.80		Russia
3.02	3	Mindyak	Russia	S Urals	58.00	53.00	300 km	Russia
3.03	4	Kraka	Russia	S Urals	57.50	52.50		Russia
3.04	3	Kempersay Massif	Russia	S Urals	58.00	50.00		Russia
3.05	3	Sakmara Massif	Russia	S Urals	57.00	52.00		Russia
3.06	3	Voykar	Russia	Polar Urals	62.00	66.00		Russia
3.07	7	Chersky	Russia	E Sakha Republic (Yakutia)	161.83	68.83		Russia
3.08	8	Mainitis Zone	Russia	Koryak Mt Central	175.83	63.83		Russia
3.09	8	Ust' - Belaya Mts	Russia	Koryak Mt North	173.00	65.83	1000 km2	Russia
3.10	8	Kuyul Mélange	Russia	Koryak Mt Peninsula	165.00	62.90		Russia
3.11	8	Upper Khatyrka	Russia	Koryak Mt Central	172.83	62.67		Russia
3.12	9	Vyvenka	Russia		169.00	61.50		Russia
3.13	9	Goven Peninsula	Russia	Koryak Mt	163.00	59.00	900 km2	Russia
3.14	8	Porotory Cape	Russia	Taigonos Peninsula (Uga - Murugal)	161.83	61.75		Russia
3.15	8	Elistratova Complex	Russia	Taigonos Peninsula (S Koryak Mt)	163.00	62.00	120 km2	Russia
3.16	8	Aluchin	Russia	NE Margin of Kolyma Omalon Block	165.50	66.50		Russia
3.17	2	Primorye	Russia	E Russia	131.33	43.03		Russia

Ophiolite #	Stratigraphic Age F	Old Age F	Young Age F	F Best Estimate	Difference Between Old Young Age F	Reliability Age F	Tectonic Environment F	Plate E	Stratigraphic Age E	Old Age E	Young Age E	E Best Estimate
2.32	PP	1970.00	1970.00	1970.00	0.00	1	MOR					0.00
2.33	Camb - e Ord	500.00	489.00	494.50	11.00	1	ICR	Norway				0.00
2.34	Camb - e Ord	492.00	486.00	489.00	6.00	1	MOR					0.00
2.35	Ord	499.00	495.00	497.00	4.00	1	MOR					0.00
2.36	l Ord - e Sil	446.00	440.00	443.00	6.00	1	ARC	Norway	l Sil - e Dev	426.00	400.00	413.00
2.37	e - m Ord	480.00	460.00	470.00	20.00	1		Canada	m Dev - e Carb	377.00	377.00	377.00
2.38	PP	1956.00	1950.00	1953.00	6.00	1	MOR					0.00
2.39				0.00	0.00	0						0.00
3.01	m - l Ord	472.00	443.00	457.50	29.00	2	IAB	Russia	e Dev	400.00	400.00	400.00
3.02	e Dev	415.00	410.00	412.50	5.00	1		Russia				0.00
3.03	Ord-Sil	490.00	417.00	453.50	73.00	3	IAB	Russia	l Dev - e Carb	370.00	327.00	348.50
3.04	m Ord - e Sil	470.00	428.00	449.00	42.00	3		Russia	l Sil - e Dev	423.00	391.00	407.00
3.05	e Ord	490.00	470.00	480.00	20.00	1		Russia	e Sil - e Dev	428.00	391.00	409.50
3.06	e Dev	417.00	391.00	404.00	26.00	2		Russia	m Dev	391.00	380.00	385.50
3.07	e Sil - m Dev	430.00	370.00	400.00	60.00	3	BAB	Russia	m Jur	174.00	170.00	172.00
3.08	l Jur - e K	159.00	121.00	140.00	38.00	2	ARC	Russia	e K	144.00	99.00	121.50
3.09	e Dev - e Carb	417.00	323.00	370.00	94.00	3		Russia	e K	137.00	132.00	134.50
3.10	l Jur - e K	155.00	121.00	138.00	34.00	2	ARC	Russia	e - l K	121.00	99.00	110.00
3.11	Tr	248.00	206.00	227.00	42.00	3	FAB	Russia	e K	144.00	112.00	128.00
3.12	l K	95.15	95.15	95.15	0.00	1		Russia				0.00
3.13	l K	83.00	65.00	74.00	18.00	1		Russia				0.00
3.14	l Jur l K	159.00	99.00	129.00	60.00	3	ARC					0.00
3.15	l Tr - l Jur	210.00	144.00	177.00	66.00	3	ARC	Russia	e - l K	121.00	99.00	110.00
3.16	m Dev - m Tr	374.00	231.00	302.50	143.00	3	MOR	Russia	e K	144.00	112.00	128.00

Ophiolite #	Difference Between Old Young Age E	Reliability Age E	Tectonic Environment E	Difference Formation Emplacement Age	Obduction Complex	Overlying Sediment Name	Mantle	Moho	Cummulates	Gabbro	Dikes	Pillows	Sediments	Completeness Score
2.32	0.00	0		1970.00										0
2.33	0.00	0	ACP	494.50										0
2.34	0.00	0		489.00										0
2.35	0.00	0		497.00										0
2.36	26.00	2	BAB	30.00	Sunnfjord Mélange		0	1	0	1	1	1	1	5
2.37	0.00	1	BAC	93.00			0	1	1	1	1	1	0	5
2.38	0.00	0		1953.00			1	0	1	1	1	1	0	5
2.39	0.00	0		0.00										0
3.01	0.00	1		57.50			1	1	0	1	1	1	1	6
3.02	0.00	0	CCC	412.50	Mindyak		1	1	0	1	1	1	1	6
3.03	43.00	3	ACP	105.00	Kraka	Filair Formation	1	1	0	1	1	0	1	5
3.04	32.00	2		42.00	Kempersay		1	1	0	1	1	1	1	6
3.05	37.00	2		70.50			1	1	0	1	1	1	1	6
3.06	11.00	1		18.50										0
3.07	4.00	1	CCC	228.00	Chersky		1	0	1	0	1	1	1	5
3.08	45.00	3		18.50										0
3.09	5.00	1	ACP	235.50										0
3.10	22.00	2	ACP	28.00	Kuyul Massif									0
3.11	32.00	2	ACP	99.00										0
3.12	0.00	0	ACP	95.15										0
3.13	0.00	0	ACP	74.00										0
3.14	0.00	0		129.00	Uga - Murugal		1	0	1	0	0	1	1	4
3.15	22.00	2	ACP	67.00	Elistratova		1	0	1	1	1	1	1	6
3.16	32.00	2	CCC	174.50	Aluchin		1	0	1	1	1	0	0	4
3.17	0.00	0		527.50	Primorye									0

Ophiolite #	Map #	Name	Country	Region	Longitude	Latitude	Area	Plate F
3.18	3	Khabarny	Russia	S Urals	57.80	51.00		Russia
3.19	1	Itmurunda zone	Russia		67.50	46.50		Russia
3.20	1	Northern Baykal	Russia	N Baykal	104.79	51.88		Russia
3.21	1	Sharyzhalgay	Russia	SW Baykal	103.97	55.00		Russia
3.22	8	Koryak	Russia	Koryak Mt NE Russia	173.00	63.00		Russia
3.23	8	Taigonos Peninsula (Uga-Murugal)	Russia	Cape Povorotny	161.50	61.12		Russia
4.01	7	NW Alaska	USA	Misheguk Mt	-161.00	68.00		US
4.02	7	Brooks Range	USA	Alaska	-152.25	68.20		US
4.03	9	Ingalls Complex	USA	Washington	-121.95	41.68		US
4.04	5	Canyon Mt	USA	E Oregon, Blue Mts Baker terrane	-119.00	44.40	200 km2	US
4.05	7	Sparta	USA	E Oregon, Blue Mts Wallowa terrane	-117.60	44.80		US
4.06	7	Josephine (Smith River)	USA	Northernmost California	-124.00	41.80		US
4.07	3	Trinity	USA	Klamath Mt	-122.50	41.10		US
4.08	7	Franciscan New Idria	USA	California	-120.60	36.40		US
4.09	7	Franciscan Burro Mt	USA	California	-121.33	36.80		US
4.10	7	Franciscan Cazadero	USA	California	-123.10	38.60		US
4.11	7	Franciscan Red Mt	USA	California	-123.70	39.85		US
4.12	7	Coast Range Del Puerto	USA	Western California	-121.40	37.40		US
4.13	7	Coast Range Point Sal	USA	Western California	-120.75	35.40		US
4.14	7	Coast Range Black Mountain	USA	Western California	-122.50	38.50		US
4.15	7	Coast Range Stonyford	USA	Western California	-122.60	39.00		US
4.16	7	Coast Range Paskenta	USA	Western California	-122.60	39.80		US
4.17	7	Coast Range Llanada	USA	Western California	-120.40	36.40		US
4.18	7	Coast Range Hospital Canyon	USA	Western California	-121.30	37.30		US
4.19	7	Great Valley Cuesta Ridge	USA	Central California	-121.30	38.00		US

Ophiolite #	Stratigraphic Age F	Old Age F	Young Age F	F Best Estimate	Difference Between Old Young Age F	Reliability Age F	Tectonic Environment F	Plate E	Stratigraphic Age E	Old Age E	Young Age E	E Best Estimate
3.18	e Ord - Sil	490.00	430.00	460.00	60.00	3						0.00
3.19	NP	820.00	775.00	797.50	45.00	3	MOR					0.00
3.20	MP	1400.00	800.00	1100.00	600.00	3	MOR					0.00
3.21	PP	2500.00	2400.00	2450.00	100.00	3	MOR					0.00
3.22	e K	144.00	121.00	132.50	23.00	2	ARC	Russia	e - l K	121.00	99.00	110.00
3.23	e K	129.00	129.00	129.00	0.00	1	ARC	Russia				0.00
4.01	m - l Jur	180.00	144.00	162.00	36.00	2		US				0.00
4.02	e - m Jur	186.00	168.00	177.00	18.00	1		US	m Jur	169.00	163.00	166.00
4.03	m - l Jur	180.00	144.00	162.00	36.00	2	MOR	US	l K	99.00	99.00	99.00
4.04	e Perm	278.00	265.50	271.75	12.50	1	ARC					0.00
4.05				0.00	0.00	0	MOR	US	l Jur - e K	157.00	157.00	157.00
4.06	m Jur	180.00	162.00	171.00	18.00	1	BAB					0.00
4.07	Ord	480.00	450.00	465.00	30.00	2	BAB	US	m - l Ord	470.00	443.00	456.50
4.08	m Jur	180.00	159.00	169.50	21.00	2	ARC	US	e K	140.00	140.00	140.00
4.09	m Jur	180.00	159.00	169.50	21.00	2	ARC	US	e K	140.00	140.00	140.00
4.10	m Jur	180.00	159.00	169.50	21.00	2		US	e K	140.00	140.00	140.00
4.11	m Jur	180.00	159.00	169.50	21.00	2		US	e K	140.00	140.00	140.00
4.12	m - l Jur	168.00	154.00	161.00	14.00	1	MOR	US	e K	140.00	140.00	140.00
4.13	l Jur	159.00	144.00	151.50	15.00	1	MOR					0.00
4.14	m - l Jur	164.00	154.00	159.00	10.00	1	MOR					0.00
4.15	m Jur	172.00	166.00	169.00	6.00	1	MOR	US	m Jur	161.00	161.00	161.00
4.16	m - l Jur	163.00	159.00	161.00	4.00	1	MOR	US	m Jur	161.00	161.00	161.00
4.17	m Jur	170.00	164.00	167.00	6.00	1	MOR	US	m Jur	161.00	161.00	161.00
4.18	m Jur	170.00	170.00	170.00	0.00	1	MOR	US	m Jur	161.00	161.00	161.00
4.19	l Jur	151.00	144.00	147.50	7.00	1						0.00

Ophiolite #	Difference Between Old Young Age E	Reliability Age E	Tectonic Environment E	Difference Formation Emplacement Age	Obduction Complex	Overlying Sediment Name	Mantle	Moho	Cummulates	Gabbro	Dikes	Pillows	Sediments	Completeness Score
3.18	0.00	0		460.00			1	1	0	1	1	1	1	6
3.19	0.00	0		797.50										0
3.20	0.00	0		1100.00										0
3.21	0.00	0		2450.00										0
3.22	22.00	2	ACP	22.50										0
3.23	0.00	0	ACP	129.00										0
4.01	0.00	0	ACP	162.00			1	0	1	1	1	0	0	4
4.02	6.00	1	ACP	11.00										0
4.03	0.00	1	ACP	63.00			1	0	1	1	1	0	0	4
4.04	0.00	0		271.75			1	0	1	1	1	0	0	4
4.05	0.00	1		-157.00										0
4.06	0.00	0		171.00		Galice formation	1	0	1	1	1	1	1	6
4.07	0.00	1		465.00		Carboniferous seds	1	0	0	0	1	1	0	3
4.08	0.00	1		29.50										0
4.09	0.00	1	ACP	29.50										0
4.10	0.00	1	ACP	29.50										0
4.11	0.00	1	ACP	29.50										0
4.12	0.00	1		21.00		Upper Jurassic & Great Valley Sequence								0
4.13	0.00	0		151.50		Upper Jurassic & Great Valley Sequence								0
4.14	0.00	0		159.00		Upper Jurassic & Great Valley Sequence								0
4.15	0.00	1		8.00		Upper Jurassic & Great Valley Sequence								0
4.16	0.00	1		0.00		Upper Jurassic & Great Valley Sequence								0
4.17	0.00	1		6.00		Upper Jurassic & Great Valley Sequence								0
4.18	0.00	1		9.00		Upper Jurassic & Great Valley Sequence								0
4.19	0.00	0		147.50										0

Ophiolite #	Map #	Name	Country	Region	Longitude	Latitude	Area	Plate F
4.20	7	Great Valley 2	USA	Central California	-121.75	38.75		US
4.21	7	Great Valley 3	USA	Central California	-122.25	40.00		US
4.22	7	Great Valley 4	USA	Central California	-120.25	36.80		US
4.23	7	Great Valley 5	USA	Central California	-119.60	36.00		US
4.24	7	Sierra Nevada Foothills 1	USA	Eastern California	-121.40	39.80		US
4.25	7	Sierra Nevada Foothills 2	USA	Eastern California	-121.30	39.00		US
4.26	7	Sierra Nevada Foothills 3	USA	Eastern California	-121.00	38.00		US
4.27	7	Sierra Nevada Foothills Smartville	USA	Eastern California	-121.40	39.25		US
4.28	7	Stanley Mountain	USA	Eastern California	-120.50	35.00		US
4.29	7	Sierra Nevada Foothills Kings River	USA	Eastern California	-118.50	36.80		US
4.30		Sarmiento	Chile	Southern	-74.00	-51.05		
4.31	7	Baja Alta Terrane	Mexico	California peninsula	-114.20	27.50		Mexico
4.32	7	Elder Creek	USA	California	-122.60	40.00		US
4.33	7	Cedros Island	Mexico	California	-115.25	28.50		Mexico
4.34	7	Vizcaino	Mexico	NW	-114.50	27.50		Mexico
4.35	10	Taitao	Chile	S	-73.00	-46.00		Chile
4.36	9	Resurrection Peninsula	USA	S Alaska	-152.00	57.50		
5.01	8	Masirah	Oman	E	58.70	20.46		Oman
5.02	9	Semail	Oman	N	57.50	24.00	60,000 km2	Oman
5.03	9	Sabzevar	Iran	NE	57.66	36.25		Iran
5.04	6	Mashod	Iran	NE	59.16	36.16		Iran
5.05	9	Tchehel Kureh	Iran		58.00	30.00		Iran
5.06	9	Iranshahr	Iran	SE	60.40	26.16		Iran
5.07	9	Fanuj Maskutan	Iran	SE	59.75	26.75		Iran
5.08	9	Kahnuj	Iran	S	57.75	27.67	600 km2	Iran

Ophiolite #	Stratigraphic Age F	Old Age F	Young Age F	F Best Estimate	Difference Between Old Young Age F	Reliability Age F	Tectonic Environment F	Plate E	Stratigraphic Age E	Old Age E	Young Age E	E Best Estimate
4.20	l Jur	151.00	144.00	147.50	7.00	1						0.00
4.21	l Jur	151.00	144.00	147.50	7.00	1						0.00
4.22	l Jur	151.00	144.00	147.50	7.00	1						0.00
4.23	l Jur	151.00	144.00	147.50	7.00	1						0.00
4.24	m - l Jur	162.00	156.00	159.00	6.00	1	ARC	US	l Jur - e K	150.00	140.00	145.00
4.25	m - l Jur	162.00	156.00	159.00	6.00	1	ARC	US	l Jur - e K	150.00	140.00	145.00
4.26	m - l Jur	162.00	156.00	159.00	6.00	1	ARC	US	l Jur - e K	150.00	140.00	145.00
4.27	m - l Jur	162.00	156.00	159.00	6.00	1	ARC	US	l Jur - e K	150.00	140.00	145.00
4.28	m Jur	168.00	164.00	166.00	4.00	1						0.00
4.29	m - l Jur	165.00	155.00	160.00	10.00	1		US	l Jur - e K	150.00	140.00	145.00
4.30				0.00	0.00	0						0.00
4.31	l Tr	221.00	220.00	220.50	1.00	1	BAB	Mexico	l Jur - e K	156.00	135.00	145.50
4.32	m Jur	172.00	165.00	168.50	7.00	1	ARC	US				0.00
4.33	m Jur	175.00	171.00	173.00	4.00	1	BAB	Mexico	l Jur - e K	156.00	135.00	145.50
4.34	l Tr	223.00	219.00	221.00	4.00	1	FAB	Mexico	l Jur - e K	156.00	135.00	145.50
4.35	l Mioc	11.20	5.30	8.25	5.90	1	FAB	Chile				0.00
4.36				0.00	0.00	0		US	l Paleoc	57.00	57.00	57.00
5.01	l Jur - e K	158.00	124.00	141.00	34.00	2	MOR	Oman	e K	132.00	121.00	126.50
5.02	l K	97.90	93.50	95.70	4.40	1	MOR	Oman	l K	95.00	90.00	92.50
5.03	l K	99.00	65.00	82.00	34.00	2	MOR	Iran	e Paleoc	65.00	65.00	65.00
5.04	l Tr	210.00	210.00	210.00	0.00	1	BAB	Iran				0.00
5.05	l K	99.00	65.00	82.00	34.00	2	MOR	Iran	e Paleoc	65.00	65.00	65.00
5.06	l K	99.00	65.00	82.00	34.00	2	BAB	Iran	e Paleoc	65.00	65.00	65.00
5.07	l K	99.00	65.00	82.00	34.00	2	BAB	Iran	e Paleoc	65.00	65.00	65.00
5.08	e K	144.00	121.00	132.50	23.00	2	MOR	Iran	l K	89.00	66.00	77.50

Ophiolite #	Difference Between Old Young Age E	Reliability Age E	Tectonic Environment E	Difference Formation Emplacement Age	Obduction Complex	Overlying Sediment Name	Mantle	Moho	Cummulates	Gabbro	Dikes	Pillows	Sediments	Completeness Score
4.20	0.00	0		147.50										0
4.21	0.00	0		147.50										0
4.22	0.00	0		147.50										0
4.23	0.00	0		147.50										0
4.24	10.00	1	ACC	14.00										0
4.25	10.00	1	ACC	14.00										0
4.26	10.00	1	ACC	14.00										0
4.27	10.00	1	ACC	14.00										0
4.28	0.00	0		166.00										0
4.29	10.00	1		15.00										0
4.30	0.00	0		0.00										0
4.31	21.00	2		75.00										0
4.32	0.00	0	ACP	168.50			0	0	1	1	1	0	0	3
4.33	21.00	2		27.50										0
4.34	21.00	2		75.50		San Hipolito								0
4.35	0.00	0	ACP	8.25	Bahia San Andres Fm		0	0	1	1	1	1	1	5
4.36	0.00	1	ACP	-57.00										0
5.01	11.00	1		14.50			1	1	0	1	1	1	1	6
5.02	5.00	1	PCM	3.20			1	1	0	1	0	0	1	4
5.03	0.00	1		17.00										0
5.04	0.00	0	PAB	210.00										0
5.05	0.00	1		17.00										0
5.06	0.00	1	BAC	17.00										0
5.07	0.00	1	BAC	17.00										0
5.08	23.00	2	PCM	55.00	Bond - e Zeyarat		0	1	1	1	1	1	1	6

Ophiolite #	Map #	Name	Country	Region	Longitude	Latitude	Area	Plate F
5.09	9	Esfandagheh	Iran		57.25	28.67		Iran
5.10	9	Shahr-Babak	Iran	Central Iran	55.25	30.66		Iran
5.11	9	Baft	Iran	South Central	56.66	29.25		Iran
5.12	9	Neyriz	Iran	South Central	54.33	29.55		Iran
5.13	9	Nain	Iran	Central Iran	53.00	33.00		Iran
5.14	9	Kermanshah	Iran	W	47.25	34.50		
5.15	6	Rasht	Iran	NW	49.00	37.00		Iran
5.16	9	Khoy	Iran	NW	44.75	38.75	770 km2	Iran
5.17	9	Baër-Bassit	Syria	NW	36.00	35.75		Syria
5.18	9	Kizildağ	Turkey	SE	36.00	36.25	900 km2	Turkey
5.19	9	Mersin	Turkey	S	34.50	36.75	900 km2	Turkey
5.20	9	Aladaj	Turkey	S	35.00	38.00		Turkey
5.21	9	Kiziltepe	Turkey	S	34.33	38.20	1.7 km2	Turkey
5.22	9	Ali Hoca	Turkey	S	34.33	38.25	161 km2	Turkey
5.23	9	Yuksekova	Turkey	SE	38.00	37.00		Turkey
5.24	9	Yayladağ	Turkey	SE	36.08	35.83		Turkey
5.25	9	Berit	Turkey	SE	37.00	37.50		Turkey
5.26	9	Pozanti-Karsanti	Turkey	SE	35.50	37.00	3000 km2	Turkey
5.27		Ovacik	Turkey	SE	32.92	39.23		
5.28	9	Sarikaramn	Turkey	Central Anatolia	34.25	38.75		Turkey
5.29	9	Antalya-Tekirova	Turkey	S	30.50	36.75		Turkey
5.30	8	Ispendere-Komurhan	Turkey	SE	38.52	38.34		Turkey
5.31	9	Cilo	Turkey	SE	43.45	37.30		Turkey
5.32	9	Gevas	Turkey	SE	43.00	38.25		Turkey
5.33	9	Guleman	Turkey	SE	39.90	38.42		Turkey

Ophiolite #	Stratigraphic Age F	Old Age F	Young Age F	F Best Estimate	Difference Between Old Young Age F	Reliability Age F	Tectonic Environment F	Plate E	Stratigraphic Age E	Old Age E	Young Age E	E Best Estimate
5.09	l K	99.00	65.00	82.00	34.00	2	MOR	Iran	e Paleoc	65.00	65.00	65.00
5.10	K	144.00	65.00	104.50	79.00	3		Iran	e Paleoc	65.00	65.00	65.00
5.11	l K	99.00	65.00	82.00	34.00	2	MOR	Iran	e Paleoc	65.00	65.00	65.00
5.12	l K	95.00	93.00	94.00	2.00	1		Iran	l K	89.00	89.00	89.00
5.13	K	144.00	65.00	104.50	79.00	3		Iran	e Paleoc	65.00	65.00	65.00
5.14				0.00	0.00	0		Iran	l K	71.00	65.00	68.00
5.15	l Tr	210.00	210.00	210.00	0.00	1		Iran				0.00
5.16	e - l K	103.00	98.00	100.50	5.00	1	MOR	Iran	l K	96.00	95.00	95.50
5.17	K	144.00	65.00	104.50	79.00	3		Syria	e - l K	100.00	86.00	93.00
5.18	l K	99.00	74.00	86.50	25.00	2	MOR	Turkey	l K	86.00	65.00	75.50
5.19	l K	96.00	91.50	93.75	4.50	1	SSZ	Turkey	l K - e Paleoc	90.00	61.00	75.50
5.20	l K	99.00	93.50	96.25	5.50	1		Turkey	l K	93.50	89.00	91.25
5.21	l K	92.00	90.00	91.00	2.00	1		Turkey	l K	78.30	65.00	71.65
5.22	l Jur - e K	152.00	132.00	142.00	20.00	1		Turkey	l K	90.00	87.00	88.50
5.23	Tr - Jur	248.00	144.00	196.00	104.00	3	ARC	Turkey	l K - l Paleoc	68.00	55.00	61.50
5.24	Tr - Jur	248.00	144.00	196.00	104.00	3		Turkey	l K - l Paleoc	68.00	55.00	61.50
5.25	Tr - K	248.00	65.00	156.50	183.00	3		Turkey	l K - l Paleoc	68.00	55.00	61.50
5.26	l K	94.00	70.00	82.00	24.00	2	FAB	Turkey	l K	78.30	65.00	71.65
5.27				0.00	0.00	0						0.00
5.28	l K	93.50	90.00	91.75	3.50	1	MOR	Turkey	l K	85.80	80.00	82.90
5.29	K	144.00	65.00	104.50	79.00	3		Turkey	l K	92.00	90.00	91.00
5.30	K	144.00	65.00	104.50	79.00	3						0.00
5.31	Tr - K	248.00	65.00	156.50	183.00	3		Turkey	l K	99.00	65.00	82.00
5.32	Tr - K	248.00	65.00	156.50	183.00	3		Turkey	l K - l Paleoc	68.00	55.00	61.50
5.33	K	144.00	65.00	104.50	79.00	3		Turkey	l K - l Paleoc	99.00	55.00	77.00

Ophiolite #	Difference Between Old Young Age E	Reliability Age E	Tectonic Environment E	Difference Formation Emplacement Age	Obduction Complex	Overlying Sediment Name	Mantle	Moho	Cummulates	Gabbro	Dikes	Pillows	Sediments	Completeness Score
5.09	0.00	1		17.00										0
5.10	0.00	1		39.50										0
5.11	0.00	1		17.00										0
5.12	0.00	1		5.00										0
5.13	0.00	1		39.50										0
5.14	6.00	1		-68.00										0
5.15	0.00	0	ACC	210.00										0
5.16	1.00	1		5.00			1	1	0	1	1	1	1	6
5.17	14.00	1	ACP	11.50										0
5.18	21.00	2		11.00			1	1	0	1	1	1	1	6
5.19	29.00	2	CCC	18.25			0	0	1	1	1	0	1	4
5.20	4.50	1	CCC	5.00				1	1	1	0	0	0	3
5.21	13.30	1	ACC	19.35			1	1	0	0	0	0	0	2
5.22	3.00	1		53.50		Halkopinar formation	0	1	0	1	1	0	0	3
5.23	13.00	1		134.50										0
5.24	13.00	1	ACP	134.50										0
5.25	13.00	1	ACP	95.00										0
5.26	13.30	1	ACP	10.35			1	0	0	1	1	1	0	4
5.27	0.00	0		0.00										0
5.28	5.80	1	ACP	8.85			0	0	0	1	1	1	1	4
5.29	2.00	1		13.50	Antalya									0
5.30	0.00	0		104.50										0
5.31	34.00	2		74.50										0
5.32	13.00	1		95.00										0
5.33	44.00	3		27.50										0

Ophiolite #	Map #	Name	Country	Region	Longitude	Latitude	Area	Plate F
5.34	9	Beysehir	Turkey	SE	31.73	37.68		Turkey
5.35	9	Troodos	Cyprus	W	33.00	35.00	3220 km2	Cyprus
5.36	7	Pindos	Greece	N	21.00	39.75		Greece
5.37	7	Vourinos	Greece	N	21.75	40.25		Greece
5.38	7	Othris	Greece	Central	22.25	39.00		Greece
5.39	7	Euboea	Greece	S	23.50	38.75		Greece
5.40	7	Agelona	Greece	S	23.00	36.75		Greece
5.41	7	Albania-Brezovica	Albania	North central	20.00	41.50		Albania
5.42	7	Krivaja-Kanjuh	Yugoslavia	SW	18.00	44.50		Yugoslavia
5.43	7	Zlatibor	Yugoslavia	SW	19.50	43.75		Yugoslavia
5.44	7	Corsican	Italy/France	SW island	9.00	42.50		Italy
5.45	7	Montgenevre	France	E	6.50	45.00		France
5.46	9	Monviso	Italy	NW	7.33	44.50		Italy
5.47	7	Zermatt-Saas-Fee	Italy	N	7.75	46.00		Italy
5.48	7	Internal Liguride (Ligurian)	Italy	N	9.50	44.25		Italy
5.49	9	External Liguride (Piedmont)	Italy	N	9.50	44.75		Italy
5.50	8	Tuscany	Italy	Central - North	11.50	43.33		Italy
5.51	9	Calabria	Italy	Central	16.00	40.00		Italy
5.52	9	Platta	Switzerland	SE	9.50	46.50		Switzerland
5.53	9	Tauern	Austria	SW	12.50	47.25		Austria
5.54	9	Apuseni (Romario)	Romania	Central	22.50	46.00		Romania
5.56	9	Lesser Caucasus	Turkey		45.00	40.00		Turkey
5.57	7	Cretan Nappe	Crete		25.00	35.20		Greece
5.58	8	Akamas	Cyprus	W	32.25	35.50		Cyprus
5.59	7	Mamonia	Cyprus	W	32.60	34.75		Cyprus

Ophiolite #	Stratigraphic Age F	Old Age F	Young Age F	F Best Estimate	Difference Between Old Young Age F	Reliability Age F	Tectonic Environment F	Plate E	Stratigraphic Age E	Old Age E	Young Age E	E Best Estimate
5.34	K	144.00	65.00	104.50	79.00	3		Turkey	l K	95.00	80.00	87.50
5.35	l K	92.00	90.00	91.00	2.00	1	BAB	Cyprus	l K	75.00	65.00	70.00
5.36	m Jur	176.00	168.00	172.00	8.00	1	BAB	Greece	m Jur	168.00	163.00	165.50
5.37	m Jur	180.00	164.00	172.00	16.00	1	MOR	Greece	m Jur	175.00	167.00	171.00
5.38	m Jur	180.00	160.00	170.00	20.00	1	MOR	Greece	m Jur	180.00	160.00	170.00
5.39	m Jur	180.00	159.00	169.50	21.00	2	MOR	Greece	m Jur	180.00	160.00	170.00
5.40	l Tr	227.00	210.00	218.50	17.00	1	MOR	Greece	m Jur	180.00	160.00	170.00
5.41	l Tr - e Jur	227.00	180.00	203.50	47.00	3	MOR	Albania	m Jur	174.00	160.00	167.00
5.42	m Jur	180.00	159.00	169.50	21.00	2	MOR	Yugoslavia	m - l Jur	180.00	145.00	162.50
5.43	m Jur	180.00	159.00	169.50	21.00	2	MOR	Yugoslavia	m - l Jur	180.00	145.00	162.50
5.44	e - m Jur	187.00	175.00	181.00	12.00	1	MOR	Italy	e - m Jur	181.00	165.00	173.00
5.45	e - m Jur	200.00	180.00	190.00	20.00	1	MOR	France	e Jur	190.00	180.00	185.00
5.46	e - l Jur	206.00	144.00	175.00	62.00	3	ARC	Italy	l K	99.00	65.00	82.00
5.47	m Jur	166.70	161.70	164.20	5.00	1	MOR	Italy	m - l Jur	161.00	152.00	156.50
5.48	m - l Jur	178.00	150.00	164.00	28.00	2	MOR	Italy	l Jur - e K	159.00	145.00	152.00
5.49	e - l Jur	185.00	145.00	165.00	40.00	2	MOR	Italy	l K	84.00	65.00	74.50
5.50	l Jur	156.00	148.00	152.00	8.00	1	MOR	Italy	K	144.00	65.00	104.50
5.51	e - l Jur	206.00	144.00	175.00	62.00	3	MOR	Italy	e - l K	106.00	65.00	85.50
5.52	e - l Jur	206.00	144.00	175.00	62.00	3	MOR	Switzerland	l K	99.00	65.00	82.00
5.53	e - l Jur	206.00	144.00	175.00	62.00	2		Austria	l K	99.00	65.00	82.00
5.54	e - m Jur	206.00	180.00	193.00	26.00	2	MOR	Romania	e K - l Paleoc	144.00	55.00	99.50
5.56	l Tr - m Jur	208.00	159.00	183.50	49.00	3		Turkey	l K	99.00	86.00	92.50
5.57	l Jur - e K	156.00	140.00	148.00	16.00	1	ARC	Greece				0.00
5.58	K	144.00	65.00	104.50	79.00	3						0.00
5.59	e Tr - l Tr	248.00	210.00	229.00	38.00	2	MOR	Cyprus	l Tr - e K	208.00	104.00	156.00

Ophiolite #	Difference Between Old Young Age E	Reliability Age E	Tectonic Environment E	Formation Emplacement Age	Obduction Complex	Overlying Sediment Name	Mantle	Moho	Cummulates	Gabbro	Dikes	Pillows	Sediments	Completeness Score
5.34	15.00	1	CCC	17.00										0
5.35	10.00	1	BAB	21.00			1	1	1	1	1	1	1	7
5.36	5.00	1	ACP	6.50			0	1	1		1	1	0	4
5.37	8.00	1		1.00			0	1	1	0	1	1	0	4
5.38	20.00	1		0.00			0	1	1	0	1	1	0	4
5.39	20.00	1		-0.50			0	1	1	0	1	1	0	4
5.40	20.00	1		48.50			0	1	1	0	1	1	0	4
5.41	14.00	1	ACP	36.50			0	1	1	0	1	1	0	4
5.42	35.00	2		7.00			0	1	1	0	1	1	0	4
5.43	35.00	2		7.00			0	1	1	0	1	1	0	4
5.44	16.00	1		8.00			0	1	1	1	1	1	1	5
5.45	10.00	1		5.00			0	1	1	0	1	1	0	4
5.46	34.00	2		93.00			0	1	1	0	1	1	0	4
5.47	9.00	1		7.70			1	0	0	1	1	1	1	5
5.48	14.00	1	ACP	12.00			1	0	0	1	0	1	1	4
5.49	19.00	1		90.50			1	0	0	1	0	1	1	4
5.50	79.00	3		47.50										0
5.51	41.00	3		89.50										0
5.52	34.00	2		93.00										0
5.53	34.00	2		93.00	Sepik									0
5.54	89.00	3	ACC	93.50										0
5.56	13.00	1		91.00										0
5.57	0.00	0	ACC	148.00										0
5.58	0.00	0		104.50			1	1	0	0	0	0	1	3
5.59	104.00	3		73.00			1	1	0	0	0	0	1	3

Ophiolite #	Map #	Name	Country	Region	Longitude	Latitude	Area	Plate F
5.60	1	Balkan-Carpathian	Bulgaria, Serbia, Romania		21.00	44.00	50,000 km2	Romania
5.61	8	Honaz	Turkey	Lycian	29.50	37.70		Turkey
5.62	7	Hellinic	Greece	Alps	23.00	38.00		Greece
5.63	7	Kure	Turkey	NE	30.20	40.00		Turkey
5.64	7	Dinaride (Central Zone of Ophiolites)	Yugoslavia	Alps	18.00	44.60		Yugoslavia
5.65		Mirdita	Albania		20.10	41.90		
5.66	10	Cyclades (Evia)	Greece		25.00	37.20		Greece
6.01	9	Bela	Pakistan		66.35	26.20		Pakistan
6.02	9	Muslim Bagh	Pakistan		67.86	30.86		Pakistan
6.03	9	Waziristan	Pakistan		70.00	33.25		Pakistan
6.04	9	Spontang	Ladakh	Pakistan Zanskar Zone	76.78	34.08	20 km2	Pakistan
6.05	10	Xigaze Dagzhuka	Tibet		88.88	29.28	450 km2	Nepal
6.06	9	Tuensang	India	Nagaland	94.50	26.00	800 km2	
6.07	10	Moreh	India	Manipur	94.40	24.50		India
6.08	9	Makran	Pakistan		63.00	26.00		Iran
6.11	9	Zhob	Pakistan		68.50	32.00		Pakistan
6.12	1	Dongwanzi	China	N China - Qinglong	118.67	40.50		China
6.13	10	Nanga Parbat	Pakistan	Himalayas	76.50	35.00		Pakistan
6.14	9	Shyok	Pakistan	NW Himalayas	76.40	34.85		Pakistan
6.15	9	Dras Sangeluma	Pakistan	NW Himalayas	75.73	34.43		Pakistan
6.16	10	Indus - Yarlung Zangbo	China	NW Himalayas	74.00	35.50		China
6.17	10	Indus - Yarlung Zangbo	China	NW Himalayas	75.00	35.00		China
6.18	10	Indus - Yarlung Zangbo	China	NW Himalayas	75.50	34.00		China
6.19	10	Indus - Yarlung Zangbo	China	Ladakh	77.50	33.40		China
6.20	10	Indus - Yarlung Zangbo	China	Ladakh	78.00	33.00		China

Ophiolite #	Stratigraphic Age F	Old Age F	Young Age F	F Best Estimate	Difference Between Old Young Age F	Reliability Age F	Tectonic Environment F	Plate E	Stratigraphic Age E	Old Age E	Young Age E	E Best Estimate
5.60	NP	568.00	558.00	563.00	10.00	1	MOR					0.00
5.61	K	144.00	65.00	104.50	79.00	3		Turkey				0.00
5.62	l Tr - l Jur	208.00	144.00	176.00	64.00	3	MOR					0.00
5.63	l Tr - l Jur	208.00	144.00	176.00	64.00	3						0.00
5.64	e - l Jur	206.00	144.00	175.00	62.00	3	ARC					0.00
5.65				0.00	0.00	0						0.00
5.66	l K	99.00	65.00	82.00	34.00	2	BAB	Greece	l Olig - e Mioc	25.00	17.00	21.00
6.01	l l K	70.00	65.00	67.50	5.00	1	MOR	Pakistan	l K - l Paleoc	66.00	64.00	65.00
6.02	l K	87.00	65.00	76.00	22.00	2	MOR	Pakistan	l K	70.00	65.00	67.50
6.03	e K	115.00	100.00	107.50	15.00	1	MOR	Pakistan	l K	70.00	68.00	69.00
6.04	l K	99.00	65.00	82.00	34.00	2	FAB	Pakistan	l K - l Paleoc	68.00	55.00	61.50
6.05	e K	110.00	100.00	105.00	10.00	1	FAB	Nepal	Eoc	50.00	40.00	45.00
6.06				0.00	0.00	0		India	l K - l Paleoc	99.00	55.00	77.00
6.07	l K	85.00	75.00	80.00	10.00	1	MOR	India	m Eoc	49.00	42.00	45.50
6.08	l K	95.00	95.00	95.00	0.00	1	MOR	Iran	l K	93.50	89.00	91.25
6.11	l Jur - l K	150.00	65.00	107.50	85.00	3	BAB	Pakistan	l K	70.00	65.00	67.50
6.12	PP	2507.20	2502.80	2505.00	4.40	1	FAB					0.00
6.13	K	144.00	65.00	104.50	79.00	3	MOR	Pakistan	Mioc	23.00	6.00	14.50
6.14	e K	144.00	99.00	121.50	45.00	3	MOR	Pakistan	l K - m Mioc	99.00	15.00	57.00
6.15	K - Paleoc	99.00	55.00	77.00	44.00	3						0.00
6.16	e K	130.00	110.00	120.00	20.00	1	MOR	China	Paleoc - Eoc	65.00	34.00	49.50
6.17	e K	130.00	110.00	120.00	20.00	1	MOR	China	Paleoc - Eoc	65.00	34.00	49.50
6.18	e K	130.00	110.00	120.00	20.00	1	MOR	China	Paleoc - Eoc	65.00	34.00	49.50
6.19	e K	130.00	110.00	120.00	20.00	1	MOR	China	Paleoc - Eoc	65.00	34.00	49.50
6.20	e K	130.00	110.00	120.00	20.00	1	MOR	China	Paleoc - Eoc	65.00	34.00	49.50

Ophiolite #	Difference Between Old Young Age E	Reliability Age E	Tectonic Environment E	Difference Formation Emplacement Age	Obduction Complex	Overlying Sediment Name	Mantle	Moho	Cummulates	Gabbro	Dikes	Pillows	Sediments	Completeness Score
5.60	0.00	0		563.00			1	1	1	1	1	1	1	7
5.61	0.00	0	pcm	104.50										0
5.62	0.00	0		176.00										0
5.63	0.00	0		176.00										0
5.64	0.00	0		175.00			1	0	1	1	0	0	1	4
5.65	0.00	0		0.00										0
5.66	8.00	1	ACP	61.00	Cycladic Blueschist Unit		1			1	1	1		4
6.01	2.00	1	ACP	2.50	Sunaro massif							1		1
6.02	5.00	1	ACP	8.50								1		1
6.03	2.00	1	ACP	38.50								1		1
6.04	13.00	1	ACC	20.50										0
6.05	10.00	1	ACC	60.00	Xigaze massif	Xigaze Group Flysch	1	1	1	1	1	1	1	7
6.06	44.00	3	CCC	-77.00	Zepuhu Fm	Disang Flysch	1	1	1	1	1	1	1	7
6.07	7.00	1	CCC	34.50			1	1	1	1	1	1	1	7
6.08	4.50	1		3.75										0
6.11	5.00	1	ACP	40.00			0	0	0	0	0	1	1	2
6.12	0.00	0		2505.00			1	1	1	1	1	1	0	6
6.13	17.00	1	ACC	90.00	Tethys belt		1	1	0	1	0	0	0	3
6.14	84.00	3		64.50										0
6.15	0.00	0		77.00			0	0	0	1	1	1	1	4
6.16	31.00	2	CCC	70.50	Indus - Yarlung Zangbo suture zone									0
6.17	31.00	2	CCC	70.50	Indus - Yarlung Zangbo suture zone									0
6.18	31.00	2	CCC	70.50	Indus - Yarlung Zangbo suture zone									0
6.19	31.00	2	CCC	70.50	Indus - Yarlung Zangbo suture zone									0
6.20	31.00	2	CCC	70.50	Indus - Yarlung Zangbo suture zone									0

Ophiolite #	Map #	Name	Country	Region	Longitude	Latitude	Area	Plate F
6.21	10	Indus - Yarlung Zangbo	China	NW Himalayas	80.00	31.80		China
6.22	10	Indus - Yarlung Zangbo	China	NW Himalayas	80.00	31.00		China
6.23	10	Indus - Yarlung Zangbo	China	NW Himalayas	81.00	31.50		China
6.24	10	Indus - Yarlung Zangbo	China	NW Himalayas	82.00	30.00		China
6.25	10	Indus - Yarlung Zangbo	China	NW Himalayas	82.50	29.80		China
6.26	10	Indus - Yarlung Zangbo	China	NW Himalayas	84.00	29.00		China
6.27	10	Indus - Yarlung Zangbo	China	NW Himalayas	85.00	28.50		China
6.28	10	Indus - Yarlung Zangbo	China	NW Himalayas	88.00	28.70		China
6.29	10	Indus - Yarlung Zangbo	China	NW Himalayas	90.00	28.80		China
6.30	10	Indus - Yarlung Zangbo	China	NW Himalayas	86.00	27.50		China
6.31	10	Indus - Yarlung Zangbo	China	NW Himalayas	91.00	28.30		China
6.32	10	Indus - Yarlung Zangbo	China	NW Himalayas	92.50	29.00		China
6.33	10	Indus - Yarlung Zangbo	China	NW Himalayas	93.00	29.00		China
6.34	10	Indus - Yarlung Zangbo	China	NW Himalayas	94.00	29.80		China
6.35	3	Hongguleleng	China	Xinjiang Uygur	83.00	40.00		China
6.36	3	Tianshan	China	S	87.00	41.00		China
6.37	3	Mishigou	China	Tianshan	88.50	42.50		China
6.38	1	Kunlun	China	E	84.00	36.00		China
6.39	4	Kunlun	China	N	84.00	36.00		China
6.40	6	Kunlun	China	S	84.00	36.00		China

Ophiolite #	Stratigraphic Age F	Old Age F	Young Age F	F Best Estimate	Difference Between Old Young Age F	Reliability Age F	Tectonic Environment F	Plate E	Stratigraphic Age E	Old Age E	Young Age E	E Best Estimate
6.21	e K	130.00	110.00	120.00	20.00	1	MOR	China	Paleoc - Eoc	65.00	34.00	49.50
6.22	e K	130.00	110.00	120.00	20.00	1	MOR	China	Paleoc - Eoc	65.00	34.00	49.50
6.23	m - l Jur	163.00	150.00	156.50	13.00	1	MOR	China	Paleoc - Eoc	65.00	34.00	49.50
6.24	m - l Jur	163.00	150.00	156.50	13.00	1	MOR	China	Paleoc - Eoc	65.00	34.00	49.50
6.25	m - l Jur	163.00	150.00	156.50	13.00	1	MOR	China	Paleoc - Eoc	65.00	34.00	49.50
6.26	m - l Jur	163.00	150.00	156.50	13.00	1	MOR	China	Paleoc - Eoc	65.00	34.00	49.50
6.27	m - l Jur	163.00	150.00	156.50	13.00	1	MOR	China	Paleoc - Eoc	65.00	34.00	49.50
6.28	m - l Jur	163.00	150.00	156.50	13.00	1	MOR	China	Paleoc - Eoc	65.00	34.00	49.50
6.29	m Jur - e K	178.00	123.00	150.50	55.00	3	MOR	China	Paleoc - Eoc	65.00	34.00	49.50
6.30	m Jur - e K	178.00	123.00	150.50	55.00	3	MOR	China	Paleoc - Eoc	65.00	34.00	49.50
6.31	m Jur - e K	178.00	123.00	150.50	55.00	3	MOR	China	Paleoc - Eoc	65.00	34.00	49.50
6.32	m Jur - e K	178.00	123.00	150.50	55.00	3	MOR	China	Paleoc - Eoc	65.00	34.00	49.50
6.33	m Jur - e K	178.00	123.00	150.50	55.00	3	MOR	China	Paleoc - Eoc	65.00	34.00	49.50
6.34	m Jur - e K	178.00	123.00	150.50	55.00	3	MOR	China	Paleoc - Eoc	65.00	34.00	49.50
6.35	Sil	443.00	418.00	430.50	25.00	2		China				0.00
6.36	Sil	443.00	418.00	430.50	25.00	2		China				0.00
6.37	l Ord - l Sil	458.00	419.00	438.50	39.00	2		China	m - l Dev	391.00	354.00	372.50
6.38	NP	900.00	543.00	721.50	357.00	3	MOR					0.00
6.39	e Carb	354.00	327.00	340.50	27.00	2	ARC					0.00
6.40	e Perm - m Tr	260.00	227.00	243.50	33.00	2	MOI					0.00

Ophiolite #	Difference Between Old Young Age E	Reliability Age E	Tectonic Environment E	Formation Emplacement Age	Obduction Complex	Overlying Sediment Name	Mantle	Moho	Cummulates	Gabbro	Dikes	Pillows	Sediments	Completeness Score
6.21	31.00	2	CCC	70.50	Indus - Yarlung Zangbo suture zone									0
6.22	31.00	2	CCC	70.50	Indus - Yarlung Zangbo suture zone									0
6.23	31.00	2	CCC	107.00	Indus - Yarlung Zangbo suture zone									0
6.24	31.00	2	CCC	107.00	Indus - Yarlung Zangbo suture zone									0
6.25	31.00	2	CCC	107.00	Indus - Yarlung Zangbo suture zone									0
6.26	31.00	2	CCC	107.00	Indus - Yarlung Zangbo suture zone									0
6.27	31.00	2	CCC	107.00	Indus - Yarlung Zangbo suture zone									0
6.28	31.00	2	CCC	107.00	Indus - Yarlung Zangbo suture zone									0
6.29	31.00	2	CCC	101.00	Indus - Yarlung Zangbo suture zone									0
6.30	31.00	2	CCC	101.00	Indus - Yarlung Zangbo suture zone									0
6.31	31.00	2	CCC	101.00	Indus - Yarlung Zangbo suture zone									0
6.32	31.00	2	CCC	101.00	Indus - Yarlung Zangbo suture zone									0
6.33	31.00	2	CCC	101.00	Indus - Yarlung Zangbo suture zone									0
6.34	31.00	2	CCC	101.00	Indus - Yarlung Zangbo suture zone									0
6.35	0.00	0	ACP	430.50										0
6.36	0.00	0	ACP	430.50										0
6.37	37.00	2	ACP	66.00										0
6.38	0.00	0		721.50										0
6.39	0.00	0		340.50										0
6.40	0.00	0		243.50										0

Ophiolite #	Map #	Name	Country	Region	Longitude	Latitude	Area	Plate F
7.01	9	Purial	Cuba	SE	-75.00	20.50		
7.02	9	Nipe-Cristal	Cuba	SE	-75.75	20.50		Cuba
7.03	10	Holguin-Gibara	Cuba	SE	-76.50	21.00		Cuba
7.04	10	Camaguey	Cuba	Central	-77.75	21.50		Cuba
7.05	10	Las Villas	Cuba	Central	-80.00	22.25		Cuba
7.06	9	Western Belt	Cuba	W	-82.00	23.00		Cuba
7.07	9	Sierra de Santa Cruz	Guatemala	NE	-89.00	15.75	715 km2	Guatemala
7.08	9	Sierra de Las Minas	Guatemala	SE	-89.00	15.25		Guatemala
7.09	9	North Coast	Hispaniola	N	-71.00	19.75		Dominican Republic
7.10	8	Cordillera Central	Hispaniola	Central	-71.00	19.00		Dominican Republic
7.11	10	Southern Peninsula	Hispaniola	S	-71.00	18.25		Dominican Republic
7.12	8	Bermeja	Puerto Rico	SW	-77.00	18.00		Jamaica
7.13	9	Blue Mountains	Jamaica	S	-76.50	18.00		Jamaica
7.14	9	Tinaquillo	Venezuela	Central	-68.50	10.00	72 km2	Venezuela
7.15	8	Siquisique	Venezuela	W	-69.50	10.50		Venezuela
7.16	9	Villa de Cura	Venezuela	E	-67.50	10.00	7000 km2	Venezuela
7.17	9	Xolopa	Mexico	S	-99.00	16.67		Mexico
7.18	9	Matapolo	Costa Rica	NW	-85.75	10.75	250 km2	Costa Rica
7.19	9	Rio Calima	Columbia	W	-77.00	4.00		Columbia
7.20	9	Esperanza	Costa Rica	NW	-85.75	10.75		Costa Rica
7.21		Las Palmas	Puerto Rico	SW	-77.00	18.00		
8.01		Meratus	Borneo	SE Indonesia	115.50	-3.50		Indonesia
8.02	10	East Timor	Timor	Hilimanu lherzolite	130.30	-3.10		
8.03	10	April Ultramafic	Papua New Guinea	W-Sepik plains	142.00	-4.25	100 km2	Papua New Guinea
8.04	10	Marum Complex	Papua New Guinea	Bismark Range	145.00	-6.00		Papua New Guinea

Ophiolite #	Stratigraphic Age F	Old Age F	Young Age F	F Best Estimate	Difference Between Old Young Age F	Reliability Age F	Tectonic Environment F	Plate E	Stratigraphic Age E	Old Age E	Young Age E	E Best Estimate
7.01				0.00	0.00	0		Cuba	Paleoc	65.00	54.80	59.90
7.02				0.00	0.00	0	MOR	Cuba	e Paleoc	65.00	61.00	63.00
7.03	e K	121.00	121.00	121.00	0.00	1		Cuba	e - m Eoc	54.80	41.30	48.05
7.04	e K	112.00	112.00	112.00	0.00	1		Cuba	e - m Eoc	54.80	41.30	48.05
7.05	e K	112.00	112.00	112.00	0.00	1		Cuba	m - l Eoc	49.00	34.00	41.50
7.06	e K	112.00	112.00	112.00	0.00	1		Cuba	e Paleoc - e Eoc	65.00	50.00	57.50
7.07	e K	132.00	99.00	115.50	33.00	2	BAB	Guatemala	l K	83.50	65.00	74.25
7.08	e K	132.00	112.00	122.00	20.00	1	BAB	Guatemala	l K	85.80	65.00	75.40
7.09	l K	93.50	89.00	91.25	4.50	1	CSS	Dominican Republic	Paleoc	65.00	55.00	60.00
7.10	e K	137.00	132.00	134.50	5.00	1	MOR	Dominican Republic	e - l K	112.00	99.00	105.50
7.11	l K	93.50	71.30	82.40	22.20	2		Dominican Republic	l Paleoc - e Plio	55.00	5.00	30.00
7.12	l Jur - e K	146.00	142.00	144.00	4.00	1		Jamaica	e - l K	112.00	99.00	105.50
7.13	l K	83.50	71.30	77.40	12.20	1	MOI	Jamaica	l K - l Paleoc	71.00	55.00	63.00
7.14	l K	89.00	85.80	87.40	3.20	1		Venezuela	l K	85.00	65.00	75.00
7.15	m Jur	176.00	164.00	170.00	12.00	1	MOR	Venezuela	l Jur - e K	159.00	99.00	129.00
7.16	e K	100.00	100.00	100.00	0.00	1		Venezuela	l K - l Paleoc	99.00	55.00	77.00
7.17	m Jur - e K	165.00	128.00	146.50	37.00	2	BAB	Mexico	l K - l Eoc	99.00	33.70	66.35
7.18	m Jur - l K	164.00	93.50	128.75	70.50	3		Costa Rica	l K	84.00	84.00	84.00
7.19	e - l K	112.00	66.00	89.00	46.00	3	AND	Columbia				0.00
7.20	l K	99.00	83.50	91.25	15.50	1		Costa Rica	l K	84.00	84.00	84.00
7.21				0.00	0.00	0						0.00
8.01				0.00	0.00	0	BAB					0.00
8.02				0.00	0.00	0		Indonesia	Mioc - Q	8.00	5.00	6.50
8.03	Eoc	54.80	33.70	44.25	21.10	2		Papua New Guinea	Olig	33.00	24.00	28.50
8.04	e - l K	121.00	65.00	93.00	56.00	3		Papua New Guinea	l Eoc - e Mioc	37.00	17.00	27.00

Ophiolite #	Difference Between Old Young Age E	Reliability Age E	Tectonic Environment E	Difference Formation Emplacement Age	Obduction Complex	Overlying Sediment Name	Mantle	Moho	Cummulates	Gabbro	Dikes	Pillows	Sediments	Completeness Score
7.01	10.20	1	ARC	-59.90			0	0	0	1	1	0	1	3
7.02	4.00	1	ARC	-63.00										0
7.03	13.50	1	ACP	72.95										0
7.04	13.50	1	CCC	63.95										0
7.05	15.00	1	ACP	70.50										0
7.06	15.00	1	ARC	54.50										0
7.07	18.50	1	ARC	41.25										0
7.08	20.80	2	BAC	46.60										0
7.09	10.00	1	ARC	31.25										0
7.10	13.00	1		29.00										0
7.11	50.00	3		52.40										0
7.12	13.00	1	ACP	38.50										0
7.13	16.00	1	ARC	14.40										0
7.14	20.00	1	ARC	12.40										0
7.15	60.00	3	ACC	41.00										0
7.16	44.00	3	ARC	23.00										0
7.17	65.30	3	ARC	80.15										0
7.18	0.00	1	ARC	44.75	Nicoya	Sabana Grande Fm	0	0	1	1	1	1	1	5
7.19	0.00	0	ARC	89.00			0	0	0	1	0	1	0	2
7.20	0.00	1	ARC	7.25										0
7.21	0.00	0		0.00										0
8.01	0.00	0		0.00			1	0	0	0	1	0	0	2
8.02	3.00	1	ACC	-6.50	Aileu Schist belt	Maubisse fm	1	1	0	0	0	1	1	4
8.03	9.00	1	ACC	15.75		Sepik complex	0	1	1	1	0	0	1	4
8.04	20.00	1	ACC	66.00		Asail shale	0	1	1	1	1	1	0	5

Ophiolite #	Map #	Name	Country	Region	Longitude	Latitude	Area	Plate F
8.05	10	Papua Ultramafic Belt	Papua New Guinea	Owen Staney Range	148.00	-7.80	3	Papua New Guinea
8.06	10	Fiji	Fiji	Viti Levu	178.00	-18.00	400 km2	Papua New Guinea
8.07	10	New Caledonia	New Caledonia		165.20	-21.00	7000 km2	Papua New Guinea
8.08	10	Northland Allochthon	New Zealand	N Island	174.00	-36.00		New Zealand
8.09	5	Yarras	Australia	Great serpentine belt zone A	152.18	-31.40		Australia
8.10	5	Attunga	Australia	Great serpentine belt zone b	150.80	-30.75		Australia
8.11	5	Port Macquarie	Australia	Aust serpentine belt zone	152.40	-31.50		Australia
8.12	10	Baryulgil	Australia	Clarence - mareton	152.45	-29.20		Australia
8.13	10	Macquarie Island	Australia	S of New Zealand	158.91	-54.58	185 km2	New Zealand
8.14	10	Obi (E Indonesia)	Indonesia	Sorong Fault	127.75	-1.25		Indonesia
8.15	5	Dun Mt	New Zealand		169.00	-45.00		New Zealand
8.16	10	New Hebrides	Vanuatu		169.00	-16.00		Papua New Guinea
8.17	10	Solomon Islands 1	Papua New Guinea		157.50	-7.00		Papua New Guinea
8.18	10	Solomon Islands 2	Papua New Guinea		160.00	-10.00		Papua New Guinea
8.19	5	Red Hills	New Zealand		175.00	-41.00		New Zealand
8.20	10	Tonga	New Zealand	Tonga Trench	173.00	-20.00		New Zealand
8.21	10	East Sulawesi	Sulawesi	Philippines	123.00	14.00		Philippines
8.22	10	Izu Bonin			121.19	5.80		Philippines
8.23	3	Tasmania	Tasmania	Dundas trough	146.00	-42.00		Australia
8.24	10	Hayama Mineoka	Japan	Central	139.60	36.70		Japan
8.25	10	Zambales	Philippines	W Pacific Indonesia	120.30	15.40		Philippines
8.26	10	West Timor	Timor	Indonesia	128.40	-3.10		Indonesia
8.27	9	Poroshiri	Japan	Hokkaido	142.52	42.41		Japan
8.28	5	Yakuno	Japan		135.00	35.30		Japan
8.29		Hovo Kanai	Japan		142.00	43.50		

Ophiolite #	Stratigraphic Age F	Old Age F	Young Age F	F Best Estimate	Difference Between Old Young Age F	Reliability Age F	Tectonic Environment F	Plate E	Stratigraphic Age E	Old Age E	Young Age E	E Best Estimate
8.05	K	144.00	65.00	104.50	79.00	3	FAB	Papua New Guinea	Eoc	55.00	34.00	44.50
8.06	l Eoc - e Olig	33.70	23.80	28.75	9.90	1	BAB	Papua New Guinea	Mioc	14.00	7.00	10.50
8.07	Paleoc	65.00	55.00	60.00	10.00	1	BAB	Papua New Guinea	l Eoc	37.00	34.00	35.50
8.08	K	144.00	65.00	104.50	79.00	3	MOR	New Zealand	l Eoc - e Mioc	40.00	20.00	30.00
8.09	m - l Dev	391.00	354.00	372.50	37.00	2	ARC	Australia	Perm	290.00	248.00	269.00
8.10	m Dev - l Carb	391.00	290.00	340.50	101.00	3		Australia	Perm	290.00	248.00	269.00
8.11	l Dev - e Carb	370.00	323.00	346.50	47.00	3		Australia	Perm	290.00	248.00	269.00
8.12	e m Pg	65.00	34.00	49.50	31.00	2		Australia	Olig	34.00	23.80	28.90
8.13	m Mioc	12.00	9.50	10.75	2.50	1	MOR	New Zealand	Plio	5.00	0.00	2.50
8.14	K-Eoc	99.00	33.70	66.35	65.30	3	ARC	Indonesia	l Olig	25.00	25.00	25.00
8.15	e Perm	290.00	256.00	273.00	34.00	2	MOR	New Zealand	l Perm	256.00	248.00	252.00
8.16	Eoc	54.80	33.70	44.25	21.10	2	FAB	Papua New Guinea	l Eoc	37.00	34.00	35.50
8.17	Eoc	54.80	33.70	44.25	21.10	2		Papua New Guinea	l Eoc	37.00	34.00	35.50
8.18	Eoc	54.80	33.70	44.25	21.10	2		Papua New Guinea	l Eoc	37.00	34.00	35.50
8.19	e Perm	280.00	280.00	280.00	0.00	1		New Zealand	l Perm	256.00	248.00	252.00
8.20	m Eoc	49.00	41.30	45.15	7.70	1	FAB					0.00
8.21	K	144.00	65.00	104.50	79.00	3	MOR	Philippines	Paleoc - Olig	65.00	23.80	44.40
8.22	m Eoc	41.80	40.80	41.30	1.00	1	FAB					0.00
8.23	Camb	512.00	490.00	501.00	22.00	2	ICR	Australia	Carb	500.00	490.00	495.00
8.24	PG	65.00	24.00	44.50	41.00	3						0.00
8.25	l Eoc	37.00	33.70	35.35	3.30	1	BAB					0.00
8.26	Ng	23.00	1.80	12.40	21.20	2		Indonesia	Mioc - Q	11.00	0.10	5.55
8.27	e K	100.00	100.00	100.00	0.00	1		Japan				0.00
8.28	e Sil - e Dev	426.00	409.00	417.50	17.00	1	MOR	Japan	e Perm	287.00	280.00	283.50
8.29				0.00	0.00	0						0.00

Ophiolite #	Difference Between Old Young Age E	Reliability Age E	Tectonic Environment E	Difference Formation Emplacement Age	Obduction Complex	Overlying Sediment Name	Mantle	Moho	Cummulates	Gabbro	Dikes	Pillows	Sediments	Completeness Score
8.05	21.00	2	ACC	60.00			1	1	1	1	1	1	1	7
8.06	7.00	1		18.25		Singatoka Sedimentary Gp	0	0	0	1	1	1	1	4
8.07	3.00	1	ACP	24.50	Tangihua		1	1	0	1	0	0	0	3
8.08	20.00	1		74.50			0	0	1	1	1	1	0	4
8.09	42.00	3		103.50			0	0	1	1	1	0	0	3
8.10	42.00	3		71.50										0
8.11	42.00	3		77.50										0
8.12	10.20	1		20.60										0
8.13	5.00	1		8.25	Macquarie Ridge		1	1	0	1	1	1	1	6
8.14	0.00	1	ACC	41.35									1	1
8.15	8.00	1	ARC	21.00			1	0	0	1	1	1	0	4
8.16	3.00	1		8.75										0
8.17	3.00	1		8.75										0
8.18	3.00	1	Intra-oceanic	8.75			1	1	0	1	0	1	0	4
8.19	8.00	1	ARC	28.00										0
8.20	0.00	0		45.15										0
8.21	41.20	3	ACC	60.10										0
8.22	0.00	0		41.30										0
8.23	10.00	1	BAC	6.00			1	1	0	1	1	1	0	5
8.24	0.00	0		44.50										0
8.25	0.00	0		35.35		U Eoc pelagic Limestone w/ tuff interbeds	1	1	1	1	1	1	1	7
8.26	10.90	1	ACC	6.85			1	1	0	0	0	1	0	3
8.27	0.00	0	ARC	100.00			1	1	1	1	1	1	1	7
8.28	7.00	1	ACC	134.00		Maizuru Group	0	0	0	1	1	1	1	4
8.29	0.00	0		0.00										0

Ophiolite #	Map #	Name	Country	Region	Longitude	Latitude	Area	Plate F
8.30		Horman Peridotite Massif	Japan	Hindaka Main zone	143.10	42.20		
8.31		Mineoka Belt	Japan		140.25	35.50		
8.32		Setogawa Belt	Japan		137.20	35.20		
8.33	10	Taiwan Ophiolite	Taiwan	Taiwan	121.00	23.50		China
8.34	1	Marlborough	Australia		149.90	-22.80		Australia
8.35	2	Tyennan - Delamerian	Australia		148.00	-32.00		Australia
8.36	3	Lachlan	Australia		147.05	-42.80		Australia
8.37	10	Koniambo Massif	New Caledonia		164.87	-21.03		Papua New Guinea
8.38	10	Cyclops	Indonesia East	Irian Jaya	137.50	-5.00		Indonesia
8.39	10	Palawan	Philippines		124.00	11.00		Philippines

Ophiolite #	Stratigraphic Age F	Old Age F	Young Age F	F Best Estimate	Difference Between Old Young Age F	Reliability Age F	Tectonic Environment F	Plate E	Stratigraphic Age E	Old Age E	Young Age E	E Best Estimate
8.30				0.00	0.00	0						0.00
8.31				0.00	0.00	0						0.00
8.32				0.00	0.00	0						0.00
8.33	l Ng	5.00	1.80	3.40	3.20	1		China	Q	1.80	1.00	1.40
8.34	NP	560.00	560.00	560.00	0.00	1	MOR					0.00
8.35	Camb	530.00	515.00	522.50	15.00	1	SSZ	Australia	Carb	515.00	515.00	515.00
8.36	Camb	505.00	495.00	500.00	10.00	1	BAB	Australia				0.00
8.37	e m Eoc	54.00	42.00	48.00	12.00	1		Papua New Guinea	m - l Eoc	49.00	34.00	41.50
8.38	m l Pg	43.00	29.00	36.00	14.00	1	BAB	Indonesia	Mioc	23.00	5.00	14.00
8.39	Tr - Jur	248.00	144.00	196.00	104.00	3	FAB	Philippines	Mioc	23.00	5.00	14.00

Ophiolite #	Difference Between Old Young Age E	Reliability Age E	Tectonic Environment E	Formation Emplacement Age	Obduction Complex	Overlying Sediment Name	Mantle	Moho	Cummulates	Gabbro	Dikes	Pillows	Sediments	Completeness Score
8.30	0.00	0		0.00										0
8.31	0.00	0		0.00										0
8.32	0.00	0		0.00										0
8.33	0.80	1		2.00										0
8.34	0.00	0		560.00										0
8.35	0.00	1		7.50										0
8.36	0.00	0	BAC	500.00										0
8.37	15.00	1		6.50										0
8.38	18.00	1	ACC	22.00			1	0	1	1	1	0	1	5
8.39	18.00	1	ACC	182.00										0

APPENDIX B

OPHIOLITE REFERENCES FOR AGE DATA

Ophiolite #	Name	Primary Reference	Secondary Reference	Secondary Reference	Secondary Reference	Secondary Reference
1.01	**Halaban-Ithilal**	Coleman, 1984	Stacey & Stoeser, 1983			
1.02	**Jabal Wask-Jabal Ess**	Coleman, 1984	Kemp et al., 1980			
1.03	**Fawakhir**	El-Sayed et al., 1999	Coleman, 1984			
1.04	**Tihama - Asir**	Coleman, 1984	Schmidt & Brown, 1982			
1.05	**Bir Umk**	Kemp et al.,. 1980	Coleman, 1984	Al-Shanti and Roobol, 1979		
1.06	**Wadi Ghadir**	Blasband et al., 2000	El Akhal, 1993	Kröner, A., 1985.	Kroner et al., 1992.	
1.07	**Quift Quseir**	Blasband et al., 2000	Blasband et al., 1997	Pallister et al., 1988.	Claesson, et al., 1984.	
1.08	**Onib & Gerf**	Blasband et al., 2000	Stern et al., 1990	Kröner, et al., 1987		
1.09	**Al Amar**	Blasband et al., 2000	Blasband et al., 1997	Berhe, S. M, 1990.		
1.10	**Quseir Marsa Alam**	Blasband et al., 2000	Ries et al., 1983			
1.11	**Meatiq Dome**	Blasband et al., 2000, 1997	Sturchio et al., 1983	Loizenbauer, 2001	Greiling et al., 1994	El-Gaby et al., 1984
1.12	**Wadi Hafafit**	Blasband et al., 2000	Greiling et al., 1994	Blasband et al., 1997		
1.13	**Nakasib**	Blasband et al., 2000	Abdelalam, 1994	Abdelsalam & Stern, 1996	Schandelmeier et al., 1994	
1.14	**Onib Sol Hamed**	Bishady et al., 1994	Shackleton, 1994			
1.15	**Wadi Lawi - Wadi Lawai**	Ahmed et al., 2001				
1.16	**Wadi 'Allaqi-Heiani**	Ren & Abdelsalam, 2005				
1.17	**Abdola-Moyale Complex**	Berhe, 1990				
1.18	**Yubdo Complex**	Berhe, 1990				
1.19	**Baragoi Complex**	Berhe, 1990				
1.20	**Ingessana Complex**	Berhe, 1990				
2.01	**Addie-Webster**	Coleman, 1977	Steuher & Murthy, 1966			
2.02	**Ballantrae Complex**	DeWit et al., 1977	Spray et al., 1984	Bluck et al., 1980	Thirwall & Bluck, 1984	
2.03	**Bay of Islands 1**	Elthon et al., 1982	Suhr & Cawood, 2001	Girardeau & Mevel, 1982	Dallmeyer & Williams 1975	Casey & Dewey, 1984
2.04	**Bay of Islands 2**	Elthon et al., 1982	Suhr & Cawood, 2001	Girardeau & Mevel, 1982	Dallmeyer & Williams 1975	Casey & Dewey, 1984
2.05	**Bay of Islands 3**	Elthon et al., 1982	Suhr & Cawood, 2001	Girardeau & Mevel, 1982	Dallmeyer & Williams 1975	Casey & Dewey, 1984
2.06	**Gibbs Islands**	Spray, 1984	DeWit et al., 1977	DeWit et al., 1977		
2.07	**Hare Bay**	Talkington & Malpas, 1980	Cawood, 1989	Dunning & Krough, 1985	Malpas et al., 1979	
2.08	**Hoch Grossen**	Ageed et al., 1980	Crowley et al., 2000	Faryad & Hoinkes, 2004		
2.09	**Kraubath**	Ageed et al., 1980	Crowley et al., 2000	Faryad & Hoinkes, 2004		
2.10	**Limousin**	Givardeau et al., 1986	Berger et al., 2005	Crowley et al., 2000		

Ophiolite #	Name	Primary Reference	Secondary Reference	Secondary Reference	Secondary Reference	Secondary Reference
2.11	**Lizard Ophiolite**	Green, 1964	Barnes & Andrews, 1984	Styles & Kirby, 1980	Clark et al, 1998	
2.12	**Massif Central**	Barde et al., 1980				
2.13	**Massif Amoricain**	Barde et al., 1980				
2.14	**Munchberg gneiss**	Franke et al., 1993	Clark et al, 1998			
2.15	**Purtuniq 1**	Scott et al., 1991	Scott et al., 1992	Laurent, 1980		
2.16	**Purtuniq 2**	Scott et al., 1991	Scott et al., 1992	Laurent, 1980		
2.17	**Purtuniq #3**	Scott et al., 1991	Scott et al., 1992	Laurent, 1980		
2.18	**Scandinavian Caledonides 1**	Furnes et al., 2001	Sturt et al., 1984	Andersen et al., 1984	Dilek et al., 1998	Sturt & Roberts, 1991
2.19	**Scandinavian Caledonides 2**	Furnes et al., 2001	Sturt et al., 1984	Andersen et al., 1984	Dilek et al., 1998	Sturt & Roberts, 1991
2.20	**Scandinavian Caledonides 3**	Furnes et al., 2001	Sturt et al., 1984	Andersen et al., 1984	Dilek et al., 1998	Sturt & Roberts, 1991
2.21	**Scandinavian Caledonides 4**	Furnes et al., 2001	Sturt et al., 1984	Andersen et al., 1984	Dilek et al., 1998	Sturt & Roberts, 1991
2.22	**Scandinavian Caledonides 5**	Furnes et al., 2001	Sturt et al., 1984	Andersen et al., 1984	Dilek et al., 1998	Sturt & Roberts, 1991
2.23	**Scandinavian Caledonides 6**	Furnes et al., 2001	Sturt et al., 1984	Andersen et al., 1984	Dilek et al., 1998	Sturt & Roberts, 1991
2.24	**Scandinavian Caledonides 7**	Furnes et al., 2001	Sturt et al., 1984	Andersen et al., 1984	Dilek et al., 1998	Sturt & Roberts, 1991
2.25	**Scandinavian Caledonides 8**	Furnes et al., 2001	Sturt et al., 1984	Andersen et al., 1984	Dilek et al., 1998	Sturt & Roberts, 1991
2.26	**Mt. Albert**	Coish & Stinton, 1992	Dunning et al., 1886	MacGregor et al., 1979	Gagnon & Jamieson, 1985	
2.27	**Mt. Orford**	Van Staal, 2005	Coish & Stinton, 1992	Dunning & Krough, 1985	Lux, 1986	
2.28	**Tauern Window**	Schuster & Kurz, 2005				
2.29	**Thetford Mines, Black Lake**	Van Staal, 2005	Lux, 1986	Coish & Stinton, 1992	Feininger, 1981	
2.30	**St. Anthony**	Girardeau & Nicolas, 1981	Jamieson, 1980			
2.31	**Shulaps**	Calon et al., 1989	Potter, 1983			
2.32	**Outokumpu Ophiolite Complex**	Andersen et al., 1990	Sturt et al., 1984			
2.33	**Karmøy**	Andersen et al., 1990	Zhou, 1996			
2.34	**Gullfjellet**	Andersen et al., 1990	Sturt, et al., 1979	Boyle, 1980	Pederson & Malpas, 1984	
2.35	**Leka**	Andersen et al., 1990	Sturt, et al., 1979	Boyle, 1980	Pederson & Malpas, 1984	
2.36	**Solund/Stavfjord**	Andersen et al., 1990	Furnes et al., 2003			
2.37	**Asbestos**	Van Staal, 2005				
2.38	**Jormua**	Furnes et al., 2005	Peltonen et al., 2003			
2.39	**Buck Creek**	Berger et al., 2001				

Ophiolite #	Name	Primary Reference	Secondary Reference	Secondary Reference	Secondary Reference	Secondary Reference
3.01	**Nurali**	Pertsev et al.,1997	Savelieva et al., 1997	Ruzhentsev & Samygin, 1979		
3.02	**Mindyak**	Pertsev et al.,1997	Savelieva et al., 1997	Ruzhentsev & Samygin, 1979		
3.03	**Kraka**	Savelieva et al., 1997	Ruzhentsev & Samygin, 1979			
3.04	**Kempersay Massif**	Savelieva et al., 1997	Ruzhentsev & Samygin, 1979			
3.05	**Sakmara Massif**	Savelieva et al., 1997	Ruzhentsev & Samygin, 1979			
3.06	**Voykar**	Saveliev et al., 1999	Sharkov et al., 1999			
3.07	**Chersky**	Oxman et al., 1995				
3.08	**Mainitis Zone**	Palandzhyan, 1986				
3.09	**Ust' - Belaya Mts**	Palandzhyan, 1986				
3.10	**Kuyul Mélange**	Palandzhyan, 1986				
3.11	**Upper Khatyrka**	Palandzhyan, 1986	Sokolov et al., 2002	Chekhovich et al., 1999		
3.12	**Vyvenka**	Palandzhjan, 1986	Suren, 1986			
3.13	**Goven Peninsula**	Palandzhyan, 1986	Suren, 1986			
3.14	**Porotory Cape**	Palandzhyan et al., 1999				
3.15	**Elistratova Complex**	Ishiwatari et al., 1998				
3.16	**Aluchin Block**	Ishiwatari et al., 1999	Sokolov et al., 2002	Lychagin, 1985	Chekhovich et al., 1999	
3.17	**Primorye**	Vyosotsky, 1994	Ishiwatari & Tsujimori, 2003			
3.18	**Khabarny**	Savelieva et al., 1997				
3.19	**Itmurunda zone**	Adveev, 1984	Koralenko et al., 1994			
3.20	**Northern Baikal**	Grudinin & Demin, 1994				
3.21	**Sharyzhalgay Block**	Gornova & Petrova, 1999				
3.22	**Koryak**	Palandzhjan, 1986				
3.23	**Taigonos Peninsula (Uga-Muruga)**	Palandzhjan et al., 1999				
4.01	**NW Alaska**	Foley, 1992	Gealey, 1980			
4.02	**Brooks Range**	Wirth et al., 1993	Moore, 1997	Nicholas, 1989		
4.03	**Ingalls Complex**	Nicolas, 1989	Miller, 1985	Miller & Mogk, 1987	Southwick, 1974	
4.04	**Canyon Mt**	Nicolas, 1989				
4.05	**Sparta Complex**	Phelps & Ave' Lallemant, 1980				
4.06	**Josephine**	Gillis & Banerjee, 2000	Harper, 1984	Wright and Wyld, 1986	Pessango et al, 1993	
4.07	**Trinity**	Spray, 1984	Wallin et al., 1988	Davies et al., 1965	Wright & Wyld, 1986	

Ophiolite #	Name	Primary Reference	Secondary Reference	Secondary Reference	Secondary Reference	Secondary Reference
4.08	**Franciscan New Idria**	Shervais et al., 2005	Saha et al., 2005	Coleman, 2000		
4.09	**Franciscan Burro Mt**	Shervais et al., 2005	Saha et al., 2005	Coleman, 2000		
4.10	**Franciscan Cazadero**	Shervais et al., 2005	Saha et al., 2005	Coleman, 2000		
4.11	**Franciscan Red Mt**	Shervais et al., 2005	Saha et al., 2005	Coleman, 2000		
4.12	**Coast Range Del Puerto**	Coleman, 2000	Shervais et al., 2005			
4.13	**Coast Range Point Sal**	Coleman, 2000	Shervais et al., 2005			
4.14	**Coast Range Black Mountain**	Coleman, 2000	Shervais et al., 2005			
4.15	**Coast Range Stonyford**	Coleman, 2000	Shervais et al., 2005			
4.16	**Coast Range Paskenta**	Coleman, 2000	Shervais et al., 2005			
4.17	**Coast Range Llanada**	Coleman, 2000	Shervais et al., 2005			
4.18	**Coast Range Hospital Canyon**	Coleman, 2000	Shervais et al., 2005			
4.19	**Great Valley Cuesta Ridge**	Shervais et al., 2005				
4.20	**Great Valley 2**	Shervais et al., 2005				
4.21	**Great Valley 3**	Shervais et al., 2005				
4.22	**Great Valley 4**	Shervais et al., 2005				
4.23	**Great Valley 5**	Shervais et al., 2005				
4.24	**Sierra Nevada Foothills 1**	Saleeby et al., 1989	Day & Bickford, 2004			
4.25	**Sierra Nevada Foothills 2**	Saleeby et al., 1989	Day & Bickford, 2004			
4.26	**Sierra Nevada Foothills 3**	Saleeby et al., 1989	Day & Bickford, 2004			
4.27	**Sierra Nevada Foothills Smartville**	Saleeby et al., 1989	Day & Bickford, 2004	Beard, 1998		
4.28	**Sierra Nevada Foothills Kings River**	Saleeby et al., 1989	Day & Bickford, 2004			
4.29	**Stanley Mountain**	Shervais et al., 2005				
4.30	**Sarmiento**					
4.31	**Baja Alta Terrane**	Busby, 2004	Moore & Kimbrough, 2005			
4.32	**Elder Creek**	Shervais et al., 2005				
4.33	**Cedros Island**	Busby, 2004	Kimbrough & Moore, 2003	Moore & Kimbrough, 2005		
4.34	**Vizcaino**	Busby, 2004	Kimbrough & Moore, 2003	Moore , 1985	Kimbrough, 1984	
4.35	**Taitao**	Nelson et al., 1993				
4.36	**Resurrection Peninsula**	Cole et al., 2006	Kusky & Young, 1999	Kusky et al., 1997		

Ophiolite #	Name	Primary Reference	Secondary Reference	Secondary Reference	Secondary Reference	Secondary Reference
5.01	**Masirah**	Gnos & Perrin, 1996	Marquer et al., 1998			
5.02	**Semail**	Nicolas & Boudier, 2000	Gray et al., 2000	Cox et al., 1999	Nicolas, 1989	Robertson & Woodcock, 1980
5.03	**Sabzevar**	Ghazi & Hassanipak, 2000a	Pamic et al., 1979			
5.04	**Mashad**	Ghazi & Hassanipak, 2000b	Chatterjee & Scotese, 2000	McCall, 1997	Şengör, 1990	
5.05	**Tchehel Kureh**	Ghazi & Hassanipak, 2000a	Pamić et al., 1979			
5.06	**Iranshahr**	Ghazi & Hassanipak, 2000a	Pamić et al., 1979			
5.07	**Fanuj Maskutan**	Ghazi & Hassanipak, 2000a	Pamić et al., 1979			
5.08	**Kahnuj**	Kananian et al., 2001				
5.09	**Esphandagheh**	Ghazi & Hassanipak, 2000a	Pamić et al., 1979			
5.10	**Shahr-Babak**	Ghazi & Hassanipak, 2000a				
5.11	**Baft**	Ghazi & Hassanipak, 2000a	Pamić et al., 1979			
5.12	**Neyriz**	Ghazi & Hassanipak, 2000a	Pamić et al., 1979	Adib & Pamić, 1980		
5.13	**Nain**	Ghazi & Hassanipak, 2000a				
5.14	**Kermanshah**	Ghazi & Hassanipak, 2000a				
5.15	**Rasht**	Ghazi & Hassanipak, 2000a	McCall, 1997	Şengör, 1990		
5.16	**Khoy**	Hassanipak & Ghazi, 2000b				
5.17	**Baër-Bassit**	Thuizat et al., 1981				
5.18	**Kizildag**	Dilek & Delaloye, 1992				
5.19	**Mersin**	Parlak & Delaloye, 1999				
5.20	**Aladaj**	Dilek & Whitney, 1997				
5.21	**Kiziltepe**	Dilek & Whitney, 1997				
5.22	**Ali Hoca**	Dilek & Whitney, 1997	Alabaster et al., 1982			
5.23	**Yuksekova**	Yilmaz, 1993				
5.24	**Yayladag**					
5.25	**Berit**	Yilmaz, 1993				
5.26	**Pozanti-Karsanti**	Palat et al., 1996				
5.27	**Ovacik**					
5.28	**Sarikaramn**	Yaliniz et al., 2000				
5.29	**Antalya-Tekirova**	Dilek et al., 1999	Yilmaz, 1993	Juteau et al., 1980		
5.30	**Ispendere-Komurhan**	Dilek et al., 1999	Yilmaz, 1993	Juteau et al., 1980		
5.31	**Cilo**	Dilek & Flower, 2003	Yilmaz, 1993			

Ophiolite #	Name	Primary Reference	Secondary Reference	Secondary Reference	Secondary Reference	Secondary Reference
5.32	**Gevas**	Dilek & Flower, 2003	Yilmaz, 1993			
5.33	**Guleman**	Dilek et al., 1999	Yilmaz, 1993	Juteau et al., 1980		
5.34	**Beysehir**	Dilek et al., 1999	Yilmaz, 1993	Juteau et al., 1980		
5.35	**Troodos**	Borradaile & Lucas, 2003	Robertson & Woodcock, 1980	Robinson et al., 1983		
5.36	**Pindos**	Rassios & Smith, 2000	Jones et al., 1991			
5.37	**Vourinos**	Rassios & Smith, 2000				
5.38	**Othris**	Rassios & Smith, 2000				
5.39	**Euboea**	Marinos, 1980				
5.40	**Agelona**	Danelian et al., 2000				
5.41	**Albania-Brezovica**	Robertson & Shallo, 2000	Vergely et al., 1998			
5.42	**Krivaja-Kanjuh**	Pamić et al., 1998	Okrusch & Seidel, 1978			
5.43	**Zlatibar**	Pamić et al., 1998	Okrusch & Seidel, 1978			
5.44	**Corsican**	Desmons, 1989	Miller & Cartwright, 2000			
5.45	**Montgenevre**	Costa & Caby, 2001				
5.46	**Monviso**	Rampone et al., 1998	Lombardo et al., 1978			
5.47	**Zermatt-Saas**	Rubatto et al., 1998	Miller & Cartwright, 2000	Amato et al., 1999		
5.48	**Internal Liguride (Ligurian)**	Piccardo, 2000	Rampone et al., 1998	Borsi et al., 1996		
5.49	**External Liguride (Piedmont)**	Rampone & Piccardo, 2000	Marroni et al., 1998	Borsi et al. 1996	Miller & Cartwright, 2000	
5.50	**Tuscany**	Tribuzio et al., 2000				
5.51	**Calabria**	Desmons, 1989	Beccaluva et al. 1980			
5.52	**Platta**	Desmons, 1989				
5.53	**Tauern**	Desmons, 1989	Zimmerman et al., 1994	Raith et al., 1977		
5.54	**Apuseni (Romario)**	Nicolae & Saccani, 2003	Herz and Savu, 1974			
5.56	**Lesser Caucasus**	Knipper, 1991				
5.57	**Cretan Nappe**	Borradaile & Lucas, 2003				
5.58	**Akamas**	Borradaile & Lucas, 2003				
5.59	**Mamonia**	Borradaile & Lucas, 2003	Dietrich, 1979			
5.60	**Balkan Carpathians**	Savov et al., 2001	Savov, 1999			
5.61	**Honaz**	Dilek & Flower, 2003				
5.62	**Hellinic**	Dilek & Flower, 2003	Spray et al., 1984			
5.63	**Kure**	Bortolotti & Principi, 2005				

Ophiolite #	Name	Primary Reference	Secondary Reference	Secondary Reference	Secondary Reference	Secondary Reference
5.64	**Dinaride**	Dilek & Flower, 2003	Pamic, 1977			
5.65	**Mirdita**	Dilek & Flower, 2003				
5.66	**Cyclades (Evia)**	Katzir et al., 2000	Dilek & Flower, 2003			
6.01	**Bela**	McCormick, 1991	Gnos et al., 1998	Ahmed & Ernst, 1999	Sarwar, 1992	Zaigham & Mallick, 2000
6.02	**Muslim Bagh**	Gnos et al., 1998	McCormick, 1991			
6.03	**Waziristan**	Shah & Khan, 1999	Moores et al., 1980	Gnos et al., 1998		
6.04	**Spontang**	Mahmood et al., 1995	Searle & Stevens 1980			
6.05	**Xigaze Dagzhuka**	Hebert et al., 2003	Nicolas, 1989			
6.06	**Tuensang (Nagaland)**	Agrawal & Kacker, 1980				
6.07	**Moreh**	Morely 2001	Vidyadharan et al., 1989			
6.08	**Makran**	McCormick, 1991				
6.09	**Cyclops**	Gnos et al., 1997				
6.10	**Palawan**	Gealey 1980				
6.11	**Zhob**	Gnos et al., 1997				
6.12	**Dongwanzi**	Kusky et al., 2001	Li et al., 2002	Li et al., 2000		
6.13	**Nanga Parbat**	Pecher et al., 2002				
6.14	**Shyot**	Pecher et al., 2002				
6.15	**Dras Sangeluma**	Robertson & Degnan, 1994				
6.16	**Indus - Yarlung Zangbo**	Hebert et al., 2003	Dupuis et al., 2005	Rowley, 1996	Rowley, 1998	
6.17	**Indus - Yarlung Zangbo**	Hebert et al., 2003	Dupuis et al., 2005	Rowley, 1996	Rowley, 1998	
6.18	**Indus - Yarlung Zangbo**	Hebert et al., 2003	Dupuis et al., 2005	Rowley, 1996	Rowley, 1998	
6.19	**Indus - Yarlung Zangbo**	Hebert et al., 2003	Dupuis et al., 2005	Rowley, 1996	Rowley, 1998	
6.20	**Indus - Yarlung Zangbo**	Hebert et al., 2003	Dupuis et al., 2005	Rowley, 1996	Rowley, 1998	
6.21	**Indus - Yarlung Zangbo**	Hebert et al., 2003	Dupuis et al., 2005	Rowley, 1996	Rowley, 1998	
6.22	**Indus - Yarlung Zangbo**	Hebert et al., 2003	Dupuis et al., 2005	Rowley, 1996	Rowley, 1998	
6.23	**Indus - Yarlung Zangbo**	Hebert et al., 2003	Dupuis et al., 2005	Rowley, 1996	Rowley, 1998	
6.24	**Indus - Yarlung Zangbo**	Dupuis et al., 2005		Rowley, 1996		
6.25	**Indus - Yarlung Zangbo**	Dupuis et al., 2005		Rowley, 1996		
6.26	**Indus - Yarlung Zangbo**	Dupuis et al., 2005				
6.27	**Indus - Yarlung Zangbo**	Dupuis et al., 2005		Rowley, 1996		

Ophiolite #	Name	Primary Reference	Secondary Reference	Secondary Reference	Secondary Reference	Secondary Reference
6.28	**Indus - Yarlung Zangbo**	Dupuis et al., 2005		Rowley, 1996		
6.29	**Indus - Yarlung Zangbo**	Dupuis et al., 2005		Rowley, 1996		
6.30	**Indus - Yarlung Zangbo**	Dupuis et al., 2005		Rowley, 1996		
6.31	**Indus - Yarlung Zangbo**	Dupuis et al., 2005		Rowley, 1996		
6.32	**Indus - Yarlung Zangbo**	Dupuis et al., 2005				
6.33	**Indus - Yarlung Zangbo**	Dupuis et al., 2005				
6.34	**Indus - Yarlung Zangbo**	Dupuis et al., 2005	Rowley, 1996			
6.35	**Hongguleleng**	Peng et al.,1995	Laurent-Charvet et al., 2005			
6.36	**Tianshan**	Laurent-Charvet et al., 2005				
6.37	**Mishigou**	Laurent-Charvet et al., 2005				
6.38	**Kunlun**	Laurent-Charvet et al., 2005				
6.39	**Kunlun**	Laurent-Charvet et al., 2005	Yuan et al., 2003			
6.40	**Kunlun**	Laurent-Charvet et al., 2005	Yuan et al., 2003			
7.01	**Purial**	Wadge et al., 1984	Cobiella, 1978	Cobiella et al., 1977		
7.02	**Nipe-Cristal**	Bortolotti & Principi, 2005	Cobiella, 1978	Cobiella et al., 1977		
7.03	**Holguin-Gibara**	Wadge et al., 1984	Kozary, 1968			
7.04	**Camaguey**	Wadge et al., 1984	Mossakovskiy & Albear, 1978			
7.05	**Las Villas**	Wadge et al., 1984	Mossakovskiy & Albear, 1978			
7.06	**Western Belt**	Wadge et al., 1984	Mossakovskiy & Albear, 1978	Fonsec et al., 1985		
7.07	**Sierra de Santa Cruz**	Rosenfeld, 1981	Wadge et al., 1984			
7.08	**Sierra de Las Minas**	Rosenfeld, 1981	Muller, 1979	Williams, 1975		
7.09	**North Coast**	Wadge et al., 1984	McCulloch et al., 1982			
7.10	**Cordillera Central**	Wadge et al., 1984	Haldemann et al., 1980			
7.11	**Southern Peninsula**	Wadge et al., 1984	Maurasse et al., 1979			
7.12	**Bermeja**	Mattson, 1974				
7.13	**Blue Mountains**	Wadge et al., 1982	Draper, 1986			
7.14	**Tinaquillo**	Seyler, et al., 1998	Gealey, 1980	MacKenzie, 1960		
7.15	**Siquisique**	Bartok et al., 1985				
7.16	**Villa de Cura**	Gealey, 1980				
7.17	**Xolopa**	Nelson & Ratschbacher, 1994				

Ophiolite #	Name	Primary Reference	Secondary Reference	Secondary Reference	Secondary Reference	Secondary Reference
7.18	**Matapolo**	Borgois et al., 1982	Wadge et al., 1984			
7.19	**Rio Calima**	Borgois et al., 1982				
7.20	**Esperanza**	Bortolotti & Principi 2005	Borgois et al., 1982			
7.21	**Las Palmas**	Tobisch, 1968				
8.01	**Meratus**					
8.02	**East Timor**	Harris & Long, 2000				
8.03	**April Ultramafic**	Milsom, 2003	Milsom, 1984			
8.04	**Marum Complex**	Milsom, 1984				
8.05	**Papua U B**	Spray, 1984				
8.06	**Fiji**	Colley, 1984				
8.07	**New Caledonia**	Audet et al., 2004	Nicholson et al., 2000a	Prinzhofer et al., 1980		
8.08	**Northland Allochthon**	Whattam et al., 2005	Malpas et al., 1992	Hopper & Smith, 1996	Cande & Kent, 1995	Nicholson et al., 2000b
8.09	**Yarras**	Offler & Shaw, 2006	Aitchison et al., 1994	Kawachi, 1991		
8.10	**Attunga**	Aitchison et al., 1994				
8.11	**Port Macquarie**	Aitchison et al., 1994				
8.12	**Baryulgil**	Aitchison et al., 1994				
8.13	**Macquarie Island**	Malpas et al., 1994	Varne et al., 2000	Hopper & Smith, 1996		
8.14	**Obi (E Indonesia)**	Hall, 2002				
8.15	**Dun Mt**	Coombs et al., 1976				
8.16	**New Hebrides**	Parrot & Dugas, 1980	Coleman, 1970			
8.17	**Solomon Islands 1**	Parrot & Dugas, 1980	Coleman, 1966			
8.18	**Solomon Islands 2**	Parrot & Dugas, 1980	Coleman, 1966			
8.19	**Red Hills**	Sano et al., 1997	Coombs et al., 1976			
8.20	**Tonga**	Banerjee et al., 2000	Fisher & Engel, 1968			
8.21	**East Sulawesi**	Rangin et al., 1990	Parkinson et al., 1998			
8.22	**Izu Bonin**	Taylor, 1992				
8.23	**Tasmania**	Brown et al., 1988				
8.24	**Hayama Mineoka**	Ogawa & Taniguchi, 1987				
8.25	**Zambales**	Zhou et al., 2000				
8.26	**W Timor Island**	Sopaheluwakan et al., 1989				

Ophiolite #	Name	Primary Reference	Secondary Reference	Secondary Reference	Secondary Reference	Secondary Reference
8.27	**Poroshiri**	Ishiwatari, 1990a	Ishiwatari, 1990b			
8.28	**Yakuno**	Herzig et al., 1997	Koide et al, 1987	Sano, 1992	Ishiwatari, 1990a; 1990b	Ishiwatari, 1985
8.29	**Hovo Kanai**					
8.30	**Horman Peridotite Massif**					
8.31	**Mineoka Belt**					
8.32	**Setogawa Belt**					
8.33	**Taiwan Ophiolite**	Bor-ming, 1996	Sopaheluwakan et al., 1989			
8.34	**Marlborough**	Spaggiari et al., 2004	Bruce & Niu, 2000			
8.35	**Tyennan - Delamerain**	Spaggiari et al., 2004	Audet et al., 2004	Comacho et al., 2002		
8.36	**Lachlan**	Audet et al., 2004	Fergusson & Coney, 1992			
8.37	**Koniambo Massif**	Audet et al., 2004				
8.38	**Cyclops**	Gnos & Peters, 1997				
8.39	**Palawan**	Gealey, 1980				

APPENDIX C

MAPS OF OPHIOLITES THROUGH GEOLOGIC TIME

Map 1 Ophiolites 750 Ma

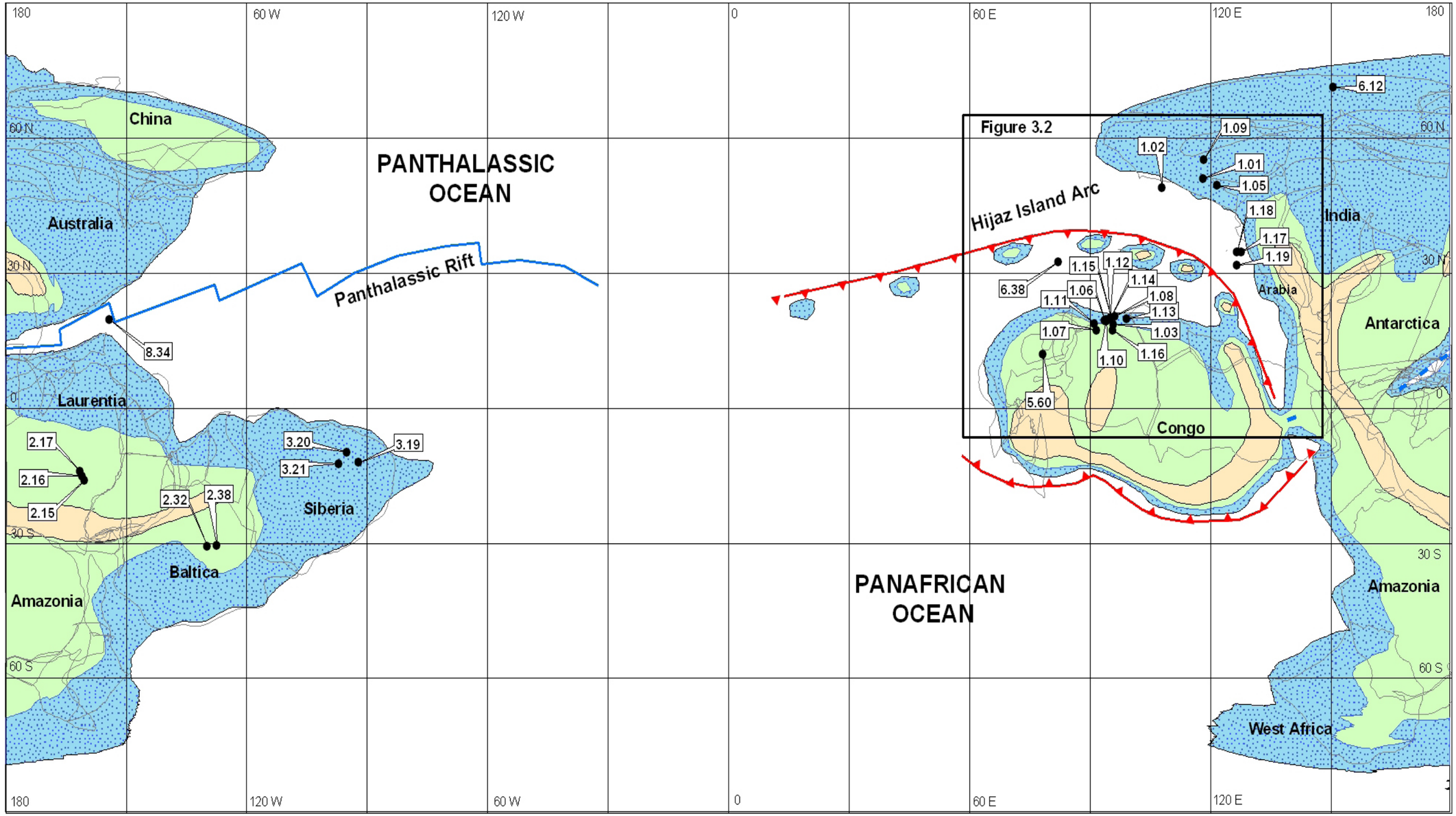

Map 2 Ophiolites 520 Ma

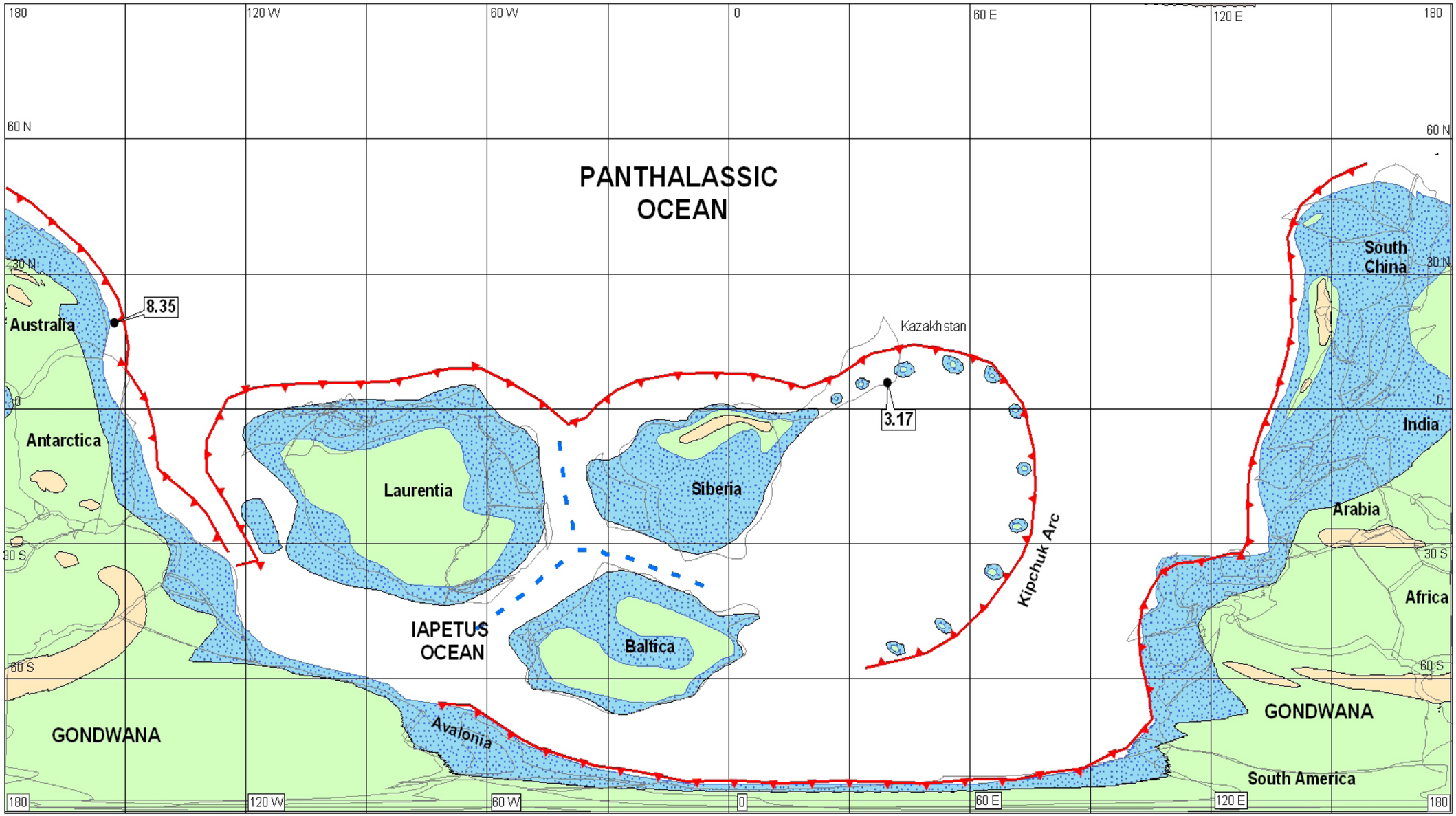

Map 3 Ophiolites 440 Ma

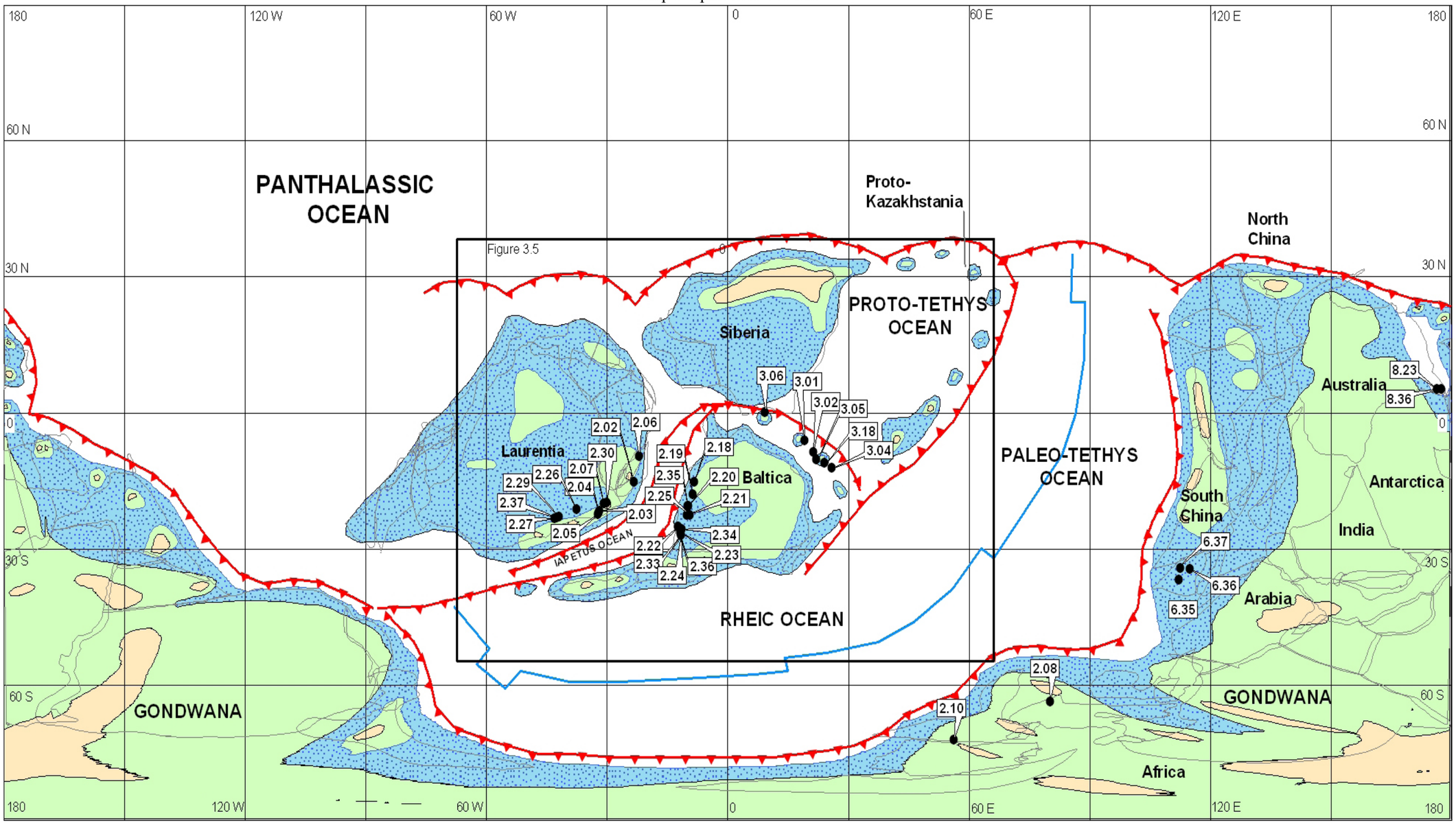

Map 4 Ophiolites 340 Ma

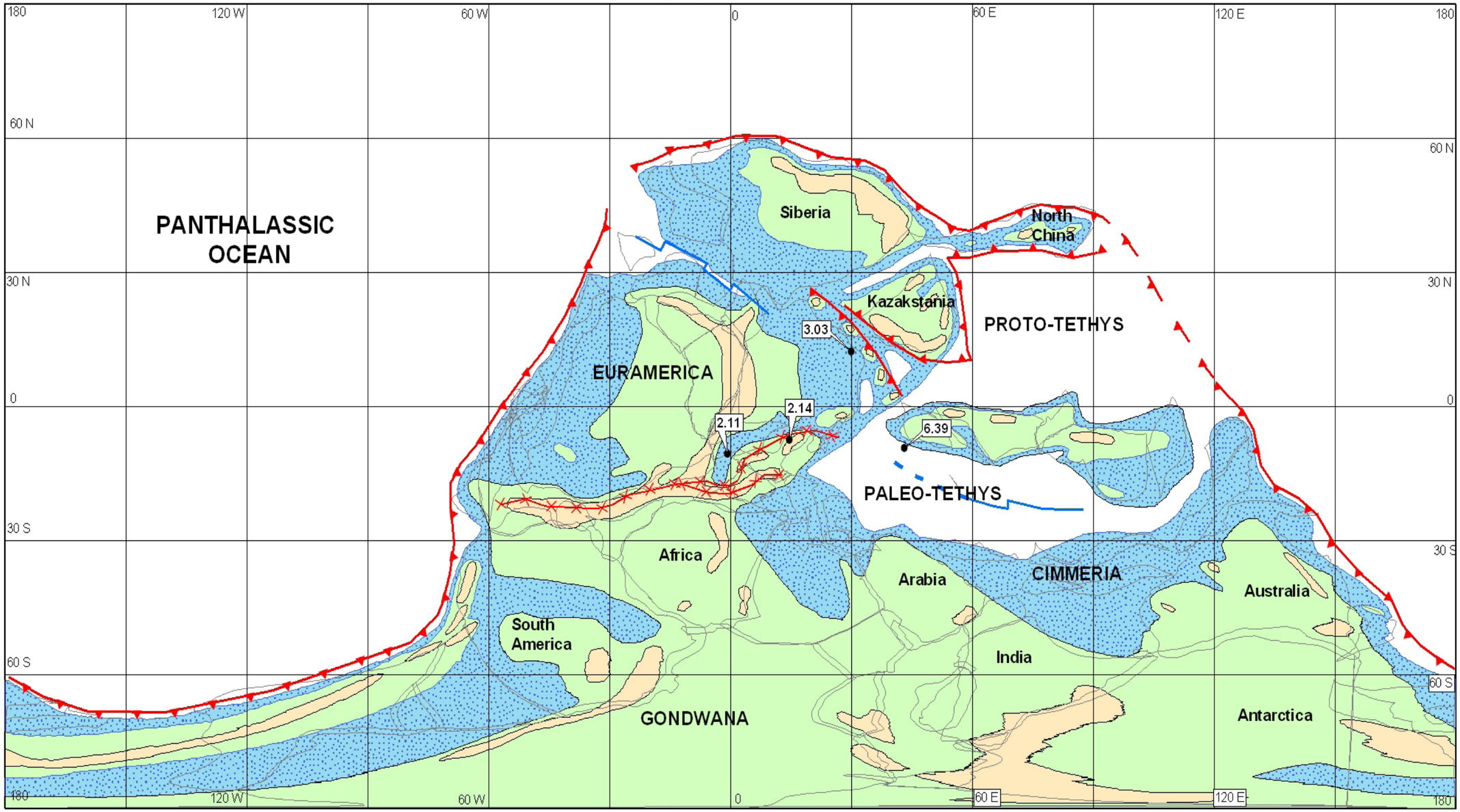

Map 5 Ophiolites 280 Ma

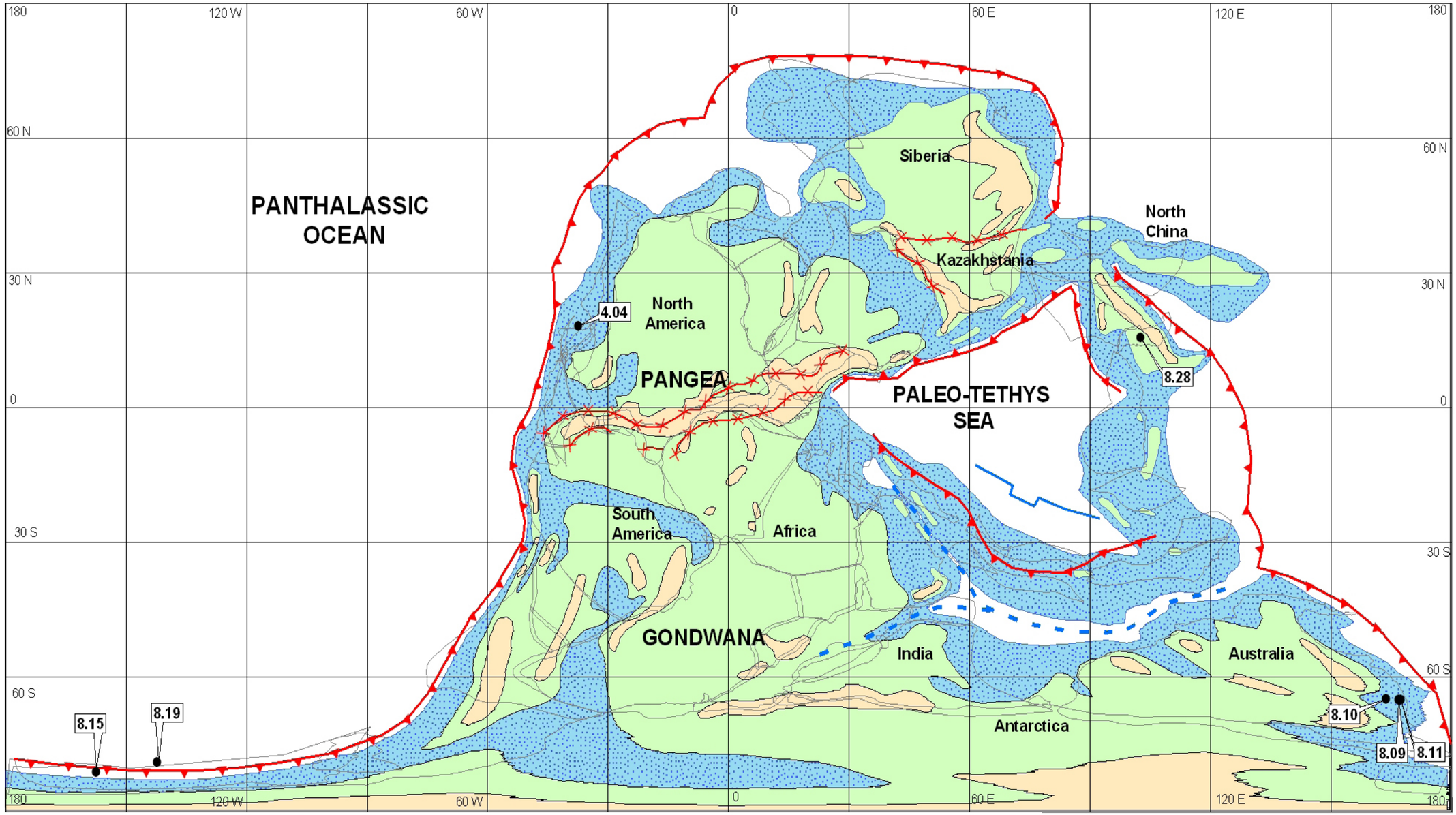

Map 6 Ophiolites 220 Ma

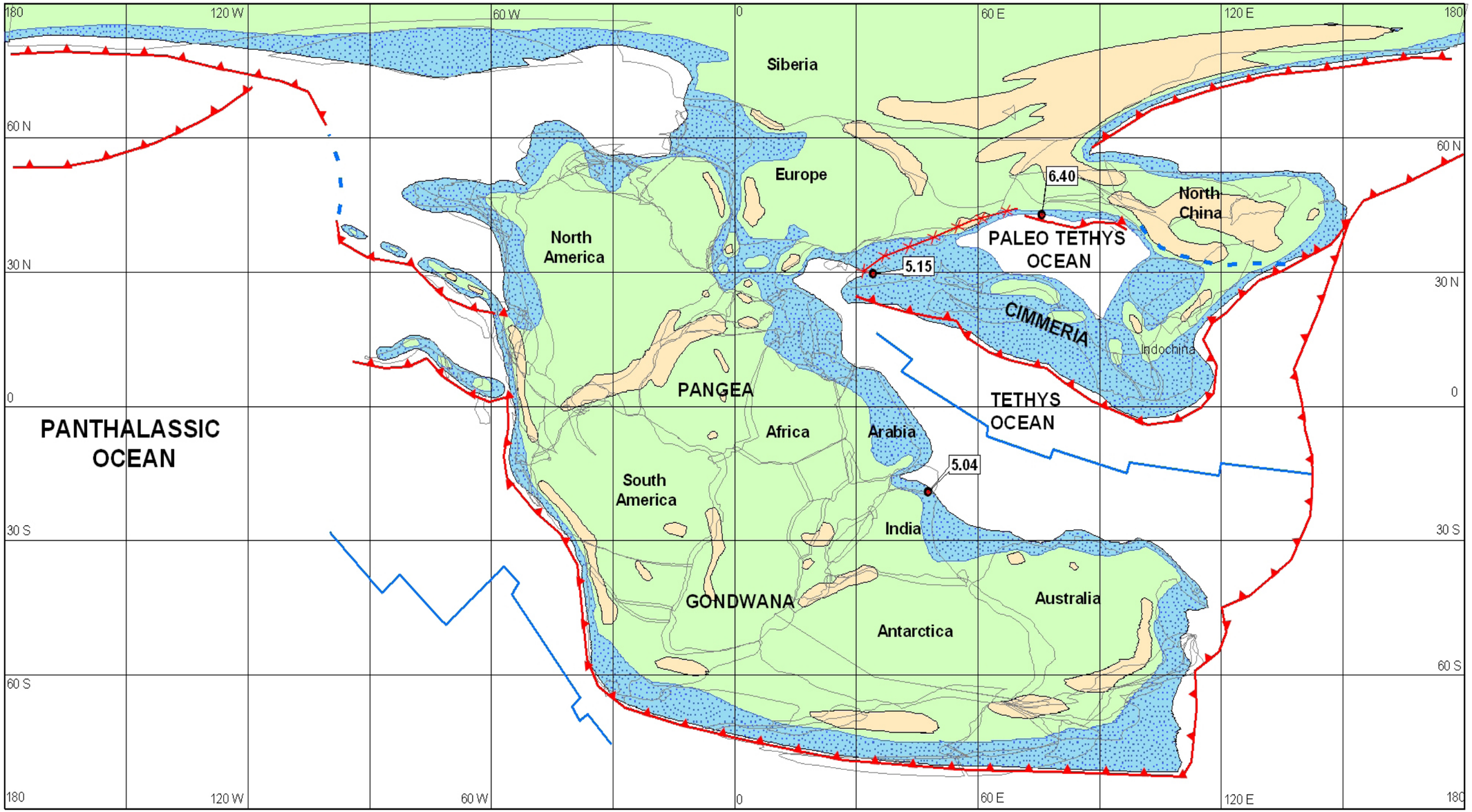

Map 7 Ophiolites 160 Ma

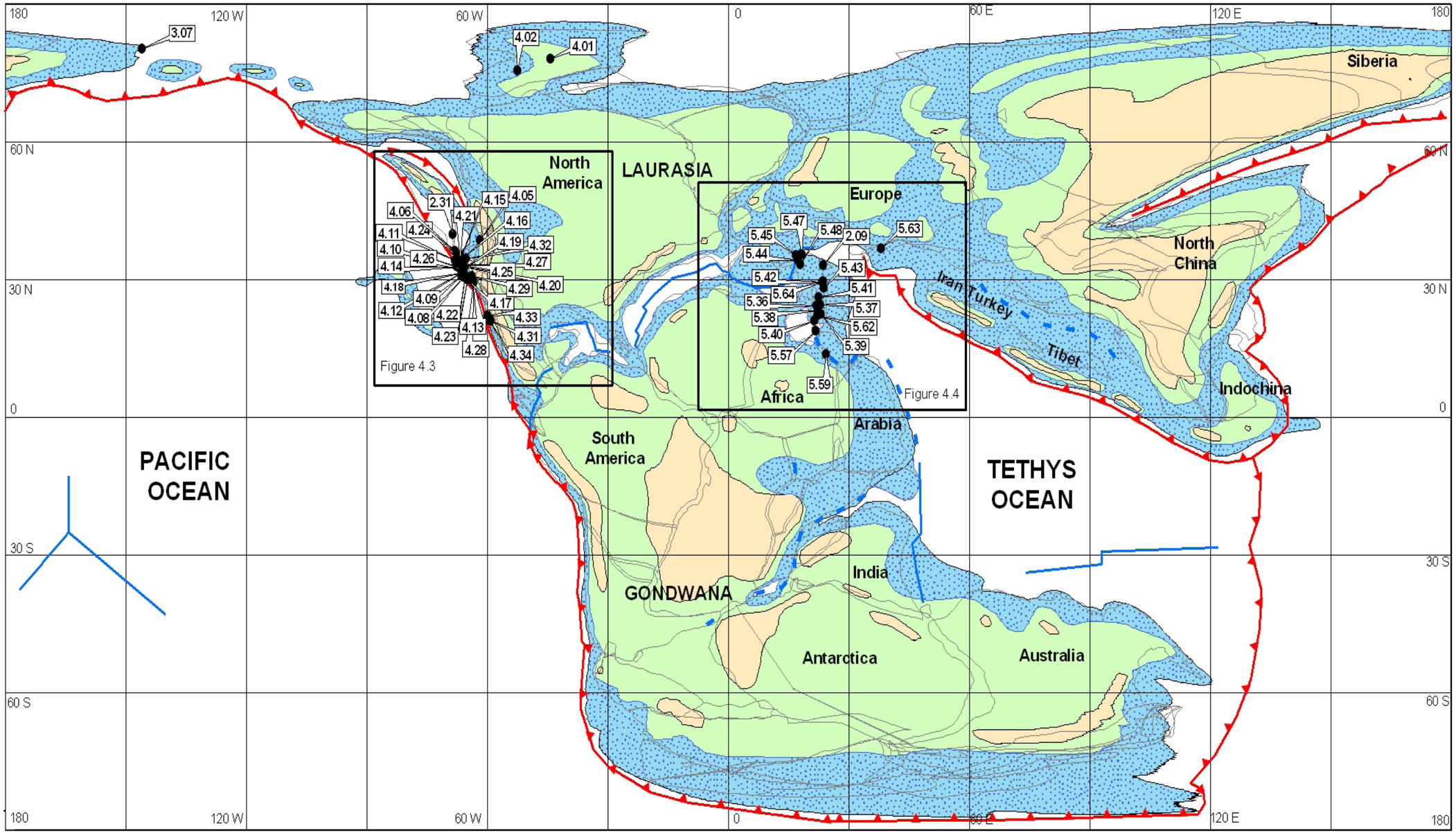

Map 8 Ophiolites 100 Ma

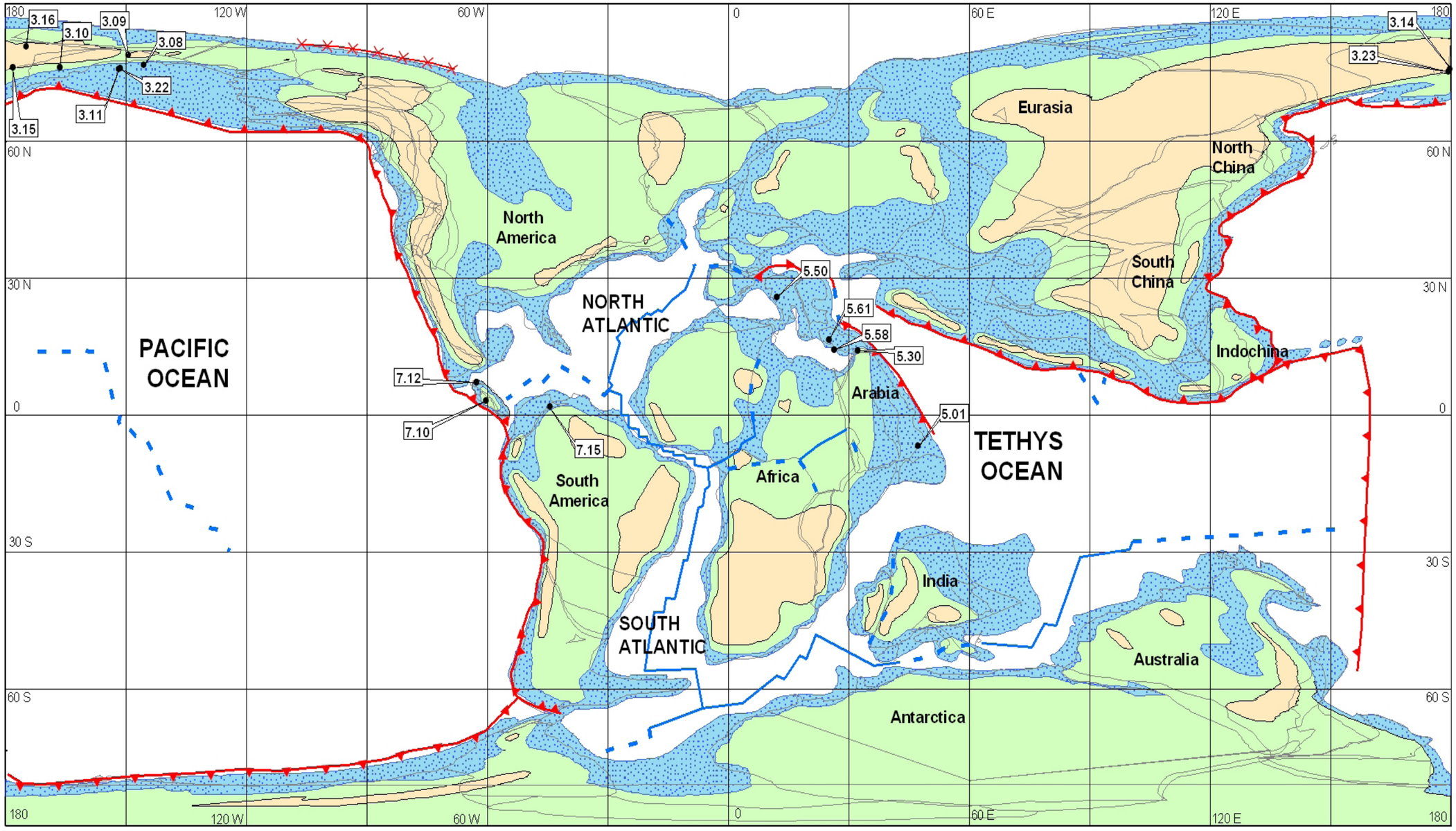

Map 9 Ophiolites 70 Ma

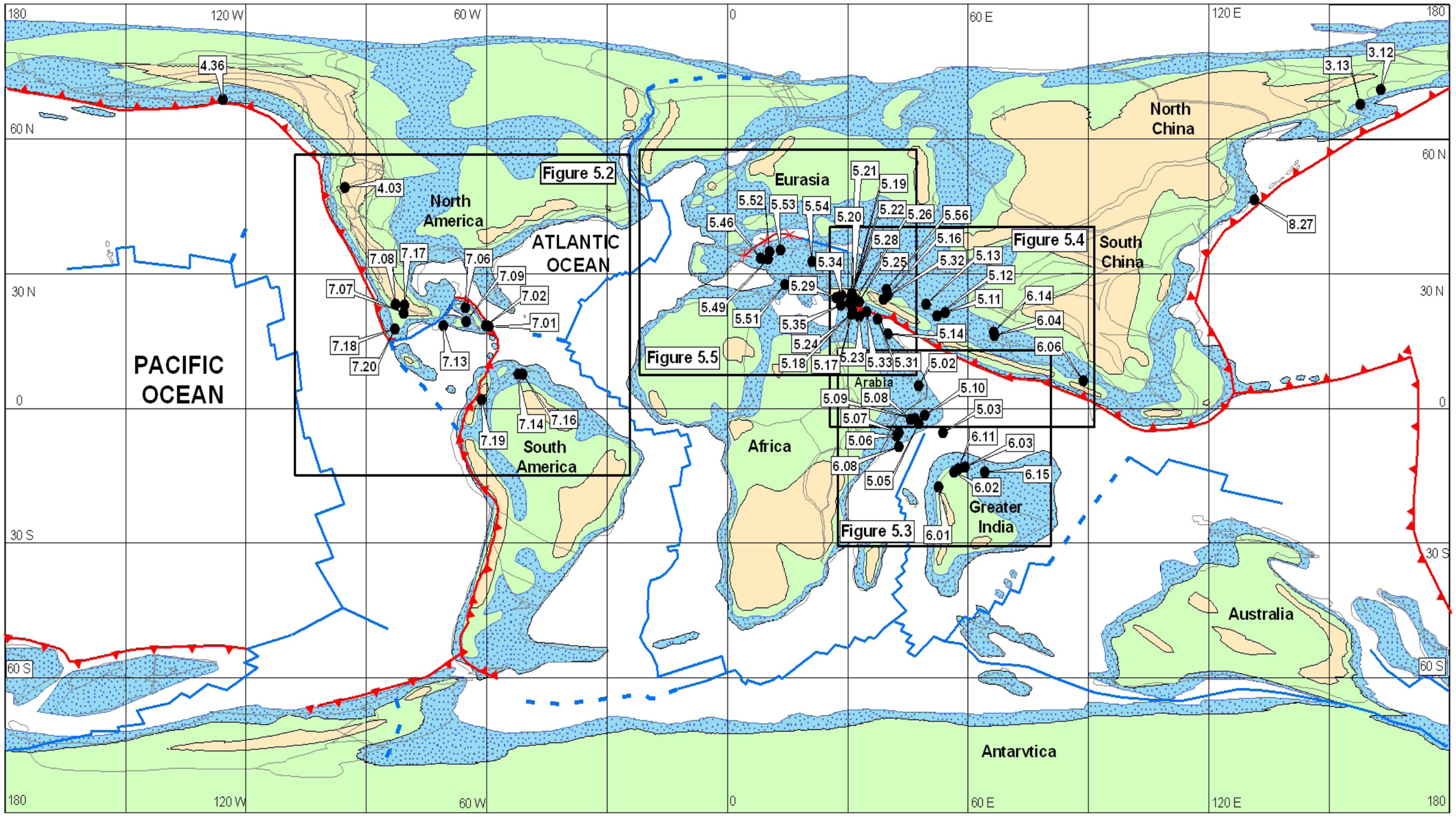

Map 10 Ophiolites 20 Ma

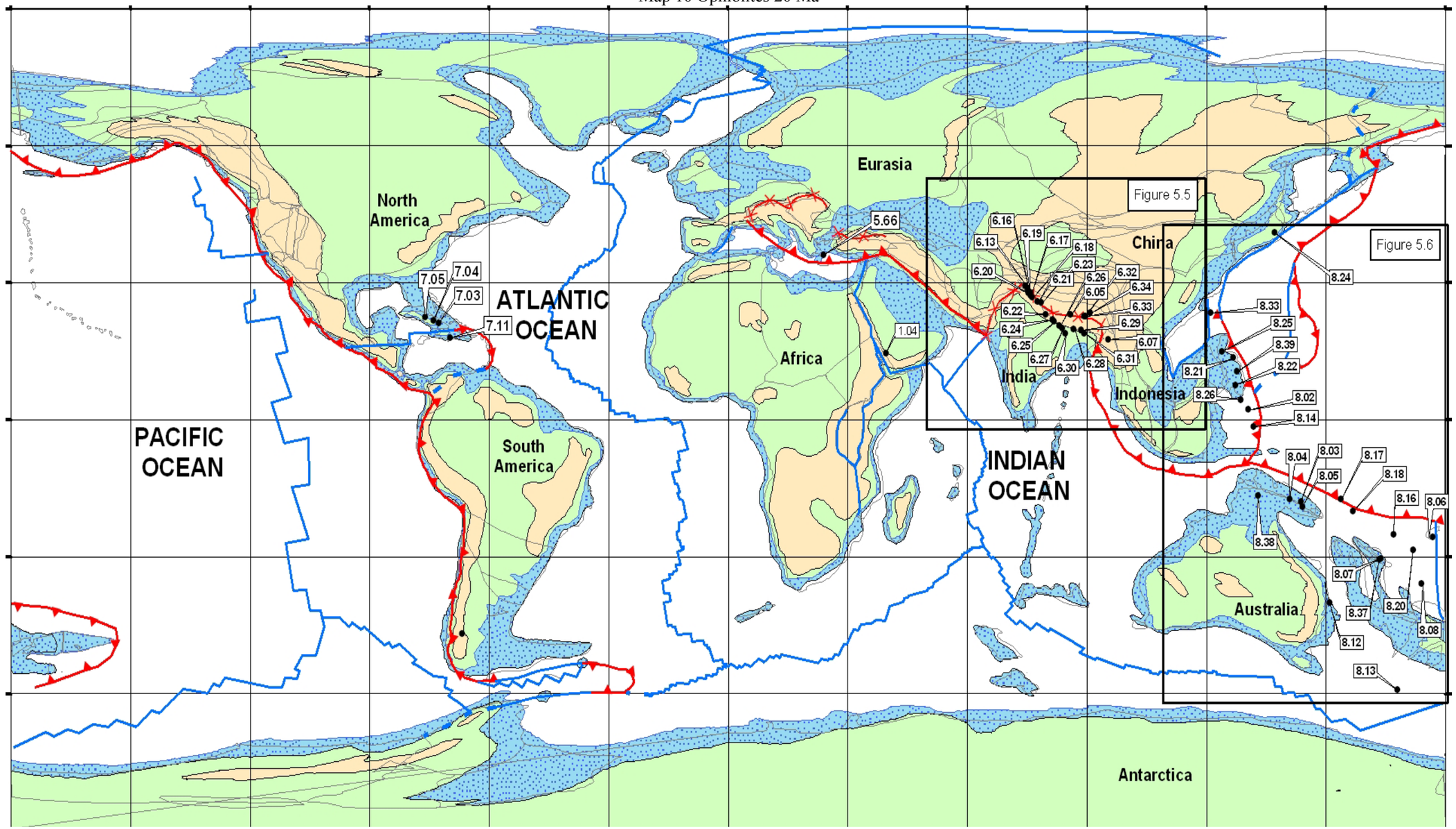

Map 11 Modern Ophiolite Locations

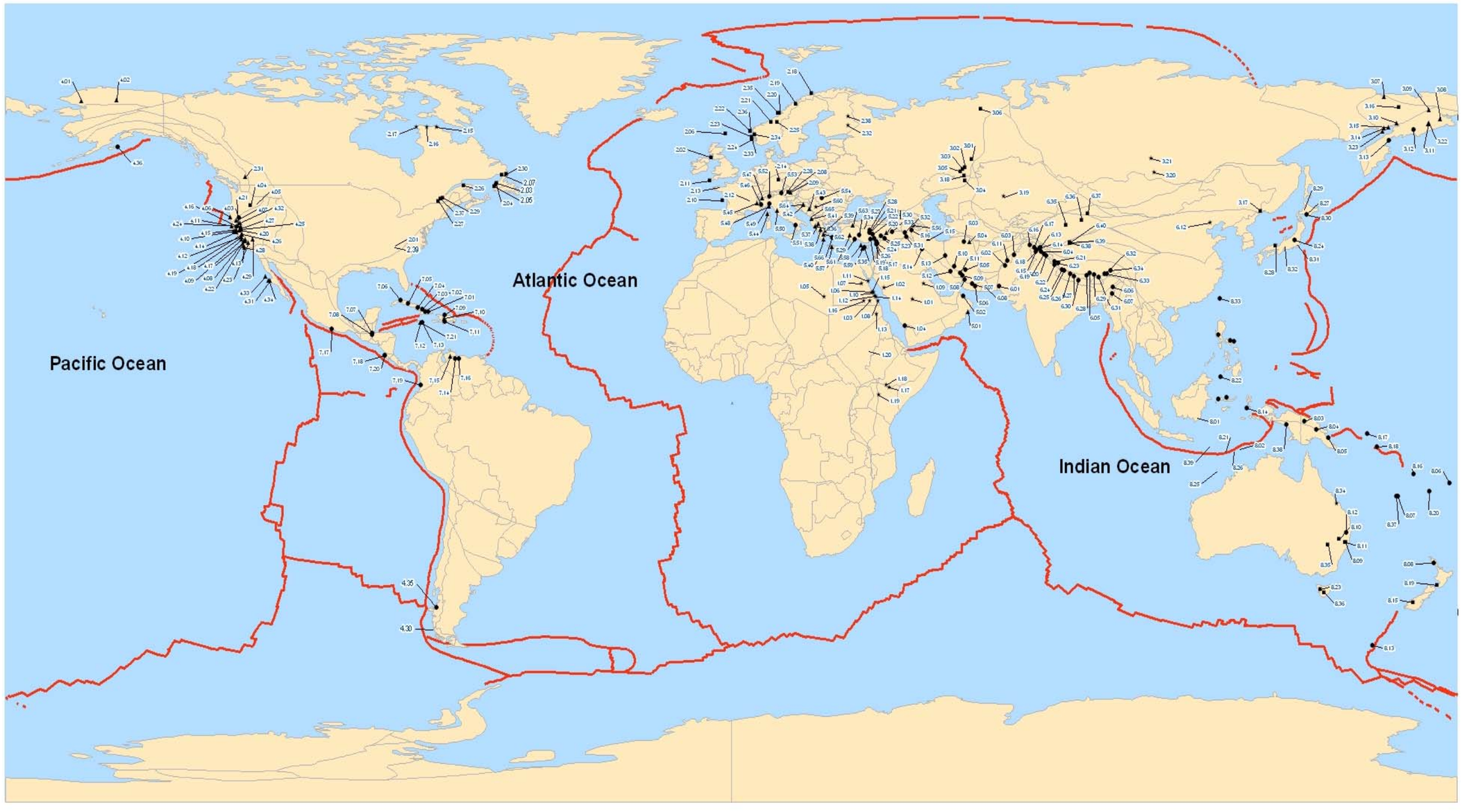

REFERENCES

Abbate, E., Bortolotti, V., Passerini, P. & Principi, G. (1985). The rhythm of Phanerozoic ophiolites. Ofioliti, 10(2), 109-138.

Abdelsalam, M.G. (1994). The Oko shear zone, Sudan: post-accretionary deformation in the Arabian-Nubian Shield. Journal of the Geological Society of London, 151, 767-776.

Abdelsalam, M.G. & Stern, R.J. (1996). Sutures and shear zones in the Arabian-Nubian Shield. Journal of African Earth Sciences, 23, 289-310.

Adib, D. & Pamić, J. (1980). Ultramafic and mafic cummulates from the Neyriz ophiolitic complex in S.E. parts of the Zagros range (Iran). *In:* Panayiotou, A. (ed). Ophiolites, Proceedings, International Ophiolite Symposium Cyprus 1979. Ministry of Agriculture and Natural Resources Geological Survey Department, 392-397.

Ageed, A., Saager, R., & Stunfi, E. (1980). Pre-alpine ultramafic rocks in the Eastern Central Alps, Austria. *In:* Panayiotou, A. (ed). Ophiolites, Proceedings, International Ophiolite Symposium Cyprus 1979. Ministry of Agriculture and Natural Resources Geological Survey Department, 601 – 606.

Agrawal, O.P. & Kacker, R.N. (1980). Nagaland ophiolites, India - a subduction zone ophiolite complex in Tethyan orogenic belt. *In:* Panayiotou, A. (ed). Ophiolites, Proceedings, International Ophiolite Symposium Cyprus 1979. Ministry of Agriculture and Natural Resources Geological Survey Department, 454-461.

Ahmed, A.H., Arai, S., & Attia, A.K. (2001). Petrological characteristics of podiform chromitites and associated peridotites of the Pan African Proterozoic ophiolite complexes of Egypt. Mineralium Deposita, 36(1), 72 – 84.

Ahmed, Z. & Ernst, W.G. (1999) Island arc-related, back-arc basinal, and oceanic-island components of the Bela Ophiolite-Mélange complex, Pakistan. International Geology Review, 41(8), 739-763.

Aitchison, J.C., Clark, B.M., Flood, P.G., & Jayko, A.S. (1994). Paleozoic ophiolitic assemblages within the southern New England orogen of eastern Australia: Implications for growth of the Gondwana margin. Tectonics 13(5), 1135-1149.

Alabaster, T., Pearce, J.A., & Malpas, J. (1982). The volcanic stratigraphy and petrogenesis of the Oman ophiolite complex. Contributions to Mineralogy and Petrology, 81(3), 168–183.

Al-Shanti, M. & Roobol, M.J. (1979). A Late Proterozoic ophiolite complex at Jabal Ess in northern Saudi Arabia. Nature, 279, 488-491.

Amato, J.M., Johnson, C.M., Baumgartner, L.P., & Beard, B.L. (1999). Rapid exhumation of the Zermatt-Saas ophiolite deduced from high-precision Sm-Nd and Rb-Sr geochronology. Earth and Planetary Science Letters, 171(3), 425-438.

Andersen, T.B., Skjerlie, K.P., & Furnes, H. (1990). The Sunnfjord Mélange: Evidence for Silurian ophiolite accretion in the West Norwegian Caledonides. Journal Geological Society of London, 147, 59-68.

Audet, M., Picard, C., & Goulet, N. (2004). The Koniambo Massif, Nouvelle-Caledonie. An overturned ophiolite sequence. EOS Trans. AGU 85(28) Western Pacific Geophysics Meeting, Supplemental Abstract V23B-96.

Avdeev, A.V. (1984). Ophiolite zones and the geologic history of Kazakhstan from the mobilist standpoint, International Geological Reviews, 26, 995-1005.

Banerjee, N.R., Gillis, K.M., Muehlenbachs, K. (2000). Discovery of epidosites in a modern oceanic setting, the Tonga forearc. Geology, 28(2), 151-154.

Barnes, B.P. & Andrews, J.R. (1984). Hot or cold emplacement of the Lizard Complex? Journal of the Geological Society of London, 141, 37-39.

Barnes & Noble Books, (2004). Hammond Atlas of the World. Hammond World Atlas Corporation, Barnes and Noble Publishing, China, scale varies by map, 287 sheets, 64 p. text.

Bartok, P.E., Renz, D., & Westermann, G.E.G. (1985). The Siquisique ophiolites, northern Lora State, Venezuela: A discussion on their Middle Jurassic ammonites and tectonics implications. Geological Society of America Bulletin, 96, 1050-1055.

Beard, J.S. (1998). Polygenetic tonalite-trondhjemite-granodiorite (TTG) magmatism in the Smartville Complex, Northern California with a note on LILE depletion in plagiogranites. Mineralogy and Petrology, 64, 1-4.

Beccaluva, L., Piccardo, G.B., & Serri, G. (1980). Petrology of Northern Apennine ophiolites and comparison with other Tethyan ophiolites. *In:* Panayiotou, A. (ed). Ophiolites, Proceedings, International Ophiolite Symposium Cyprus 1979. Ministry of Agriculture and Natural Resources Geological Survey Department, 314-331.

Berger, J., Femenias, O., Mercier, J.C.C., & Demaiffe, D. (2005). Ocean-floor hydrothermal metamorphism in the Limousin ophiolites (western French Massif Central): evidence of a rare preserved Variscan ocean marker. Journal of Metamorphic Geology, 23, 795-812.

Berhe, S.M. (1990). Ophiolites in Northeast and East Africa: implications for Proterozoic crustal growth. Journal of the Geological Society of London, 147, 41-57.

Bishady, A.M., Attia, M.S., Hathout, M., & Omar, M I.B. (1994). Petrography and Geochemistry of the Ophiolitic Mélange in the Area of Wadi Lawi and Wadi Lawawi, South of Eastern Desert, Egypt. Archiwum Mineralogiczne, 50(1), 69-96.

Blasband, B., Brooijmans, P., Dirks, P., Visser, W., & White, S. (1997). A Pan-African core complex in the Sinai, Egypt. Geologie en Mijnbouw, 76(3), 247 – 266.

Blasband, B., White, S., Brooijmans, P., De Boorder, H., & Visser, W. (2000). Late Proterozoic extensional collapse in the Arabian–Nubian Shield. Journal of the Geological Society, 157, 615 - 628.

Bluck, B.J., Halliday, A.N., Aftalion, M., & Macintyre, R.M. (1980). Age and Origin of the Ballantrae ophiolite and its significance to the Caledonia orogeny and Ordovician time scale. Geology, 8, 492-495.

Bor-ming, J. (1996). Mid-ocean ridge or marginal basin origin of the East Taiwan Ophiolite: chemical and isotopic evidence. Contributions to Mineralogy and Petrology, 92 (2), 194 – 206.

Borradaile, G.J. & Lucas, K. (2003). Tectonics of the Akamas and Mamonia ophiolites, Western Cyprus: magnetic petrofabrics and paleomagnetism. Journal of Structural Geology, 25(12), 2053-2076.

Borsi, L., Schaerer, U., Gaggero, L., & Crispini, L. (1996). Age, origin and geodynamic significance of plagiogranites in lherzolites and gabbros of the Piedmont-Ligurian ocean basin. Earth and Planetary Science Letters, 140, 227-241.

Bortolotti, V. & Principi, G. (2005). Tethyan ophiolites and Pangea breakup. The Island Arc, 14, 442-470.

Bourgois, J., Calle, B., Tournon, J., & Toussaint, J.F. (1982). The Andean ophiolitic megastructures on the Buga-Buenaventura transverse (Western Cordillera--Valle Colombia). Tectonophysics, 82(3-4), 207-229.

Boyle, A.P. (1980). The Sulitjelma amphibolites, Norway: Part of a flower Paleozoic ophiolite complex? *In:* Panayiotou, A. (ed). Ophiolites, Proceedings, International Ophiolite Symposium Cyprus 1979. Ministry of Agriculture and Natural Resources Geological Survey Department, 567-575.

Brown, A.V., Page, N.J., Love, & A.H. (1988). Geology and platinum-group-element geochemistry of the Serpentine Hill complex, Dundas Trough, western Tasmania. Canadian Ministry, 26, 161-175.

Bruce, M.C., & Niu, Y. (2000). Evidence for Palaeozoic magmatism recorded in the Late Neoproterozoic Marlborough ophiolite, New England Fold Belt, central Queensland: Australian Journal of Earth Sciences, 47(6), 1065-1076.

Busby, C. (2004). Continental growth at convergent margins facing large ocean basins: a case study from Mesozoic convergent-margin basins of Baja California, Mexico. Tectonophysics, 392, 241-277.

Calon, T.J., Malpas, J.G., & McDonald, R. (1989). The Anatomy of the Shulaps Ophiolite. Geological Fieldwork Paper 1990-1, British Columbia Geological Survey Branch, 375 - 386.

Cande, S.C. & Kent, D.V. (1995). Revised calibration of the geomagnetic polarity time scale for the Late Cretaceous and Cenozoic. Journal of Geophysical Research, 100B, 6093-6095.

Casey, J.F. & Dewey, J.F. (1984). Initiation of subduction zones along transform and accretionary plate boundaries, triple-junction evolution and fore arc spreading centers- Implications for Ophiolitic geology and obduction. *In:* Gass, I.G., Lippard, S. J., & Shelton, A.W. (eds.). Ophiolites and Oceanic Lithosphere. Geological Society of London Special Publication 13, 269-290.

Cawood, P.A. (1989). Acadian remobilization of a Taconian ophiolite: Hare Bay allocthon northwestern Newfoundland. Geology, 17(3), 257-260.

Chatterjee, S. and Scotese, C. R. 1999. The breakup of Gondwana and the evolution and biogeography of the Indian plate. Proceedings of Indian National Science Academy, 65A: 397-425.

Chekhovich, V., Kovalenko, D., & Ledneva, G. (1999). Cenozoic History of the Bering Sea and its northwestern margin. The Island Arc, 8(2), 168-180.

Claesson, S., Pallister, J.S., & Tatsumoto, M. (1984). Samarium-neodymium data on two late Proterozoic ophiolites of Saudi Arabia and implications for crustal and mantle evolution: Contributions to Mineralogy and Petrology, 85, 244-252.

Clark, A.H., Scott, D.J., Sandeman, H.A., Bromley, A.V., & Farrar, E. (1998). Siegenian generation of the Lizard ophiolite: U-Pb zircon age data for plagiogranites, Porthkerris, Cornwall. Journal of the Geological Society of London, 155, 595-598.

Cobiella, J.L. (1978). Una mélange en Cuba Oriental. Minera en Cuba, 4(4), 46-51.

Cobeilla, J.L, Campos, M., Boiteau, A., & Quintas, F. (1977). Geologia del flanco sur de la Sierra del Purial. Minera en Cuba, 3(1), 55-62 and 3(2), 44-53.

Coish, R.A., Bramley, A., Gavigan, T., & Masinter, R. (1991). Progressive changes in volcanism during Iapetan rifting: Comparisons with the East African Rift-Red Sea system. Geology, 19, 1021–1024.

Coish, R A., & Sinton, C.W. (1992). Geochemistry of mafic dikes in the Adirondack Mountains: implications for late Proterozoic continental rifting. Contributions to Mineralogy and Petrology, 110, 500–514.

Cole, R.B., Nelson, S.W., Layer, P.W., & Oswald, P.J. (2006). Eocene volcanism above a depleted mantle slab window in southern Alaska. Geological Society of America Bulletin, 118(1-2), 140–158.

Coleman, P.J. (1966). The Solomon Islands as an island arc. Nature, 211, 1249-1251.

Coleman, P.J. (1970). Geology of the Solomon and New Hebrides Islands, as part of the Melanesian re-entrant, southwest Pacific. Pacific Science, 24, 289-314.

Coleman, R.G. (1977). Ophiolites. Springer-Verlag, Berlin. pp 229.

Coleman, R.G. (1984). Ophiolites and Tectonic Evolution of the Arabian Peninsula. *In:* Gass, I.G., Lippard, S. J., & Shelton, A.W. (eds.). Ophiolites and Oceanic Lithosphere. Geological Society of London Special Publication 13, 359-366.

Coleman, R.G. (2000). Prospecting for ophiolites along the California continental margin. *In:* Dilek, Y., Moores, E., Elthon, D., & Nicholas, A. (eds.). Ophiolites and oceanic crust: new insights from field studies and the Ocean Drilling Program. Geological Society of America Special Paper 349, 351–364.

Colley, H. (1984). An ophiolite suite in Fiji?. *In:* Gass, I.G., Lippard, S. J., & Shelton, A.W. (eds.). Ophiolites and Oceanic Lithosphere. Geological Society of London Special Publication 13, 333-340.

Comacho, A., Hensen, B.J. & Armstrong, R. (2002). Isotopic test of a thermally driven intraplate orogenic model, Australia. Geology, 30(10), 887-890.

Coombs, D.S., Landis, C.A., Norris, R.J., Sinton, M., Borns, D.J., & Craw, D. (1976). The Dun Mountain ophiolite belt, New Zealand, its tectonic setting, constitution, and origin, with special reference to the southern portion. American Journal of Science, 276, 561-603.

Costa, S., Caby, R. (2001). Evolution of the Ligurian Tethys in the Western Alps: Sm/Nd and U/Pb geochronology and rare-earth element geochemistry of the Montgenevre ophiolite (France). Chemical Geology, 175, 449-466.

Cox, J., Searle, M., & Pedersen, R. (1999). The petrogenic origin of leucogranitic dykes intruding the northern Semail ophiolite, United Arab Emirates: field relationships, geochemistry and Sr/Nd isotope systematics. Contributions to Mineralogy and Petrology, 137-287.

Crowley, Q.G., Floyd, P.A., Winchester, J.A., Franke, W., & Holland, J.G. (2000). Early Paleozoic rift-related magmatism in Variscan Europe: fragmentation of the Armorican Terrane Assemblage. Terra Nova, 12, 171-180.

Dallmeyer, R.D., & Williams, H. (1975). $^{40}Ar/^{39}Ar$ ages from the Bay of Islands metamorphic aureole: their bearing on the timing of Ordovician ophiolite obduction. Canadian Journal of Earth Science, 12, 1865-1890.

Danelian, T., Lekkas, S., & Alexopoulos, A. (2000). Discovery of Triassic radiolarites in an ophiolitic complex of the southernmost Peloponnese (Agelona, Lakonia, Greece). Earth and Planetary Sciences 330, 639-644.

Davies, G.A., Holdaway, M.J., Lipman, P.W., & Romey, W.D. (1965). Structure, metamorphism and plutonism in the south-central Klamath Mountains, California. Geological Society of America Bulletin, 76, 933-966.

Davis, H.L. (1971). Peridotite- Gabbro-Basalt complex in eastern Papua: an overthrust plate of oceanic mantle and crust. Bureau of Mineral Resources of Australia, Bulletin, 128.

Day, H.W. & Bickford, M.E. (2004), Tectonic setting of the Jurassic Smartville and Slate Creek complexes, northern Sierra Nevada, California. Geological Society of America Bulletin, 116(11-12), 1515-1528.

Desmons, J. (1989). Different metamorphic evolutions in the Alpine-Apenninic ophiolites (France-Italy-Switzerland-Austria). Chemical Geology, 77, 229-250.

Dewit, M.J., Dutch, S., Kligfield, R., Allen, R. & Stern, C. (1977). Deformation, Serpentinization and Emplacement of a Dunite Complex, Gibbs Island, South-Shetland Islands - Possible Fracture Zone Tectonics. Journal of Geology, 85(6), 745-762.

Dietrich, V.J. (1979). Ophiolitic belts of the central Mediterranean. In: International Atlas of Ophiolites, Geological Society of America Map and Chart Series, MC-33.

Dilek, Y. (2003a). Ophiolite concept and its evolution. *In:* Dilek, Y. & Newcomb, S. (eds.). Ophiolite concept and the evolution of geological thought. Geological Society of America Special Paper 373, 1-16.

Dilek, Y. (2003b). Ophiolite pulses, mantle plumes orogeny *In:* Dilek, Y. & Robinson, P.T. (eds.). Ophiolites in Earth History. Geological Society, London Special Publication 218, 9-19.

Dilek, Y. & Delaloye, M. (1992). Structure of the Kizildag Ophiolite, a Slow-Spread Cretaceous Ridge Segment North of the Arabian Promontory. Geology, 20(1), 19-22.

Dilek, Y. & Flower, M.F.J. (2003). Arc-trench rollback and forearc accretion: A model template for ophiolites in Albania, Cyprus, and Oman. *In:* Dilek, Y. & Robinson, P.T. (eds.). Ophiolites in Earth History. Geological Society, London Special Publication 218, 43-68.

Dilek, Y., Moores, E.M., & Furnes, H. (1998). Structure of modern oceanic crust and ophiolites and implications for faulting and magmatism at oceanic spreading centers. *In*: Buck, R., Karson, J., Delaney, P., & Lagabrielle, Y. (eds). Faulting and Magmatism at Mid-Ocean Ridges. American Geophysical Union Monograph, 106, 219–66.

Dilek, Y. & Whitney, D.L. (1997) Counterclockwise P-T-t trajectory from the metamorphic sole of a Neo-Tethyan ophiolite (Turkey). Tectonophysics, 280(3-4), 295-310.

Dilek, Y., Whitney, D.L., & Tekeli, O. (1999). Links between tectonic processes and landscape morphology in an alpine collision zone, south-central Turkey. Z. Geomorphology N. F. Supplemental Bd. 118, 147-164.

Draper, G. (1986). Blueschists and associated rocks in eastern Jamaica and their significance for Cretaceous plate-margin development in the northern Caribbean. Geological Society of America Bulletin, 97(1), 48-60.

Dunning, G.R. & Krough, T.E. (1985). Geochronology of ophiolites of the Newfoundland Appalachians. Canadian Journal of Earth Sciences, 22, 1659-1670.

Dunning, G.R., Krough, T.E., & Pederson, R.B. (1986). U-Pb zircon ages of Appalachian-Caledonian ophiolites: Terra Cognita, 6, L51 (abstract).

Dupuis, C., Hérbert, R., Dubois-Côté, V., Guilmette, C., Wang, C.S., Li, Y.L., & Li, Z.J. (2005). The Yarlung Zangbo suture zone ophiolitic mélange (southern Tibet): new insights from geochemistry of ultramafic rocks. Journal of Asian Earth Sciences, 25, 937-960.

El Akhal, H. (1993). A transect from a tectonic mélange to an island-arc in the Pan-African of SE Egypt (Wadi Ghadir area). Scientific Series of the International Bureau, Forschungszentrum Juelich, 20, 244 p.

El-Sayed, M.M., Furnes, H. & Mohamed, F.H. (1999). Geochemical constraints on the tectonomagmatic evolution of the Late-Precambrian Fawakhir ophiolite, Central Eastern Desert, Egypt. Journal of African Earth Sciences, 29(3), 515-533.

Elthon, D., Casey, J.F., & Komor, S. (1982). Mineral chemistry of ultramafic cumulates from the North Arm Mountain Massif of the Bay of Island ophiolite, Newfoundland: evidence for high pressure crystal fractionation of oceanic basalts. Journal of Geophysical Research, 87, 8717–8734.

Ernst, W.G. (2005). Alpine and Pacific styles of Phanerozoic mountain building: Subduction zone petrogenesis of continental crust. Terra Nova, 17, 165-188.

Faryad, S.W. & Hoinkes, G. (2004). Complex Growth Textures in a Polymetamorphic Metabasite from the Kraubath Massif (Eastern Alps). Journal of Petrology, 45(7), 1441-1451.

Feininger, T. (1981). Amphibolite associated with the Thetford Mines ophiolite complex at Belmina Ridge, Quebec. Canadian Journal of Earth Science, 18, 1878-1892.

Fergusson, C.L. & Coney, P.J. (1992). Implications of a Bengal Fan-type deposit in the Paleozoic Lachlan fold belt of southeastern Australia. Geology, 20(11), 1047-1049.

Fisher, R.L. & Engel, C.G. (1968). Dunite Dredged from Nearshore Flank of Tonga Trench on Expedition Nova 1967. Transactions-American Geophysical Union, 49(1), 217.

Foley, J.Y. (1992). Ophiolitic and other mafic-ultramafic metallogenic provinces in Alaska (west of the 141st meridian). U.S. Geological Survey Open-File Report 92-20B, 55 p.

Fonsec, E., Zelepugin, V.N. & Eredia, M. (1985). Structure of the Ophiolite Association of Cuba. Geotectonics, 19(4), 321-329.

Franke, W., Żelázniewicz, A., Porćebski, S. J., & Wajspyrch, B. (1993). Saxothuringian zone in Germany and Poland: differences and common features. International Journal of Earth Sciences, 82(3), 583 – 599.

Furnes, H., Banerjee, N.R., Muehlenbach, S., & Kontinen, A. (2005). Preservation of biosignatures in metaglassy volcanic rocks from the Jormua ophiolite complex, Finland. Precambrian Research, 136, 125-137.

Furnes, H., Hellevang, B., & Dilek, Y. (2001). Cyclic volcanic stratigraphy in a Late Ordovician marginal basin, west Norwegian Caledonides. Bulletin of Volcanology, 63(2–3), 164 – 178.

Furnes, H., Hellevang, B., Robins, B., & Gudmundsson, A. (2003). Geochemical stratigraphy of the lavas of the Solund-Stavfjord Ophiolite Complex, W. Norway, and magma-chamber dynamics. Bulletin of Volcanology, 65(6), 441–457.

Furnes, H., Thon, A., Nordås, J., & Garmann, L.B. (1982). Geochemistry of Caledonian metabasalts from some Norwegian ophiolite fragments. Contributions to Mineralogy and Petrology, 79(3), 295 – 307.

Gagnon Y.D. & Jamieson, R.A. (1985). Geology of the Mont Albert region, Gaspe Peninsula. Geological Survey of Canada Paper 85(1A), 783-788.

Gealey, W.K (1977). Ophiolite obduction and geologic evolution of the Oman Mountains and adjacent areas. Geological Society of America Bulletin, 88, 1183-1191.

Gealey, W.K. (1980). Ophiolite obduction mechanisms. *In:* Panayiotou, A. (ed). Ophiolites, Proceedings, International Ophiolite Symposium Cyprus 1979. Ministry of Agriculture and Natural Resources Geological Survey Department, 228-243.

Ghazi, A.M. and Hassanipak, A.A. (1999). Geochemistry of subalkaline and alkaline extrusives from the Kermanshah ophiolite, Zagros Suture Zone, Western Iran: Implications for Tethyan plate tectonics. Journal of Asian Earth Sciences, 17(3), 319-332.

Ghazi, A.M. & Hassanipak, A.A. (2000). Petrology and geochemistry of the Shahr-Babak ophiolite, central Iran. *In:* Dilek, Y., Moores, E., Elthon, D., & Nicholas, A. (eds.). Ophiolites and oceanic crust: new insights from field studies and the Ocean Drilling Program. Geological Society of America Special Paper 349, 485-498.

Gillis, K.M. & Banerjee, N.R. (2000). Hydrothermal alteration patterns in supra-subduction zone ophiolites. *In:* Dilek, Y., Moores, E., Elthon, D., & Nicholas, A. (eds.). Ophiolites and oceanic crust: new insights from field studies and the Ocean Drilling Program. Geological Society of America Special Paper 349, 283-298.

Girardeau, J., Dubuisson, G., & Mercier, J.C.C. (1986). Kinematic of Thrusting of Ophiolite and Crystalline Nappes in Limousin, Western French Massif-Central. Bulletin De La Societe Geologique De France, 2(5), 849-860.

Girardeau, J., & Mevel, C. (1982). Amphibolitized sheared gabbros from ophiolites as indicators of the evolution of the oceanic crust: Bay of Islands, Newfoundland. Earth Planetary Science Letters, 61, 151-165.

Girardeau, J. & Nicolas, A. (1981). The structures of two ophiolite massifs, Bay-of-Islands, Newfoundland: A model for the oceanic crust and upper mantle. Tectonophysics, 77(1-2), 1-34.

Gnos, E., Immenhauser, A., & Peters, Tj. (1997). Late Cretaceous/early Tertiary convergence between the Indian and Arabian plates recorded in ophiolites and related sediments. Tectonophysics, 271, 1-19.

Gnos, E., Khan, M., Mahmood, K., Khan, A.S., Shafique, N.A., & Villa, I.M. (1998). Bela oceanic lithosphere assemblage and its relation to the Reunion hotspot. Terra Nova, 10(2), 90-95.

Gnos, E. & Perrin, M. (1996). Formation and evolution of the Masirah ophiolite constrained by paleomagnetic study of volcanic rocks. Tectonophysics, 253, 53-64.

Gornova, M.A. & Petrova, Z.I. (1999). Mantle peridotites of Granulite-Gneiss complexes as fragments of Archean ophiolites in the Baikal Region. Ofioliti, 24(2).

Gray, D.R., Gregory., R.T., & Miller, J.Mc. (2000). A New structural profile along the Muscat-Ibra transect, Oman: Implications for emplacement of the Semail ophiolite. *In:* Dilek, Y., Moores, E., Elthon, D., & Nicholas, A. (eds.). Ophiolites and oceanic crust: new insights from field studies and the Ocean Drilling Program. Geological Society of America Special Paper 349, 513-523.

Green, D. H. (1964). The metamorphic aureole of the peridotite at the Lizard, Cornwall. Journal of Geology, 72, 543-563.

Greiling, R.O., Abdeen, M.M., Dardir, A.A., Akhal, H., Ramly, M.F., Kamal, G.M., Osman, A.F., Rashwan, A.A., Rice, A.H.N., & Sadek, M.F. (1994). A structural synthesis of the Proterozoic Arabian-Nubian Shield in Egypt. International Journal of Earth Sciences, 83(3), 484 – 501.

Grudinin, M.I. & Demin, I.A. (1994). Riphean ophiolites of the Northern Baikal region (east Siberia). *In:* Ishiwatari, A., Malpas, J., & Ishizuka, H. (eds). Proceedings of the 29th International Geological Congress Part D, VSP, 263-272.

Hacker, B.R., (1994). Rapid emplacement of young oceanic lithosphere: Argon geochronology of the Oman ophiolite. Science, 265, 1563-1565.

Haldemann, E.G., Brouwer, S.B., Blowes, J.H., & Snow, W.E. (1980). Lateritic nickel deposits at Bonao Falconridge Dominica. Field Guide 9th Caribbean Geological Conference, Santo Domingo, 69-78.

Hall, R. (2002). Cenozoic geological and plate tectonic evolution of SE Asia and the SW Pacific: computer-based reconstructions, model and animations. Journal of Asian Earth Sciences, 20, 353-431.

Harper, G.D. (1984). The Josephine Ophiolite. Geological Society of America Bulletin, 95, 1009-1026.

Harris, R. & Long, T. (2000). The Timor ophiolite, Indonesia: Model or myth? *In:* Dilek, Y., Moores, E., Elthon, D., & Nicholas, A. (eds.). Ophiolites and oceanic crust: new insights from field studies and the Ocean Drilling Program. Geological Society of America Special Paper 349, 321 – 330.

Hassanipak, A.A. & Ghazi, A.M. (2000). Petrology, geochemistry and tectonic setting of the Khoy ophiolite, northwest Iran: implications for Tethyan tectonics. Journal of Asian Earth Sciences, 18(1), 109-121.

Hébert, R., Huot, F., Wang, C., & Liu, Z. (2003). Yarlung Zangbo ophiolites, southern Tibet revisited: geodynamic implications from the mineral record. *In:* Dilek, Y. & Robinson, P.T. (eds.). Ophiolites in Earth History. Geological Society, London Special Publication 218, 165-190.

Herz, N. & Savu, H. (1974). Plate tectonic history of Romania. Geological Society of America Bulletin, 85, 1429-1440.

Herzig, C.T., Kimbrough, D.L., & Hayasaka, Y. (1997). Early Permian zircon uranium-lead ages for plagiogranites in the Yakuno ophiolite, Asago district, Southwest Japan. The Island Arc, 6(4), 396-403.

Hopper, D.J. & Smith, I.E.M. (1996). Petrology of the gabbro and sheeted basaltic intrusives at North Cape, New Zealand. New Zealand Journal of Geology and Geophysics, 39, 389-402.

Ingersoll, R.V. & Busby, C.J. (1995). Tectonics of sedimentary basins. In: Busby, C.J.& Ingersoll, R.V. (Eds.), Tectonics of Sedimentary Basins. Blackwell, Cambridge, MA, pp. 1 – 52.

Ishiwatari, A. (1985). Igneous petrogenesis of the Yakuno ophiolite (Japan) in the context of the diversity of ophiolites. Contribution to Mineralogy and Petrology, 89, 155-67.

Ishiwatari, A. (1990a). Time-space distribution and petrologic diversity of Japanese ophiolites. *In:* Peters, T.J., Nicolas, A., & Coleman R.G. (eds). Ophiolite Genesis and Evolution of the Oceanic Lithosphere. Ministry of Petroleum and Minerals, Sultanate of Oman. Kluwer Academic Publications, Amsterdam, 723-744.

Ishiwatari, A. (1990b). Yakuno ophiolite and related rocks in the Maizuru terrane. *In:* Ichikawa, K. Mizutani, S., Hara, I., Hada, S., & Yao, A (eds). Pre-Cretaceous terranes of Japan. IGCP Project 224, 109 – 120.

Ishiwatari, A. & Tsujimori, T. (2003). Paleozoic ophiolites and bluschists in Japan and Russian Primorye in the Tectonic framework of east Asia: A Synthesis. The Island Arc, 12(2), 190.

Ishiwatari, A., Sokolov, S., Saito, D., Tsujimori, T., & Miyashita, S. (1998). Geology and Petrology of Elistratova Ophiolites in Taigonos peninsula, Northeastern Russia: an island-arc ophiolites intruded into oceanic mantle. International Ophiolite Symposium, Oulu, Finland August 10-15.

Ishiwatari, A., Sokolov, S., Saito, D., Tsujimori, T., & Miyashita, S. (1999). Superplume-related ophiolites among western Pacific accretionary complexes: Examples from Koryak Mountains, Northeastern Russia. Superplume International Workshop, Poster and abstract P-31. Wako City, Japan January 28-31.

Iturralde-Vinent, M.A. (1989). Role of Ophiolites in the Geological Structure of Cuba. Geotectonics, 23(4), 332-342.

Iturralde-Vinent, M.A., ed. (1996). Ofiolitas y Arcos Volcanicos de Cuba, IUGS Project 364. Caribbean Ophiolites and Volcanic Arcs, Special Contribution No. 1.

Ivanov, K.S., Puchkov, V.N., & Babenko, V.A. (1990). Finds of Conodonts and graptolites in metamorphic units of South Urals. Dokl. Akad. Nauk SSSR 310, 676-679 (translated from Russian).

Jamieson, R.A. (1980). Formation of metamorphic aureoles beneath ophiolites. Evidence from the St. Anthony complex, Newfoundland. Geology, 8, 150-154.

Jones, G., Robertson, A.H.F., & Cann, J.R. (1991). Genesis and emplacement of the supra-subduction zone Pindos ophiolite, northwestern Greece. *In:* Peters, T.J., Nicolas, A., & Coleman R.G. (eds). Ophiolite Genesis and Evolution of the Oceanic Lithosphere. Ministry of Petroleum and Minerals, Sultanate of Oman. Kluwer Academic Publications, Amsterdam, pp. 771-800.

Juteau, T. (2003) Identification of a mantle unit in ophiolites: A major step in the evolution of the ophiolite concept. *In:* Dilek, Y. & Newcomb, S. (eds.). Ophiolite concept and the evolution of geological thought. Geological Society of America Special Paper 373, 31-54.

Juteau, T. & Whitechurch, H. (1980). The magmatic cummulates of Antalya (Turkey): Evidence of multiple intrusions in an ophiolitic magma chamber. *In:* Panayiotou, A. (ed). Ophiolites, Proceedings, International Ophiolite Symposium Cyprus 1979. Ministry of Agriculture and Natural Resources Geological Survey Department, 377-391.

Kananian, A., Juteau, T., Bellon, H., Darvishzadeh, A., Sabzehi, M., Whitechurch, H., & Ricou, L.E. (2001). The ophiolite massif of Kahnuj (western Makrãn, southern Iran): new geological and geochronological data. Comptes Rendus De L Academie Des Sciences Serie Ii Fascicule a-Sciences De La Terre Et Des Planetes, 332(9), 543-552.

Katzir, Y., Avigad, D., Matthews, A., Garfunkel, Z., Evans, B.W. (2000). Origin, HP/LT metamorphism and cooling of ophiolitic mélanges in southern Evia (NW Cyclades), Greece. Journal of Metamorphic Geology, 18, 699-718.

Kawachi, Y. (1991)."Rhodonite" - bearing manganese deposits in the New England fold belt of eastern Australia, with special reference to the deposit of Woods Mine. Bending of the Great Serpentine Belt and Tectonic History of the Arc-type Crust around the Belt, Eastern Australia. Preliminary Report on the Geology of the New England Fold Belt, Australia, No. 2, 55-61.

Kemp, J., Pellatn, C., & Calvez, J.V. (1980). Geochronological investigation and geological history in the Precambrian of northwestern Saudi Arabia. Bureau des Recherches Gtologiques et Minieres Open File-01-1.

Khain, E.V., Bibikova, E.V., Salnikova, E.B., Kroner, A., Gibsher, A.S., Didenko, A.N., Degtyarev, K.E. and Fedotova, A.A. (2003). The Palaeo-Asian ocean in the Neoproterozoic and early Palaeozoic: new geochronologic data and palaeotectonic reconstructions. Precambrian Research, 122(1-4), 329-358.

Kimbrough, D.L. (1984). Paleogeographic significance of the Middle Jurassic Gran Canon Formation, Cedros Island, Baja California. *In:* Frizzell, V.A. (ed.). Geology of the Baja California Peninsula, Book 39. Pacific Section Society Economic Paleontologists and Mineralogists, Los Angeles, 107-118.

Kimbrough, D.L. & Moore, T.E. (2003). Ophiolite and volcanic arc assemblages on the Vizcaino peninsula and Cedros Island, Baja California Sur, Mexico: Mesozoic forearc lithosphere of the Cordilleran magmatic arc. *In:* Johnson, S.E., Paterson, S.R., Fletcher, J.M., Girty, G.H., Kimbrough, D.L., Martin-Barajas A. (eds) Tectonic evolution of Northwest Mexico and Southwestern USA, Geological Society of America Special Paper 374, 43-71.

Knipper, A.L. (1991). Upper Triassic-Early Jurassic sedimentary breccias in the ophiolitic suite of the Lesser Caucasus. *In:* Peters, T.J., Nicolas, A., & Coleman R.G. (eds). Ophiolite Genesis and Evolution of the Oceanic Lithosphere. Ministry of Petroleum and Minerals, Sultanate of Oman. Kluwer Academic Publications, Amsterdam, 705-714.

Koide, Y., Sano, S., Ishiwatari, A., & Kagami, H. (1987). Geochemistry of the Yakuno ophiolite in southwest Japan. Journal of the Faculty of Science, Hokkaido University, IV (22), 297-312.

Koistinen, T. J. (1981). Structural evolution of an early Proterozoic stratabound Cu-Co-Zn deposit, Outokumpu, Finland. Transactions of the Royal Society of Edinburgh: Earth Sciences, 72, 115-158.

Kontinen, A. (1987). An early Proterozoic ophiolite - The Jormua mafic-ultramafic complex, northeastern Finland. Precambrian Research, 35, 313-341.

Koralenko, I., Aerov, G., & Bagrova, Z. (1994). Geological and structural conditions localizing ornamental stone occurrences in the ophiolites of Itmurunda zone, Kazakhstan, Russia. *In:* Ishiwatari, A., Malpas, J., & Ishizuka, H. (eds.). Proceedings of the 29th International Geological Congress Part D, VSP, 255-262.

Kozary, M.T. (1968). Ultramafic rocks in thrust zones of northwestern Oriente province, Cuba. American Association of Petroleum Geologists Bulletin, 52, 2298-2317.

Kröner, A. (1985). Ophiolites and the evolution of tectonic boundaries in the late Proterozoic Arabian-Nubian shield of northeast Africa and Arabia. Precambrian Research, 27, 277-300.

Kröner, A., Greiling, R., Reischman, T., Hussein, I.M., Stern, R.J., Durr, S., Kruger, J., & Zimmer, M. (1987). Pan-African crustal evolution in the Nubian segment of Northeast Africa. *In:* Kröner, A. (ed.). Proterozoic Lithospheric Evolution. American Geophysical Union Geodynamics Series Volume 17, International Lithosphere Program Contribution, 235-257.

Kröner, A., Todt, W., Hussein, I.M., Mansour, M., & Rashwan, A.A. (1992). Dating of late Proterozoic ophiolites in Egypt and the Sudan using the single grain zircon. Precambrian Research, 59(1-2), 15-32.

Kusky, T.M., and Bradley, D.C. & Haeussler, P. (1997), Progressive deformation of the Chugach accretionary complex, Alaska, during a Paleogene ridge-trench encounter. Journal of Structural Geology, 19(2), 139-157.

Kusky, T.M., Li, J.H., & Tucker, R.T. (2001). The Archean Dongwanzi ophiolite complex, North China Craton: 2.505 Billion Year Old Oceanic Crust and Mantle. Science, 292, 1142-1145.

Kusky, T.M. & Young, C. (1999). Emplacement of the Resurrection Peninsula ophiolite in the southern Alaska Forearc During a Ridge-Trench Encounter, Journal of Geophysical Research, 104(B12), 29025-29054.

Laurent, R. (1980). Environment of formation, evolution and emplacement of the Appalachian ophiolites from Quebec. *In:* Panayiotou, A. (ed). Ophiolites, Proceedings, International Ophiolite Symposium Cyprus 1979. Ministry of Agriculture and Natural Resources Geological Survey Department, 628-636.

Laurent-Charvet, S., Charvet, J., Shu, L. S. (2005). Middle and Late Palaeozoic Northward deformations in Tianshan (NW China): New structural insights along field cross-sections in south, central and north Tianshan units. International Geoscience Programme Tectonics of Central Asia 480, 234-239.

Li, J.H., Kusky, T.M., & Huang, X. (2002). Neoarchean podiform chromitites and harzburgite tectonite in ophiolitic mélange, North China Craton, Remnants of Archean oceanic mantle, Geological Society of America Today, 12(7), 4-11.

Li, J.H., Qian, X.L., & Huang, X.N. (2000). The tectonic framework of the basement of north China craton and its implication for early Precambrian cratonization. Acta Petrologica Sinica, 16(1), 1-10 (English abstract).

Loizenbauer, J., Wallbrecher, E., Fritz, H., Neumayr, P., Khudeir, A.A., & Kloetzli, U. (2001). Structural geology, single zircon ages and fluid inclusion studies of the Meatiq metamorphic core complex: Implications for Neoproterozoic tectonics in the Eastern Desert of Egypt. Precambrian Research, 110(1-4), 357-383.

Lombardo, B., Nervo, R., Compagnoni, R., Messiga, B., Kienast, J.R., Mevel, C., Fiora, L., Piccardo, G.B., & Lanza, R. (1978). Osservazioni preliminari sulle ofioliti metamorfiche del Monviso (Alpi Occidentali). Rend. Soc. Ital. Min. Petrol., 34(2), 253-305.

Lux, D. R. (1986), $^{40}Ar/^{39}Ar$ ages for minerals from the amphibolite dynamothermal aureole, Mont Albert, Gaspe´, Québec. Canadian Journal of Earth Sciences, 23, 21-26.

Lychagin, P.P. (1985). Aluchin massif and the problem of ophiolitic ultramafic and gabbroic rocks in Mesozoic System of northeastern USSR. Pacific Geology, 5, 33-41.

Lytwyn, J., Casey, J., Gilbert, S., & Kusky, T. (1997). Arc-like mid-ocean ridge basalt formed seaward of a trench-forearc system just prior to ridge subduction: An example from subaccreted ophiolites in southern Alaska. Journal of Geophysical Research, 102(B5), 10225-10244.

MacGregor, I., Asish, D., & Basu, R. (1979). Petrogenesis of the Mount Albert Ultramafic Massif, Quebec: Summary. Geological Society of America Bulletin, 90(10), 898-900.

Mackenzie, D.B. (1960). High-temperature alpine-type peridotite from Venezuela. Geological Society of America Bulletin, 71, 303-318.

Mahmood, K., Boudier, F., Gnos, E., Monie, P., & Nicolas, A. (1995). $^{40}Ar/^{39}Ar$ dating of the emplacement of the Muslim Bagh ophiolite, Pakistan. Tectonophysics, 250, 169-181.

Malpas, J., Smith, I.E.M., & Williams, D. (1994). Comparative genesis and tectonic setting of ophiolitic rocks of the South and North Islands of New Zealand. *In:* Ishiwatari, A., Malpas, J., & Ishizuka, H. (eds.). Circum-Pacific Ophiolites. VSP, Utrecht, 29-46.

Malpas, J., Spörli, K.B., Black, P.M., & Smith, I.E.M. (1992). Northland ophiolite, New Zealand, and implications for plate tectonic evolution of the southwest Pacific. Geology, 20(2), 149-152.

Malpas, J., Stevens, R.K. & Strong, D.F. (1973). Amphibolite associated with the Newfoundland ophiolite: its classification and tectonic significance. Geology, 1(1), 45-47.

Mantovani, E., Viti, M., Babbucci, D., Tamburelli, C. & Albarello, D. (2001). Back arc extension: which driving mechanism? *In*: Jessell, M.W. (ed.). General Contributions: Journal of the Virtual Explorer, 3, 17-45.

Marinos, G.P. (1980). Do the ophiolites of eastern Greece represent an old oceanic crust? *In:* Panayiotou, A. (ed). Ophiolites, Proceedings, International Ophiolite Symposium Cyprus 1979. Ministry of Agriculture and Natural Resources Geological Survey Department, 347-348.

Marquer, D., Mercolli, I., & Peters, T. (1998). Early cretaceous intra-oceanic rifting in the Proto-Indian Ocean recorded in the Masirah ophiolite. Tectonophysics, 292 1-16.

Marroni, M., Molli, G., Montanini, A. & Tribuzio, R., (1998). The association of continental crust rocks with ophiolites in the Northern Apennines (Italy): implications for the continent-ocean transition in the Western Tethys. Tectonophysics, 292(1-2), 43-66.

Mason, R. (1980). Temperature and Pressure estimates in the contact aureole of the Sulitjelma gabbro, Norway: Implications for an ophiolite origin. *In:* Panayiotou, A. (ed). Ophiolites, Proceedings, International Ophiolite Symposium Cyprus 1979. Ministry of Agriculture and Natural Resources Geological Survey Department, 576-581.

Mattson, P.H. (1974). Middle Cretaceous nappe structures and their relation to the tectonic history of the Greater Antilles. Geological Society of America Bulletin, 84, 21-38.

Maurasse, F.J.M., Husler, J., Georges, G., Schmidt, R., & Damond, P. (1979). Upraised Caribbean seafloor below acoustic reflection B" at the southern peninsula of Haiti. Geol. Mijnb. 58, 71-83.

McCaig, A.M. (1983). P-T conditions during emplacement of the Bay of Islands ophiolite complex. Earth and Planetary Science Letters, 65, 459-473.

McCall, G.J.H. (1997). The geotectonic history of the Makrãn and adjacent areas of southern Iran. Journal of Asian Earth Sciences, 15, 517-531.

McCormick, G.R. (1991). Origin of volcanics in the Tethyan suture zone of Pakistan. *In:* Peters, T.J., Nicolas, A., & Coleman R.G. (eds). Ophiolite Genesis and Evolution of the Oceanic Lithosphere. Ministry of Petroleum and Minerals, Sultanate of Oman. Kluwer Academic Publications, Amsterdam, 715-722.

Miller, J.A. & Cartwright, I. (2000). Distinguishing between seafloor alteration and fluid flow during subduction using stable isotope geochemistry: examples from Tethyan ophiolites in the Western Alps. Journal of Metamorphic Geology, 18, 467-482.

Miller, R.B. (1985). The Ophiolitic Ingalls Complex, North Cascades, Washington. Geological Society of America Bulletin, 96, 27-42.

Miller, R.B. & Mogk, D.W. (1987). Ultramafic rocks of a fracture-zone ophiolite, North Cascades, Washington. Tectonophysics, 142, 261-289.

Milsom, J. (1984). The gravity filed of the Marum ophiolite complex, Papua New Guinea. *In:* Gass, I.G., Lippard, S. J., & Shelton, A.W. (eds.). Ophiolites and Oceanic Lithosphere. Geological Society of London Special Publication 13, 351-357.

Milsom, J. (2003) Forearc ophiolites: a view from the Western Pacific. *In:* Dilek, Y. & Robinson, P.T. (eds.). Ophiolites in Earth History. Geological Society, London Special Publication 218, 507-516.

Moore, D.H. (1997). A geological interpretation of the geophysical data for the Ouyen 1:250 000 map sheet area. Victorian Initiative for Minerals and Petroleum Report 39. Geological Survey of Victoria, Department of Natural Resources and Environment.

Moore, T.E. (1985). Stratigraphy and tectonic significance of the Mesozoic tectonostratigraphic terranes of the Vizcaino Peninsula, Baja California Sur, Mexico. Circum-Pacific Council for Energy and Mineral Resources Earth Sciences Series, 1, 315-329.

Moore, T.E. & Kimbrough, D.L. (2005). Tectonostratigraphy of Baja California Triassic Ophiolites; a Southern Perspective of Alta California Ophiolite Terranes. GSA Cordilleran Section - 101st Annual Meeting (April 29 - May 1) Paper No. 36-8.

Moore, T.E., Wallace, W.K., Mull, C.G., Adams, K.E., Plafker, G. & Nokleberg, W.J. (1997). Crustal implications of bedrock geology along the Trans-Alaska Crustal Transect (TACT) in the Brooks Range, northern Alaska. Journal of Geophysical Research-Solid Earth, 102(B9), 20645-20684.

Moores, E.M. (2002). Pre-1 Ga (pre-Rodinian) ophiolites: their tectonic and environmental implications. Geological Society of America Bulletin, 114, 80-95.

Moores, E.M. (2003). A personal history of the ophiolite concept. *In:* Dilek, Y. & Newcomb, S. (eds.). Ophiolite concept and the evolution of geological thought. Geological Society of America Special Paper 373, 17-30.

Moores, E.M., Kellogg, L.H., & Dilek, Y. (2000). Tethyan ophiolites, mantle convection, and tectonic "historical contingency": A resolution of the "ophiolite conundrum." *In:* Dilek, Y., Moores, E., Elthon, D., & Nicholas, A. (eds.). Ophiolites and oceanic crust: new insights from field studies and the Ocean Drilling Program. Geological Society of America Special Paper 349, 3-12.

Moores, E.M., Roeder, D.H., Abbas, S.G., & Ahmad, Z. (1980). Geology and emplacement of the Muslim Bagh ophiolite complex. *In:* Panayiotou, A. (ed). Ophiolites, Proceedings, International Ophiolite Symposium Cyprus 1979. Ministry of Agriculture and Natural Resources Geological Survey Department, 424-429.

Moores, E.M. & Twiss, R.J. (1995). Tectonics. W. H. Freeman and Company, USA. pp 415.

Morely, C.K. (2001). Combined escape tectonics and subduction rollback–back arc extension: a model for the evolution of Tertiary rift basins in Thailand, Malaysia and Laos. Journal of the Geological Society, 158(3), 461-474.

Morozov, O., Alexyutin, M., Sokolov, S., & Harbert, W. (2004). Paleomagnetic results from accretional complexes of Taigonos peninsula and their paleotectonic application. American Geophysical Union, Fall Meeting abstract #GP41A-0827.

Mossakovskiy, A.A. & Albear, J.F. (1978). Nappe structure of western and northern Cuba and history of it's emplacement in the light of a study of olistostromes and molasses. Geotectonics, 12, 225-236.

Muller, P.D. (1979). Geology of the Los Amates quadrangle and vicinity, Guatemala, Central America. PhD Thesis, New York State University at Binghamton, 326 pp.

Nekrasov, G.Y., Oro, J., Sokolov, S.D., Flores, R. & Shavyrina, M.V. (1989). Ophiolites of Eastern Cuba. Geotectonics, 23(1), 60-71.

Nelson, B.K. & Ratschbacher, L. (1994). The origin of a terrane: U/Pb zircon geochronology and tectonic evolution of the Xolopa complex (southern Mexico). Tectonics, 13(2), 455-475.

Nelson, E., Forsythe, R., Diemer, J., & Allen, M. (1993). Taitao ophiolite: a ridge collision ophiolite in the forearc of southern Chile (46ºS). Revista Geológica de Chile, 20(2), 137-165.

Nicholson, K.N., Black, P.M., & Picard, C. (2000a). Geochemistry and tectonic significance of the Tangihua Ophiolite Complex, New Zealand. Tectonophysics, 321, 1-15.

Nicholson, K.N., Picard. C., & Black. P.M. (2000b). A comparative study of Late Cretaceous ophiolitic basalts from New Zealand and New Caledonia: implications for the tectonic evolution of the SW Pacific. Tectonophysics, 327, 157-171.

Nicolae, I. & Saccani, E. (2003). Petrology and geochemistry of the late Jurassic calc-alkaline series associated to Middle Jurassic ophiolites in the South Apuseni Mountains (Romania). Schweizerische Mineralogische Und Petrographische Mitteilungen, 83(1), 81-96.

Nicolas, A. (1989). Structure of Ophiolites and Dynamics of Oceanic Lithosphere. Kluwer Academic, Dordrecht. pp 367.

Nicolas, A. & Boudier, F. (2000). Large Mantle Upwellings and Related Crustal Thickness in the Oman Ophiolite. *In:* Dilek, Y., Moores, E., Elthon, D., & Nicholas, A. (eds.). Ophiolites and oceanic crust: new insights from field studies and the Ocean Drilling Program. Geological Society of America Special Paper 349, 67-74.

Nicolas, A. & Boudier, F. (2003). Where ophiolites come from and what they tell us. *In:* Dilek, Y. & Newcomb, S. (eds.). Ophiolite concept and the evolution of geological thought. Geological Society of America Special Paper 373, 137-152.

Nokelberg, W.J., Parfenov, L.M., Monger, J.W.H., Norton, I.O., Khanchuk, A.I., Stone, D.B., Scotese, C.R., Scholl, D.W., & Fujita, K. (1998). Phanerozoic tectonic evolution of the circum-north Pacific. U.S. Geological Survey Professional Paper 1626, 100 pp.

Offler, R. & Shaw, S. (2006). Hornblende Gabbro Block in Serpentinite Mélange, Peel-Manning Fault System, New South Wales, Australia: Lu-Hf and U-Pb Isotopic Evidence for Mantle-Derived, Late Ordovician Igneous Activity. The Journal of Geology, 114(2), 211-230.

Ogawa Y. & Taniguchi, H. (1987). Ophiolitic mélange in forearc area and formation of the Mineoka Belt. Science Reports, Kyushu University, Geology, 15, 1-23.

Okrusch, M. & Seidel, E. (1978). Jurassic age of metamorphism at the base of the Brezovica peridotite (Yugoslavia). Earth and Planetary Science Letters, 39, 291-297.

Oxman, V.S., Parfenov, L.M., Prokopiev, A.V., Timofeev, V.F., Tretyakov, F.F., Nedosekin, Y.D., Layer, P.W., & Fujita, K. (1995). The Chersky Range ophiolite belt, Northeastern Russia. Journal of Geology, 103, 539-557.

Palandzhjan, S.A. (1986). Ophiolite belts in the Koryak Upland, Northeast Asia. Tectonophysics, 127(3-4), 341-360.

Palandzhjan, S.A., Sokolov, S., & Ganelin, A. (1999). Tectonic setting and compositional heterogeneity of the accreted Mesozoic ophiolite in Povorotny Cape, Taigonos Peninsula, Northeastern Russia, Journal of Conference Abstracts, 4, 1.

Palat, A., Casey, J.F., Kerrich, R. (1996). Geochemical characteristics of accreted material beneath the Pazanti-Karsanti ophiolite, Turkey: Intra-oceanic detachment, assemble and obduction. Tectonophysics, 263(1-4), 249-276.

Pallister, J.S., Stacey, J.S., Fischer, L.B., & Premo, W.R. (1988). Precambrian ophiolites of Arabia: Geologic settings, U-Pb geochronology, Pb-isotope characteristics, and implications for continental accretion. Precambrian Research, 38, 1-54.

Pamić, J. (1977). Variation in geothermometry and geobarometry of peridotite intrusions in the Dinaride central ophiolite zone. Yugoslavia. Am. Min., 62, 874-886.

Pamić, J., Gusic, I. & Jelaska, V., (1998). Geodynamic evolution of the central Dinarides. Tectonophysics, 297(1-4), 251-268.

Pamić, J., Sestini, G., Adib, D. (1979)Alpine magmatic and metamorphic processes and plate tectonics in the Zagros Range, Iran. Geological Society of America Bulletin, 90, 569-576.

Parkinson, C.D., Miyazaki, K., Wakita, K., Barber, A.J., & Carswell, D.A. (1998). An overview and tectonic synthesis of the pre-Tertiary very-high-pressure metamorphic and associated rocks of Java, Sulawesi and Kalimantan, Indonesia. The Island Arc, 7(1-2), 184.

Parlak, O. & Delaloye, M. (1999). Precise Ar-40/Ar-39 ages from the metamorphic sole of the Mersin ophiolite (southern Turkey). Tectonophysics, 301(1-2), 145-158.

Parrot, J.F. & Dugas, F. (1980). The disrupted ophiolite belt of the southwest Pacific: Evidence of an Eocene subduction zone. Tectonophysics, 66, 349-372.

Pearce, J.A.(2003). Supra-subduction zone ophiolites-Implications for the origin of ophiolites. *In:* Dilek, Y. & Newcomb, S. (eds.). Ophiolite concept and the evolution of geological thought. Geological Society of America Special Paper 373, 269-294.

Pêcher, A., Giuliani, G., Garnier, V., Maluski, H., Kausar, A.B., Malik, R.H. and Muntaz, H.R. (2002). Geology, geochemistry and Ar-Ar geochronology of the Nangimali ruby deposit, Nanga Parbat Himalaya (Azad Kashmir, Pakistan). Journal of Asian Earth Sciences, 21(3), 265-282.

Pedersen, R.B. & Malpas, J. (1984). The origin of oceanic plagiogranites from the Karmøy ophiolite, western Norway. Contributions to Mineralogy and Petrology, 88 (1-2), 36-52.

Peltonen, P., Manttari, I., Huhma, H., & Kontinen, A. (2003). Archean zircons from the mantle: the Jormua ophiolite revisited. Geology 31, 645-648.

Peng, G., Lewis, J.F., Lipin, B.R., McGee, J.J., Peisheng, B., & Xibin, W. (1995). Inclusions of phlogopite and phlogopite hydrates in chromite from the Hongguleleng Ophiolite in Xinjiang, Northwest China. American Mineralogist, 80(11-12), 1307-1316.

Pertsev, N., Spadea, P., Savelieva, G.N., & Gaggero, L. (1997). Nature of the transition zone in the Nurali ophiolite, southern Urals. Tectonophysics, 276(1-4), 163-180.

Pessagno, E.A., Jr., Blome, C.D., Hull, D.M., & Six, W.M. (1993). Jurassic Radiolaria from the Josephine ophiolite and overlying strata, Smith River subterrane (Klamath Mountains), northwestern California and southwestern Oregon. Micropaleontology, 39(2), 93-166.

Peters, T. & Mercolli, I. (1997). Formation and evolution of the Masirah ophiolite (Sultanate of Oman). Ofioliti, 22(1).

Phelps, D. & Ave'Lallemant, H.G. (1980). The Sparta ophiolite complex, northeast Oregon: a plutonic equivalent to low K2O island-arc volcanism. American Journal of Science, 280-A, 345-358.

Pindell, J. & Dewey, J.F. (1982). Permo-Triassic reconstruction of western Pangea and the evolution of the Gulf of Mexico/Caribbean region. Tectonics, 1, 179-212.

Ping, J., Dunyi, L., Yuruo, S., & Fuqin, Z., (2005). Shrimp dating of SSZ ophiolites from northern Xinjiang province, China: implications for generation of oceanic crust in the central Asian orogenic belt. International Geoscience Programme IGCP-480 Tectonics of Central Asia, 246-251.

Potter, C.J. (1983). Geology of the Bridge River Complex, Southern Shulaps Range, British Columbia: A Record of Mesozoic Convergent Tectonics. Ph.D. Dissertation, University of Washington, 192 pages.

Prestvik, T. (1980). The Caledonian ophiolite complex of Leka, north central Norway. *In:* Panayiotou, A. (ed). Ophiolites, Proceedings, International Ophiolite Symposium Cyprus 1979. Ministry of Agriculture and Natural Resources Geological Survey Department, 555-566.

Prinzhofer, A, Nicolas, A., Cassard, D., Moutte, J., Leblanc, M., Paris, J.P, & Rabinovitch, M. (1980). Structures in the New Caledonia peridotites-gabbros: Implications for oceanic mantle crust. Tectonophysics, 69(1-2), 85-112.

Puchkov, V.N. (1997). Tectonics of the Urals: Modern Concepts, Geotectonics, 31, 294-312.

Raith, M., Hormann, P.K., & Abraham, K. (1977). Petrology and metamorphic evolution of the Penninic ophiolites in the western Tauern window (Austria). Schweiz. Min. Petrogr. Mitt., 57, 187-232.

Rampone, E., Hofmann, A.W., & Raczek, I. (1998). Isotopic contrasts within the Internal Liguride ophiolite (N. Italy): the lack of a genetic mantle-crust link. Earth and Planetary Science Letters, 163(1-4), 175-189.

Rampone, E. & Piccardo, G.B. (2000). The ophiolite-oceanic lithosphere analogue: New insights from the Northern Apennines (Italy). *In:* Dilek, Y., Moores, E., Elthon, D., & Nicholas, A. (eds.). Ophiolites and oceanic crust: new insights from field studies and the Ocean Drilling Program. Geological Society of America Special Paper 349, 21-34.

Rangin, C., Jolivet, L., Pubellier, M., and The Tethys Pacific Working Group (1990). A simple model for the tectonic evolution of southeast Asia and Indonesia region for the past 43 m.y. Geological Society of France Bulletin, 8(6), 889-905.

Rassios, A. & Smith, A.G. (2000). Constraints on the formation and emplacement age of western Greek ophiolites (Vourinos, Pindos, and Othris) inferred from deformation structures in peridotites. *In:* Dilek, Y., Moores, E., Elthon, D., & Nicholas, A. (eds.). Ophiolites and oceanic crust: new insights from field studies and the Ocean Drilling Program. Geological Society of America Special Paper 349, 473-484.

Ren, D. & Abdelsalam, M.G. (2005). Tracing along strike structural continuity in the Neoproterozoic Allaqi-Heiani Suture, Southern Egypt using Principal Component Analysis (PCA), Fast Fourier Transform (FFT0, and Redundant Wavelet Transform (RWT) of ASTER data. Geological Society of America, South-Central Section, 39th annual meeting, 37(3), 5.

Ries, A.C., Shackelton, R.M., Graham, R.H., & Fitches, W.R. (1983). Pan African structures, ophiolites and mélange in the Eastern Desert of Egypt: a traverse at 26°N. Journal of the Geological Society, London, 140, 75-95.

Robertson, A. & Degnan, P. (1994). The Dras Arc Complex - Lithofacies and Reconstruction of a Late Cretaceous Oceanic Volcanic Arc in the Indus Suture Zone, Ladakh-Himalaya. Sedimentary Geology, 92(1-2), 117-145.

Robertson, A.H.F. & Woodcock, N.H. (1980). Tectonic setting of the Troodos massif in the east Mediterranean. *In:* Panayiotou, A. (ed). Ophiolites, Proceedings, International Ophiolite Symposium Cyprus 1979. Ministry of Agriculture and Natural Resources Geological Survey Department, 36-49.

Robertson, A.H.F., & Shallo, M. (2000). Mesozoic–Tertiary evolution of Albania in its regional eastern Mediterranean context. Tectonophysics, 316, 197-254.

Robinson, P.T., Melson, W.G., Ohearn, T., & Schmincke, H.U. (1983). Volcanic Glass Compositions of the Troodos Ophiolite, Cyprus: Geology, 11(7), 400-404.

Rosenfeld, J.H. (1981). Geology of the western Sierra de Santa Cruz, Guatemala, Central America. Ph.D. Dissertation, New York State University at Binghamton, 313 pp.

Rowley, D.B. (1996). Age of initiation of collision between India and Asia: A review of Stratigraphic data. Earth and Planetary Science Letters, 145, 1-13.

Rowley, D.B., (1998). Minimum age of initiation of collision between India and Asia North of Everest based on the subsidence history of the Zhepure Mountain section. The Journal of Geology 106, 229-235.

Rubatto, D., Gebauer, D., & Fanning, M. (1998). Jurassic formation and Eocene subduction of the Zermatt-Saas-Fee ophiolites: implications for the geodynamic evolution of the Central and Western Alps. Contributions to Mineralogy and Petrology, 132(3), 269-287.

Ruzhentsev, S.V. & Samygin, S.G. (1979). Tectonic evolution of the South Uralian ophiolites. *In:* R.W. Talkington & J. Malpas (eds.). Ophiolites of Canadian Appalachians and Soviet Urals. Contribution to IGCP Project 39, 115-126.

Saha, A., Basu, A.R., Wakabayashi, J., & Wortman, G.L. (2005). Geochemical evidence for a subducted infant arc in Franciscan high-grade-metamorphic tectonic blocks. Geological Society of America Bulletin, 117(9-10), 1318-1335.

Saleeby, J.B., Shaw, H.F., Niemeyer, S., Moores, E.M., & Edelman, S.H. (1989). U/Pb, Sm/Nd and Rb/Sr geochronological and isotopic study of northern Sierra Nevada ophiolitic assemblages, California. Contributions to Mineralogy and Petrology, 102(2), 205-220.

Sano, S. (1992). Neodymium isotopic compositions of SilurianYakuno metagabbros. Journal of the Japanese Association of Mineralogy, Petrology and Economic Geology, 87, 272-282. (in Japanese with English abstract).

Sano, S., Tazaki, K., Koide, Y., Nagao, T., Watanabe, T, & Kawachi, Y. (1997). Geochemistry of dike rocks in Dun Mountain ophiolite, Nelson New Zealand. New Zealand Journal of Geology and Geophysics, 40, 127-136.

Sarwar, G. (1992). Tectonic Setting of the Bela Ophiolites, Southern Pakistan. Tectonophysics, 207(3-4), 359-381.

Saveliev, A.A., Sharaskin, A.J., & D'Orazio, M. (1999). Plutonic to volcanic rocks of the Voykar ophiolite massif (Polar Urals): structural and geochemical constraints on their origin. Ofioliti, 24(1), 21.

Savelieva, G.N., Sharaskin, A.Ya., Saveliev, A.A., Spadea, P., & Gaggero, L. (1997). Ophiolites of the southern Uralides adjacent to the East European continental margin. Tectonophysics, 276(1-4), 117-137.

Savov, I. P. (1999). Petrology and Geochemistry of the Precambrian Balkan-Carpathian Ophiolite, Bulgaria and Serbia. M.S. Thesis, University of South Florida, 106 pp.

Savov, I., Ryan, J., Haydoutov, I., & Schijf, J. (2001). Late Precambrian Balkan-Carpathian ophiolite- a slice of the Pan-African ocean crust?: geochemical and tectonic insights from the Tcherni Vrah and Deli Jovan Massifs, Bulgaria and Serbia. Journal of Volcanology and Geothermal Research, 110, 299-318.

Schandelmeier, H., Wipfler, E., Küster, D., Sultan, M., Becker, R., Stern, R.J., & Abdelsalam, M.G. (1994). Atmur-Delgo suture: A Neoproterozoic oceanic basin extending into the interior of northeast Africa. Geology, 22(6), 563-566.

Schmidt, D.L. & Brown, G.F. (1982). Major element chemical evolution of the Late Proterozoic shield of Saudi Arabia. Deputy Ministry for Mineral Resources Open File Report USGS-OF-02-88.

Schroetter, J.M., Bédard, J.H., & Tremblay, A. (2005). Structural evolution of the Thetford Mines Ophiolite Complex, Canada: Implications for the southern Quebec ophiolitic belt. Tectonics, 24(1-2), 1.

Schuster, R. & Kurz, W. (2005). Eclogites in the Eastern Alps: High-pressure metamorphism in the context of the alpine orogeny. Mitt. Österr. Miner. Ges. 150, 173-188.

Scotese, C.R. (1986). Phanerozoic reconstructions: an new look at the assembly of Asia. University of Texas, Geophysical Tech Reports 66:55.

Scotese, C.R. (1991) Jurassic and Cretaceous plate reconstructions. Paleogeography, Paleoclimatology, and Paleoecology, 87, 493-501.

Scotese, C.R. (1997). Paleogeographic Atlas, PALEOMAP Progress Report 90-497, Department of Geology, University of Texas at Arlington, Arlington, Texas, p 1-45.

Scotese, C.R. (2001) Atlas of Earth History. PALEOMAP Project, Arlington, Texas, 79 pp.

Scotese, C.R., Gahagan, L.M., Larson, R.L. (1988). Plate tectonic reconstruction of the Cretaceous and Cenozoic ocean basins. Tectonophysics, 55, 22-48.

Scotese, C.R. and Golonka, J. (1993). Phanerozoic paleogeographic maps. American Association of Petroleum Geologists.

Scotese C.R. & Rees, P.M. (2004). The Spatial-Temporal Information Matrix (STIM CUBE): An efficient way to store geological information. Geological Society of America Annual Meeting, Denver, Colorado. Abstract 61-16.

Scott, D.J., Helmstaedt, H., & Bickle, M.J. (1992). Purtuniq ophiolite, Cape Smith belt, Northern Quebec, Canada: A reconstructed section of early Proterozoic oceanic crust. Geology, 20, 173-176.

Scott, D.J., St-Onge, M.R., Lucas, S.B., & Helmstaedt, H. (1991). Geology and chemistry of the Early Proterozoic Purtuniq ophiolite, Cape Smith Belt, northern Quebec, Canada. *In:* Peters, T.J., Nicolas, A., & Coleman R.G. (eds). Ophiolite Genesis and Evolution of the Oceanic Lithosphere. Ministry of Petroleum and Minerals, Sultanate of Oman. Kluwer Academic Publications, Amsterdam, 817-850.

Searle, M.P. & Stevens, R.K. (1980). Obduction Processes in ancient, modern and future ophiolites *In:* Panayiotou, A. (ed). Ophiolites, Proceedings, International Ophiolite Symposium Cyprus 1979. Ministry of Agriculture and Natural Resources Geological Survey Department, 300-319.

Şengör, A.M.C. (1990). A new model for the late Paleozoic-Mesozoic tectonics evolution of Iran and implications for Oman. *In:* Robertson, A.H.F, Searle, M.P., & Ries, A.C. (eds.). The geology and tectonics of the Oman region. Geological Society of London Special Publication 49, 797-831.

Seyler, M., Paquette, J.L., Ceuleneer, G., Kienast, J.R. & Loubet, M., (1998). Magmatic underplating, metamorphic evolution and ductile shearing in a Mesozoic lower crust-upper mantle unit (Tinaquillo, Venezuela) of the Caribbean Belt. Journal of Geology, 106(1), 35-58.

Shackleton, R.M. (1994). Review of Late Proterozoic sutures, ophiolitic mélanges and tectonics of eastern Egypt and north-east Sudan, International Journal of Earth Sciences, 83(3), 537-546.

Shah, M.T. & Khan, A. (1999). Geochemistry and origin of Mn-deposits in the Waziristan ophiolite complex, north Waziristan, Pakistan. Mineralium Deposita, 34(7), 697-704.

Sharkov, E.V., Chistyakov, A.V., Laz'ko, E.E., & Quick, J.E. (1999). Evolution of composition of major mineral phases in layered complex of ophiolite assemblage: evidence for the Voykar ophiolites (Polar Urals, Russia). Ofioliti, 24(2), 249.

Shervais, J.W., Murchey, B.L., Kimbrough, D.L., Renne, P.R., Hannan, B. (2005). Radioisotopic and biostratigraphic age relations in the Coast Range Ophiolite, northern California: Implications for the tectonic evolution of the Western Cordillera. Geological Society of America Bulletin, 117(5-6), 633-653.

Sleep, N.H. & Windley, B.F., (1982). Archean plate tectonics: constraints and inferences. Journal of Geology, 90, 363-380.

Smith, A.G., Smith, D.G., & Funnell, B.M. (1994). Atlas of Mesozoic and Cenozoic coastlines. Cambridge University Press, Cambridge, 99 pp.

Sokolov, S.D., Bondarenko, G.Ye., Morozov, O.L., Shekhovstov, V.A., Glotov, S.P., Ganelin, A.V., & Kravchenko-Berezhnoy, I.R. (2002). South Anyui suture, Northeast Arctic Russia: facts and problems. *In:* Miller, E., Grantz, A, & Klemperer ,S. Tectonic Evolution of the Bering Shelf-Chukchi Sea-Artic Margin and Adjacent Landmasses. Geological Society of America Special Paper 360, 209-224.

Sopaheluwakan, J., Helmers, H., Tjokrosapoetro, S. & Nila, E.S. (1989). Medium Pressure Metamorphism with Inverted Thermal-Gradient Associated with Ophiolite Nappe Emplacement in Timor. Netherlands Journal of Sea Research, 24(2-3), 333-343.

Southwick, D.L. (1974). Geology of the alpine-type ultramafic complex near Mount Stuart, Washington. Geological Society of America Bulletin, 85, 391-402.

Spaggiari, C.V., Gray, D.R., & Foster, D.A. (2003). Tethyan- and Cordilleran-type ophiolites of eastern Australia: implications for the evolution of Tasmanides. *In:* Dilek, Y. & Robinson, P.T. (eds.). Ophiolites in Earth History. Geological Society, London Special Publication 218, 517-540.

Spaggiari, C.V., Pidgeon, R.T., & Wilde, S.A. (2004) Structural and tectonic framework of >4.0 Ga detrital zircons from the Jack Hills Belt, Narryer Terrane, Western Australia. Geological Society of America Annual Meeting Denver, Colorado, Paper No. 82-11 (abstract).

Spray, J.G. (1984). Possible causes and consequences of upper mantle decoupling and ophiolite displacement. *In:* Gass, I.G., Lippard, S. J., & Shelton, A.W. (eds.). Ophiolites and Oceanic Lithosphere. Geological Society of London Special Publication 13, 255-268.

Spray, J.G., Bébien, J., Rex, D.C., & Roddick, J.C. (1984). Age constraints on the igneous and metamorphic evolution of the Hellenic-Dinaric ophiolites. *In:* Dixon J.E., & Robertson, A.H.F. (eds). The Geological Evolution of the Eastern Mediterranean. Geological Society of London, Special Publication 173, 619-627.

Stacey, J.S. & Stoeser, D.B. (1983). Distribution of oceanic and continental leads in the Arabian-Nubian Shield. Contributions to Mineralogy and Petrology, 84, 91-105.

Stern, R.J. (2005) Evidence from ophiolites, blueshcists, and ultrahigh-pressure metamorphic terranes that the modern episode of subduction tectonics began in Neoproterozoic time. Geology, 33(7), 557-560.

Stern, R.J., Nielsen, K.C., Best, E., Sultan, M., Arvidson, R.E., & Kröner, A. (1990). Orientation of late Precambrian sutures in the Arabian-Nubian shield. Geology, 18(11), 1103-1106.

Sturchio, N.C, Sultan, M., & Batiza, R. (1983). Geology and origin of Meatiq Dome, Egypt: A Precambrian metamorphic core complex? Geology, 11(2), 72-76.

Sturt, B.A. & Roberts, D. (1991). Tectonostratigraphic relationships and obduction histories of Scandinavian ophiolithic terranes. *In:* Peters, T.J., Nicolas, A., & Coleman R.G. (eds). Ophiolite Genesis and Evolution of the Oceanic Lithosphere. Ministry of Petroleum and Minerals, Sultanate of Oman. Kluwer Academic Publications, Amsterdam, 745-769.

Sturt, B.A., Roberts, D., & Furnes, H. (1984). A conspectus of Scandinavian Ophiolites. *In:* Gass, I.G., Lippard, S. J., & Shelton, A.W. (eds.). Ophiolites and Oceanic Lithosphere. Geological Society of London Special Publication 13, 381-391.

Sturt, B.A., Thon, A., & Furnes, H. (1979). The Karmøy ophiolite, southwest Norway. Geology, 7(6), 316-320.

Styles, M.T. & Kirby, G.A. (1980). New investigations of the Lizard complex, Cornwall, England and a discussion of an ophiolite model. *In:* Panayiotou, A. (ed). Ophiolites, Proceedings, International Ophiolite Symposium Cyprus 1979. Ministry of Agriculture and Natural Resources Geological Survey Department, 517-526.

Suhr, G. & Cawood, P.A. (2001). Southeastern Lewis Hills (Bay of Islands Ophiolite): Geology of a deeply eroded, inside-corner, ridge-transformation intersection. Geological Society of America Bulletin, 113(8), 1025-1038.

Suren, P. (1986). Ophiolite belts in Koryak uplands, Northeast Asia. Tectonophysics, 127, 341-360.

Talkington, R.W. & Malpas, J. (1980). Spinel phases of the White Hills Peridotite, St. Anthony Complex, Newfoundland: Part 1. Occurrence and chemistry. *In:* Panayiotou, A. (ed). Ophiolites, Proceedings, International Ophiolite Symposium Cyprus 1979. Ministry of Agriculture and Natural Resources Geological Survey Department, 607-619.

Taylor, B. (1992). Rifting and the volcanic-tectonic evolution of the Izu-Bonin-Mariana arc. *In:* Proceedings from ODP, Science Results, 126, 672-652.

Thirwall, M.F. & Bluck, B.J. (1984). Sr-Nd isotope and chemical evidence that the Ballantrae 'ophiolite', SW Scotland, is Polygenic. *In:* Gass, I.G., Lippard, S. J., & Shelton, A.W. (eds.). Ophiolites and Oceanic Lithosphere. Geological Society of London Special Publication 13, 215-230.

Thuizat, R. Whitechurch, H. Montigny, R. Juteau, T. (1981). K-Ar dating of some infra-ophiolitic metamorphic soles from the eastern Mediterranean; new evidence for oceanic thrustings before obduction. Earth and Planetary Science Letters, 52, 302-310.

Tribuzio, R., Tiepolo, M., Vanucci, R. (2000). Evolution of gabbroic rocks of the Northern Apennine ophiolites (Italy): Comparison with the lower oceanic crust from modern slow-spreading ridges. *In:* Dilek, Y., Moores, E., Elthon, D., & Nicholas, A. (eds.). Ophiolites and oceanic crust: new insights from field studies and the Ocean Drilling Program. Geological Society of America Special Paper 349, 129-138.

Van Staal, C.R. (2005). Pre-Carboniferous Metallogeny of the Canadian Appalachians. Geological Survey of Canada, Mineral Deposits of Canada, 32 p.

Varne, R., Brown, A.V. & Falloon, T (2000). Macquarie Island: Its geology, structural history, and the timing and tectonic setting of its N-MORB. *In:* Dilek, Y., Moores, E., Elthon, D., & Nicholas, A. (eds.). Ophiolites and oceanic crust: new insights from field studies and the Ocean Drilling Program. Geological Society of America Special Paper 349, 301-320.

Vergely, P., Dimo, A., & Monie, P. (1998). Datation des semelles metamorphiques ophiolitiques d'Albanie par la methode 40Ar/39Ar: consequences sur le mecanisme de leur mise en place. C.R. Acad. Sci. Paris, Sci. Terre Planet., 326, 717-722.

Vidyadharan, K.T., Joshi, A., Ghose, S., Gaur, M.P., Shukla, R. (1989). Manipur ophiolites: its geology, tectonic settings and metallogeny with special reference to podiform chromite. *In:* Ghose, N.C. (ed.). Phanerozoic ophiolites of India and associated mineral resources. Sumna Publications, Patna, India, 197-212.

Vyosotsky, S.V. (1994). High and low pressure cummulates of the Paleozoic ophiolites in Primorye, Eastern Russia. *In:* Ishiwatari, A., Malpas, J., & Ishizuka, H. (eds). Proceedings of the 29th International Geological Congress Part D, VSP, 145-162.

Wadge, G., Draper, G., & Lewis, J.F. (1984). Ophiolites of the northern Caribbean: A reappraisal of their roles in the evolution of the Caribbean plate boundary. *In:* Gass, I.G., Lippard, S. J., & Shelton, A.W. (eds.). Ophiolites and Oceanic Lithosphere. Geological Society of London Special Publication 13, 367-380.

Wadge, G., Jackson, T.A., Isaacs, M.C., & Smith, T.E. (1982). The ophiolitic Bath-Dunrobin Formation, Jamaica: Significance for Cretaceous plate margin evolution in the north-western Caribbean. Journal of the Geological Society of London, 139, 321-333.

Wallin, T.E., Mattinson, J.M., & Potter, A.W. (1988). Early Paleozoic magmatic events in Eastern Klamath Mountains, northern California. Geology, 16(2), 144-148.

Whattam, S.A., Malpas, J., Ali, J.R., Lo, C., & Smith, I.E.M. (2005). Formation and emplacement of the northland ophiolite, northern New Zealand: SW Pacific tectonic implications. Journal of the Geological Society, 162, 225-241.

Williams, M.D. (1975). Emplacement of Sierra de Santa Cruz, eastern Guatemala. American Association of Petroleum Geologists Bulletin, 59, 1211-1216.

Wirth, K.R., Bird, J.M., Blythe, A.E., Harding, D.J., & Heizler, M.T. (1993). Age and Evolution of Western Brooks Range Ophiolites, Alaska - Results from Ar-40/Ar-39 Thermochronometry. Tectonics, 12(2), 410-432.

Wright, J.E. & Wyld, S.J. (1986). Significance of xenocrystic Precambrian zircon contained within the southern continuation of the Josephine ophiolite: Devils Elbow ophiolite remnant, Klamath Mountains, northern California. Geology, 14(8), 671-674.

Yaliniz, M.K., Floyd, P.A. & Goncuoglu, M.C., (2000). Petrology and geotectonic significance of plagiogranite from the Sarikaraman Ophiolite (Central Anatolia, Turkey). Ofioliti, 25(1), 31-37.

Yaliniz, M.K., Goncuoglu, M.C. & Ozkan-Altiner, S., (2000). Formation and emplacement ages of the SSZ-type Neotethyan ophiolites in Central Anatolia, Turkey: palaeotectonic implications. Geological Journal, 35(2), 53-68.

Yilmaz, Y. (1993). New Evidence and Model on the Evolution of the Southeast Anatolian Orogen. Geological Society of America Bulletin, 105(2), 251-271.

Yuan, C., Sun, M., Zhou, M.F., Zhou, H., Xiao, W., & Li, J. (2003). Absence of Archean basement in the South Kunlun Block: Nd-Sr-O isotopic evidence of granotiods. The Island Arc, 12, 13-21.

Zaigham, N.A. & Mallick, K.A. (2000). Bela ophiolite zone of southern Pakistan: Tectonic setting and associated mineral deposits. Geological Society of America Bulletin, 112(3), 478-489.

Zhou, M.F. (1996), An early Proterozoic podiform chromitite in the Outokumpu Ophiolite complex, Finland - A discussion. Economic Geology and the Bulletin of the Society of Economic Geologists, 91(1), 221-222.

Zhou, M.F., Lewis, J., Malpas, J. & Munoz-Gomez, N. (2001). The Mayari-Baracoa paired ophiolite belt, eastern Cuba: Implications for tectonic settings and platinum-group elemental mineralization. International Geology Review, 43(6), 494-507.

Zhou, M.F., Yumul, G.P., Malpas, J., & Sun, M. (2000). Comparative study of platinum- group elements in the Coto and Acoje blocks of the Zambales ophiolite complex, Philippines. The Island Arc, 9, 556-564.

Zimmermann, R., Hammerschmidt, K., & Franz, G. (1994). Eocene high pressure metamorphism in the Penninic units of the Tauern Window (Eastern Alps). Evidence from 40Ar-39Ar dating and Petrological investigations. Contributions to Mineralogy and Petrology, 117, 175-186.

BIOGRAPHICAL INFORMATION

Stacey Metzler earned a Bachelor of Science in Geology from the University of Texas at Arlington in 1999. She pursued a teaching career for a few years where she taught high school and junior high science and math classes. After returning to earn her Master of Science in Geology and Spatial Information Certification for GIS, she will work in the Engineering and Teaching industries where both of her interest lie; showing college students the fascination she has always held for science and math concepts as well as working in the Engineering industry as a Geologist and GIS analyst.